doi : 10.17596/0003573

Cruise Report

MR06-04

LEG1 and 2

Aug. 1- Sep. 29, 2006

Leg 1: Sekinehama – Kushiro

Leg 2: Kushiro-(Dutch Harbor, USA) -Sekinehama

Content

1. Preface

This volume includes the simply notes instruments, methods, and preliminary results obtained on-board of the MR06-04 legs 1 and 2 cruises carried out by R/V MIRAI in the Okhotsk Sea, the Japan/East Sea, the Bering Sea and the Chukchi Sea in 2006. The cruise is divided in two legs of which research area are the Okhotsk and Japan Seas area (from Sekinehama to Kushiro; leg. 1) and the Arctic area (from Kushiro -(Dutch Harbor, USA) to Sekinehama; leg. 2). The investigation started in (leg 1), and then to (leg 2).

Main purpose of this cruise is to understanding of glacial and inter-glacial climate changes and abrupt changes in the above area, especially the sea surface temperature and salinity changes and impact of the Amur River discharge on the thermohaline circulation and sea-ice formation in the Okhotsk Sea. In addition, we investigate the Arctic area to understand the relationship between methane release events and climate changes.

The main observation items are site survey (Sea beam and sub-bottom profiler system), sediment coring (Piston corer, Gravity corer, and Multiple corer), conductivity, temperature, and depth observation and water collection in the water column (CTD/Rosette sampler) and its physical and chemical analyses (Temperature, Salinity, dissolved oxygen, total carbonate, Alkalinity, pCO_2, pH, nutrients and *Chl* a), XCTD and XCP measurements and plankton collection in the surface water (Norpac net). We also successfully observed Under way of Geological, Geophysical, Meteorological, Biogeochemical (*Chl* a, and pCO_2), Physical property (temperature and salinity) investigations, Shipboard ADCP, Satellite, Aerosol and rain collections except for the inside the Russian Exclusive Economic Zone.

The cruise has been completed almost of what we planed. On behalf of the scientists on-board, I thank all Japanese, American and Canadian authorities; the Ministry of Education, Culture, Sports, Science, and Technology of Japan, the Ministries of Foreign Affair of Japan, USA, and Canada, the Coast Guard of USA and Canada, for allowing us to work inside the American and Canadian EEZ. Without their help, the cruise would have never been realized. I really appreciate Captain, Dr. Akamine, Chief officer, Mr. Inoue, and crew members for their hard works on board the ship. Finally, I would like to thank Canadian Ice Navigator, Mr. Cordeiro for his best advices about roots for safety navigation in the sea-ice covered area in Chukuti Sea.

MR06-04 Chief Scientist
Naomi Harada
Japan Agency for Marine-Earth Science and Technology (JAMSTEC)
Institute of Observational Research for Global Change (IORGC)
Paleoclimatology and Paleoceanography Group

2. Cruise summary

2.1 Ship

R/V MIRAI

L x B x D	128.58m x 19m x 13.2m
Gross Tonnage	8,672 tons
Call Sign	JNSR

2.2 Cruise Code

MR06-04

2.3 Title of the cruise

Study on the paleoceanography in high latitude of the North Pacific and its adjacent seas and the Arctic area.

2.4 Institute

Japan Agency for Marine-Earth Science and Technology (JAMSTEC)

2-15 Natsushima-cho, Yokosuka 237-0061, Japan

2.5 Chief Scientist

Naomi Harada (JAMSTEC)

2.6 Cruise periods and ports of call

Leg.1: August, 1, 2006 (Sekinehama, Japan) to August, 20, 2006 (Kushiro, Japan)

Leg.2: August, 21, 2006 (Kushiro, Japan) to September, 29, 2006 (Sekinehama, Japan) (call at Dutch harbor, USA for August, 28, 2006 and September, 19, 2006)

2.7 Observation summary

Piston coring	24 casts
Multiple coring	43 casts
Gravity coring	5 casts
Plankton net	196 casts
CTD/water sampling	40 casts
XBT	3 casts
XCTD	44 casts
XCP	3 casts
Radiosonde launching	48 casts
CO_2 profiler	23 stations (leg.2)
Sub bottom profiling	11 stations
Meteorological water sampling	Continuous data except for the non-permission area from Russian,

	USA, and Canadian Governments
Aerosol sampling	Continuous data except for the non-permission area from Russian, USA, and Canadian Governments
Surface Meteorology	Continuous data except for the non-permission area from Russian, USA, and Canadian Governments
Cloud observation with lider	Continuous data except for the non-permission area from Russian, USA, and Canadian Governments
Eddy flux measurement	Continuous data except for the non-permission area from Russian, USA, and Canadian Governments
Aerosol observation with sky radio meter	Continuous data except for the non-permission area from Russian, USA, and Canadian Governments
Sea surface water monitoring	Continuous data except for the non-permission area from Russian, USA, and Canadian Governments
Sea surface Gravity	Continuous data except for the non-permission area from Russian, USA, and Canadian Governments
Shipboard ADCP	Continuous data except for the non-permission area from Russian, USA, and Canadian Governments
Sea bottom topography	Continuous data except for the non-permission area from Russian, USA, and Canadian Governments
Surface Tree Component	Continuous data except for the non-permission area from Russian, USA, and Canadian Governments
Magnetic Field Measurement	Continuous data except for the non-permission area from Russian, USA, and Canadian Governments

2.8 Data Policy

All data collected during this cruise will be under the control of the Data Management Office (DMO) of JAMSTEC.

2.9 Overview

(1) Leg.1: August 1, 2006 (Sekinehama) – August 20, 2006 (Kushiro)

Total 18 piston and 7 multiple cores were collected at seven stations in this leg.1. Two piston cores were collected at the St.1 (42˚31N, 144˚20'E, water depth 996m) and St.2 (41˚52'N, 143˚57'E, water depth 1043m), respectively with multiple cores at the Off Kushiro. For PC01, the major lithology is glass, pumice-bearing sandy silt and fossils such as foraminifera and diatom are rare. For PC02, the major lithology is bioturbated olive black diatom, spicule-bearing silt clay or clayey silt. Three piston cores were collected at the St.3 (45˚45'N, 140˚47'E, water depth 774m) in the northern Japan Sea. The major lithology is dark olive gray clayey diatom ooze and partly thin lamination layers appear. Three piston cores were collected at St.4 (44˚32'N, 145˚E, water depth 1217m) off Shiretoko in the Okhotsk Sea. The major lithology is homogeneous olive black silty clay. Three piston cores were collected at St.6 (53˚17'N, 150˚05'E, 1143m) and St.7 (51˚17'N, 149˚13'E, water depth 1249m), respectively in the international water of the central Okhotsk Sea. Two piston cores also are collected at St.5 (54˚19'N, 149˚10'E, water depth 831m) in the international water. For PC06, the major lithology is grayish olive diatom bearing silty clay. For PC07, the major lithology is grayish olive silty clay. For PC05, the major lithology is similar as those of PC06 and 07, and the shipboard age of core bottom is estimated to be older than the past 40 kyr. At seven stations, 13 casts of CTD/hydrography and 99 casts of plankton net observations were done.

(2) Leg.2: August, 21, 2006 (Kushiro) – August, 29, 2006 (Sekinehama)

On Sep. 2nd (local time), R/V MIRAI observed sea ice free area in the Chukchi Sea where most northern site (72-36˚N, 166W) as navigating as possible MIRAI can. In order to go to the Beaufort Sea, although R/V MIRAI tried to go to close the Alaskan coast, the presence of heavy and thick multi-year sea ice prohibited the navigation of R/V MIRAI toward the east. Consequently, the final decision that R/V MIRAI does not observe in the Beaufort Sea was made on Sep. 5th.

Total 6 piston, 5 gravity and 36 multiple cores were collected at 23 stations in the southeastern Bering Sea during leg.2. Two piston cores were collected at the St.23 (60˚N, 179˚28'W, water depth 1002m), St.24 (60˚16'N, 179˚25'W, water depth 852m), 25 (60˚04'N, 179˚28'W, water depth 1158m), respectively in the Bering Sea. For PC23, 24, 25, the major lithology is olive black silty clay. Some microfossils such as diatom, foraminifera are found and some lamination layers appear throughout the cores. In addition, 27 casts of CTD/hydrography and 97 casts of plankton net observations were done.

Bloom of haptophyto plankton was found on courses from St.29 (59˚N, 167˚W) to St.30 (59˚N, 177˚W) and from St.31 (59˚N, 170˚W) to St.32 (57˚N, 167˚W) since the observation in 2000

Fig.2.1 Haptophyto plankton bloom (area of turquoise blue)

(Fig.2.1). The community was composed of *Eminilania huxleyi*.

3. List of Instruments on MIRAI

(1) Multi Narrow Beam Echo Sounding System

SeaBeam 2112.004, (SeaBeam Instruments Inc., USA)

Frequency: 12kHz

Beam resolution: 1 degree

Depth measurement accuracy: <0.5%

Depth range: 100~11000 m

① Sub-bottom profiler

SeaBeam 2112.004, (SeaBeam Instruments Inc. USA)

Transmission frequency range: 2.5~6.5kHz

Depth penetration: about 70m beneath the sea floor

Beam withth: 5 degree x 5 degree

Depth measurement accuracy: <0.5%

(2) Current profiler

Broadband Acoustic Doppler Current Profiler, VM-75 (RD Instruments Inc., USA)

Frequency (averaged): 300 second

Measurement depth range: 30~650m

Measurement depth cell number: 40

Measurement resolution: 1mm/s

Measurement accuracy: 0.25%

(3) Ship board Magnet system

① Gravity Meter: S-116 (LaCoste-Romberg. Inc., USA)

Measurement accuracy: 1 mGal

② Magnet Meter: Three component magnetometer, SFG-1214 (Tierra Tecnica Ltd., USA)

Measurement resolution: 0.01 nT

(4) General Weather Observation

① Anemometer: KE-500 (Koshin Denki, Japan)

② Thermometer FT (Koshin Denki, Japan)

③ Dewpoint Meter: DW-1 (Koshin Denki, Japan)

④ Barometer: F451 (Yokogawa Co., Japan)

⑤ Radiometer: MS-801, MS-202 (Eiko Seiki, Japan)

(5) SOAR Insolation-Radiation observation system

① Anemometer: 5106 (R.M. Young, USA)

② Barometer: 61201 (R.M. Young, USA)

③ Rain gauge: 50202 (R.M. Young, USA)

④ Radiometer: PSP, PIR (Eppley labs, USA)

(6) Ceilometer: CT-25K (VAISARA, Finland)
Observation range: 0-7.5 km
Observation resolution: 50 ft

(7) Radiosonde system
① GPS Radiosonde: RS-80-15G (VAISARA, Finland)

(8) CTD/Rosetta water sampling system
① Carousel Water Sampler, SBE32 (Sea-Bird Electronics Inc., USA)
② Conductivity/Temperature/Depth Profiler, SBE9plus, SBE11 (Sea-Bird Electronics Inc., USA)
Conductivity measurement accuracy: 0.0003 S/m
Temperature measurement accuracy: 0.001˚C
Pressure measurement accuracy: 0.015%
③ Niskin Water sampler (General Oceanics Inc. USA)

(9) XBT system, T-05, T-07 (Tsurumi-Seiki Ltd., Japan)
Measurement accuracy: 0.2 ˚C

(10) XCTD system, XCTD-1 (Tsurumi-Seiki Ltd., Japan)
Conductivity measurement accuracy: 0.03 S/m
Temperature measurement accuracy: 0.02˚C

(11) XCP system (Tsurumi-Seiki Ltd., Japan)
Observation depth range: ~1000m

(12) Partial pressure CO_2 (pCO_2) measurement system, Non-dispersive infrared analyzer (BINOS, Inc. USA)
Observation depth range: 150~400ppm
Measurement resolution: 0.1 ppm

(13) Bottle Salinity measurement
① AutoSal, 8400B, (Guildline)
② Thermometer, Digital Platinum Resistance Thermometer, (Guildline)

(14) Nutrients measurement, Continuous Flow Analytical System, Model TRAACS 800 (4 channels), (Bran+Lubbe)

(15) Total Dissolved Inorganic Carbon (TCO_2) Measurement, (Carbon Dioxide Coulometer Model 5012, UIC Inc.)

(16) Total Alkalinity

① Titrator, TitraLab TIM 900 (Radiometer)

② Autoburette, TitraLab ABU 901 (Radiometer)

(17) Dissolved Oxygen Measurement

① Titrator, Metrohm, Model 716 DMS Titrino/10ml of titration vessel

② Detector, Metrohm, Pt Electrode/ 6.0408.100

(18) Surface Sea water Monitoring

① Temperature and Salinity Sensor, SEACAT Thermosalinograph SBE-21 (SeaBird Electronics Inc., USA)

Conductivity: 0.001 S/m

Temperature measurement accuracy: 0.01˚C

② Dissolved Oxygen Sensor, 2127A (Oubisufair Laboratory Japan Inc., Japan)

Measurement accuracy: 1%

③ Fluorometer, 10-AU-005 (Turner Designs)

Fluorescence detection limit: 5 ppt

(19) Multiple corer (Rigosha, Japan)

(20) Piston corer (Riosha, Japan)

(21) Giant Gravity corer (OUYO, Japan)

4. Cruise Track and Log

4.1 Cruise Track

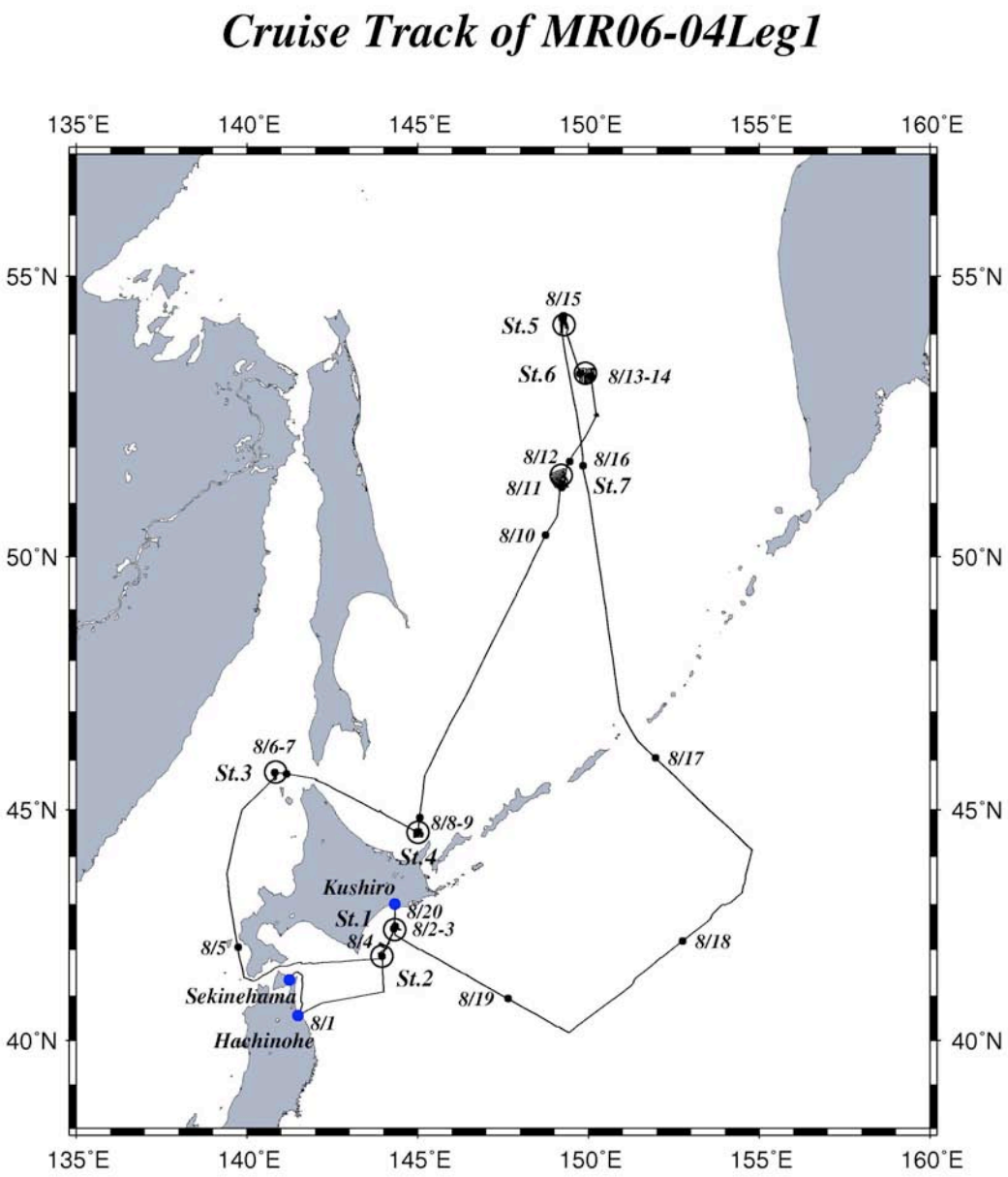

Fig. 4.1.1 Cruise track, noon position and observational points in MR06-04 Leg1

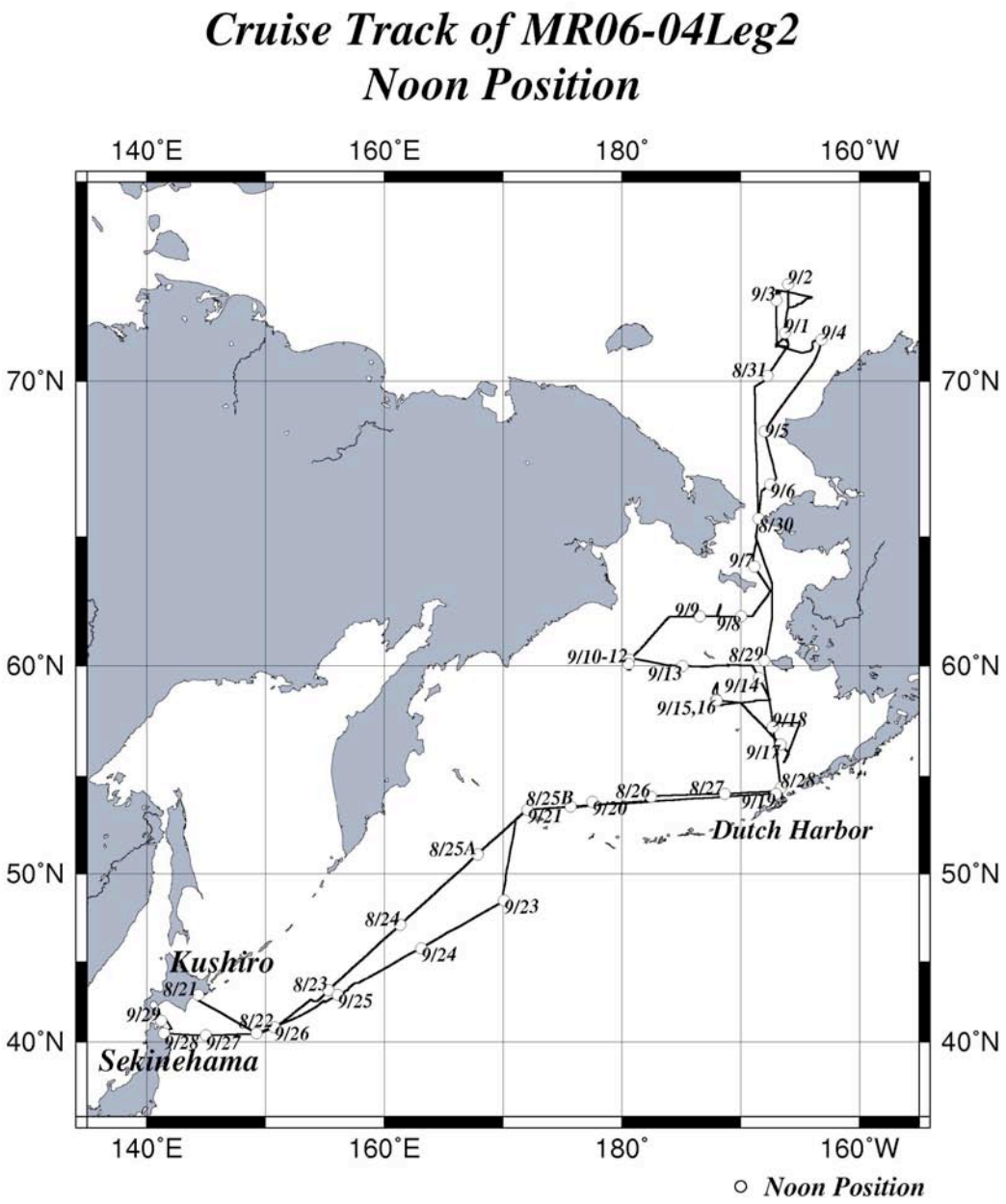

Fig. 4.1.2 Cruise track and noon position in MR06-04 Leg2

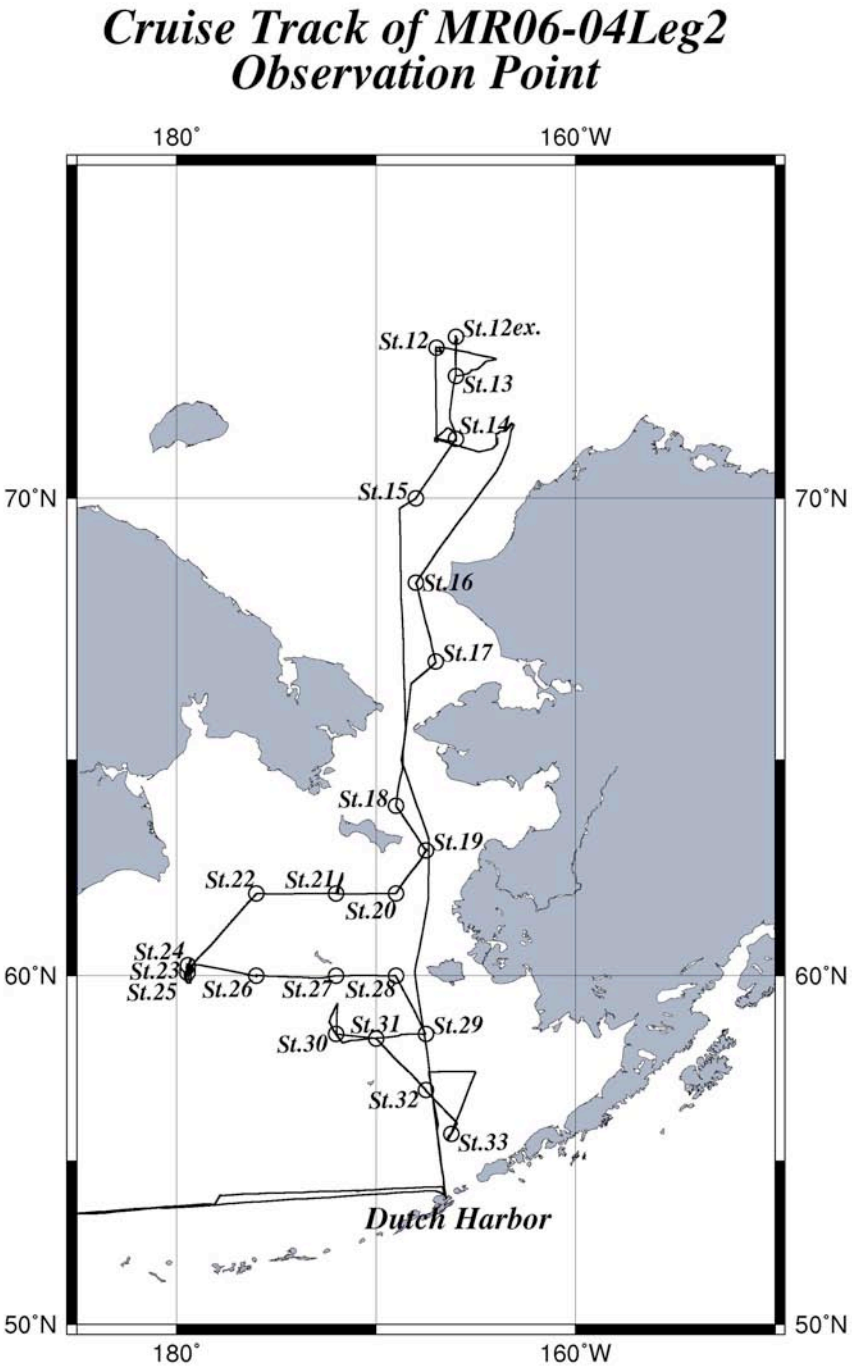

Fig. 4.1.3 Cruise track and observational points in MR06-04 Leg2

4.2 Cruise Log

(Leg1)

S.M.T.		U.T.C.		Position		Event
Date	Time	Date	Time	Lat.	Long.	
8/1	6:00	7/31	21:00	41-22N	141-14E	Departure for Sekinehama
8/1	12:20	8/1	3:20	40-33N	141-30E	Arrival at Hachinohe
	17:00		8:00	40-33N	141-30E	Departure for Hachinohe
	20:17		11:17	40-51.33N	142-19.65E	XCTD SB-01
8/2	1:48	8/1	16:48	41-05.60N	144-00.37E	Arrival at Free Fall point
	2:05		17:02	41-05.60N	144-00.37E	Free Fall (3,200m)
	3:54		18:54	-	-	Departure for Free Fall Point
	4:01		19:01	41-05.43N	144-00.30E	XCTD NC-01
	8:30		23:30	42-08.33N	144-08.75E	Radiosonde RS-01
8/2	10:00	8/2	1:00	42-27N	144-19E	Arrival at Station 1
	10:05		1:05	42-27.66N	144-17.50E	CTD cast St.1-01 (1,020m)
	11:30		2:30	42-28.12N	144-17.44E	Radiosonde RS-02
	11:35		2:35	42-28.15N	144-17.44E	Plankton Net (Calibration; 500m, 200m, 50m)
	12:26		3:26	42-28.59N	144-17.49E	Plankton Net St.1-01 (200m, 100m, 50m, 25m)
	13:43		4:43	42-29.53N	144-17.85E	Plankton Net St.1-02 (200m - 20m)
	14:30		5:30	42-29.67N	144-17.80E	Radiosonde RS-03
	15:13		6:13	42-29.64N	144-18.20E	XCTD NC-02
	15:18		6:18	-	-	Site survey (4hour)
	20:30		11:30	42-30.58N	144-19.73E	Radiosonde RS-04
	20:30		11:30	42-30.58N	144-19.72E	XCTD NC-03
8/3	2:30	8/2	17:30	42-30.57N	144-19.65E	Radiosonde RS-05
	4:02		11:30	42-30.58N	144-19.72E	XCTD NC-04
	7:04		22:04	42-30.71N	144-20.06E	Start Multiple Core St.1-01
	7:39		22:39	42-30.59N	144-19.65E	Multiple Core at bottom St.1-01 (993m)
	8:30		23:30	42-30.72N	144-19.94E	Radiosonde RS-06
	8:42		23:42	42-30.69N	144-19.86E	Start Piston Core St.1-01
	9:46	8/3	0:46	42-30.57N	144-19.67E	Piston Core at bottom St.1-01 (996m)
	9:53		0:53	42-30.56N	144-19.63E	XCTD NC-05
	13:10		4:10	42-30.69N	144-19.83E	Start Piston Core St.1-02

S.M.T.		U.T.C		Position		Event
Date	Time	Date	Time	Lat.	Long.	
	14:13		5:13	42-30.58N	144-19.70E	Piston Core at bottom St.1-02 (995m)
	14:30		5:30	42-30.65N	144-19.60E	Radiosonde RS-07
	15:06		6:06	–	-	Departure for Station 1
	15:20		6:20	42-30.63N	144-19.80E	XCTD NC-06
	17:30		8:30	41-52N	143-57E	Arrival at Station 2
	17:30		8:30	-	-	Site survey (6hour)
	20:50		11:50	42-01.49N	144-19.03E	Radiosonde RS-08
8/4	2:30	8/3	17:30	42-01.49N	144-19.03E	Radiosonde RS-09
	5:55		20:55	41-51.80N	143-57.46E	Start Multiple Core St.2-01
	6:11		21:11	41-51.91N	143-57.21E	XCTD NC-07
	6:25		21:25	41-52.02N	143-56.98E	Multiple Core at bottom St.2-01 (1,043m)
	7:38		22:38	41-51.90N	143-57.30E	Start Piston Core St.2-01
	8:30		23:30	41-52.01N	143-56.97E	Radiosonde RS-10
	8:35		23:35	41-52.01N	143-56.92E	Piston Core at bottom St.2-01 (1,045m)
	9:36	8/4	0:36	41-51.63N	146-56.41E	CTD cast St.2-01 (1,000m)
	11:06		2:06	41-51.01N	143-56.75E	Start Piston Core St.2-02
	12:04		3:04	41-52.01N	143-56.95E	Piston Core at bottom St.2-02 (1,043m)
	13:02		4:02	41-51.18N	143-56.75E	CTD cast St.2-02 (1000m)
	14:30		5:30	41-52.13N	143-57.23E	Radiosonde RS-11
	14:40		5:30	41-52.02N	143-57.22E	Plankton Net St.2-01 (200m)
	15:02		6:02	41-51.88N	143-57.25E	Plankton Net St.2-02 (20m - 603m)
	18:38		9:38	41-51.57N	143-56.30E	Calibration for magnetometer
	19:00		12:00	-	-	Departure for Station 2
	20:30		11:30	41-47.80N	143-25.98E	Radiosonde RS-12
8/5	2:30	8/4	17:30	41-43.26N	141-35.78E	Radiosonde RS-13
	8:30		23:30	41-20.22N	140-07.79E	Radiosonde RS-14
	13:36	8/5	4:36	42-27.34N	139-38.04E	XCTD SB-02
	14:30		5:30	41-20.22N	140-07.79E	Radiosonde RS-15
	20:30		11:30	44-04.81N	139-32.58E	Radiosonde RS-16
8/6	2:55	8/5	17:55	45-36.27N	140-44.06E	Radiosonde RS-17
	3:03		18:03	45-36.85N	140-44.83E	XCTD SB-03

S.M.T.		U.T.C		Position		Event
Date	Time	Date	Time	Lat.	Long.	
	3:18		18:18	45-46N	140-50E	Arrival at Station 3
	3:18		18:18	-	-	Site Survey (5hour)
	8:30		23:30	45-45.40N	140-47.20E	Radiosonde RS-18
	9:03	8/6	0:03	45-45.49N	140-47.01E	Start Piston Core St.3-01
	9:56		0:56	45-45.46N	140-46.95E	Piston Core at bottom St.3-01 (774m)
	10:48		1:48	45-45.13N	140-47.08E	CTD cast St.3-01 (720m)
	13:05		4:05	45-45.47N	140-46.97E	Start Piston Core St.3-02
	13:59		4:59	45-45.46N	140-46.94E	Piston Core at bottom St.3-02 (772m)
	14:30		5:30	45-45.55N	140-47.07E	Radiosonde RS-19
	14:53		5:53	45-45.50N	140-47.15E	Plankton Net St.3-1 (200m, 100m, 60m, 25m)
	15:55		6:55	45-45.61N	140-48.53E	Plankton Net St.3-2 (200m, 75m, 60m ,25m)
	16:29		7:29	45-45.61N	140-49.28E	Plankton Net St.3-3 (20m - 700m)
	20:30		11:30	45-45.40N	140-52.97E	Radiosonde RS-20
	20:31		11:31	45-45.50N	140-52.93E	Calibration for magnetometer
8/7	2:30	8/6	17:30	45-36.00N	140-48.74E	Radiosonde RS-21
	6:55		21:30	45-45.56N	140-47.09E	Start Piston Core St.3-3
	7:47		22:47	45-45.46N	140-46.95E	Piston Core at bottom St.3-3 (772m)
	8:35		23:35	45-45.50N	140-47.02E	Radiosonde RS-22
	9:00	8/7	0:00	45-45.50N	140-47.02E	CTD cast St.3-02 (720m)
	10:10		1:10	45-45.55N	140-47.06E	Start Multiple Core St.3-01
	10:35		1:35	45-45.46N	140-46.97E	Multiple Core at bottom St.3-01 (774m)
	11:00		2:00	-	-	Departure for Station 3
	14:50		5:50	45-36.02N	142-01.49E	Radiosonde RS-23
	20:30		11:30	44-58.38N	143-53.24E	Radiosonde RS-24
	22:20		13:20	44-44.55N	144-25.32E	XCTD SB-04
	23:48		14:48	44-31N	145-00E	Arrival at Station 4
	23:48		14:48	-	-	Site survey (6hour)
8/8	2:30	8/7	17:30	44-28.91N	145-01.73E	Radiosonde RS-25
	6:55		21:55	44-31.65N	145-00.36E	Start Piston Core St.4-01
	7:58		22:58	44-31.64N	145-00.20E	Piston Corer at bottom St.4-01 (1,213m)
	8:30		23:30	44-31.58N	145-00.16E	Radiosonde RS-26
	8:54		23:54	44-31.76N	145-00.45E	CTD cast St.4-01 (1,200m)
	10:05	8/8	1:05	44-31.65N	145-04.96E	Start Piston Core St.4-02
	11:05		2:05	44-31.65N	145-00.16E	Piston Core at bottom St.4-02 (1,225m)

S.M.T.		U.T.C.		Position		Event
Date	Time	Date	Time	Lat.	Long.	
	12:03		3:03	44-31.76N	144-59.58E	CTD cast St.4-02 (1,200m)
	13:26		4:26	44-31.88N	144-59.25E	Plankton Net St.4-01 (200m, 100m, 50m, 25m)
	14:10		5:10	44-31.88N	144-59.14E	Plankton Net St.4-02 (20m - 1,000m)
	14:30		5:30	44-31.90N	144-59.18E	Radiosonde RS-27
	1836		9:36	44-32.79N	144-52.98E	Calibration for magnetometer
	18:55		9:55	-	-	Site survey (Expansion, 11hour)
	20:30		11:30	44-32.08N	144-58.78E	Radiosonde RS-28
8/9	2:30	8/8	17:30	44-28.68N	144-53.19E	Radiosonde RS-29
	6:54		21:54	44-31.57N	145-00.33E	Start Piston Core St.4-03
	7:54		22:54	44-31.69N	145-00.30E	Piston Corer at bottom St.4-03 (1,222m)
	8:30		23:30	44-31.76N	145-00.34E	Radiosonde RS-30
	8:54		23:54	44-31.78N	145-00.26E	Start Multiple Core St.4-01
	9:27	8/9	0:27	44-31.61N	145-00.25E	Multiple Core at bottom St.4-01 (1,218m)
	10:00		1:00	-	-	Departure for Station 4
	15:30		6:30	45-42N	145-12E	EEZ of Russian Federation In
8/10	13:38	8/10	4:38	50-45N	149-05E	EEZ of Russian Federation Out
	15:19		6:19	51-11.12N	149-09.18E	XCTD SB-05
	15:42		6:42	51-20N	149-12E	Arrival at Station 7
	15:42		6:42	-	-	Site survey (15hour)
	21:02		12:02	51-16.81N	149-05.98E	XCTD NC-08
8/11	3:00	8/10	18:00	51-25.97N	149-07.82E	XCTD NC-09
	6:55		21:55	51-16.75N	149-12.51E	Start Piston Core St.7-01
	7:52		22:52	51-16.55N	149-12.47E	Piston Core at bottom St.6-01 (1,256m)
	8:52		23:52	51-16.53N	149-12.43E	CTD cats St.7-01 (1,200m)
	10:16	8/11	1:16	51-16.75N	149-12.49E	Start Piston Core St.7-02
	11:20		2:20	51-16.56N	149-12.60E	Piston Core at bottom St.7-02(1,249m)
	12:21		3:21	51-16.65N	149-12.64E	Plankton Net St.7-01 (200m, 100m, 50m, 25m)
	13:04		4:04	51-16.75N	149-12.94E	Plankton Net St.7-02 (20m - 1,000m)
	15:30		6:30	51-17.50N	149-08.32E	XBT NT-01
	15:36		6:36	51-14.47N	149-09.72E	Calibration for magnetometer
	16:30		6:30	-	-	Site survey (Expansion, 12hour)
	21:00		12:00	51-29.58N	149-08.32E	XCTD NC-10

S.M.T.		U.T.C.		Position		Event
Date	Time	Date	Time	Lat.	Long.	
8/12	3:05	8/11	18:05	51-29.58N	149-08.32E	XCTD NC-11
	6:30		21:30	51-17.35N	149-12.22E	XCP CP-01
	6:44		21:44	51-17.37N	149-12.26E	XCTD NC-12
	6:53		21:53	51-16.88N	149-12.60E	Start Piston Core St.7-03
	7:52		19:52	51-16.54N	149-12.54E	Piston Core at bottom St.7-03 (1,256m)
	8:50		23:50	51-16.75N	149-12.57E	Start Multiple Core St.7-01
	9:23	8/12	0:23	51-16.65N	149-12.60E	Multiple Core at bottom St.7-01 (1,250m)
	9:54		0:54	-	-	Departure for Station 7
8/12	15:00	8/12	6:00	52-24.53N	150-04.96E	XCTD NC-13
	15:40		6:40	52-34.9N	150-13.6E	Site survey (Station 6 extra, 2hour)
	19:04		10:04	53-02.92N	150-07.34E	XCTD SB-06
8/12	19:30	8/12	3:30	53-20N	150-06E	Arrival at Station 6
	19:30		3:30	-	-	Site survey (11hour)
8/13	3:00	8/12	18:00	53-14.05N	149-57.50E	XCTD NC-14
	6:53		21:53	53-17.05N	150-04.81E	Start Piston Core St. 6-01
	7:48		22:48	53-16.86N	150-04.67E	Piston Core at bottom St.6-01(1,149m)
	8:42		23:42	53016.66N	150-04.67E	CTD cast St.6-01 (1,100m)
	10:16	8/13	1:16	53-16.99N	150-04.40E	Start Piston Core St.6-02
	11:14		2:14	53-16.88N	150-04.73E	Piston Core at bottom St.6-02 (1,143m)
	12:08		3:08	53-16.77N	150-04.49E	Plankton Net (calibration; 100m)
	12:35		3:35	53-16.80N	150-04.78E	Plankton Net St.6-01 (200m, 100m, 50m, 25m)
	13:19		4:19	53-16.89N	150-05.17E	Plankton Net St.6-02 (20m - 1,000m)
	14:38		5:38	53-17.11N	150-05.81E	XBT NT-02
	16:50		7:50	-	-	Site survey (Expansion, 12hour)
	21:12		12:12	53-213.84N	149-45.11E	XBT NT-03
8/14	3:00	8/13	3:05	53-16.93N	149-52.29E	XCTD NC-15
	6:53		21:52	53-17.22N	150-04.77E	Start Piston Core St.6-03
	7:59		22:59	53-16.87N	150-04.71E	Piston Corer at bottom St.6-03 (1,143m)
	8:52		23:52	53-17.13N	150-04.53E	Start Multiple Core St.6-01
	9:24	8/14	0:24	53-17.13N	150-04.70E	Multiple Core at bottom St.6-01 (1,144m)
	12:51		3:51	53-19.19N	149-44.26E	XCTD NC-16
	13:05		4:05	53-19.41N	149-44.26E	XCTD NC-17
	13:14		4:14	53-19.59N	149-44.26E	XCTD NC-18
	13:25		4:25	53-19.81N	149-44.26E	XCTD NC-19

S.M.T.		U.T.C.		Position		Event
Date	Time	Date	Time	Lat.	Long.	
	13:33		4:33	53-19.98N	149-44.26E	XCTD NC-20
	13:44		4:44	53-20.20N	149-44.26E	XCTD NC-21
	14:17		5:17	53-19.9N	149-44.3E	XCP CP-02
	14:24		5:24	-	-	Departure for Station 6
8/14	17:34	8/14	8:38	54-04.59N	149023.20E	XCTD SB-07
8/14	17:42	8/14	8:42	54-10N	149-17E	Arrival at Station 5
	17:42		8:42	-	-	Site survey (12hour)
8/15	2:56	8/14	17:56	54-16.04N	149-11.73E	XCTD NC-22
	6:52		21:52	54-19.20N	149-15.81E	Start Piston Core St.5-01
	7:47		22:47	54-18.95N	149-16.05E	Piston Core at bottom St.5-01 (831m)
	8:32		23:32	54-19.26N	149-15.96E	CTD cast St.5-01 (781m)
	9:46	8/15	0:46	54-19.70N	149-16.27E	Plankton Net St.5-01 (200m)
	10:03		1:03	54-10.75N	149-16.23E	Plankton Net St.5-02 (20m - 800m)
	12:35		3:35	54-19.54N	149-15.87E	Start Piston Core St. 5-02
	13:27		4:27	54-18.95N	149-16.06E	Piston Core at bottom St.5-02 (830m)
	14:17		5:17	54-19.12N	149-15.81E	Start Multiple Core St. 5-01
	14:46		5:46	54-18.96N	149-16.05E	Multiple Core at bottom St.5-01 (828m)
	15:12		6:12	54-18.87N	49-16.22E	Plankton Net St.5-03 (300m, 200m, 150m)
	16:10		7:10	54-10N	149-17E	Site survey (Expansion, 2hour)
	18:17		9:17	54-06.51N	149-13.38E	XCTD NC-23
	18:39		9:39	54-08.811N	149-13.40E	XCTD NC-24
	19:00		10:00	54-06.51N	149-13.38E	XCTD NC-25
	19:24		10:24	54-11.68N	149-13.31E	XCTD CP-3
	19:37		10:37	54-11.67N	149-13.44E	XCTD NC-26
	19:54		10:54	54-12.41N	149-12.92E	XCTD NC-27
	20:05		11:05	54-13.21N	149-11.59E	XCTD NC-28
	20:16		11:16	54-13.63N	149-11.63E	XCTD NC-29
	20:33		11:33	54-14.47N	149-11.59E	XCTD NC-30
	20:50		11:50	54-15.99N	149-11.60E	XCTD NC-31
	21:04		12:04	54-17.50N	149-11.61E	XCTD NC-32
	21:15		12:15	54-19.00N	149-11.59E	XCTD NC-33
	21:25		12:25	54-20.49N	149-11.57E	XCTD NC-34
	21:32		12:32	54-21.50N	149-11.58E	Calibration for magnetometer
	22:23		13:23	54-17.48N	149-13.40E	XCTD NC-35
	22:30		13:30	-	-	Departure for Station 5

S.M.T.		U.T.C.		Position		Event
Date	Time	Date	Time	Lat.	Long.	
8/16	3:00	8/15	18:00	54-10.93N	149-28.23E	XCTD NC-36
	8:52		23:57	52-07.98N	149-46.59E	XCTD NC-37
	12:15		3:15	51-38N	149-50E	EEZ of Russian Federation In
8/18	0:07	8/17	15:07	44-09N	154-47E	EEZ of Russian Federation Out
	0:24		15:24	44-07.00N	154-46.62E	Radiosonde RS-31
	2:30		17:30	43-39.57N	154-36.62E	Radiosonde RS-32
	3:40		18:40	43-20.56N	154-31.16E	Radiosonde RS-33
	5:27		2027	43-05.60N	154-15.29E	Radiosonde RS-34
	8:33		23:33	42-40.48N	153-33.50E	Radiosonde RS-35
	11:30	8/18	2:30	42-15.84N	152-51.42E	Radiosonde RS-36
	14:30		5:30	41-49.84N	152-05.78E	Radiosonde RS-37
	17:30		8:30	41-24.53N	151-24.59E	Radiosonde RS-38
	20:30		11:30	41-01.54N	150-54.63E	Radiosonde RS-39
	23:30		14:30	40-41.45N	150-18.31E	Radiosonde RS-40
8/19	2:30	8/18	14:30	40-21.21N	149-42.25E	Radiosonde RS-41
	5:31		17:31	40-18.13N	149-05.68E	Radiosonde RS-42
	8:32		20:32	40-35.78N	148-26.37E	Radiosonde RS-43
	11:30		23:30	40-53.13N	147-44.98E	Radiosonde RS-44
	14:30	8/19	2:30	41-10.72N	147-03.74E	Radiosonde RS-45
	17:36		5:36	41-28.30N	146-23.87E	Radiosonde RS-46
	20:37		8:37	41-44.53N	145-44.49E	Radiosonde RS-47
	23:31		11:31	41-57.76N	145-12.23E	Radiosonde RS-48
8/20	8:40	8/19	23:40	42-59N	144-22E	Arrival at Kushiro

(Leg2)

S.M.T.		U.T.C.		Position		Event
Date	Time	Date	Tme	Latitude	Longitude	
8/21	15:30	8/21	06:30	42-59N	144-22E	Departure for Kushiro
	22:00		12:00	-	-	Time adjustment (+1hr)
8/22	22:00	8/22	11:00	-	-	Time adjustment (+1hr)
8/23	18:02			44-16.55N	156-51.88E	Calibration for magnetometer
	22:00	8/23	10:00	-	-	Time adjustment (+1hr)
8/24	22:00	8/24	09:00	-	-	Time adjustment (+1hr)
8/25A	22:00	8/25	08:00	-	-	Time adjustment (+1hr)
						Crossed Date line
8/25B	22:00	8/26	05:00	-	-	Time adjustment (+1hr)
8/26	22:00	8/27	06:00	-	-	Time adjustment (+1hr)
8/27	13:16	8/27	21:16	54-07.71N	170-54.77W	Calibration for magnetometer
8/28	09:20	8/28	17:20	53-54N	161-31W	Arrival at Dutch Harbor Off
	09:30		17:30	-	-	Departure for Dutch Harbor Off
8/31	05:42	8/31	13:42	69-49.63N	168-49.36W	Mooring buoy check (M03-04)
	07:42		15:42	70-00N	168-00W	Arrival at Station 15
	08:00		16:00	-	-	CO_2 profile measurement start
	08:10		16:10	69-59.98N	167-59.96W	Start Multiple Core St.15-01
	08:16		16:16	67-59.90N	167-59.96W	Multiple Core at bottom St.15-01 (48m)
	08:34		16:34	70-00.02N	167-59.97W	CTD cast St.15-01 (35m)
	09:12		17:12	70-00.02N	168-00.00W	Start Multiple Core St.15-02
	09:17		17:17	70-00.19N	168-00.48W	Multiple Core at bottom St.15-02 (48m)
	10:00		18:00	70-00.00N	157-59.92W	CTD cast St.15-02 (35m)
	10:30		18:30	70-00.21N	167-59.83W	Plankton Net St.15-01 (20m, 40m)
	10:50		18:50	70-00.14	167-59.66W	Plankton Net St.15-02 (20m, 40m)
	10:56		18:56	-	-	CO_2 profile measurement finish
	11:18		19:18	-	-	Departure for Station 15
	14:18		22:18	70-37.79N	166-45.12W	Mooring buoy check (M04-04)
	16:24	9/1	00:24	71-00N	166-00W	Arrival at Station 14

S.M.T.		U.T.C.		Position		Event
Date	Time	Date	Time	Lat.	Long.	
	16:28		00:28	70-59.97N	165-59.88W	Start multiple Core St.14-01
	16:34		00:34	70-59.97N	166-59.85W	Multiple Core at bottom St.14-01 (44m)
	16:50		00:50	71-00.04N	165-59.80W	CTD cast St.14-01 (33m)
	21:24		05:24	70-57.64N	166-54.22W	Calibration for magnetometer
9/1	08:06	9/1	16:06	70-59.96N	165-59.88W	Start multiple Core St.14-02
	08:11		16:11	70-59.99N	165-59.94W	Multiple Core at bottom St.14-02 (43m)
	08:17		16:17	-	-	CO_2 profile measurement start
	08:27		16:27	71-00.01N	165-59.92W	Plankton Net St.14-01 (20m, 40m)
	08:44		16:44	71-00.02N	165-59.89W	Plankton Net St.14-02 (20m, 40m, 20m)
	09:02		17:02	71-00.05N	165-59.84W	Plankton Net St.14-03 (20m, 35m)
	09:32		17:32	71-00.02N	165-59.99W	Start gravity Core St.14-01
	09:58		17:58	71-00.01N	166-00.02W	Gravity Core at bottom St.14-01 (43m)
	10:27		18:27	-	-	CO_2 profile measurement finish
	10:30		18:30	-	-	Departure for Station 14
	14:30		22:30	72-00N	166-00W	Arrival at Station 13
	14:44		22:44	72-00.30N	166-00.05W	Start Multiple Core St.13-01
	14:49		22:49	72-00.04N	165-59.97W	Multiple Core at bottom St.13-01 (46m)
	15:06		23:06	72-00.03N	165-59.83W	Plankton Net St.13-01 (20m)
	15:11		23:11	72-00.04N	165-59.78W	Plankton Net St.13-02 (40m, 24m)
	15:25		23:25	72-00.78N	165-59.68W	Plankton Net St.13-03 (20m, 40m)
	15:52		23:52	-	-	CO_2 profile measurement start
	15:59		23:59	71-59.99N	165-59.97W	Gravity Corer sampling St.13-01 (46m)
	16:39	9/2	00:39	72-00.01N	165-59.89W	CTD cast St.13-01 (30m)
	17:05		01:05	-	-	CO_2 profile measurement finish
	17:12		01:12	-	-	Departure for Station 13
	19:55		03:55	72-31.40N	165-59.68W	Calibration for magnetometer
	20:12		04:12	72-36N	166-00W	Arrival at Station 12extra
9/2	08:07	9/2	16:07	72-35.99N	166-00.23W	Start Multiple Core St.12ex-01
	08:12		16:12	72-35.93N	166-00.23W	Multiple Core at bottom St.12ex-01 (53m)
	08:12		16:12	-	-	CO_2 profile measurement start
	08:23		16:23	72-36.00N	166-00.01W	CTD cast St.12ex-01 (40m)
	09:48		17:48	72-35.99N	166-00.29W	CTD cast St.12ex-02 (40m)
	10:19		18:19	72-36.02N	165-59.96W	Start Multiple Core St.12ex-02
	10:24		18:24	72-36.02N	165-59.96W	Multiple Core at bottom St.12ex-02 (53m)
	10:41		18:41	72-36.00N	165-59.88W	Start Gravity Core St.12ex-01
	10:53		18:53	72-36.00N	165-59.97W	Gravity Core at bottom St.12ex-01 (53m)
	12:31		20:31	72-36.18N	165-59.69W	Plankton Net St.12ex-01 (20m)

S.M.T.		U.T.C.		Position		Event
Date	Time	Date	Time	Lat.	Long.	
	12:36		20:36	72-36.13N	165-59.63W	Plankton Net St.12ex-02 (45m, 20m)
	12:44		20:44	72-36.16N	165-59.60W	Plankton Net St.12ex-03 (20m)
	12:51		20:51	72-36.17N	165-59.53W	Plankton Net St.12ex-04 (45m, 20m)
	12:57		20:57	72-36.23N	165-59.56W	Plankton Net St.12ex-05 (45m)
	13:00		21:00	-	-	CO_2 profile measurement finish
	13:12		21:12	-	-	Departure for Station 12extra
	15:42		23:42	72-00N	166-00W	Arrival at Station 13
	16:12	9/3	00:12	72-00.01N	165-59.97W	Start Multiple Core St.13-02
	16:16		00:16	72-00.01N	165-59.99W	Multiple Core at bottom St.13-02 (46m)
	16:24		00:24	72-00.03N	165-59.97W	CTD cast St.13-02 (30m)
	17:00		01:00	-	-	Departure for Station 13
9/3	07:30	9/3	15:30	72-26N	166-58W	Arrival at Station 12
	08:07		16:07	72-25.93N	166-57.83W	Start Multiple Core St.12-01
	08:09		16:09	72-25.93N	166-57.81W	Multiple Core at bottom St.12-01 (53m)
	08:14		16:14	-	-	CO_2 profile measurement start
	08:23		16:23	72-25.90N	166-57.70W	CTD cast St.12-01 (40m)
	09:11		17:11	-	-	CO_2 profile measurement finish
	10:00		18:00	72-25.88N	166-57.85W	CTD cast St.12-02 (40m)
	10:30		18:30	-	-	Departure for Station 12
9/4	06:50	9/4	14:50	71-05.01N	163-57.57W	Calibration for magnetometer
9/5	06:45	9/5	14:45	68-31.25N	167-56.16W	Calibration for magnetometer
	07:30		15:30	68-30N	168-00W	Arrival at Station 16
	08:06		16:06	68-30.02N	167-59.98W	Start Multiple Core St.16-01
	08:12		16:12	68-30.30N	167-59.95W	Multiple Core at bottom St.16-01 (54m)
	08:13		16:13	-	-	CO_2 profile measurement start
	08:22		16:22	68-30.02N	167-59.96W	CTD cast St.16-01
	08:56		16:56	68-29.98N	168-00.09W	Start Gravity Core St.16-01
	09:11		17:11	68-29.97N	167-59.99W	Gravity Core at bottom St.16-01 (54m)
	10:00		18:00	68-29.97N	168-00.11W	Plankton Net St.16-01 (20m, 40m)
	10:18		18:18	68-29.97N	168-00.08W	Plankton Net St.16-02 (40m)
	10:27		18:27	68-29.97N	168-00.11W	Plankton Net St.16-03 (40m)
	10:37		18:37	68-29.98N	168-00.09W	Plankton Net St.16-04 (40m)
	10:44		18:44	68-29.98N	167-59.95W	Start Multiple Core St.16-02
	10:50		18:50	68-29.99N	167-59.96W	Multiple Core at bottom St.16-02 (54m)
	11:48		19:48	-	-	CO_2 profile measurement finish
	12:00		20:00	-	-	Departure for Station 16

S.M.T.		U.T.C.		Position		Event
Date	Time	Date	Time	Lat.	Long.	
9/6	07:42	9/6	15:42	67-00N	167-00W	Arrival at Station 17
	08:05		16:05	66-59.94N	166-59.93W	Start Multiple Core St.17-01
	08:09		16:09	-	-	CO_2 profile measurement start
	08:10		16:10	66-59.99N	166-59.95W	Multiple Core at bottom St.17-01 (40m)
	08:16		16:16	66-59.95N	166-59.93W	CTD cast St.17-01 (30m)
	09:30		17:30	66-59.98N	167-00.31W	Plankton Net St.17-01 (30m)
	09:42		17:42	66-59.89N	166-59.25W	Plankton Net St.17-02 (30m)
	09:53		17:53	66-59.89N	166-59.26W	Plankton Net St.17-03 (30m)
	10:30		18:30	-	-	CO_2 profile measurement finish
	10:42		18:42	-	-	Departure for Station 17
9/7	10:18	9/7	18:18	64-00N	169-00W	Arrival at Station 18
	10:21		18:21	63-59.89N	168-59.97W	Start multiple Core St.18-01
	10:24		18:24	-	-	CO_2 profile measurement start
	10:25		18:25	63-59.88N	168-59.97W	Multiple Core at bottom St.18-01 (35m)
	10:31		18:31	63-59.88N	169-00.01W	Plankton Net St.18-01 (25m)
	10:38		18:38	63-59.86N	168-59.98W	Plankton Net St.18-02 (25m)
	10:44		18:44	63-59.86N	168-59.95W	Plankton Net St.18-03 (25m)
	10:55		18:55	63-59.88N	168-59.96W	CTD cast St.18-01 (26m)
	11:21		19:21	63-59.99N	169-00.18W	Start Multiple Core St.18-02
	11:24		19:24	63-59.99N	169-00.18W	Multiple Core at bottom St.18-02 (35m)
	11:25		19:25	-	-	CO_2 profile measurement finish
	11:30		19:30	-	-	Departure for Station 18
	16:30	9/8	00:30	63-00N	167-30W	Arrival at Station 19
	16:34		00:34	-	-	CO_2 profile measurement start
	16:34		00:34	63-00.01N	167-29.91W	Start Multiple Core St.19-01
	16:38		00:38	63-00.01N	167-29.94W	Multiple Core at bottom St.19-01 (33m)
	16:48		00:48	63-00.11N	167-29.26W	Plankton Net St.19-01 (25m)
	16:55		00:55	63-00.19N	167-29.85W	Plankton Net St.19-02 (25m)
	17:03		01:03	63-00.24N	167-29.70W	Plankton Net St.19-03 (25m)
	17:17		01:17	63-00.48N	167-29.57W	CTD cast St.19-01 (26m)
	18:12		02:12	63-00.01N	167-30.01W	Start Multiple Core St.19-02
	18:16		02:16	62-59.99N	167-30.01W	Multiple Core at bottom St.19-02 (33m)
	18:23		02:23	63-00.13N	167-29.87W	CTD cast St.19-02 (24m)
	18:47		02:47	-	-	CO_2 profile measurement finish
	18:55		02:55	63-00.68N	167-27.34W	Calibration for magnetometer
	19:24		03:24	-	-	Departure for Station 19
9/8	07:48	9/8	15:48	62-00N	169-00W	Arrival at Station 20

S.M.T.		U.T.C.		Position		Event
Date	Time	Date	Time	Lat.	Long.	
	08:07		16:07	62-00.02N	169-00.03W	Start Multiple Core St.20-01
	08:08		16:08	-	-	CO_2 profile measurement start
	08:11		16:11	62-00.01N	169-00.04W	Multiple Core at bottom St.20-01 (37m)
	08:20		16:20	62-00.07N	169-00.11W	CTD cast St.20-01 (28m)
	08:50		16:50	62-00.07N	169-00.44W	Plankton Net St.20-01 (25m)
	08:59		16:59	62-00.10N	169-00.51W	Plankton Net St.20-02 (25m)
	09:21		17:21	62-00.07N	168-59.91W	Start Multiple Core St.20-02
	09:26		17:26	62-00.07N	168-59.91W	Multiple Core at bottom St.20-02 (37m)
	09:32		17:32	62-00.10N	168-59.95W	CTD cast St.20-02 (28m)
	09:55		17:55	-	-	CO_2 profile measurement finish
	10:00		18:00	-	-	Departure for Station 20
	16:30	9/9	00:30	62-00N	172-00W	Arrival at Station 21
9/9	08:05	9/9	16:05	-	-	CO_2 profile measurement start
	08:06		16:06	62-00.02N	172-00.02W	Start Multiple Core St.21-01
	08:10		16:10	62-00.03N	172-00.03W	Multiple Core at bottom St.21-01 (55m)
	08:18		16:18	62-00.10N	172-00.20W	CTD cast St.21-01 (40m)
	08:52		16:52	62-00.26N	172-00.77W	Plankton Net St.21-01 (20m)
	09:02		17:02	62-00.27N	172-00.88W	Plankton Net St.21-02 (40m, 25m)
	09:04		17:04	-	-	CO_2 profile measurement finish
	09:12		17:12	-	-	Departure for Station 21
	17:00	9/10	01:00	62-00N	176-00W	Arrival at Station 22
	17:02		01:02	-	-	CO_2 profile measurement start
	17:03		01:03	62-00.30N	176-00.16W	Start Multiple Core St.22-01
	17:09		01:09	62-00.30N	176-00.16W	Multiple Core at bottom St.22-01 (96m)
	17:17		01:17	61-59.94N	176-00.12W	Plankton Net St.22-01 (20m, 50m, 24m, 96m, 58m)
	17:47		01:47	61-59.64N	176-00.12W	CTD cast St.22-01 (84m)
	18:19		02:19	-	-	CO_2 profile measurement finish
	18:24		02:24	-	-	Departure for Station 22
9/10	04:06	9/10	12:06	-	-	Arrival at Station 23
	04:07		12:07	-	-	Site survey (4 hours)
	09:04		17:04	60-09.51N	179-27.82W	Start Multiple Core St.23-01
	09:06		17:06	-	-	CO_2 profile measurement start
	09:36		17:36	60-09.51N	179-27.79W	Multiple Core at bottom St.23-01 (1,000m)
	10:10		18:10	60-09.50N	179-27.80W	Start Piston Core St.23-01
	11:04		19:04	60-09.53N	179-27.82W	Piston Core at bottom St.23-01 (1,001m)
	12:58		20:58	60-09.53N	179-27.87W	Start piston Core St.23-02

S.M.T.		U.T.C.		Position		Event
Date	Time	Date	Time	Lat.	Long.	
	13:48		21:48	60-09.53N	179-27.82W	Piston Core at bottom St.23-02 (1,011m)
	14:41		22:41	60-09.53N	179-27.78W	CTD cast St.23-01 (904m)
	15:47		23:47	60-09.53N	179-27.86W	Start Multiple Core St.23-02
	16:18	9/11	00:18	60-09.53N	179-27.85W	Multiple Core at bottom St.23-02 (1,000m)
	16:42		00:42	60-09.67N	179-28.16W	CTD cast St.23-02 (995m)
	17:59		01:59	60-09.71N	179-28.40W	Plankton Net St.23-01 (20m - 900m)
	20:59		04:59	60-09.52N	179-28.36W	Plankton Net St.23-02 (20m - 200m)
	21:29		05:29	60-09.49N	179-28.33W	Plankton Net St.23-03 (20m - 200m)
	21:48		05:48	-	-	CO_2 profile measurement finish
	22:06		06:06	-	-	Departure for Station 23
	22:12		06:12	-	-	Arrival at Station 24
	22:13		06:13	-	-	Site survey (7 hours)
9/11	08:06	9/11	16:06	-	-	CO_2 profile measurement start
	08:06		16:06	60-15.72N	179-25.35W	Start Multiple Core St.24-01
	08:33		16:33	60-15.72N	179-25.35W	Multiple Core at bottom St.24-01 (851m)
	09:03		17:03	60-15.70N	179-25.34W	Start Piston Core St.24-01
	09:47		17:47	60-15.70N	179-25.34W	Piston Core at bottom St.24-01 (851m)
	10:40		18:40	60-15.71N	179-25.33W	Start Piston Core St.24-02
	11:27		19:27	60-15.70N	179-25.35W	Piston Core at bottom St.24-02 (851m)
	13:09		21:09	60-15.71N	179-25.37W	Start multiple Core St.24-02
	13:34		21:34	60-15.70N	179-25.35W	Multiple Core at bottom St.24-02 (851m)
	13:56		21:56	60-15.68N	179-25.03W	CTD cast St.24-01 (836m)
	15:09		23:09	60-15.65N	179-24.57W	Plankton Net St.24-01 (20m - 700m)
	16:54	9/12	00:54	-	-	CO_2 profile measurement finish
	17:00		01:00	60-14.39N	179-29.63W	Calibration for magnetometer
	17:30		01:30	-	-	Site survey (13 hours)
9/12	07:30	9/12	15:30	-	-	Departure for Station 24
	08:48		16:48	-	-	Arrival at Station 25
	09:14		17:14	60-04.49N	179-27.77W	Start Piston Core St.25-01
	09:56		17:56	-	-	CO_2 profile measurement start
	10:09		18:09	60-04.48N	179-27.80W	Piston Core at bottom St.25-01 (1,160m)
	11:11		19:11	60-04.49N	179-27.77W	Start piston Core St.25-02
	12:02		20:02	60-04.50N	179-27.78W	Piston Core at bottom St.25-02 (1,156m)
	13:00		21:00	60-04.49N	179-27.82W	Start multiple Core St.25-01
	13:30		21:30	60-04.56N	179-27.79W	Multiple Core at bottom St.25-01 (1,156m)
	14:00		22:00	-	-	CO_2 profile measurement finish
	14:33		22:33	60-04.48N	179-27.79W	Start Multiple Core St.25-02

S.M.T.		U.T.C.		Position		Event
Date	Time	Date	Time	Lat.	Long.	
	15:02		23:02	60-04.50N	179-27.75W	Multiple Core at bottom St.25-02 (1,160m)
	15:36		23:36	-	-	Departure for Station 25
	16:30	9/13	00:30	-	-	Arrival at Station 24
	16:38		00:38	60-15.96N	179-24.48W	CTD cast St.24-02 (750m)
	17:42		01:42	-	-	Departure for Station 24
9/13	06:30	9/13	14:30	60-00N	176-00W	Arrival at Station 26
	06:35		14:35	-	-	Site survey (1 hour)
	08:06		16:06	-	-	CO_2 profile measurement start
	08:08		16:08	60-00.02N	175-59.99W	Start Multiple Core St.26-01
	08:16		16:16	59-59.78N	176-00.00W	Multiple Core at bottom St.26-01 (131m)
	08:25		16:25	60-00.05N	175-59.55W	CTD cast St.26-01 (114m)
	09:15		17:15	60-00.30N	175-59.39W	Plankton Net St.26-01 (40m, 100m)
	09:23		17:23	-	-	CO_2 profile measurement finish
	09:36		17:36	-	-	Departure for Station 26
	17:54	9/14	01:54	60-00N	172-00W	Arrival at Station 27
	18:02		02:02	59-59.99N	171-59.98W	Start Multiple Core St.27-01
	18:06		02:06	60-00.01N	172-00.00W	Multiple Core at bottom St.27-01 (68m)
	18:10		02:10	-	-	CO_2 profile measurement start
	18:17		02:17	59-59.94N	171-59.48W	Plankton Net St.27-01 (20m, 50m, 20m)
	18:35		02:35	59-59.83N	171-59.94W	CTD cast St.27-01 (52m)
	19:06		03:06	-	-	CO_2 profile measurement finish
	19:45		03:45	60-00.00N	171-59.97W	Start Multiple Core St.27-02
	19:50		03:50	60-00.01N	172-00.00W	Multiple Core at bottom St.27-02 (69m)
	20:00		04:00	-	-	Departure for Station 27
9/14	06:42	9/14	14:42	59-59.48N	169-02.78W	Calibration for magnetometer
	07:48		15:48	60-00N	169-00W	Arrival at Station 28
	08:06		16:06	60-00.00N	169-00.00W	Start Multiple Core St.28-01
	08:08		16:08	-	-	CO_2 profile measurement start
	08:09		16:09	60-00.00N	168-59.99W	Multiple Core at bottom St.28-01 (43m)
	08:28		16:28	60-00.02N	169-00.32W	CTD cast St.28-01 (31m)
	09:08		17:08	60-00.05N	169-00.40W	Plankton Net St.28-01 (30m)
	09:14		17:14	60-00.04N	169-00.51W	Plankton Net St.28-02 (30m)
	09:15		17:15	-	-	CO_2 profile measurement finish
	09:24		17:24	-	-	Departure for Station 28
	16:42	9/15	00:42	-	-	Arrival at Station 29
	16:46		00:46	58-29.97N	167-30.04W	Start Multiple Core St.29-01

S.M.T.		U.T.C.		Position		Event
Date	Time	Date	Time	Lat.	Long.	
	16:51		00:51	58-30.00N	167-30.04W	Multiple Core at bottom St.29-01 (51m)
	16:51		00:51	-	-	CO_2 profile measurement start
	16:57		00:57	58-30.00N	167-30.02W	Plankton Net St.29-01 (20m, 40m, 20m)
	17:18		01:18	58-29.95N	167-30.02W	CTD cast St.29-01 (38m)
	17:53		01:53	58-30.00N	167-30.03W	Start Multiple Core St.29-02
	17:57		01:57	58-29.99N	167-30.03W	Multiple Core at bottom St.29-02 (51m)
	18:27		02:27	58-29.94N	167-30.10W	CTD cast St.29-02 (37m)
	18:48		02:48	-	-	CO_2 profile measurement finish
	18:54		02:54	-	-	Departure for Station 29
9/15	05:00	9/15	13:00	-	-	Site survey (6 hours)
	11:12		19:12	58-30N	172-00W	Arrival as Station 30
9/16	10:05	9/16	18:05	58-29.99N	172-00.13W	Start Multiple Core St.30-01
	10:05		18:05	-	-	CO_2 profile measurement start
	10:14		18:14	58-30.01N	172-00.13W	Multiple Core at bottom St.30-01(100m)
	10:21		18:21	58-30.02N	172-00.13W	CTD cast St.30-01 (86m)
	11:02		19:02	58-30.01N	172-00.76W	Plankton Net St.30-01 (20m, 50m, 80m)
	11:32		19:32	58-29.98N	172-01.42W	Plankton Net St.30-02 (20m, 50m, 80m)
	11:43		19:43	-	-	CO_2 profile measurement finish
	12:00		20:00	-	-	Departure for Station 30
	16:24	9/17	00:24	58-23N	170-00W	Arrival at Station 31
	16:30		00:30	-	-	CO_2 profile measurement start
	16:31		00:31	58-22.95N	170-00.00W	Start Multiple Core St.31-01
	16:36		00:36	58-22.99N	170-00.40W	Multiple Core at bottom St.31-01 (74m)
	16:45		00:45	58-22.08N	169-59.99W	Plankton Net St.31-01 (20m, 60m, 20m)
	17:03		01:03	58-23.00N	169-59.94W	Plankton Net St.31-01 (30m, 60m)
	17:21		01:21	58-22.93N	169-59.82W	CTD cast St.31-01 (60m)
	17:54		01:54	-	-	CO_2 profile measurement finish
	18:00		02:00	-	-	Departure for Station 31
9/17	07:42	9/17	15:42	57-00N	167-30W	Arrival at Station 32
	08:06		16:06	56-59.99N	167-30.01W	Start Multiple Core St.32-01
	08:06		16:06	-	-	CO_2 profile measurement start
	08:12		16:12	57-00.01N	167-30.03W	Multiple Core at bottom St.32-01 (77m)
	08:20		16:20	56-59.99N	167-30.07W	CTD cast St.32-01 (64m)
	08:57		16:57	56-59.79W	167-30.63W	Plankton Net St.32-01 (20m, 60m)
	09:05		17:05	-	-	CO_2 profile measurement finish
	09:12		17:12	-	-	Departure for Station 32

S.M.T.		U.T.C.		Position		Event
Date	Time	Date	Time	Lat.	Long.	
	14:24		22:24	55-46N	166-14W	Arrival at Station 33
	14:24		22:24	-	-	Site survey (4 hours)
	18:09	9/18	02:09	55-46.36N	166-13.39W	CTD cast St.33-01 (115m)
	18:14		02:14	-	-	CO_2 profile measurement start
	18:46		02:46	55-46.42N	166-13.59W	Start Multiple Core St.33-01
	18:54		02:54	55-46.42N	166-13.59W	Multiple Core at bottom St.33-01 (132m)
	19:05		03:05	55-46.42N	166-13.56W	Start Gravity Core St.33-01
	19:20		03:20	55-46.41N	166-13.57W	Gravity Core at bottom St.33-01 (132m)
	19:35		03:35	55-46.42N	166-13.57W	Plankton Net St.33-01 (20m - 120m)
	20:11		04:11	55-46.49N	166-13.68W	Plankton Net St.33-02 (40m - 120m)
	20:40		04:40	55-46.51N	166-13.84W	Plankton Net St.33-03 (40m - 110m)
	21:05		05:05	-	-	CO_2 profile measurement finish
	21:18		05:18	-	-	Departure for Station 33
9/18	15:20	9/18	23:20	-	-	Site Survey (14 hours)
9/19	09:20	9/19	17:20	53-54N	161-31W	Arrival at Dutch Harbor Off
	09:35		17:35	-	-	Departure for Dutch Harbor Off
	22:00	9/20	07:00	-	-	Time adjustment (-1hr)
9/20	22:00	9/21	08:00	-	-	Time adjustment (-1hr)
9/21	22:00	9/22	09:00	-	-	Time adjustment (-1hr)
						Crossed Date line, SMT's 9/22 was skipped
9/23	13:37	9/23	00:37	48-30.85N	170-06.10E	Calibration for magnetometer
	22:00		10:00	-	-	Time adjustment (-1hr)
9/24	22:00	9/24	11:00	-	-	Time adjustment (-1hr)
9/25	22:00	9/25	12:00	-	-	Time adjustment (-1hr)
9/26	18:05	9/26	08:05	40-31.19N	149-16.65E	Calibration for magnetometer
	22:00	9/26	13:00	-	-	Time adjustment (-1hr)
9/28	08:50	9/27	23:50	40-34N	141-29E	Arrival at Hachinohe
	15:20	9/28	06:20	-	-	Departure for Hachinohe
9/29	09:00	9/29	00:00	41-22N	141-14E	Arrival at Sekinahama

5. List of Participants

(1) Chief Scientist

Naomi Harada*† Japan Agency for Marine-Earth Science and Technology (JAMSTEC)
Institute of Observational Research for Global Change (IORGC)
Paleoclimatology and Paleoceanography Group
2-15 Natsushima-cho, Yokosuka 237-0061, Japan

(2) Other participants

Katsunori Kimoto* JAMSTEC
IORGC
Paleoclimatology and Paleoceanography Group

Yusuke Okazaki* JAMSTEC
IORGC
Paleoclimatology and Paleoceanography Group

Kana Nagashima† JAMSTEC
IORGC
Paleoclimatology and Paleoceanography Group

Miyako Sato* JAMSTEC
IORGC
Paleoclimatology and Paleoceanography Group

Tatsuhiko Sakamoto* JAMSTEC
Institute for Research on Earth Evolution (IFREE),
Research Program for Paleoenvironment and Earth system evolution

Takashi Toyofuku† JAMSTEC
IFREE
Research Program for Paleoenvironment and Earth system evolution

Kouichi Iijima*† JAMSTEC
IFREE
Research Program for Paleoenvironment and Earth system evolution

Saiko Sugisaki*† JAMSTEC
IFREE
Research Program for Paleoenvironment and Earth system evolution

Atsushi Kurasawa* JAMSTEC
IFREE
Research Program for Paleoenvironment and Earth system evolution

Kyung Eun Lee* Division of Marine Environment & Bioscience
College of Ocean Science and Technology
Korea Maritime University
Busan 606-791, South Korea

Sergey A. Gorbarenko* V.l.ll'ichev Pacific Oceanological Institute, Far Eastern
Branch, Russian Academy of Sciences
43 Baltiyskaya Str., Vladivostok 690041, Russia

Alexandr N. Derkachev* V.l.ll'ichev Pacific Oceanological Institute, Far Eastern
Branch, Russian Academy of Sciences
43 Baltiyskaya Str., Vladivostok 690041, Russia

Yriyi P. Vasilenko* V.l.ll'ichev Pacific Oceanological Institute, Far Eastern
Branch, Russian Academy of Sciences
43 Baltiyskaya Str., Vladivostok 690041, Russia

Alexandr A. Bosin* V.l.ll'ichev Pacific Oceanological Institute, Far Eastern
Branch, Russian Academy of Sciences
43 Baltiyskaya Str., Vladivostok 690041, Russia

Tomohiro Nakamura* Institute of Low Temperature Science, Hokkaido University
Kita 19 Nishi 8, Kita-ku, Sapporo 060-0819, Japan

Ryoko Oohira* Graduate School of Science and Engineering, Yamagata University
1-4-12 Koshirakawa-cho, Yamagata 990-8560, Japan

Susumu Konno† Graduate School of Science and Engineering, Yamagata University
1-4-12, Koshirakawa-cho, Yamagata 990-8560, Japan

Frank Griessbaum*† Ocean Research Institute, University of Tokyo
1-15-1 Minamidai Nakano-ku, Tokyo 164-8639, Japan

Takuya Itaki*† Department of Earth and Planetary Science, University of Tokyo
7-3-1 Hongo Bunkyo-ku, Tokyo 113-0033, Japan

Fumiko Nakagawa* Faculty of Science, Hokkaido University
Kita 10 Nishi 8 Kita-ku, Sapporo, 060-0810, Japan

Akinari Hirota*† Faculty of Science, Hokkaido University
Kita 10 Nishi 8 Kita-ku, Sapporo, 060-0810, Japan

Toyoho Ishimura* Faculty of Science, Hokkaido University
Kita 10 Nishi 8 Kita-ku, Sapporo, 060-0810, Japan

Akira Ijiri*† Faculty of Science, Hokkaido University
Kita 10 Nishi 8 Kita-ku, Sapporo, 060-0810, Japan

Daisuke Komatsu† Faculty of Science, Hokkaido University
Kita 10 Nishi 8 Kita-ku, Sapporo, 060-0810, Japan

Yasutomo Ookubo† Faculty of Science, Hokkaido University
Kita 10 Nishi 8 Kita-ku, Sapporo, 060-0810, Japan

Hisashi Narita† Graduate School of Marine Science and Technology, Tokai University
3-20-1 Orito, Shimizu-ku, Shizuoka 424-8610, Japan

Yoko Kishi*† Graduate School of Marine Science and Technology, Tokai University
3-20-1 Orito Shimizu-ku, Shizuoka 424-8610, Japan

Masayo Okabe* Tokai University
1117 Kitakinme, Hiratsuka 259-1292, Japan

Harumi Murayama* Faculty of Science, Toyama Uniersity
3190 Gofuku, Toyama 930-8555, Japan

Ajit Kumar Manda† Graduate School of Science, Toyama University
3190 Gofuku, Toyama 930-8555, Japan

Stephan Rella† Department of Earth and Planetary Science, University of Tokyo
7-3-1 Hongo Bunkyo-ku Tokyo113-0033, Japan

Toru Iwata† Graduate School of Environmental Science, Okayama University
3-1-1 Tsushimanaka Okayama 700-8530, Japan

Ippei Nagao† Graduate School of Environmental Science, Nagoya University
Furo-cho, Chikusa-ku, Nagoya 464-8601, Japan

Fumi Takeuchi† Graduate School of Environmental Science, Nagoya University
1 Furo-cho, Chikusa-ku, Nagoya 464-8602, Japan

Motoo Utsumi† Graduate School of Life and Environmental Sciences, Tsukuba University
1-1-1 Tennodai, Tsukuba, 305-8572

Kota Katsuki† Research Center for Coastal Lagoon Environments, Shimane University
1060 Nishikawa-cho, Matsue 690-0852, Japan

Hidemine Kumata† Graduate School of Life Science, Tokyo University of Pharmacy and Life Science
1432-1 Horinouchi, Hachioji 192-0392, Japan

Yasuyo Koike† Graduate School of Life Science, Tokyo University of Pharmacy and Life Science
1432-1 Horinouchi, Hachioji 192-0392, Japan

Satoshi Okumura* Global Ocean Development Inc. (GODI)
Mitsuiseimei-kamiooka building 1-13-8 Kamiooka-nishi,
Kounann-ku, Yokohama 233-0002, Japan

Shinya Okumura† GODI

Soichiro Sueyoshi* GODI

Wataru Tokunaga† GODI

Kazuho Yoshida*† GODI

Ryo Ooyama† GODI

Kazuya Yamashita* GODI

Yutaka Matsuura*† Marine Works Japan Ltd. (MWJ)
1-1-7 2F Mutsuura, Kanazawa-ku, Yokohama 236-0031, Japan

Yusuke Sato*† MWJ

Tamami Ueno*† MWJ

Yuko Sagawa* MWJ

Hiroyuki Hayashi* MWJ

Takami Mori*† MWJ

Ei Hatakeyama* MWJ

Kazuhiro Yoshida† MWJ

Yohei Taketomo† MWJ

Yasushi Hashimoto† MWJ

Hideki Yamamoto* MWJ

Hiroshi Matsunaga* MWJ

Mikio Kitada*† MWJ

Keisuke Wataki* MWJ

Masaki Moro* MWJ

Ayumi Takeuchi* MWJ

Junji Matsushita* MWJ

Tatsuya Tanaka*	MWJ
Fuyuki Shibata†	MWJ
Naoko Takahashi†	MWJ
Tomoyuki Takamori†	MWJ
Kenichiro Sato†	MWJ
Takayoshi Seike†	MWJ
Kimiko Nishijima†	MWJ
Ayaka Hatsuyama†	MWJ
Paul Cordeiro	P.O. BOX846
(Ice Pilot)	Kensington, PE, C0B 1M0, Canada

Regend

* Leg.1 (Sekinehama-Kushiro)

† Leg.2 (Kushiro-Sekinehama)

*† Leg.1, 2 (Sekinehama-Sekinehama)

Intentionally left blamk

Intentionally left blamk

Intentionally left blamk

6. Observations

6.1 Weather and Sea condition

Leg.1: 1-20 August, 2006 (Sekinehama-Kushiro)

The leg.1 cruise of MR06-04 started on 1 August, 2006 from Sekinehama. The research area of leg.1 was the off Tokachi, the Japan/East Sea and the Okhotsk Sea. The first research area (Sts.1 and 2) was off Tokachi. The weather condition was calm, weak wind speed (4-5 m/s) and cool air temperature (19-20˚C) for summer season due to active "Yamase". The next research area (St.3) was the northern part of Japan/East Sea and wind speed (10 m/s) and air temperature (25˚C) were higher than those at off Tokachi. The last research area of the leg.1 was Okhotsk Sea. Because of weak wind speed and active Okhotsk high, the condition of foggy and low air temperature (14-16˚C) for summer continued during the observation period in the Okhotsk Sea. The weather and sea condition was suitable for sediment coring, CTD/water sampling and plankton net sampling during the whole leg.1.

Leg.2: 21 August – 29 September, 2006 (Kushiro-Sekinehama)

The leg.2 was 21 August-29 September, 2006 and the first priority research area of leg.2 was the Chukchi and Beaufort Seas and Mackenzy delta. The R/V MIRAI departed for the Chukchi Sea through the Bering Sea. During the 25-26 August, when the R/V MIRAI was navigating around the continental shelf in the eastern Bering Sea (55-58˚S, 165-170˚W), the enormous coccolithophorid (*Emiliania huxleyi*) bloom was found (Fig.6.1.1). Such occurrence of large *E. huxleyi* bloom was since 2000, and this bloom area was close to where a *E. huxleyi* bloom was found during the MR00-K06 cruise on September and October, 2000.

On the 30 August, R/V MIRAI passed through the Bering Strait and entered in the Chukchi Sea and the air temperature were 4-5˚C, warm for the Arctic Ocean. On the 2nd September, R/V MIRAI observed sea ice free area in the Chukchi Sea where most northern site (72-36˚N, 166˚W) as navigating as possible MIRAI can. In order to go to the Beaufort Sea, although R/V MIRAI tried to go to close the Alaskan coast, the presence of heavy and thick multi-year sea ice prohibited the navigation of R/V MIRAI toward the east (Fig.6.1.2). Consequently, we made the final decision that R/V MIRAI does not observe in the Beaufort Sea.

The second priority area for observation was the continental shelf in the eastern Bering Sea. Although the weather and sea condition in the Bering Sea was changeable with high frequency, suitable condition for observation such as air temperature ranged 8-13 ˚C and relatively weak wind velocity, 4-12m/s continued during the leg. 2 cruise period. Almost all planed observation, piston coring at three sites, multiple coring at 36 sites, gravity coring at 5 sites, CTD/water sampling and plankton sampling at 27 sites were done.

Fig. 6.1.1 *E. huxleyi* bloom (turquoise blue green color) observed in the Bering Sea.

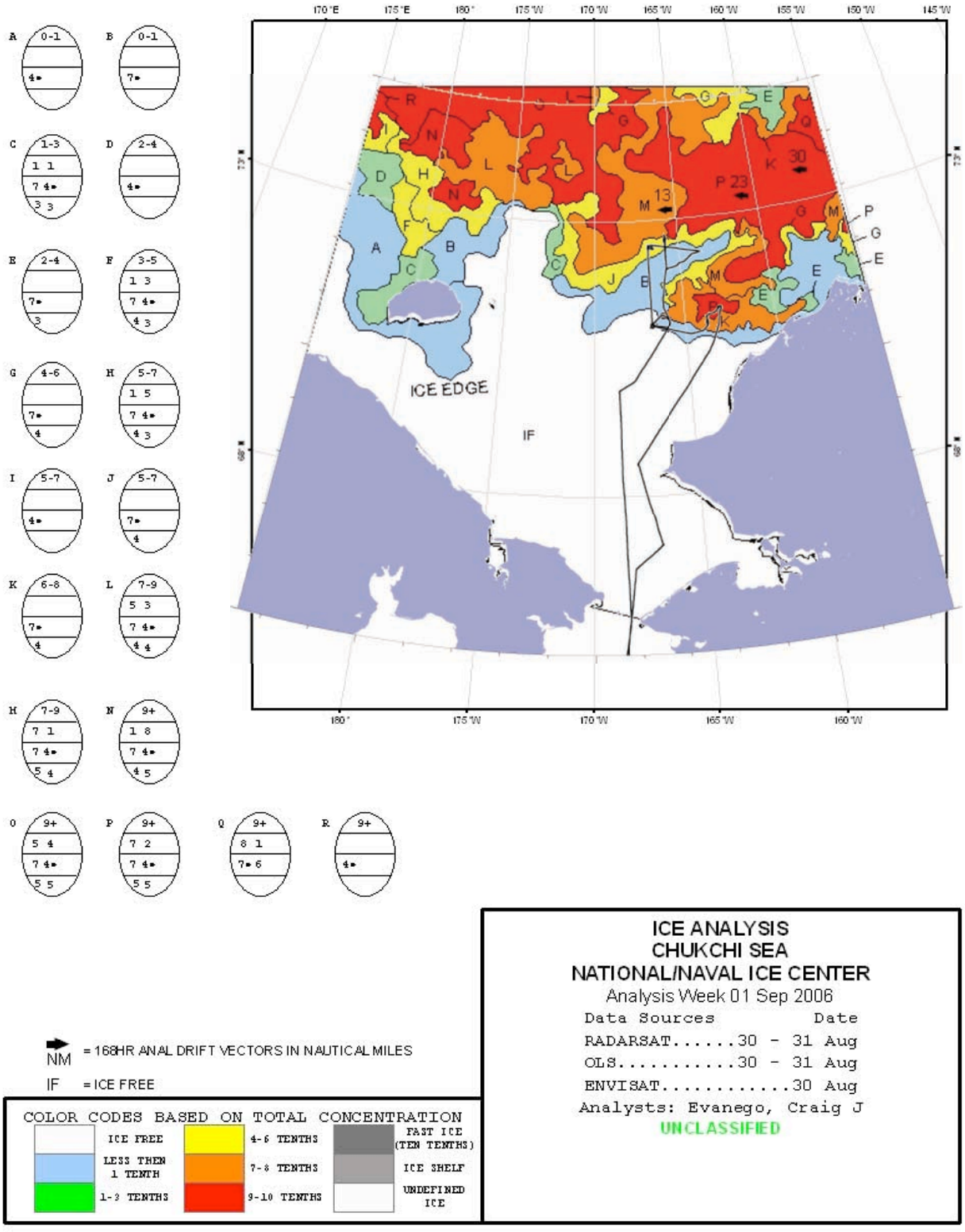

Fig.6.1.2 The R/V MIRAI's navigation route during the MR06-04 in the Arctic Sea (solid line).

6.2. Meteorological observations

6.2.1 Surface Meteorological Observation

(1) Personnel

Satoshi Okumura	(Global Ocean Development Inc., GODI)	-leg1-
Souichoro Sueyoshi	(GODI)	-leg1-
Kazuya Yamashita	(GODI)	-leg1-
Shinya Okumura	(GODI)	-leg2-
Wataru Tokunaga	(GODI)	-leg2-
Ryo Ohyama	(GODI)	-leg2-
Kazuho Yoshida	(GODI)	-leg1, 2-
Kunio Yoneyama	(JAMSTEC) : Principal Investigator (Not on-board)	

(2) Objectives

The surface meteorological parameters are observed as a basic dataset of the meteorology. These parameters bring us the information about the temporal variation of the meteorological condition surrounding the ship.

(3) Methods

The surface meteorological parameters were observed throughout the MR06-04 cruise from the departure of Sekinehama on 31 July 2006 to arrival of Sekinehama on 29 September 2006, and called at port Kushiro on 20 - 21 August, except for the EEZ of Russia.

. At this cruise, we used two systems for the surface meteorological observation.

1) MIRAI Surface Meteorological observation (SMet) system
2) Shipboard Oceanographic and Atmospheric Radiation (SOAR) system

1) MIRAI Surface Meteorological observation (SMet) system

Instruments of SMet system are listed in Table 6.2.1-1 and measured parameters are listed in Table 6.2.1-2. Data was collected and processed by KOAC-7800 weather data processor made by Koshin-Denki, Japan. The data set has 6-second averaged.

2) Shipboard Oceanographic and Atmospheric Radiation (SOAR) system

SOAR system designed by BNL (Brookhaven National Laboratory, USA) consists of major three parts.

i) Portable Radiation Package (PRP) designed by BNL – short and long wave downward radiation.
ii) Zeno Meteorological (Zeno/Met) system designed by BNL – wind, air temperature, relative humidity, pressure, and rainfall measurement.
iii) Scientific Computer System (SCS) designed by NOAA (National Oceanic and Atmospheric Administration, USA) – centralized data acquisition and logging of all data sets.

SCS recorded PRP data every 6 seconds, Zeno/Met data every 10 seconds. Instruments and their locations are listed in Table6.2.1-3 and measured parameters are listed in Table 6.2.1-4.

We have carried out inspecting and comparing about following three kinds of sensors, before and after the cruise.

a) Young Rain gauge (SMet and SOAR)
Inspecting the linearity of output value from the rain gauge sensor to change input value by adding fixed quantity of test water.
b) Barometer (SMet and SOAR)
Comparing with the portable barometer value, PTB220CASE, VAISALA.

c) Thermometer (air temperature and relative humidity) (SMet and SOAR)
Comparing with the portable thermometer value, HMP41/45, VAISALA.

(4) Preliminary results

Figures 6.2.1-1 shows the time series of the following parameters;
Wind (SOAR)
Air temperature (SOAR)
Relative humidity (SOAR)
Precipitation (SOAR, ORG)
Short/long wave radiation (SOAR)
Pressure (SOAR)
Sea surface temperature (EPCS)
Significant wave height (SMet)

(5) Data archives

The raw data obtained during this cruise will be submitted to JAMSTEC. Corrected data sets will also be available from K. Yoneyama of JAMSTEC.

(6) Remarks

1. SOAR Anemometer, SOAR capacitive rain gauge and SOAR Optical rain gauge were installed on 50 - 70cm higher locations than original in 28 July. And SOAR capacitive rain gauge was installed on 61cm upper from the original location at 00:20, 2 August. We showed their altitudes in Table 6.2.1-3 after 2 August.

2. Following period, Sea Surface Temperature data was valid because surface water pump worked.
   06:50 UTC, 1 August - 00:40, 9 August
   04:43 UTC, 10 August - 02:00, 16 August
   15:13 UTC, 17 August - 07:30, 19 August
   07:26 UTC, 21 August - 16:58, 28 August
   18:30 UTC, 28 August - 15:57, 19 September
   18:36 UTC, 19 September - 22:56, 27 September

3. We used No.1 gyrocompass from 09:54:51UTC to 12:07:01, 5 September 2006 (The default gyrocompass of this cruise was No.2 gyrocompass).

4. Data acquisition stopped in the EEZ of Russian Federation.
   (SMet)
   01:00 UTC, 9 August - 04:37, 10 August
   02:00 UTC, 16 August - 15:19, 17 August
   (SOAR)
   00:49 UTC, 9 August - 04:39, 10 August
   02:00 UTC, 16 August - 15:23, 17 August

Table 6.2.1-1 Instruments and installations of MIRAI Surface Meteorological system

Sensors	Type	Manufacturer	Location (altitude from surface)
Anemometer	KE-500	Koshin Denki, Japan	foremast (24 m)
Tair / RH	HMP45A	Vaisala, Finland	
with 43408 Gill aspirated radiation shield		R.M. Young, USA	compass deck (21 m)
			starboard side and port side
Thermometer: SST	RFN1-0	Koshin Denki, Japan	4th deck (-1m, inlet -5m)
Barometer	AP-370	Koshin Denki, Japan	captain deck (13 m)
			weather observation room
Capacitive rain gauge	50202	R. M. Young, USA	compass deck (19 m)
Optical rain gauge	ORG-815DR	Osi, USA	compass deck (19 m)
Radiometer (short wave)	MS-801	Eiko Seiki, Japan	radar mast (28 m)
Radiometer (long wave)	MS-202	Eiko Seiki, Japan	radar mast (28 m)
Wave height meter	MW-2	Tsurumi-seiki, Japan	bow (10 m)

Table 6.2.1-2 Parameters of MIRAI Surface Meteorological observation system

	Parameter	Units	Remarks
1	Latitude	degree	
2	Longitude	degree	
3	Ship's speed	knot	Mirai log, DS-30 Furuno
4	Ship's heading	degree	Mirai gyro, TG-6000, Tokimec
5	Relative wind speed	m/s	6sec./10min. averaged
6	Relative wind direction	degree	6sec./10min. averaged
7	True wind speed	m/s	6sec./10min. averaged
8	True wind direction	degree	6sec./10min. averaged
9	Barometric pressure	hPa	adjusted to sea surface level
			6sec. averaged
10	Air temperature (starboard side)	degC	6sec. averaged
11	Air temperature (port side)	degC	6sec. averaged
12	Dewpoint temperature (starboard side)	degC	6sec. averaged
13	Dewpoint temperature (port side)	degC	6sec. averaged
14	Relative humidity (starboard side)	%	6sec. averaged
15	Relative humidity (port side)	%	6sec. averaged
16	Sea surface temperature	degC	6sec. averaged
17	Rain rate (optical rain gauge)	mm/hr	hourly accumulation
18	Rain rate (capacitive rain gauge)	mm/hr	hourly accumulation
19	Down welling shortwave radiation	W/m^2	6sec. averaged
20	Down welling infra-red radiation	W/m^2	6sec. averaged
21	Significant wave height (bow)	m	hourly
22	Significant wave height (aft)	m	hourly
23	Significant wave period (bow)	second	hourly
24	Significant wave period (aft)	second	hourly

Table 6.2.1-3 Instruments and installation locations of SOAR system

Sensors (*Zeno/Met*)	Type	Manufacturer	Location (altitude from surface)
Anemometer	05106	R.M. Young, USA	foremast (25 m)
Tair/RH	HMP45A	Vaisala, Finland	
with 43408 Gill aspirated radiation shield		R.M. Young, USA	foremast (23 m)
Barometer	61201	R.M. Young, USA	
with 61002 Gill pressure port		R.M. Young, USA	foremast (22 m)
Capacitive rain gauge	50202	R. M. Young, USA	foremast (24 m)
Optical rain gauge	ORG-815DA	Osi, USA	foremast (24 m)

Sensors (*PRP*)	Type	Manufacturer	Location (altitude from surface)
Radiometer (short wave)	PSP	Epply Labs, USA	foremast (24 m)
Radiometer (long wave)	PIR	Epply Labs, USA	foremast (24 m)
Fast rotating shadowband radiometer (FRSR)		Yankee, USA	foremast (24 m)

Table 6.2.1-4 Parameters of SOAR system

	Parameter	Units	Remarks
1	Latitude	degree	
2	Longitude	degree	
3	SOG	knot	
4	COG	degree	
5	Relative wind speed	m/s	
6	Relative wind direction	degree	
7	Barometric pressure	hPa	
8	Air temperature	degC	
9	Relative humidity	%	
10	Rain rate (optical rain gauge)	mm/hr	
11	Precipitation (capacitive rain gauge)	mm	reset at 50 mm
12	Down welling shortwave radiation	W/m^2	
13	Down welling infra-red radiation	W/m^2	
14	Defuse irradiance	W/m^2	

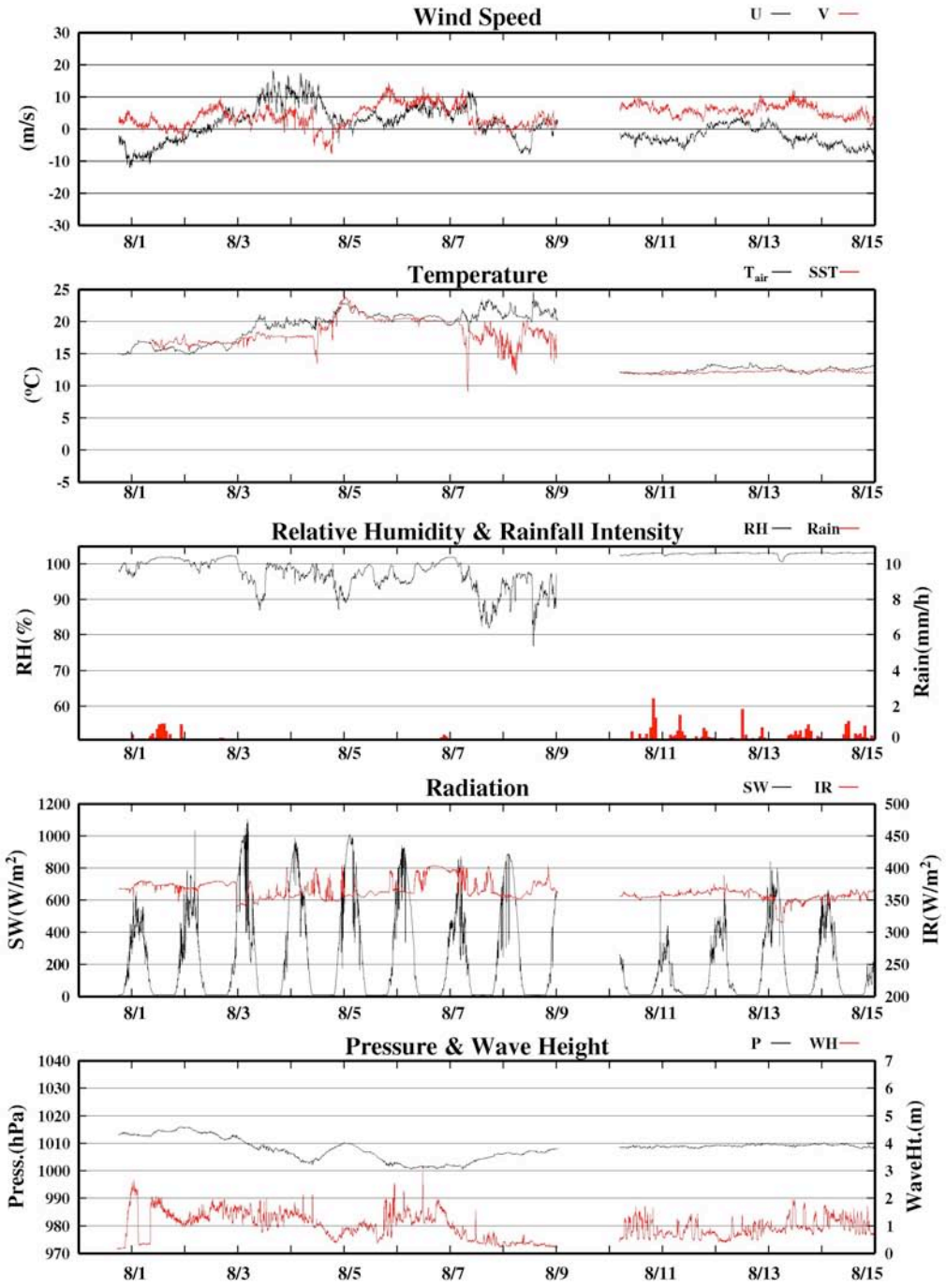

Fig.6.2.1 Time series of surface meteorological parameters during the cruise

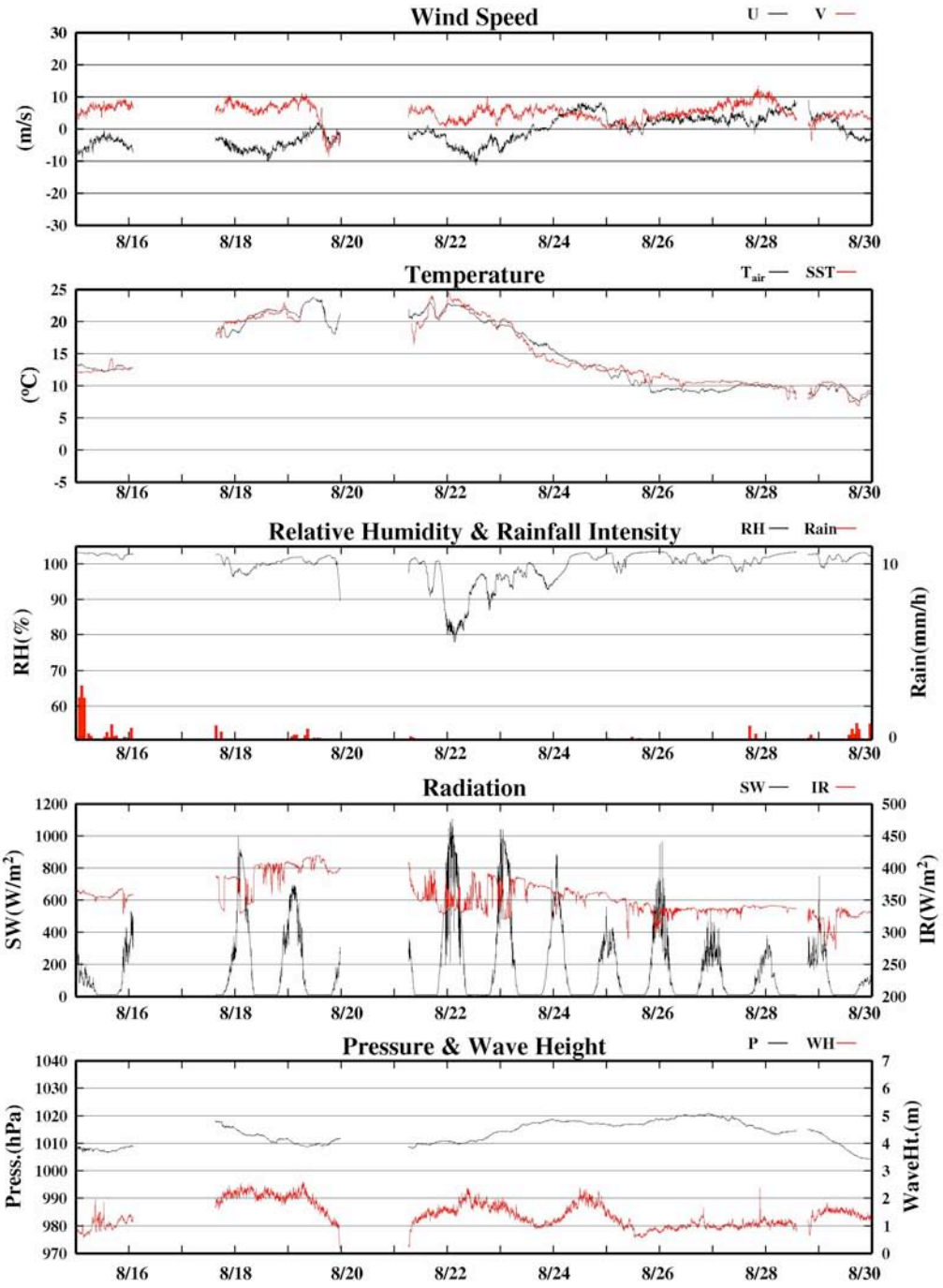

Fig.6.2.1 Continue

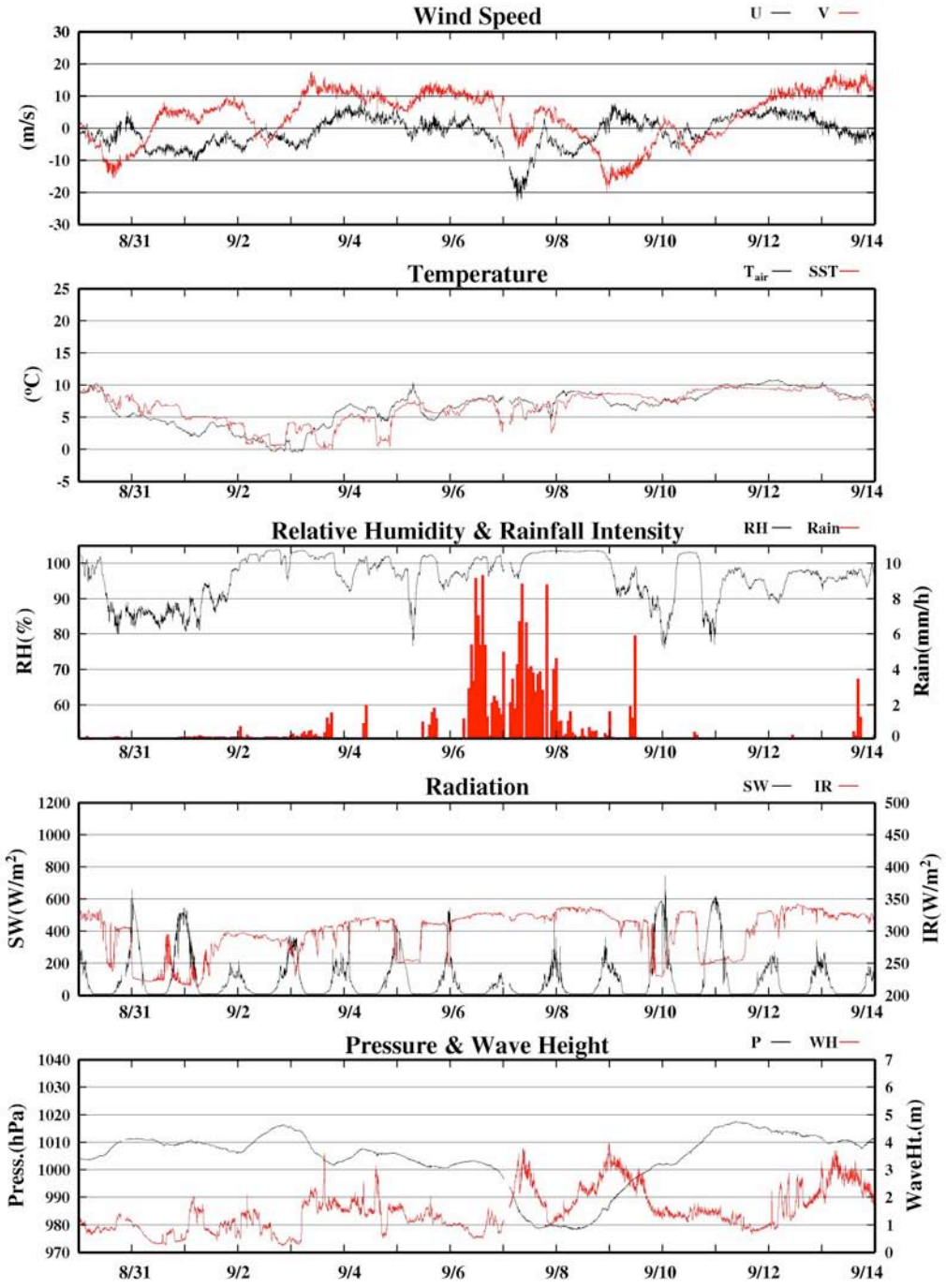

Fig.6.2.1 Continue

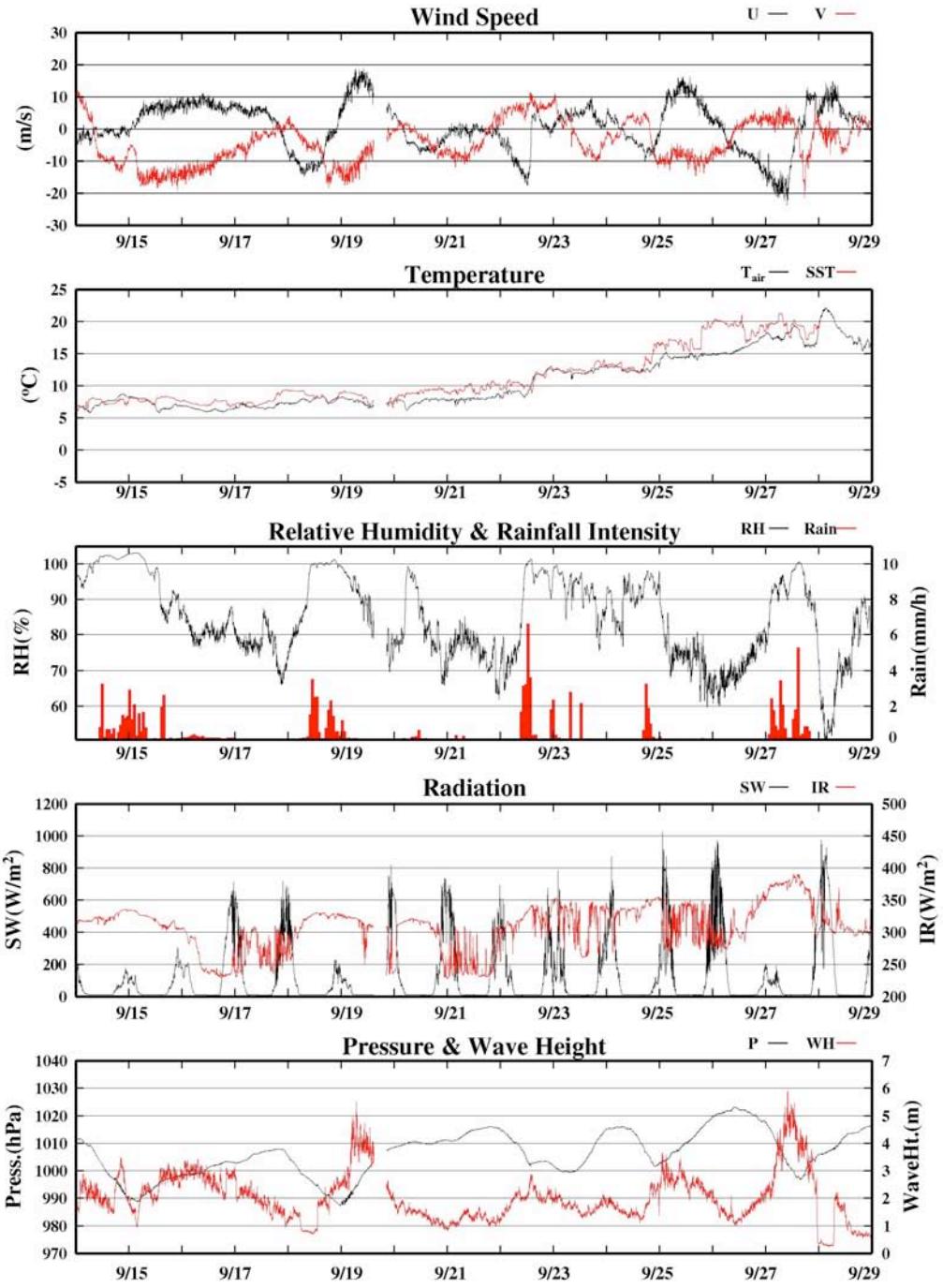

Fig.6.2.1 Continue

6.2.2 Ceilometer Observation

(1) Personnel

Satoshi Okumura	(Global Ocean Development Inc., GODI)	-leg1-
Souichoro Sueyoshi	(GODI)	-leg1-
Kazuya Yamashita	(GODI)	-leg1-
Shinya Okumura	(GODI)	-leg2-
Wataru Tokunaga	(GODI)	-leg2-
Ryo Ohyama	(GODI)	-leg2-
Kazuho Yoshida	(GODI)	-leg1,2-
Kunio Yoneyama	(JAMSTEC) : Principal Investigator (Not on-board)	

(2) Objectives

The information of cloud base height and the liquid water amount around cloud base is important to understand the process on formation of the cloud. As one of the methods to measure them, the ceilometer observation was carried out.

(3) Parameters

1. Cloud base height [m].
2. Backscatter profile, sensitivity and range normalized at 30 m resolution.
3. Estimated cloud amount [oktas] and height [m] ; Sky Condition Algorithm.

(4) Methods

We measured cloud base height and backscatter profile using ceilometer (CT-25K, VAISALA, Finland) throughout the MR06-04 cruise, from 1 August 2006 (departure of Sekinehama) to 29 September 2006 (arrival of Sekinehama), except for the EEZ of Russia and territorial waters of U.S.A.

Major parameters for the measurement configuration are as follows;

Laser source:	Indium Gallium Arsenide (InGaAs) Diode
Transmitting wavelength:	905±5 mm at 25 degC
Transmitting average power:	8.9 mW
Repetition rate:	5.57 kHz
Detector:	Silicon avalanche photodiode (APD) Responsibility at 905 nm: 65 A/W
Measurement range:	0 ~ 7.5 km
Resolution:	50 ft in full range
Sampling rate:	60 sec
Sky Condition	0, 1, 3, 5, 7, 8 oktas (9: Vertical Visibility) (0: Sky Clear, 1: Few, 3: Scattered, 5-7: Broken, 8: Overcast)

On the archive dataset, cloud base height and backscatter profile are recorded with the resolution of 30 m (100 ft).

(5) Preliminary results

The figure 6.2.2-1 shows the time series of the first, second and third lowest cloud base height.

(6) Data archives

The raw data obtained during this cruise will be submitted to JAMSTEC.

(7) Remarks

1. Data acquisition stopped in the EEZ of Russian Federation and the territorial waters of U.S.A.
   00:53, 9 August - 04:38, 10 August (Russia EEZ)
   02:08, 16 August - 15:25, 18 August (Russia EEZ)
   14:00 - 19:10, 28 August (USA, territorial waters)
   19:00 - 21:15, 30 August (USA, territorial waters)
   00:20 - 02:45, 7 September (USA, territorial waters)
   14:50 - 20:30, 19 September (USA, territorial waters)

2. Window cleaning (UTC): 06:51, 3 August
   06:14, 5 August
   02:35, 18 August
   05:11, 21 August
   08:00, 22 August
   06:55, 24 August
   05:28, 26 August
   01:53, 31 August
   00:43, 5 September
   22:21, 15 September
   19:25, 20 September

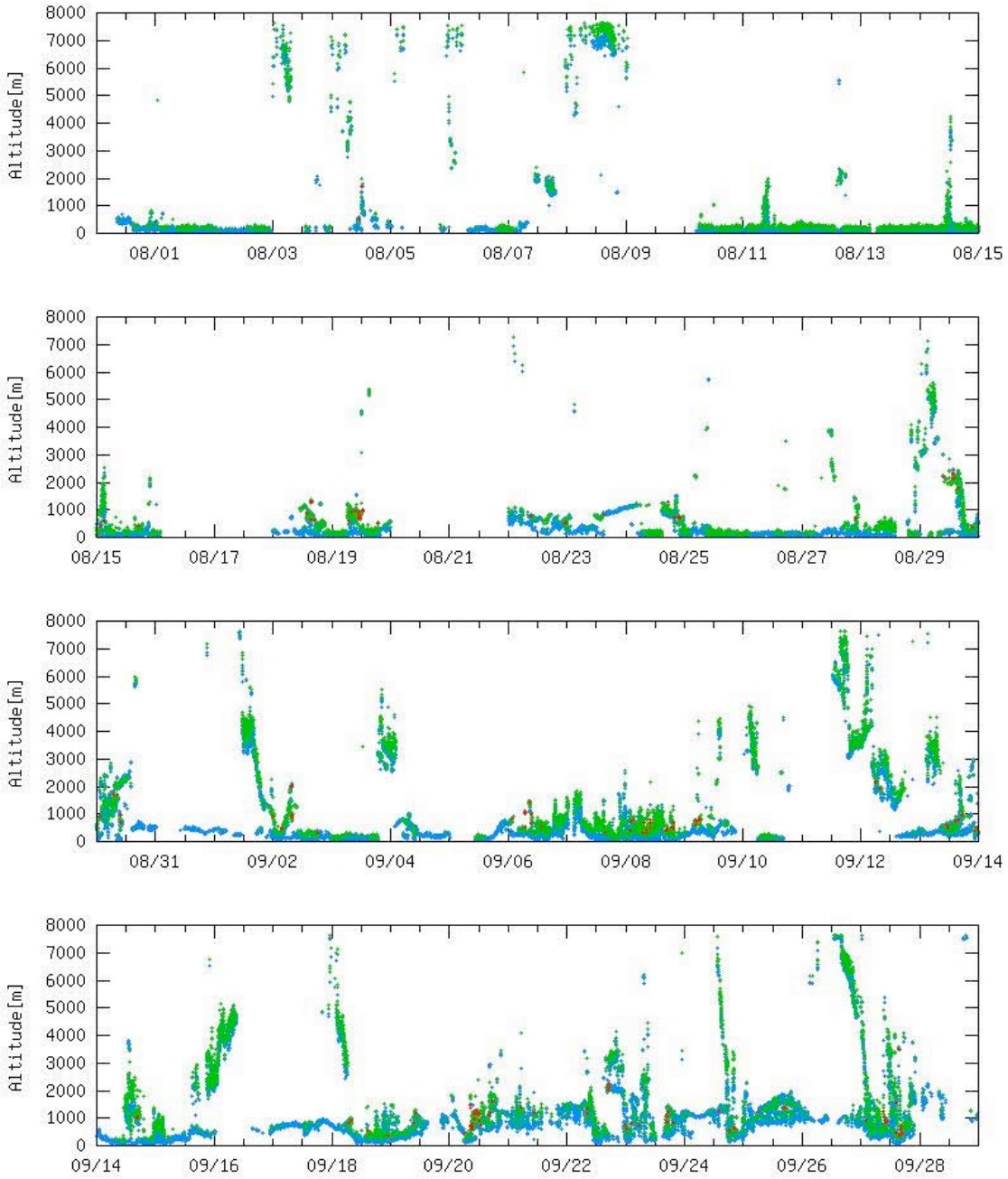

Fig.6.2.2.1 1st (blue) 2nd (green) and 3rd (red) lowest cloud base height during MR06-04 cruise.

6.2.3 Radiosonde Observation

(1) Personnel

Yoshihiro Tachibana (Tokai University/JAMSTEC)

(2) Motivations

The marine boundary-layer cloud, a general term including fog, stratus, and stratocumulus, widely and statically covers world oceans. Such cloud cover plays an important role in the Earth's climate through radiation processes, i.e., through direct shading (the "parasol effect") and its greenhouse effect. To parameterize the global radiation effects of the clouds, it is quite essential to know whether (and under what conditions) the cloud forms. Because most atmospheric general circulation models (AGCMs) and objective analysis data are not able to properly reproduce the marine boundary-layer clouds, the role that such clouds play in the air-sea interaction may be underestimated. We are still far from a satisfactory understanding of the importance of the marine boundary-layer cloud in affecting climate. One reason for this is the lack of observational studies. According to the climatology of low-level cloud distribution over the Pacific compiled by the International Satellite Cloud Climatology Project (ISCCP), the southern part of the Okhotsk Sea around the Kuril Islands is known to be one of the world's most stratocumulus-covered areas during the summer. It is also common that stationery anticyclones, referred to the Okhotsk highs, occur there in summer. These anticyclones play an important role in the hemispheric scale summer climate. The Okhotsk high usually occurs in association with cold marine boundary-layer clouds, which are called Yamase in Japanese. In years when Yamase occurs, the summer climate in Japan is anomalously cold, and rice production, which forms an economic basis of many Asian nations, dramatically decreases. This decreased production might influence the global economy, given Japan's place as a leading economic power.

(3) Objectives

Although the marine boundary-layer cloud or the marine fog in these regions is important, no direct upper-air radiosonde observations in the Okhotsk Sea have been executed by Japanese research vessels, partially due to the Cold War. The lack of observations has prevented us from understanding not only the mechanisms by which the marine boundary-layer cloud or the marine cloud develops but also the fog's vertical structure. Filling up this observational blank area should enable further progress in the knowledge of the air-sea interaction and the role of the marine boundary-layer cloud and the marine fog in climate, and allow better parameterization of the marine boundary-layer cloud and marine fog in GCMs.

In order to understand the reasons for the fog's concurrence with the Okhotsk high, interaction processes among the occurrence of the anticyclone, the marine fog, and sea surface temperature (SST) have been suggested. It is believed that cold SSTs due to sea ice remaining until the beginning of summer is a cause of the marine fog occurring in this region. However, previous studies have not clearly presented

observational evidence for interactions among the marine fog, the cold SST, and the anticyclone. For example, the question of whether the cold SST is the cause of or the response to the marine fog has not been solved. It is not even clear whether the Okhotsk high is always accompanied by marine fog or not.

The goal of this study is to better understand air-sea interaction processes, mainly based on GPS radiosonde observations 1) showing the difference in the atmospheric and oceanic vertical structures between the foggy and fogless anticyclones, 2) showing whether the cold SST is the cause of or the response to the marine fog, 3) estimating the sign of the atmospheric horizontal temperature advection, 4) proposing possible causes of the occurrence of the marine fog, and 5) estimating the approximate pressure rise due to the formation of the cold marine fog. Through the observations of air-sea interactive processes, we consider reasons why this area is one of the foggiest areas in the northern hemisphere. Finding the relationship between the fog formation and the anticyclone based on observational evidence provides us perspective on the air-sea interaction processes in the Okhotsk Sea as well as its surrounding areas such as the northwestern North Pacific. Furthermore, the observational results may provide a caution on potentially misleading values of the sea level pressure based on the objective analyses and numerical models in which marine fog is not correctly reproduced.

(4) Measured Parameters

Temperature, Relative Humidity, Wind Direction/Speed

(5) Instruments

VAISALA DigiCORA MW11 semi-automatic Radiosonde system

VAISALA RS92-SGP

(6) Preliminary results

The upper air soundings using GPS radiosondes were conducted from 2 August to 9 August and from 17 August through 19 August. Detailed dates and positions of the radiosonde observations are listed in Table 1. In former periods, fog with the Okhotsk high occasionally appeared.

(7) Data Archive

All the radiosonde data obtained during this cruise have been shared with all the personnel listed above. Also the data will be submitted to DOM (Data Management Office), JAMSTEC, and under their control.

Table 6.2.3.1 Radiosonde launch log

DATE &TIME				Position		Altitude
				Lon. E	Lat. N	
YY	MM	DD	HH	(deg.)	(deg.)	(gpm)
06	08	02	00	144.075	42.0710	24174
06	08	02	03	144.292	42.4660	22984
06	08	02	06	144.297	42.4920	24739
06	08	02	12	144.322	42.5190	20283
06	08	02	18	144.305	42.5380	30304
06	08	03	00	144.326	42.5120	25312
06	08	03	06	------	42.5100	22249
06	08	03	12	144.065	42.0350	20336
06	08	03	18	143.951	41.8631	22524
06	08	04	00	143.952	41.8660	24811
06	08	04	06	143.948	41.8460	24475
06	08	04	12	143.597	41.7960	25173
06	08	04	18	141.690	41.7060	24514
06	08	05	00	140.156	41.3320	22514
06	08	05	06	139.620	42.5270	25339
06	08	05	12	139.551	44.1070	19498
06	08	05	18	140.705	45.5770	22033
06	08	06	00	140.779	45.7650	25143
06	08	06	06	140.783	45.7590	22299
06	08	06	12	140.885	45.7480	23701
06	08	06	18	140.812	45.6040	24906
06	08	07	00	140.783	45.7580	24853
06	08	07	06	142.021	45.6020	18275
06	08	07	12	143.770	44.9780	22034
06	08	07	18	144.932	44.4830	25127
06	08	08	00	145.005	44.5270	25650
06	08	08	06	144.987	44.5310	23314
06	08	08	12	145.023	44.5380	23462
06	08	08	18	144.899	44.5120	15137
06	08	09	00	145.005	44.5280	22213
06	08	17	15	154.783	44.1515	15958
06	08	17	18	154.647	43.7447	6945

06	08	17	19	154.562	43.4290	17704
06	08	17	21	154.318	43.1383	24072
06	08	18	00	153.611	42.7556	21959
06	08	18	03	152.992	42.3435	22108
06	08	18	06	152.148	41.8472	21720
06	08	18	09	151.451	41.4332	21736
06	08	18	12	150.957	41.0538	19779
06	08	18	15	150.368	40.7257	21885
06	08	08	18	149.780	40.3886	21731
06	08	18	21	149.189	40.2771	20799
06	08	19	00	148.534	40.5547	21769
06	08	19	03	147.802	40.8627	20865
06	08	19	06	147.163	41.1365	22337
06	08	19	09	146.442	41.4534	21969
06	08	19	12	145.802	41.7157	22483
06	08	19	15	145.266	41.9362	22066

6.2.4 Lidar observations of clouds and aerosols

(1) Personnel

Nobuo Sugimoto, Ichiro Matsui, Atsushi Shimizu (National Institute for Environmental Studies, not on board), operation was supported by GODI.

(2) Objectives

Objectives of the observations in this cruise is to study distribution and optical characteristics of ice/water clouds and marine aerosols using a two-wavelength lidar.

(3) Measured parameters

- Vertical profiles of backscattering coefficient at 532 nm
- Vertical profiles of backscattering coefficient at 1064 nm
- Depolarization ratio at 532 nm

(4) Method

Vertical profiles of aerosols and clouds were measured with a two-wavelength lidar. The lidar employs a Nd:YAG laser as a light source, which generates the fundamental output at 1064 nm and the second harmonic at 532 nm. Transmitted laser energy is typically 30 mJ per pulse at both of 1064 and 532 nm. The pulse repetition rate is 10 Hz. The receiver telescope has a diameter of 20 cm. The receiver has three detection channels to receive the lidar signals at 1064 nm and the parallel and perpendicular polarization components at 532 nm. An analog-mode avalanche photo diode (APD) is used as a detector for 1064 nm, and photomultiplier tubes (PMTs) are used for 532 nm. The detected signals are recorded with a digital oscilloscope and stored on a hard disk with a computer. The lidar system was installed in the radiosonde container on the compass deck. The container has a glass window on the roof, and the lidar was operated continuously regardless of weather. Every 10 (leg1) or 15(leg2) minutes vertical profiles of three channel are recorded.

(5) Results

Although data obtained in this cruise has not been analyzed, lower clouds and fog were very frequently appeared and laser light could not penetrate into middle and upper troposphere especially in leg 2. Quick-look figures of backscattering intensity at 532 nm , depolarization ratio at 532 nm and ratio of backscattering intensities between 1064 nm and 532 nm up to 15 km are shown in Fig. 1-3. Whity area in

time-height indications means that laser light did not reach such region and lidar did not detect any meaningful signals. In the former half of leg 1, a surface aerosol layer was detected. Simultaneously cirrus clouds appeared between 10 and 13 km height. Data in the latter half was very poor. In leg 2, there was a log of lower clouds. As shown in Fig. 2, clouds were frequently detected below 500 m. However, cloud bottom height was higher at the end of leg 2 in Fig. 3. And a vertical structure of cloud system accompanying low pressure was detected on 11-16 September.

(6) Data archive

- raw data
  - lidar signal at 532 nm
  - lidar signal at 1064 nm
  - depolarization ratio at 532 nm
  - temporal resolution 15 min/ vertical resolution 6 m
  - data period : August 1, 2006 – September 29, 2006
- processed data
  - cloud base height, apparent cloud top height
  - phase of clouds (ice/water)
  - cloud fraction
  - boundary layer height (aerosol layer upper boundary height)
  - backscatter coefficient of aerosols
  - particle depolarization ratio of aerosols

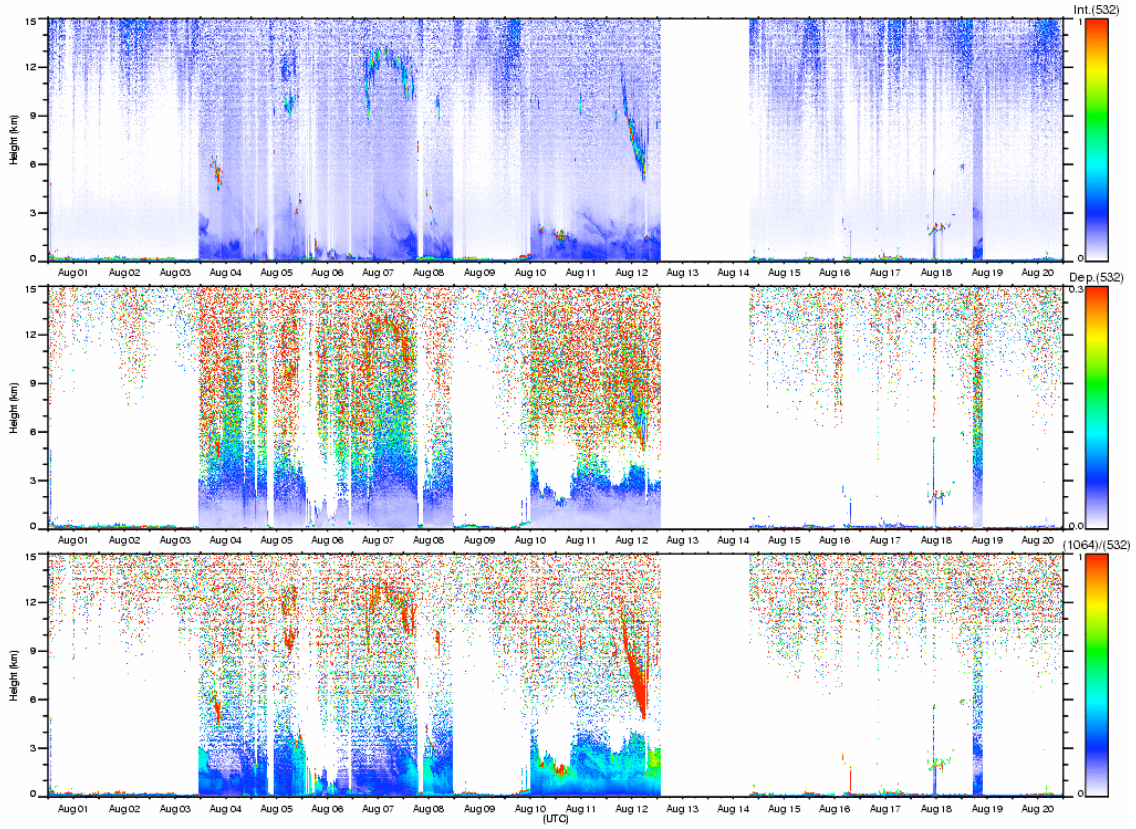

Figure 6.2.4.1 Time-height indications of backscattering intensity at 532 nm (top), depolarization ratio at 532 nm (middle), and ratio of backscattering intensities between 1064 nm and 532 nm (bottom), during MR06-04 leg 1. Depolarization ratio is a measure of non-sphericity of particles, and ratio of two wavelengths is a measure of particle size.

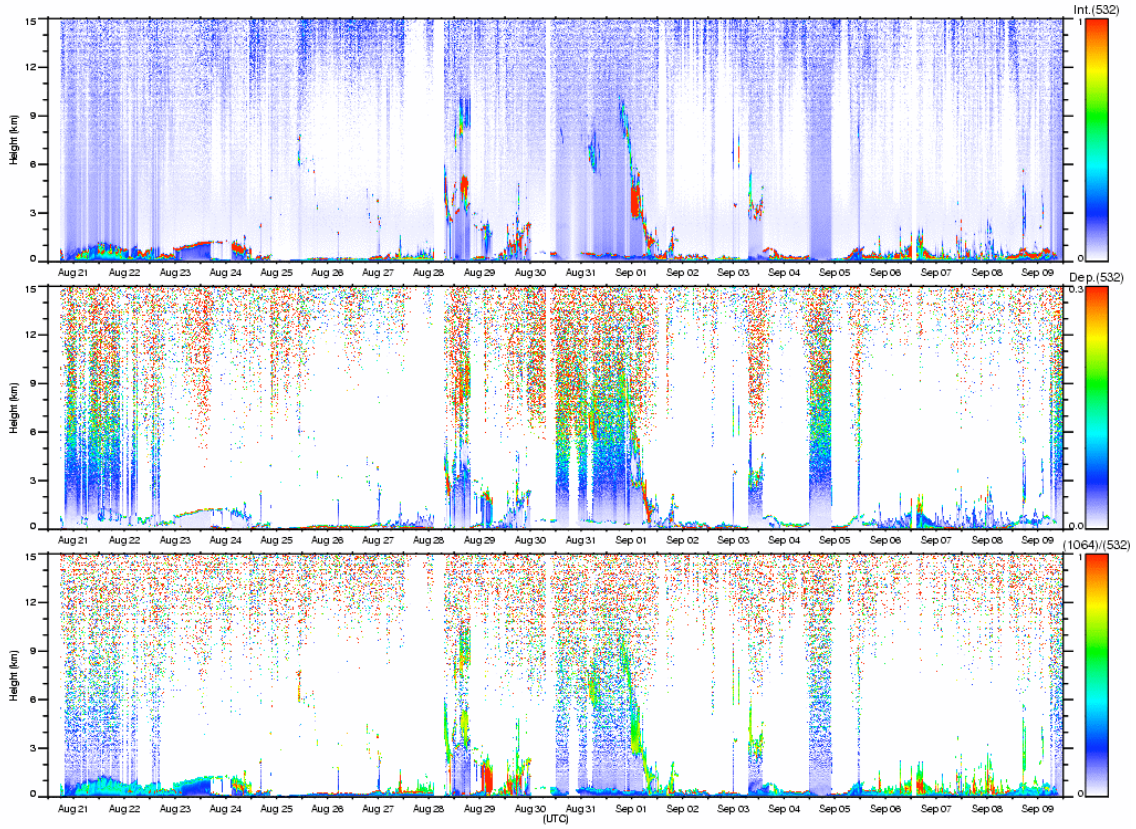

Figure 6.2.4.2 Same as Figure 1 but for first half of MR06-04 leg2.

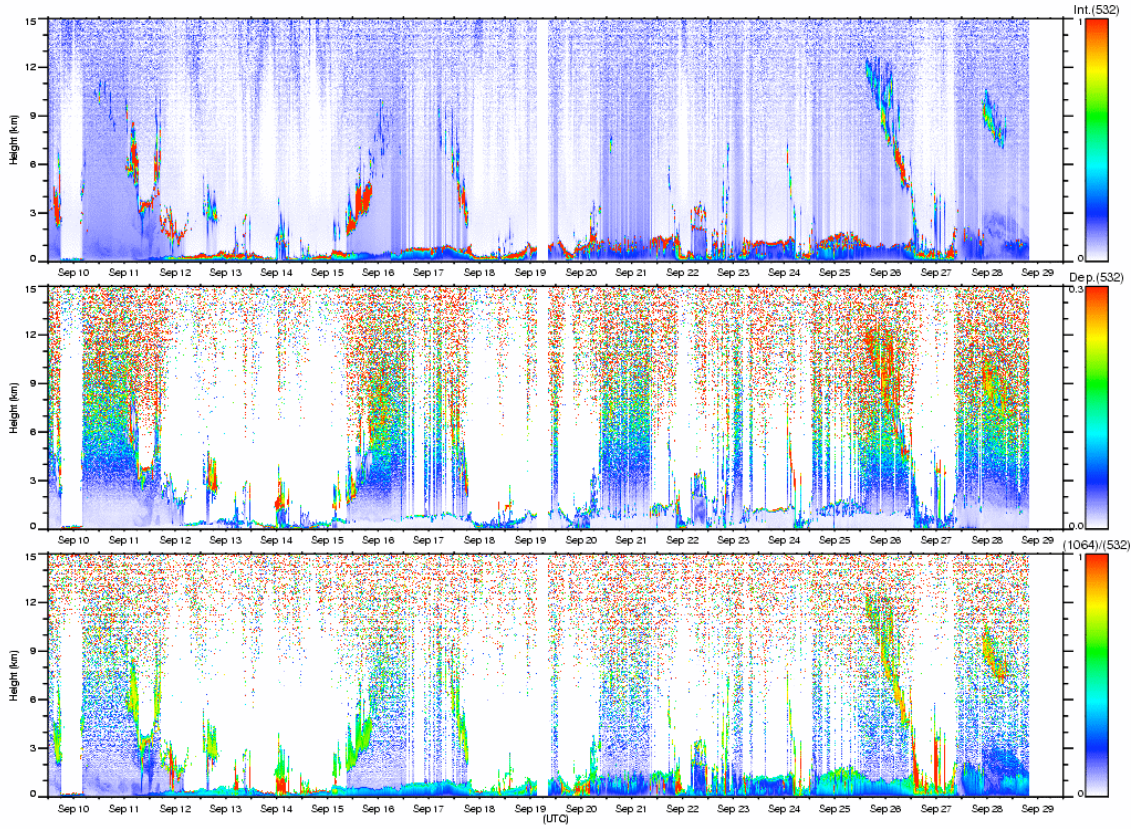

Figure 6.2.4.3 Same as Figure 1 but for second half of MR06-04 leg2.

6.2.5 On-board automated eddy flux measurement

(1) Personnel

Toru Iwata (Okayama University): Principal Investigator

On-shore scientists

Osamu Tsukamoto (Okayama University)

Fumiyoshi Kondo (Okayama University)

Hiroshi Ishida (Kobe University)

(2) Objective

Current interest in air-sea interaction calls for accurate measurements of eddy fluxes of momentum, surface heat, water vapor and carbon dioxide (CO_2) in order to achieve our deeper understanding on the relationships between recent CO_2 increase and global climate dynamics. The most promising technique for these fluxes measurements is the eddy covariance technique.

(3) Methods

The surface turbulent flux system consists of turbulence sensors and ship motion sensors (Kanto Aircraft Instrument Co.,Ltd.). The turbulence sensors are installed at the top of the foremast. A three-dimensional sonic anemometer-thermometer (KAIJO SONIC, DA-600) has been in continuous operation since June 2000 (MR00-K04), and an infrared gas analyzer (LI-COR, LI-7500) since May 2002. The sonic anemometer measures three-dimensional wind velocity components relative to the ship including apparent wind velocity due to ship motion. The ship motions are independently measured by ship motion sensors, including a two-axis inclinometer (Applied Geomechanics, MD-900-T), a three-axis accelerometer (Applied signal Inc., QA-700-020), and a three-axis rate gyro (Systron Donner, QRS-0050-100). LI-7500 is a CO_2/H_2O turbulence sensor (generally called "Open-path system") that measures turbulent signals of carbon dioxide and water vapor simultaneously.

These turbulence and ship motion signals are sampled at 10Hz by a PC-based data logging system (Labview, National Instruments Co.,Ltd.). The PC system is connected to the MIRAI network system to obtain ship speed and heading data that are used to derive absolute wind components relative to the ground. Combining these turbulence data and ship motion data, turbulent fluxes and statistics are calculated in a real-time basis and displayed on the PC. The dataset include every 0.1 sec raw data and 1min mean statistic data.

In addition to these turbulent flux measurement instruments, an improved "closed-path system" was mounted during the present cruise for the purpose of comparison between open- and closed-path systems. Another LI-7500 sensor was installed at the top of the foremast. Its light path was sealed up with SUS

cylinder and the air was introduced into the cell by an air pump. We call this instruments "Open-Closed system". Figure 1 shows the installation of the instruments.

(4) Preliminary results

Based on the raw 10Hz turbulence data, apparent wind velocities were corrected and eddy-covariance method was applied to lead eddy fluxes of sensible heat, latent heat and CO_2. Fig.2 shows the preliminary results during Leg2 based on preliminary quality control. Eddy fluxes were originally calculated every 10 minutes and averaged over an hour. Due to low SST around the Arctic ocean, latent heat flux was small and sensible heat flux contribution is larger than the tropical or mid-latitude ocean.

(5) Future plan and Data Archives

All the data obtained during this cruise are archived at Okayama University, and will be open to public after quality checks and corrections. Interested scientists should contact Prof. Osamu Tsukamoto at Okayama University. The corrected data and inventory information will be submitted to JAMSTEC Data Management Office.

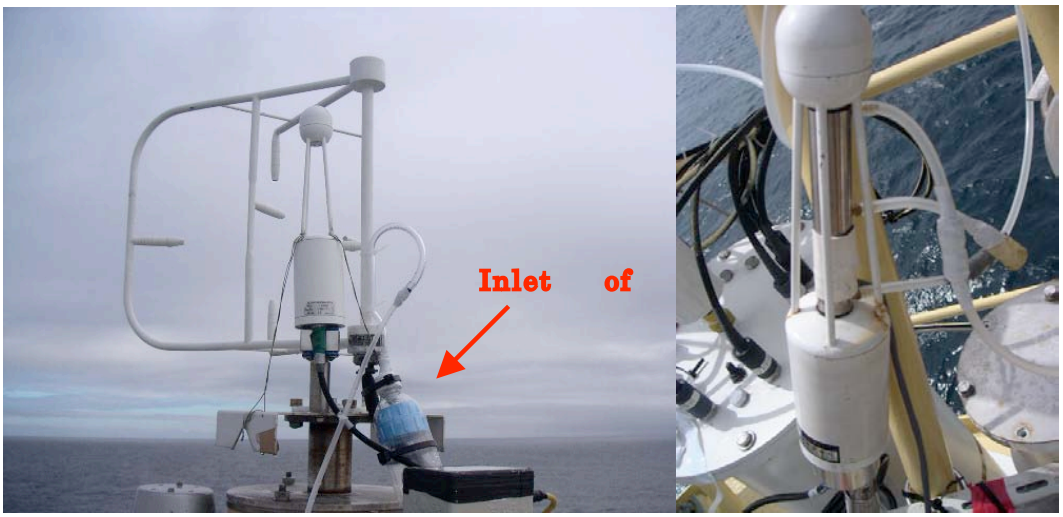

Figure 6.2.5.1 The installation of the turbulence measurement sensors and inlet of sample gas (left panel), and a sealed-up LI7500 (right panel).

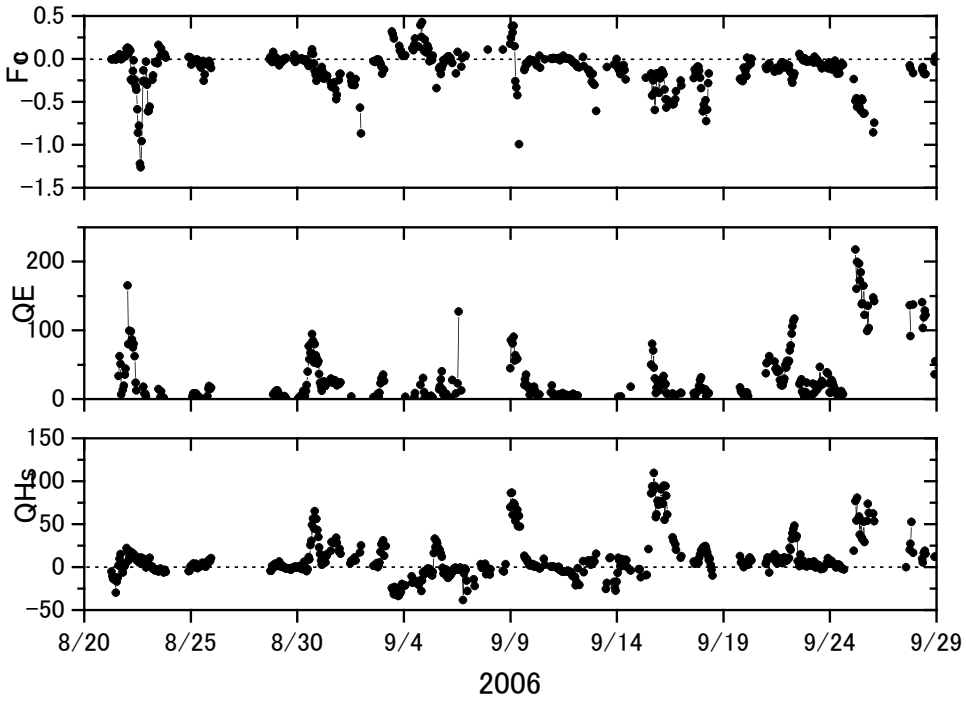

Figure 6.2.5.2 Preliminary results of eddy fluxes of sensible heat (QHs), latent heat(QE) and CO_2(Fco) calculated with eddy-covariance method. The sensible heat flux and the latent heat flux were given in W m^{-2} and CO_2 flux is given in mgCO_2 m^{-2} s^{-1}. Corrections were not applied to the sensible heat flux (QHs) for water vapor contribution, and to the CO_2 flux (Fco) for the Webb correction.

6.2.6. Aerosol optical characteristics measured by Sky radiometer

(1) Personnel

Principal Investigator :

Kazuma Aoki (University of Toyama) Associate Professor / not onboard

Co-workers:

Tatsuo Endoh (Tottori University of Environmental Studies) Professor / not onboard

Tamio Takamura (CEReS, Chiba University) Professor / not onboard

Teruyuki Nakajima (CCSR, The University of Tokyo) Professor / not onboard

Nobuo Sugimoto (NIES) Chief Research Scientist / not onboard

Operation was supported by Global Ocean Development Inc. (GODI).

(2) Objective

Objective of the observations in this aerosol is to study distribution and optical characteristics of marine aerosols by using a sky radiometer (POM-01 MKII). Furthermore, collections of the data for calibration and validation to the remote sensing data were performed simultaneously

(3) Measured parameters

- Aerosol optical thickness at 5 wavelengths (400, 500, 675, 870 and 1020 nm)
- Ångström exponent
- Single scattering albedo at 5 wavelengths
- Size distribution of volume (0.01 μm – 20 μm)

GPS provides the position with longitude and latitude and heading direction of the vessel, and azimuth and elevation angle of sun. Horizon sensor provides rolling and pitching angles.

(4) Methods

Sky radiometer is measuring the direct solar irradiance and the solar aureole radiance distribution, has seven interference filters. Analysis of these data is performed by SKYRAD.pack version 4.2 developed by Nakajima *et al.* 1996.

(5) Results

Data obtained in this cruise will be analyzed at University of Toyama.

(6) Data Archives

Measurements of aerosol optical data are not archived so soon and developed, examined, arranged and finally provided as available data after a certain duration. All data will archived at University of Toyama (K.Aoki, SKYNET/SKY: http://skyrad.sci.u-toyama.ac.jp/) and Chiba University (T.Takamura, SKYNET) after the quality check and submitted to JAMSTEC within 3-year.

6.2.7 Intergrated Eddy Covariance Measurements of Turbulent Fluxes of Atmospheric Aerosols and CO_2 from a Moving Ship

(1) Personnel

Frank Griessbaum (Ocean Research Institute, The University of Tokyo) Legs.1 and 2

(2) Objectives

In recent years promising attempts have been conducted to directly quantify the emission and deposition fluxes of atmospheric aerosols (solid and liquid) in the terrestrial (TBL) as well as the marine boundary layer (MBL) by eddy covariance (EC). This study is focusing on employing the EC method in a unique integration of trace gas and aerosol measuring equipment on a mobile platform (ship) in order to cover wide areas of the MBL and also to have the ability to measure while the ship is underway.

(3) Measured parameters

- Turbulent fluxes obtained by EC-System located at top of foremast (10 Hz sample rate),
  - Atmospheric aerosol particle flux in one size class from 5 nm to 3 µm particle diameter
  - Fogwater fluxes in 40 size classes from 2 to 50 µm fog droplet diameter
  - CO_2 and water vapor fluxes
- Fog droplet spectra in 40 size classes from 2 to 50 µm fog droplet diameter
- Atmospheric aerosol particle number concentrations measured at compass deck,
  - Particle size classes: 0.10 – 0.15 µm, 0.15 – 0.20 µm, 0.20 – 0.30 µm, 0.30 – 0.50 µm, 0.50 – 1.0 µm, 1.0 – 2.0 µm, 2.0 – 5.0 µm
- High volume filter samples of atmospheric aerosol particles for post-chemical analysis
  - $PM_{2.5}$ and $PM_{>2.5}$
- Passive string fogwater collection for post-chemical analysis
- Two-stage fog impactor fog water collection for post-chemical analysis
  - Stage 1: Aerodynamical droplet diameter of > 13 µm
  - Stage 2: Aerodynamical droplet diameter from 6 to 13 µm
- Ozone (from pre-dried air sample)

(4) Instruments and Methods

The configuration and the sensors of the EC system as deployed at the top of the foremast are depicted in Figure 6.2.7.1. Each sensor is connected via RS232 through a RS232-LAN server to the recording PC below the deck (see Figure 6.2.7.2). The combination of serial communication and TCP/IP-protocol based system enable us to record the data free of noise as well as get besides the parameters also all available status information of the sensors for consecutively quality assurance.

From computational fluid dynamics (CFD) calculations of the airflow around vessels it is known that the most suitable place of undistorted airflow for the measurements is at the very bow and the most elevated location. For this reason, the entire EC instrumentations were fixed at the very top of the foremast. In order to be able to employ the condensation particle counter also underway during rough weather conditions, the maximum tilt angle of the device was technically improved to up to 30 degree.

Furthermore, a set of instruments for physical and chemical characterization of atmospheric aerosols (liquid and solid) as well as Ozone was located at the compass deck:

- Optical Particle counters, Rion KC01D and KC18
- High volume aerosol particle filter sampler, Kimoto AS9
- Passive string fogwater collector
- Two-stage fogwater impactor, Enviscope
- Wind sector control unit

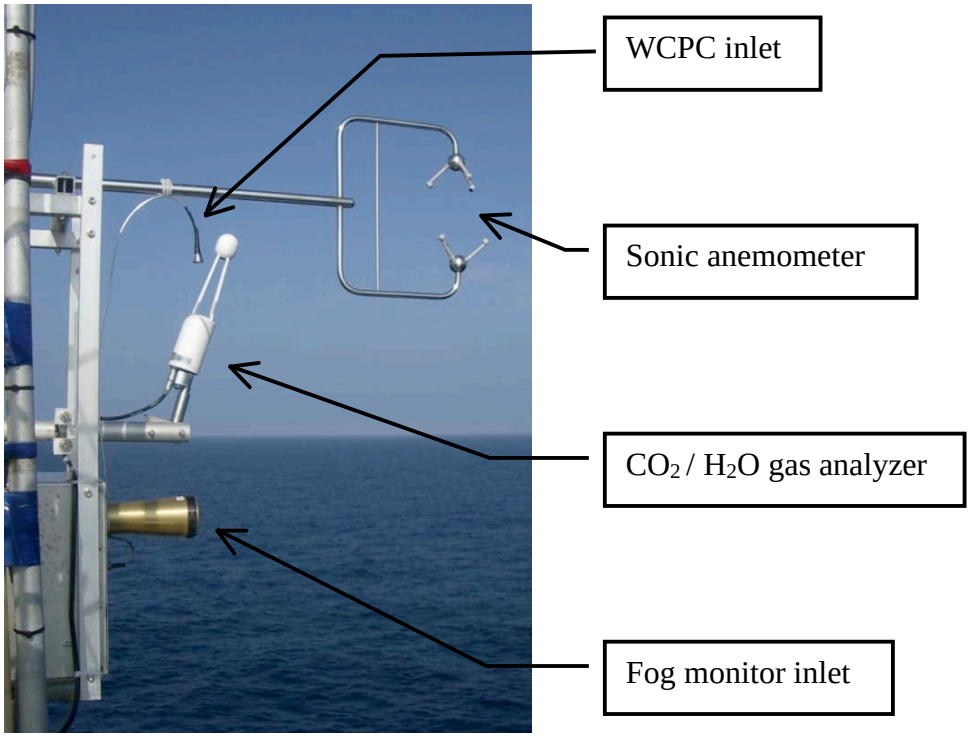

Figure 6.2.7.1. Integrated Eddy Covariance System

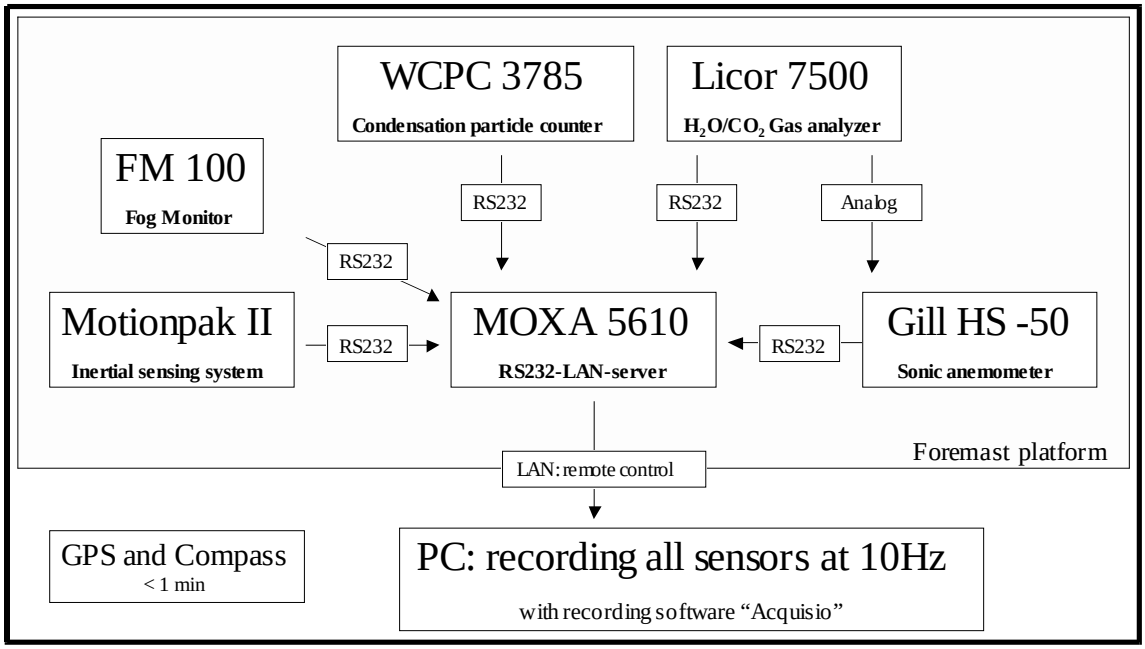

Figure 6.2.7.2. Technical layout of the EC-System

(5) Preliminary and expected results

Three sets of data obtained during MR06-4 (Leg1 & 2) are expected:

(i) Turbulent flux data of aerosol particles, fogwater and CO_2. This data is in processing and results are not yet available.

(ii) Chemical analysis of aerosol particle filters and fogwater samples. Analytics are not yet done.

(iii) Aerosol particle number concentration in various size classes as well as Ozone measurements. Preliminary data of the time series is depicted in Figure 6.2.7.3. The data is not filtered for ship exhaust contamination.

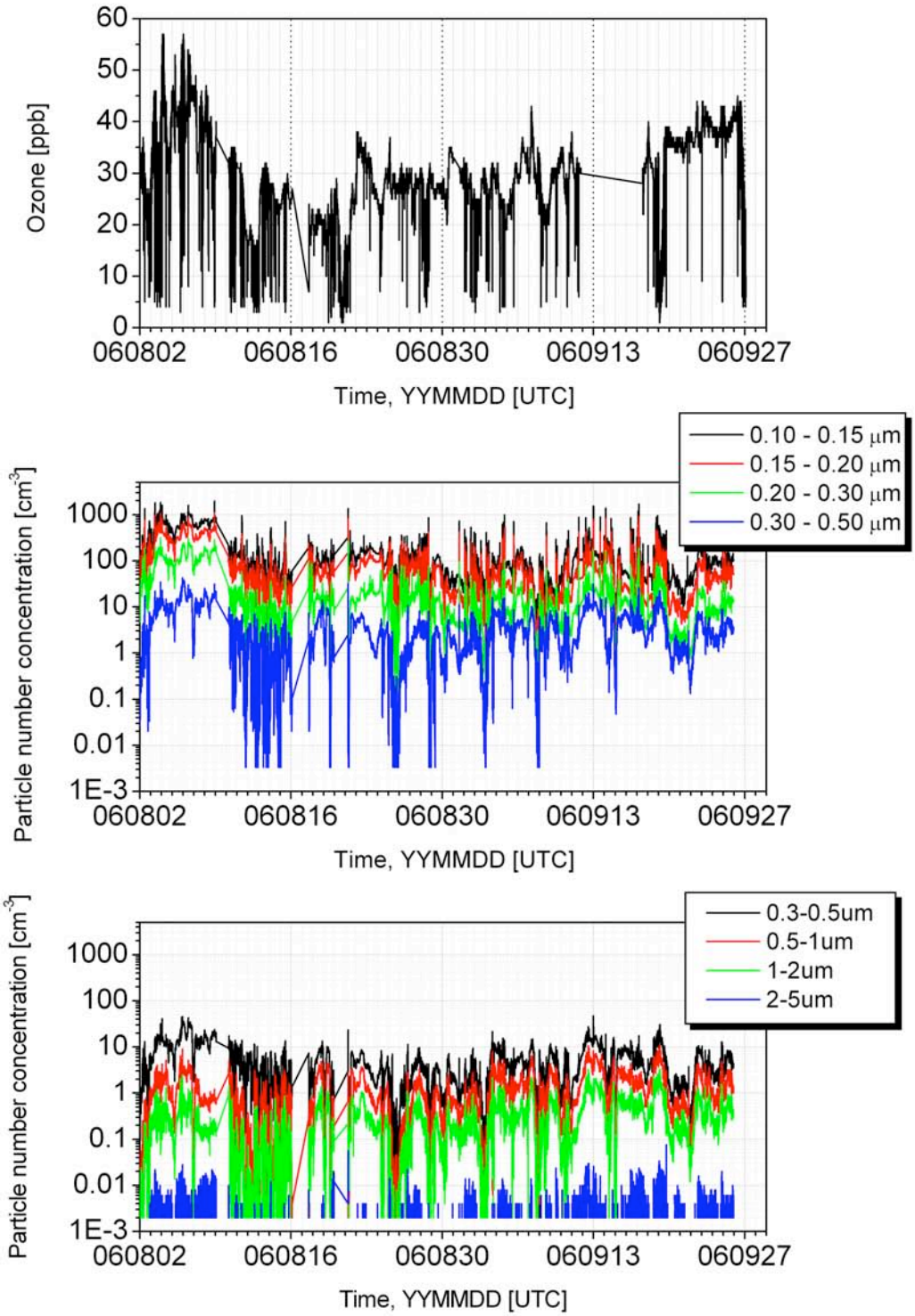

Figure 6.2.7.3 Time series of Ozone and particle number concentrations during MR06-4 Leg1 & Leg2

(6) Data archives

The data obtained during MR06-04 will be accessible upon request at Ocean Research Institute, The University of Tokyo.

6.2.8 Rain Sampling for Stable Isotopes

(1) Personnel

Kimpei Ichiyanagi (JAMSTEC) (Not on board)

(2) Objective

To determine the spatial distribution of isotopic composition of rainfall on the Ocean

(3) Method

Rainfall samples are collected in 6cc glass bottle with plastic cap. Isotopic compositions for hydrogen and oxygen in rainfall are determined by the Isotope Ratio Mass Spectrometry (IRMS).

(4) Preliminary results

During this cruise, we collected 28 samples in total. Table 6.2.8.1 lists the date and location of rainfall samples. Analysis will be done after the cruise.

(5) Data archive

Original samples will be analyzed by IORGC. Inventory and analyzed digital data will be submitted to JAMSTEC Data Management Office.

Table 6.2.8.1 Dates and locations to show when and where rain water were sampled.

Sample No.	Date (UTC)		Location (lat/lon)		Rain (mm)
1	2006/8/1	0:40	40-58.69N	141-35.16E	1.6
2	2006/8/1	21:39	41-43.06N	143-58.11E	0.4
3	2006/8/11	19:46	51-21.36N	149-20.98E	7.9
4	2006/8/13	3:47	53-16.80N	150-04.81E	0.2
5	2006/8/14	21:58	54-19.18N	149-15.85E	3.0
6	2006/8/15	23:45	52-08.92N	149-46.18E	1.8
7	2006/8/27	16:57	54-07.25N	172-23.41W	0.7
8	2006/8/27	21:18	54-07.41N	170-54.52W	0.2
9	2006/8/28	6:58	54-13.17N	168-14.00W	0.1
10	2006/8/28	19:14	54-25.35N	166-33.97W	1.4
11	2006/8/29	20:55	60-25.63N	167-55.42W	2.7
12	2006/8/30	4:20	62-04.70N	167-21.60W	1.7
13	2006/9/2	8:58	72-32.24N	166-00.48W	0.1
14	2006/9/6	15:50	67-00.01N	166-59.80W	5.0
15	2006/9/7	4:05	65-18.70N	168-36.40W	9.7
16	2006/9/7	20:09	63-44.79N	168-35.82W	12.4
17	2006/9/9	3:03	62-05.50N	171-52.10W	7.2
18	2006/9/13	19:36	59-59.10N	175-04.12W	0.9
19	2006/9/14	20:45	59-19.06N	168-17.40W	3.2
20	2006/9/16	17:50	59-30.00N	172-00.00W	4.0
21	2006/9/18	22:00	56-57.36N	167-11.32W	12.8
22	2006/9/20	1:43	54-04.60N	169-18.80W	3.9

23	2006/9/20	19:15	53-46.79N	176-48.04W	0.6
24	2006/9/23	1:40	48-26.17N	169-56.00E	3.4
25	2006/9/23	19:15	46-20.49N	164-30.34E	2.4
26	2006/9/25	0:11	43-03.45N	156-20.07E	4.0
27	2006/9/27	8:35	40-24.96N	144-05.26E	22.1
28	2006/9/27	21:00	40-28.80N	142-01.70E	5.0

6.2.9 CO_2 profiling observation

(1) Personnel

Toru Iwata (Okayama University): Principal Investigator (on board)

On-shore scientists

Osamu Tsukamoto (Okayama University)

(2) Objective

The aerodynamic gradient technique has been used to estimate CO_2 fluxes over the land surface by some micrometeorologists. In order to estimate CO_2 flux by this technique, the profile of CO_2 concentration in the surface boundary layer must be measured and the eddy diffusivity correctly evaluated.

(3) Methods

The CO_2 content at four levels in the surface atmosphere (5, 50, 200 and 710cm above the sea surface) was measured with a non-dispersive infrared (NDIR) gas analyzer (Licor Co., LI-6252) to estimate the CO_2 fluxes by the aerodynamic gradient technique. Air samples drawn from four levels were alternately introduced into the measuring cell of the NDIR every 45 second by the electrical switch at the rate of 0.8-0.9 L/min (Figure 6.2.9.1). Sample air was pre-dried by passing through a fiber drier. The calibration of NDIR was made twice at every stations using other standard gas concentrations (351 and 410 ppm) of CO_2. Data was logged at 1Hz by a laptop PC and statistically analyzed for 20 seconds every 45 second.

Air is sampled by using "Albedo boom" at the head of the ship with 6x9 vinyl hose attached with a profiling buoy (Figure 6.2.9.2). A water-repellent filter was attached to the end of hoses. Sample airs at the four levels are introduced to the laboratory with 4x6 teflon hose (65m). They are extended every stations. Summary of surface CO_2 profiling measurements is shown in Table 6.2.9.1

(4) Preliminary Results

Figure 6.2.9.3 shows an example of time variations of the CO_2 concentration at St.13 on Sep. 1st, 2006. CO_2 concentrations of lower levels show lower values. Obvious difference between levels is not shown from 8:40 till 8:55 in which time buoy was hung up at higher levels about 5m ASL. The profile may present semilogarithmic fit and the difference of CO_2 concentration between surface and 7m height is about 0.3 ppm (Figure 6.2.9.4). Semilogarithmic profile of CO_2 concentration was presented as following equation.

$$c(z) = \alpha \log z + \beta$$

Figure 6.2.9.5 shows relationship between $\triangle pCO_2$ and α at all stations of data. α shows clear dependency on $\triangle pCO_2$.

(5) Future plan and Data Archives

All the data obtained during this cruise are archived at Okayama University, and will be open to public after quality checks and corrections. Interested scientists should contact Dr. Toru Iwata at Okayama University. The corrected data and inventory information will be submitted to JAMSTEC Data Management Office.

Table.6.2.9.1 List of surface CO_2 profiling measurements

St.No.	DATE(LST	DOY(LST)	Time(LST)	Duration
15	31-Aug	243	8:30- 11:30	3:00
14	1-Sep	244	8:15-10:30	1:00×2
13	1-Sep	244	15:00-17:00	0:40, 1:10
12EX	2-Sep	245	8:10-13:00	4:50
12	3-Sep	246	8:15-9:05	0:50
16	5-Sep	248	8:10-11:45	3:35
17	6-Sep	249	8:10-10:30	2:20
18	7-Sep	250	10:20-11:20	1:00
19	7-Sep	250	16:35-18:45	2:10
20	8-Sep	251	8:10-9:50	1:40
21	9-Sep	252	8:05-9:00	0:55
22	9-Sep	252	17:05-18:15	1:10
23	10-Sep	253	9:05-21:40	3:40, 8:50
24	11-Sep	254	8:05-16:45	8:40
25	12-Sep	255	9:55-13:40	3:45
26	13-Sep	256	8:05-9:30	1:25
27	13-Sep	256	18:30-19:00	0:30
28	14-Sep	257	8:10-9:10	1:00
29	14-Sep	257	16:50-18:45	1:55
30	16-Sep	259	10:05-11:40	1:35
31	16-Sep	259	16:30-17:50	1:20
32	17-Sep	260	8:05-9:05	1:00
33	17-Sep	260	18:15-21:05	2:50

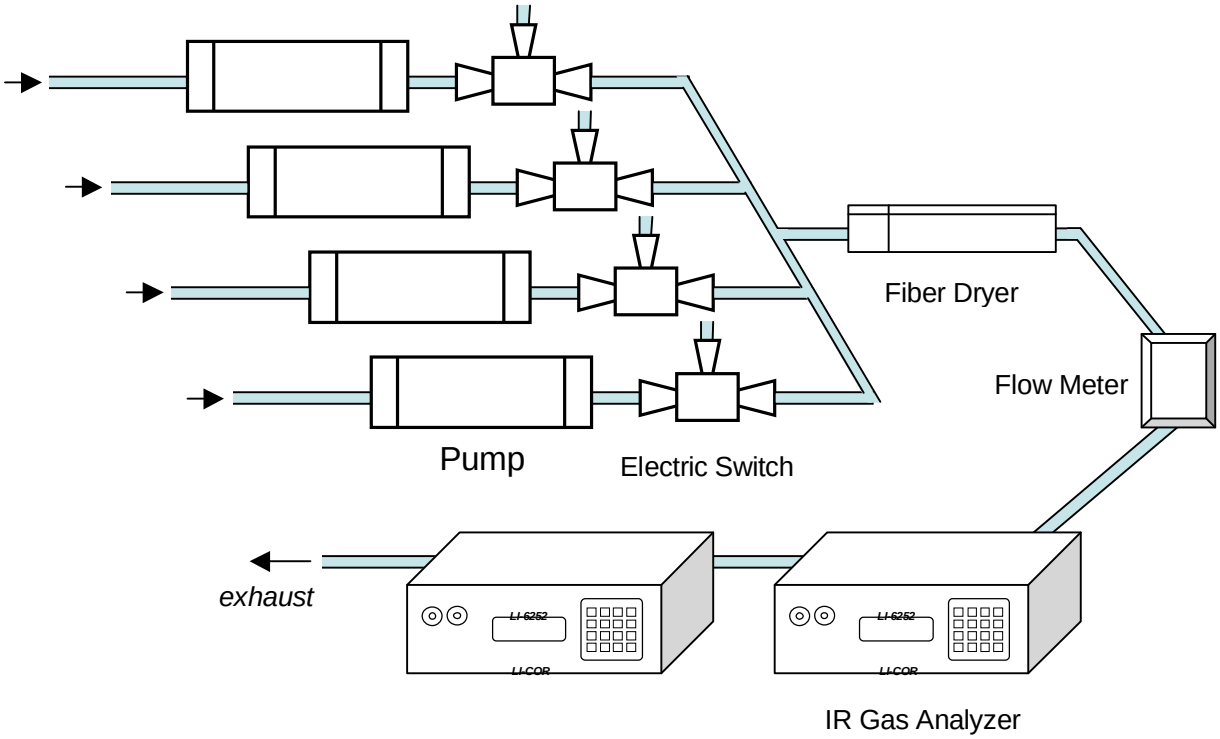

Figure 6.2.9.1 CO_2 profile measurement system.

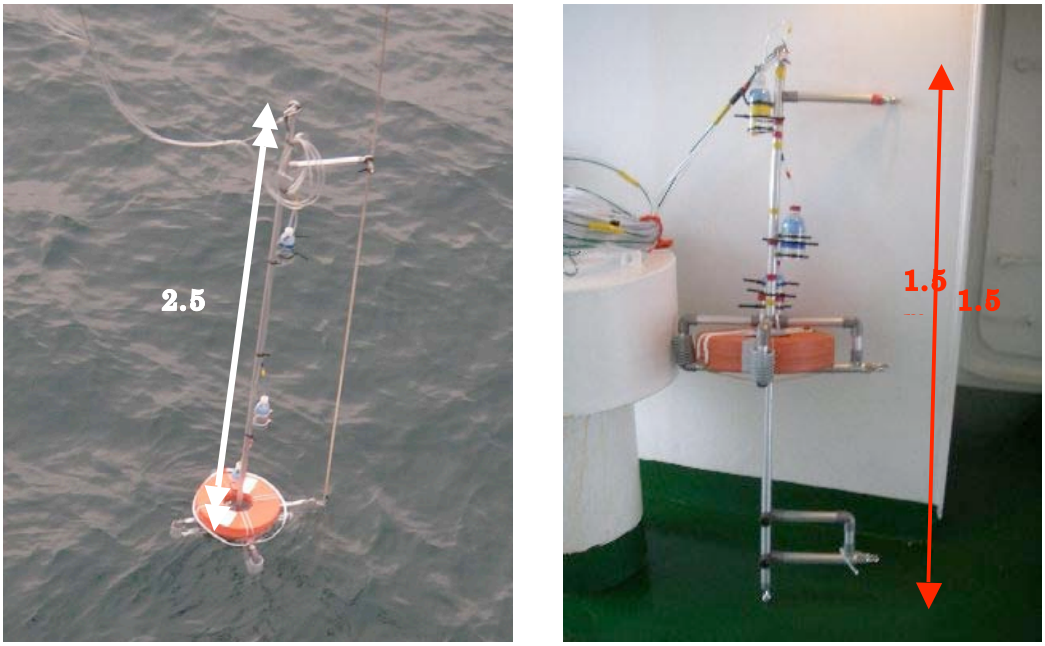

Figure 6.2.9.2 Buoys for gas sampling for fine condition (a) and for rough condition (b).

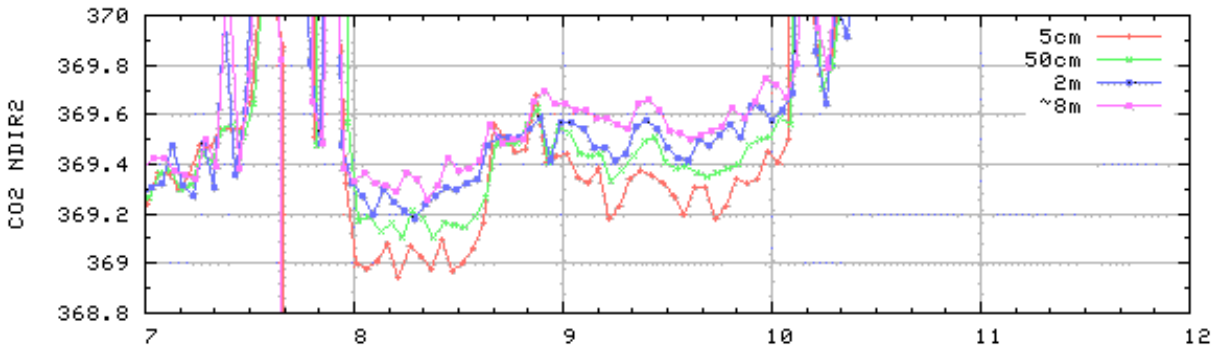

Figure 6.2.9.3 Time variations of CO_2 concentration for 4 levels (5, 50, 200 and 710 cm) at St.13 from 800 till 1000 on Sep. 1st 2006.

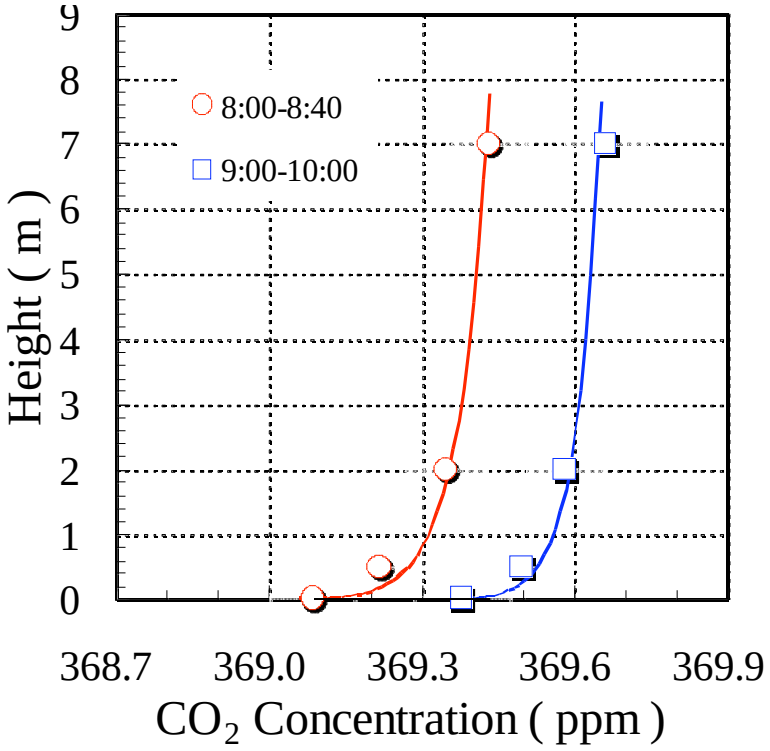

Figure 6.2.9.4 Examples of vertical profile of CO_2 concentration at St.13 on Sep. 1st 2006.

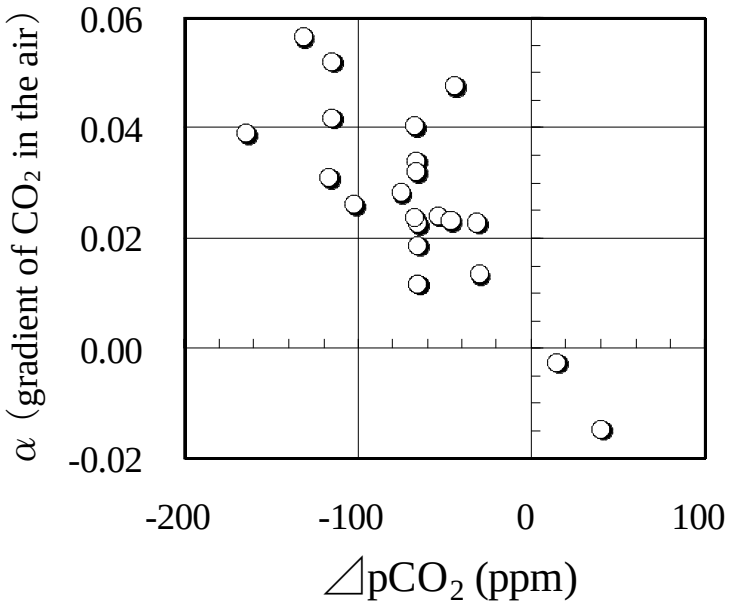

Figure 6.2.9.5 Relationship between ΔpCO_2 and gradient coefficient of log-linear profile, α.

6.2.10 Dimetylsulfide measurement

(1) Personnel

Ippei Nagao (Nagoya University)

(2) Objectives

During this cruise in the northern North Pacific and the Arctic Ocean, my research objectives are as follows;

・to investigate spatial and temporal variations of dimethylsulfide (DMS) and its precursor dimethylsulfoniopropionate (DMSP) in the seawater.

・to attempt to measure turbulent DMS flux from ocean to atmosphere by using fluorine induced chemiluminescence technique which can measure the atmospheric DMS concentration fast enough for the eddy-correlation method.

(3) Measured parameters

・Atmospheric DMS concentration

・DMS and DMSP (particulate DMSP and dissolved DMSP) concentrations in the seawater

(4) Instruments and Methods

4-1 Fluorine induced DMS measurement system for DMS in the atmosphere

High speed sensor for DMS based on its fast chemiluminescence reaction with molecular fluorine (F_2) was developed following the document by Hills et al [1998]. Intense chemiluminescence occurred upon reaction of F_2 with a sulfur-containing compound, as follows;

CH_3SCH_3 (DMS) + F_2 ⟶ multi steps ⟶ HF* and HCF** (R1)

HCF** ⟶ HCF** + hv (λ =500~700 nm) (R2)

HF* ⟶ HF + hv (λ =660~750 nm) (R3)

Emission in the wavelength range 450~650 nm was monitored via photon counting with a photomultiplier tube (R2228P, Hamamatsu Photonics, Co. Ltd.). Residence time of the sample air in the reaction cell was very short (much less than 0.1 sec). Assuming that reaction (R1) was a pseudo 1st order reaction, within the residence time of sample air in the cell (0.012sec), reaction (R1) was expected to almost complete. Product gases were evacuated from the reaction cell and then scrubbed of F_2 and HF via a two-stage chemical trap, which first converts excess F_2 to CF_4 on activated carbon and then HF to H_2O on Ascarite II. This system was installed in the stainless steel shelter at the lower stage of the foremast of R/V Mirai. Sample air was introduced from the top of the foremast through a Teflon-tube (10mm o. d. and c.a. 20m of length). Signals of this reaction were recorded in personal computer, and then analyzed to calculate the DMS concentration.

4-2 GC/FPD system

4-2-1 DMS in the atmosphere

Continuous measurement of the atmospheric DMS concentration was carried out during this cruise every 2 hours. Air was introduced through the Teflon tube (10mm o.d., 40m of length) from the compass deck to the Atmospheric Survey Room of R/V Mirai with 30 L/min. Then, air for DMS measurement was sampled from the manifold by sampling pump system. The traps for cryogenic pre-concentration were silico-steel stainless tubes (1/8 inches o.d., 5cm of length). This tube was packed with Tenax GR (GL Science Co. Ltd. 60/80 mesh). During pre-concentration, this trap was kept at -70 C with a liquid CO_2. A Nafion dryer (Perma-Pure Inc. Co. Ltd.) was located between the manifold and the cryogenic trap to avoid ice blocking in the trap tube. Sampling air volume was set to 3.0 L and monitored by personal computer to accurately estimate the sample air volume. Then pre-concentration tube was heated at +160 ℃ within 1.5 min to introduce DMS to a gas chromatography equipped with flame photometric detector (GC/FPD) (Shimadzu, GC-14B). This GC/FPD system designed for the analysis of volatile sulfur compounds was used for determination of DMS both in the seawater and atmosphere. Packed column was filled with β-β' ODPN (Shimadzu Co. Ltd.), and the carrier gas was 99.9999% quality nitrogen. Temperature in the column oven was set to be 60 C. The detection limit (DL) was estimated to be 12 pptv in 3.0 liter of STP.

4-2-2 Seawater DMS and DMSP

Purge and Trap method was applied to measure the seawater concentrations of DMS and DMSP. A glass bubbling flask was used for purge of volatiles including DMS from water. After introducing 30 ml of water samples to a degasification vessel by syringe, samples were purged with pure N_2 gas (99.9999%, Nagoya Kosan Co. Ltd) with 60 mL min^{-1} for 20 min. The extracted DMS was then concentrated by the same method as that for air sample. A Nafion dryer was located between the purge flask and the cryogenic trap to avoid ice blocking in the trap tube. The DL was estimated to be 0.05 nM of DMS for a 30 mL of seawater sample.

Dissolved DMSP (DMSPd) was determined as DMS by the cold alkali treatment method. After removal of volatiles from filtered water by purging, the sample was transferred to a 30 mL glass vial. Then 100 mg of NaOH was added to set the pH to ~13. The sample was left to react at room temperature for a day to achieve the full transformation of DMSP into DMS. The newly formed DMS was purged from the solution and measured as described above. For particulate DMSP (DMSPp), the GF/F filter (Whatman Co. Ltd. Φ25mm) used during the sample filtration to the purge flask was replaced into a 30 mL glass vial, filled with MillQ water, and allowed to react for a day with 100 mg NaOH. The entire volume was taken with a syringe to follow the usual purging procedure.

(5) Results (preliminary or expected)

5-1 Atmospheric DMS concentration

Figure 6.2.10.1 shows the time course of the atmospheric DMS concentration measured by GC/FPD

system during this cruise. A large variation of DMS concentration ranged from DL to 1000 pptv was observed. For instance, high concentration was observed on Aug. 25, Sep. 4, Sep. 7 and Sep. 22, while low concentration was observed on Aug. 22, Sep. 2, and Sep. 18~20. Maximum concentration (c.a. 1000 pptv) was observed on Aug. 25 when R/V was located around 50N and 170E. As shown in Figure 6.2.10.2, these periods of relatively high DMS concentration roughly correspond to those when seawater concentration of DMS were high.

5-2 Seawater DMS and DMSP concentrations

Figure 6.2.10.2 shows the time course of the DMS concentration in the surface seawater (around 10m depth) obtained during this cruise. Temporal variation of DMSPp showed a similar pattern to that of DMS in the surface seawater (Figure 6.2.10.3). High concentrations of DMS and DMSPp were observed around Aug. 25, and Sep. 20~25 when R/V was located around 40~45 N.

5-3 Future plan

DMS fluxes will be calculated both by the bulk method and the eddy-correlation method with data measured during this cruise. Then the DMS fluxes by two methods will be compared to discuss their validity particularly the exchange coefficient of DMS as a function of the wind speed, and if possible recommended relationship between the wind speed and the exchange coefficient will be proposed.

(6) Data archives

All data will be archived at Graduate School of Environmental Studies, Nagoya University.

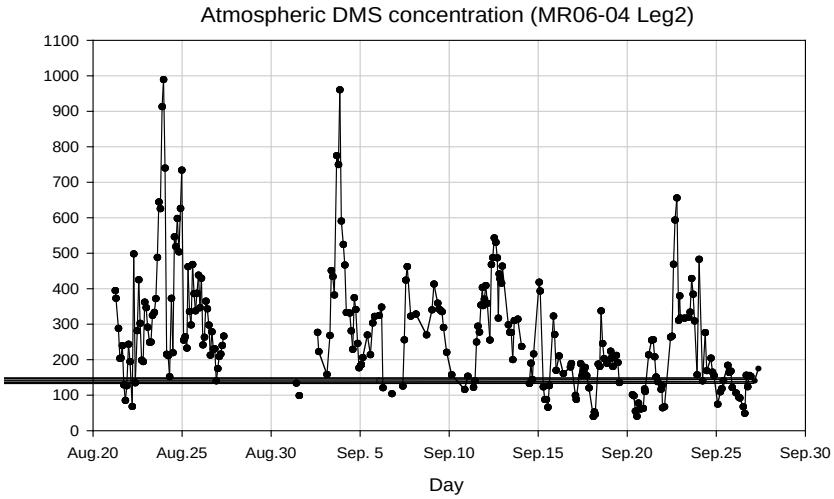

Figure 6.2.10.1. Time course of the atmospheric DMS concentration measured during MR06-04 cruise.

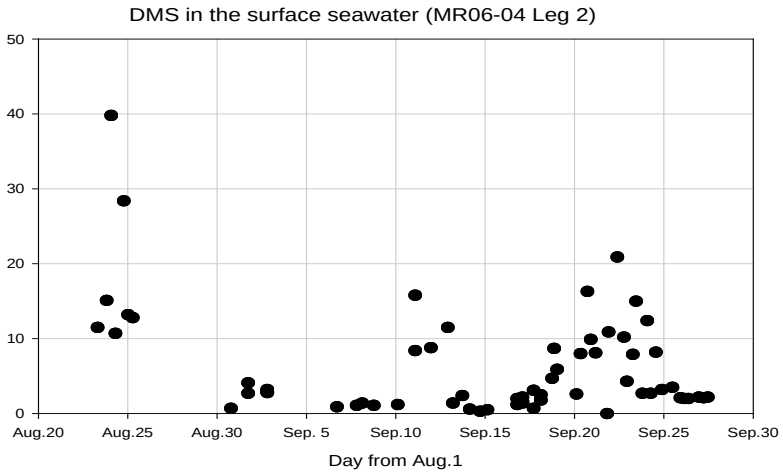

Figure 6.2.10.2. Time course of the DMS concentration in the surface seawater (10m depth) measured during MR06-04 cruise.

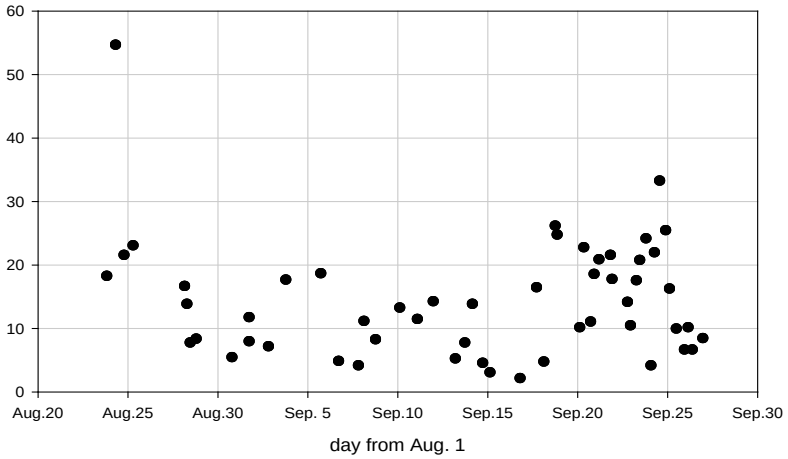

Figure 6.2.10.3. Same as Figure 6.2.10.2, but except for DMSPp.

6.3 Physical Oceanographic observations

6.3.1 XCTD, XBT and XCP obserevations (Leg 1)

(1) Personnel

Tomohiro Nakamura	(Inst. of Low Temp. Sci., Hokkaido Univ.): Principal Investigator	-leg1-
Satoshi Okumura	(Global Ocean Development Inc., GODI)	-leg1-
Souichiro Sueyoshi	(GODI)	-leg1-
Kazuho Yoshida	(GODI)	-leg1-
Kazuya Yamashita	(GODI)	-leg1-

(2) Objectives

In order to investigate water mass structure and its variability and to estimate vertical mixing rate, vertical profiles of temperature, salinity, and current velocity were observed using XCTD, XBT, and XCP systems.

(3) Instruments and Parameters

The equipments and specifications of the XCTD, XBT, and XCP systems are shown in Tables 6.3.1.1 and 6.3.1.2, respectively;

Table 6.3.1.1 Equipments of XCTD, XBT and XCP.

XCTD	Probe	XCTD-1	Tsurumi-Seiki Co.
	Converter	MK-100	Tsurumi-Seiki Co.
	Software	WinXCTD software (Ver.1.08)	Tsurumi-Seiki Co.
XBT	Probe	T-7	Tsurumi-Seiki Co.
	Converter	MK-30	Tsurumi-Seiki Co.
	Software	XBT system (Ver.1.46)	Tsurumi-Seiki Co.
XCP	Probe	XCP	Sippican Inc.
	Receiver	MK-10N	Sippican Inc.
	Software	XCP menu program (Ver.1.0),	Sippican Inc., Tsurumi-Seiki Co.

Table 6.3.1.2 Specifications of XCTD, XBT and XCP.

	Parameter	Range	Accuracy
XCTD	Conductivity	0~60 mS/cm	+/- 0.03 mS/cm
	Temperature	-3~35 deg-C	+/- 0.02 deg-C
	Depth	0~1,000m	+/- 5m or +/-2%
XBT (T-7)	Temperature	-2.22~35.55 deg-C	+/- 0.2 deg-C
	Depth	0~760m	-
XCP	Temperature	0~35 deg-C	+/- 0.2 deg-C
	Current Velocity (east/west, north/south)	-70~+70 cm/sec	+/-3% RMS
	Depth	0~1,500m	+/- 7m or +/- 3%

(4) Methods

XCTD and XBT are expendable devices that measure temperature (XCTD and XBT) and salinity (only XCTD). We launched 44 XCTD probes (including 7 XCTD probes for correcting the sound velocity of MNBES, i.e., sites SB1-7) and 3 XBT probes by the automatic launcher and the hand launcher. The summary of XCTD and XBT observations are shown in Tables 6.3.1-3 and 6.3.1-4, respectively.

XCP is an expendable device that measures current velocity and temperature. Data collected by the probe as it falls through the water column is transferred to the buoy assembly at the sea surface. A radio frequency transmitter is contained within the buoy. The data acquisition box (MK-10N) accepts the radio frequency output of the probe in real time and converts the signal into a digital format. We launched 3 XCP probes. The summary of XCP observation is shown in Table 6.3.1-5.

(5) Preliminary Results

The results of XCTD, XBT, and XCP observations are shown in Figures 6.3.1-1 to 6.3.1-3, respectively. Figure 6.3.1-1 shows XCTD stations and the vertical sections of potential temperature and salinity along the course. The locations of XBT (XCP) stations and the vertical profiles of observed temperature (velocity) are shown in Figrue 6.3.1-2 (6.3.1-3).

(6) Data archive

XCTD, XBT and XCP data obtained during this cruise will be submitted to JAMSTEC and will be available via “R/V Mirai Data Web Page” in JAMSTEC home page under the JAMSTEC data policy.

Table 6.3.1.3 XCTD observation launching log

Station No.	Date	Launched time	Finish time	Launch Position Latitude	Launch Position Longitude	Measured Depth [m]	Water Depth [m]	Surface Temp. [deg-C]	Surface Salinity [PSU]	Probe S/N
SB01	2006/8/1	11:16:53	11:22	40-51.3331 N	142-19.6458 E	1036	1089	16.600	32.682	03042883
NC01	8/1	19:01:23	19:06	41-054340 N	144-00.3000 E	1036	3517	16.810	32.774	06037193
NC02	8/2	6:12:41	6:18	42-29.6380 N	144-18.1980 E	963	966	16.671	32.831	06037189
NC03	8/2	11:30:10	11:35	42-30.5879 N	144-19.7196 E	991	996	16.726	32.853	06037190
NC04	8/2	19:01:59	19:07	42-30.9214 N	144-19.6890 E	1002	1010	16.611	32.861	06037192
NC05	8/3	0:52:45	0:58	42-30.5637 N	144-19.6321 E	987	993	17.025	32.879	06037191
NC06	8/3	6:20:34	6:26	42-30.6271 N	144-19.7951 E	997	993	17.639	32.875	06037194
NC07	8/3	21:11:23	21:16	41-51.9134 N	143-57.2147 E	1035	1046	17.608	32.735	06037189
SB02	8/5	4:36:18	4:41	42-27.3424 N	139-38.0445 E	1036	2244	22.448	33.714	03042882
SB03	8/5	18:03:36	18:09	45-36.8481 N	140-44.8381 E	738	752	20.004	33.866	04120655
SB04	8/7	13:20:27	13:25	44-44.5582 N	144-25.3220 E	1035	1082	17.111	32.310	04120658
SB05	8/10	6:19:39	6:25	51-11.1188 N	149-09.1782 E	1035	1297	12.030	32.632	04120661
NC08	8/10	12:02:00	12:07	51-16.8192 N	149-05.9822 E	1033	1271	11.938	32.673	06037186
NC09	8/10	18:00:12	18:05	51-25.9678 N	149-07.8173 E	1035	1231	11.788	32.679	06037187
NC10	8/11	12:00:06	12:05	51-29.5773 N	149-08.3173 E	1035	1242	11.772	32.642	06037184
NC11	8/11	18:00:02	18:05	51-33.6947 N	149-17.0062 E	1035	1167	11.889	32.621	06037183
NC12	8/11	21:43:56	21:49	51-17.3703 N	149-12.2609 E	1035	1243	12.192	32.582	06037185
NC13	8/12	5:59:58	6:05	52-24.5314 N	150-04.9648 E	1034	1079	12.081	32.787	06058643
SB06	8/12	10:04:07	10:09	53-02.8812 N	150-07.3457 E	1025	1034	12.176	32.813	06058640
NC14	8/12	18:00:00	18:05	53-14.0522 N	149-57.5027 E	1036	1120	12.267	32.795	06037387
NC15	8/13	18:00:02	18:05	53-16.9316 N	149-52.2883 E	1035	1120	12.200	32.806	06058637
NC16	8/14	3:51:09	3:56	53-19.1933 N	149-44.2626 E	1100	1096	12.362	32.814	06058641
NC17	8/14	4:05:10	4:10	53-19.4087 N	149-44.2619 E	1100	1085	12.343	32.811	06058634
NC18	8/14	4:14:34	4:20	53-19.5926 N	149-44.2626 E	1090	1080	12.324	32.812	06058633
NC19	8/14	4:25:43	4:31	53-19.8135 N	149-44.2580 E	1094	1105	12.313	32.813	06058638
NC20	8/14	4:33:48	4:39	53-19.9839 N	149-44.2594 E	1100	1208	12.284	32.812	06058636
NC21	8/14	4:44:09	4:49	53-20.2028 N	149-44.2578 E	1100	1289	12.260	32.816	06058639
SB07	8/14	8:34:14	8:38	54-04.5876 N	149-23.2033 E	834	844	12.199	32.807	06058644
NC22	8/14	17:56:24	18:01	54-16.0370 N	149-11.7271 E	896	900	12.134	32.783	06037388
NC23	8/15	9:17:16	9:22	54-06.5113 N	149-13.3971 E	850	856	12.323	32.785	06037578
NC24	8/15	9:39:09	9:44	54-08.8191 N	149-13.4066 E	834	839	12.256	32.765	06037545
NC25	8/15	9:59:48	10:04	54-11.2272 N	149-13.4247 E	832	835	12.326	32.798	06037546
NC26	8/15	10:37:13	10:42	54-11.6742 N	149-13.4463 E	885	884	12.393	32.809	06037547
NC27	8/15	10:53:39	10:59	54-12.4109 N	149-12.9217 E	927	933	12.388	32.805	06037393
NC28	8/15	11:05:00	11:10	54-13.2129 N	149-11.5974 E	970	985	12.400	32.804	06037394

Table 6.3.1.3 XCTD observation launching log (continue)

Station No.	Date	Launched time	Finish time	Launch Position Latitude	Launch Position Longitude	Measured Depth [m]	Water Depth [m]	Surface Temp. [deg-C]	Surface Salinity [PSU]	Probe S/N
NC29	2006/8/15	11:15:35	11:21	54-13.6390 N	149-11.6343 E	1019	1024	12.407	32.798	06037549
NC30	8/15	11:32:35	11:38	54-14.4797 N	149-11.5906 E	964	970	12.393	32.793	06037548
NC31	8/15	11:49:44	11:55	54-15.9938 N	149-11.6066 E	896	901	12.311	32.792	06037389
NC32	8/15	12:03:52	12:09	54-17.5010 N	149-11.6105 E	853	863	12.266	32.783	06037390
NC33	8/15	12:14:41	12:20	54-19.0002 N	149-11.5990 E	819	826	12.168	32.795	06037391
NC34	8/15	12:25:23	12:30	54-20.4938 N	149-11.5698 E	788	796	12.173	32.809	06037392
NC35	8/15	13:22:39	13:28	54-17.4867 N	149-13.4073 E	856	860	12.150	32.805	06037395
NC36	8/15	18:00:02	18:05	53-10.9191 N	149-28.2264 E	1036	1157	12.568	32.783	06037398
NC37	8/15	23:52:15	23:57	52-07.9839 N	149-46.3941 E	919	926	12.486	32.763	06037397

Table 6.3.1.4 XBT observation launching log

Station No.	Date	Launched time	Finish time	Launch Position LAT (N)	Launch Position LON (E)	MD [m]	WD [m]	SST [deg-C]	SSS [PSU]	Probe Type	Launcher
NT01	2006/8/11	6:29:40	6:32	51-17.50	149-13.01	789	1244	11.976	32.645	T-7	Auto
NT02	8/13	5:38:06	5:40	53-17.11	150-05.81	789	1149	12.498	32.790	T-7	Auto
NT03	8/13	12:11:45	12:14	53-23.85	149-45.12	789	1254	12.108	32.806	T-7	Auto

Table 6.3.1.5 XCP observation launching log

Station No.	Date	Launched time	Finish time	Launch Position LAT (N)	Launch Position LON (E)	MD [m]	WD [m]	SST [deg-C]	SSS [PSU]	CD [deg]	CV [knot]	Probe S/N
XCP01	2006/8/11	21:30	21:37	51-17.3	149-12.2	1169	1245	12.193	32.577	309	0.3	05121011
XCP02	8/14	5:17	5:23	53-19.9	149-44.3	1256	1209	12.271	32.812	209	0.4	05121010
XCP03	8/15	10:24	10:28	54.11.7	149-13.3	858	885	12.370	32.811	139	0.0	05121012

Acronyms in Table 6.3.1.3 to Table 6.3.1.5 are as follows;

SST: Sea surface temperature [deg-C] measured by Continuous Sea Surface Monitoring System

SSS: Sea surface salinity [PSU] measured by Continuous Sea Surface Monitorring System

MD: Maximum measured depth [m]

WD: Water Depth [m]

CD: Surface Current Direction [deg] measured by Doppler Sonar

CV: Surface Current Velocity [knot] measured by Doppler Sonar

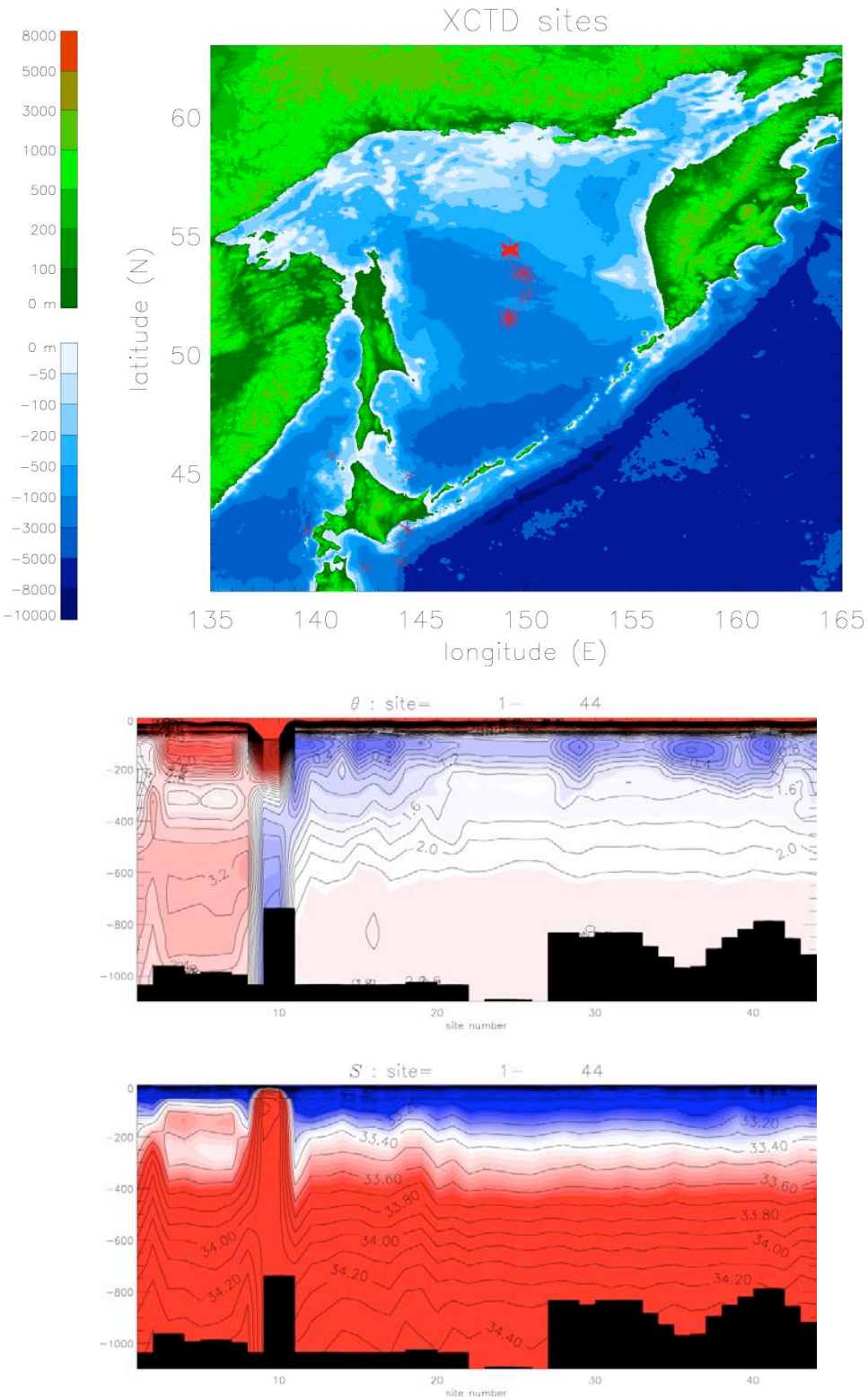

Figure 6.3.1.1: (Upper) The locations of XCTD stations and (lower) the vertical sections of potential temperature and salinity along the ship track.

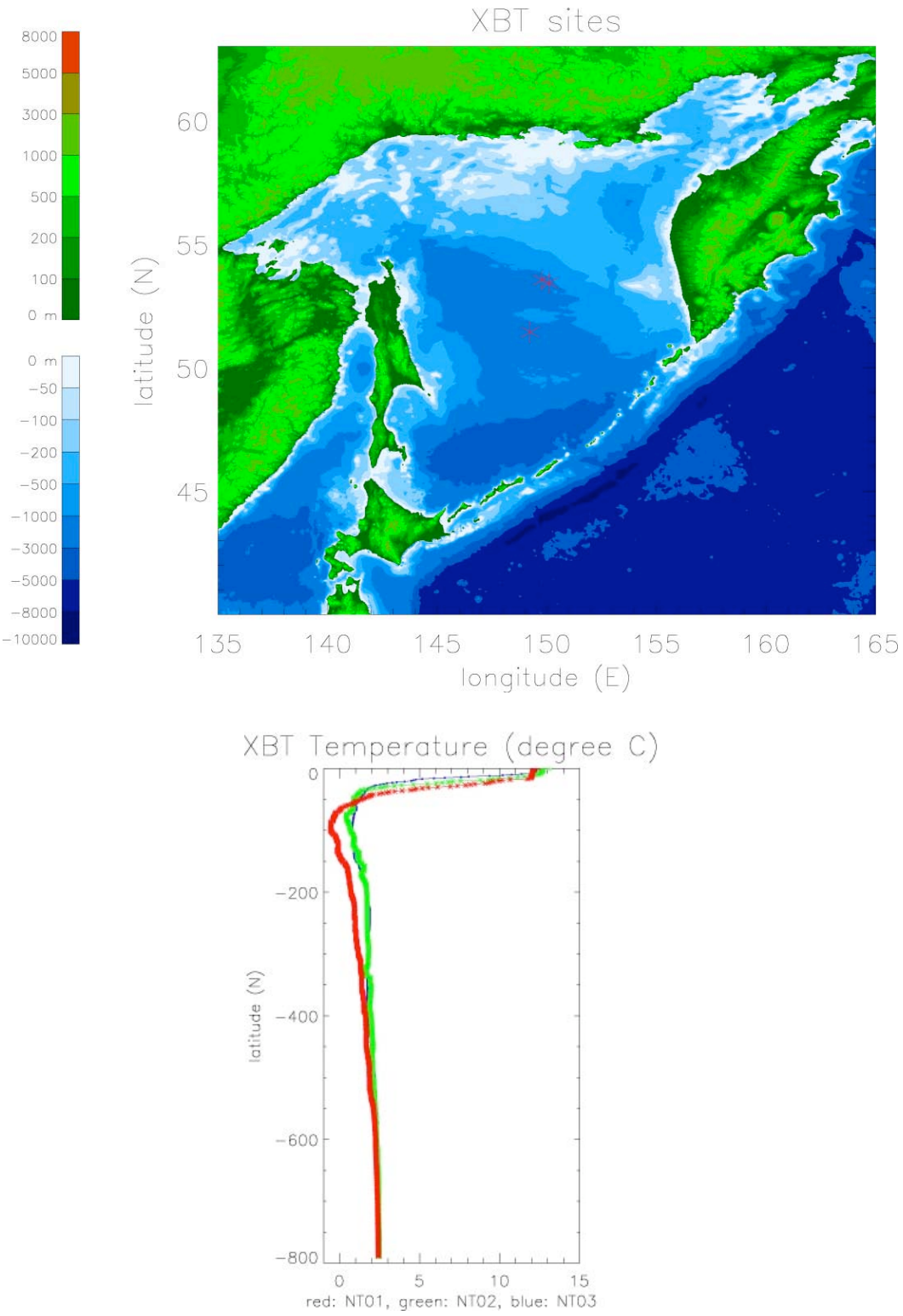

Figure 6.3.1.2: (Left) The locations of XBT stations and (right) the vertical sections of observed temperature.

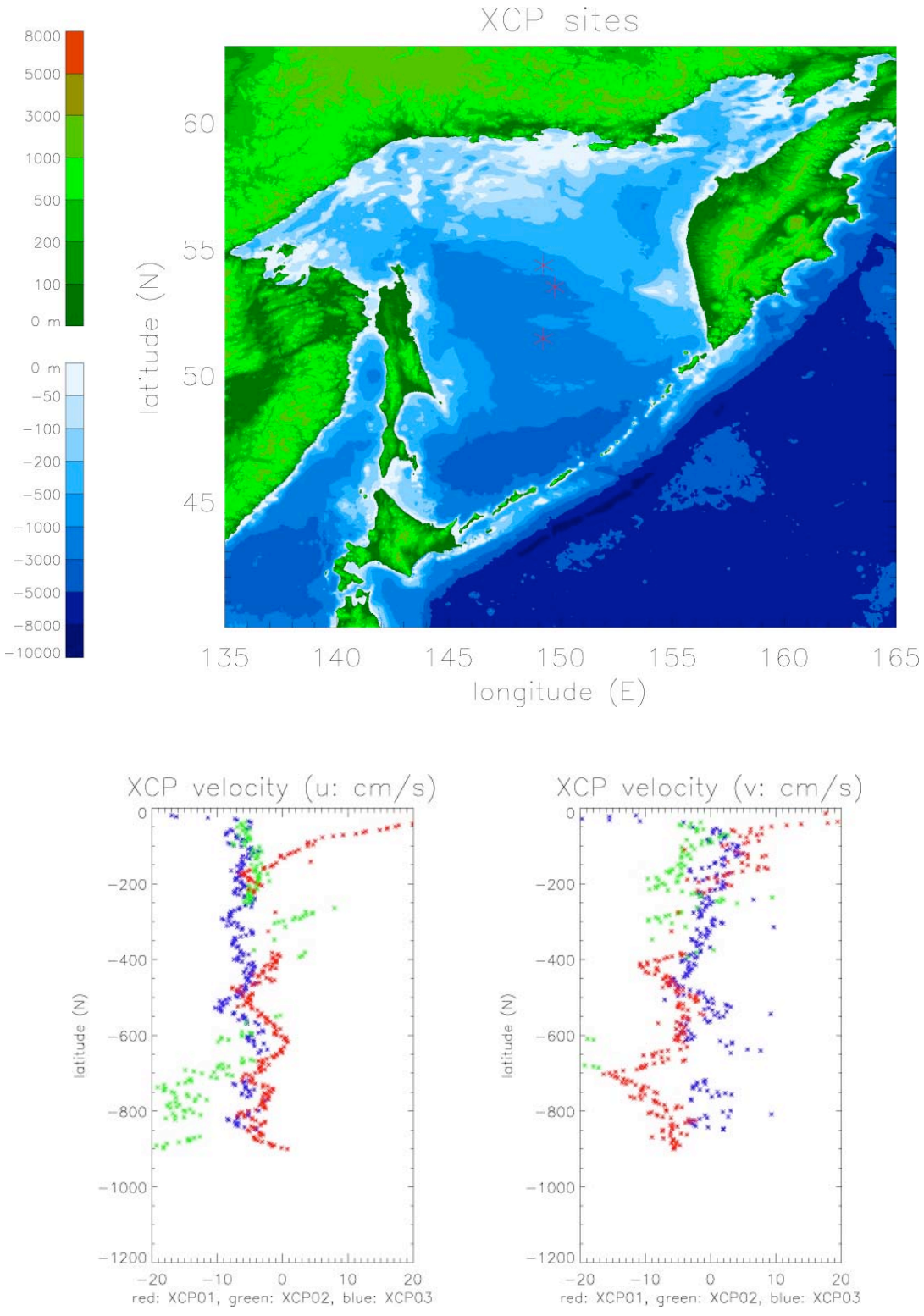

Figure 6.3.1.3: (Upper) The locations of XCP stations and (Lower) the vertical profiles of observed velocity.

6.3.2 Shipboard ADCP (Leg 1)

(1) Personnel

Tomohiro Nakamura (Inst. of Low Temp. Sci., Hokkaido Univ.): Principal Investigator
Satoshi Okumura (Global Ocean Development Inc., GODI)
Souichiro Sueyoshi (GODI)
Kazuho Yoshida (GODI)
Kazuya Yamashita (GODI)

(2) Objective

Continuous measurement of the current profile along the ship track, except in the Russian exclusive economic zone (EEZ), using the shipboard ADCP which provides current velocity [cm/s] and echo intensity [dB] of each depth cell.

(3) Instruments and Methods

Continuous upper ocean current measurement along ship's track, except in the Russian EEZ, was conducted using hull-mounted Acoustic Doppler Current Profiler, RD Instruments VM-75 system, which is installed on the centerline and approximately 28 m aft from the bow. The firmware version was 5.59 and the data acquisition software was VmDas Ver.1.40. The system consists of following components;

1. a 75 kHz Broadband (coded-pulse) profiler with 4-beam Doppler sonar operating at 75 KHz (RD Instruments, USA), mounted with beams pointing 30 degrees from the vertical and 45 degrees azimuth from the keel;
2. the Ship's main gyro compass (TG-6000 Tokimec, Japan), continuously providing ship's heading measurements to the ADCP;
3. a GPS navigation receiver (Trimble DS4000) providing position fixes;
4. a personal computer running data acquisition software. The clock of the logging PC is adjusted to GPS time every 10 minutes.

Raw data was recorded in beam coordinates, and then converted to the earth coordinates using ship's heading data from ship's main gyrocompass. The position fix data from ship's navigation system was also recorded in NMEA0183 format and merged with ensemble data in the VmDas.
The ADCP was configured for 5-m processing bin, a 12-m blanking interval. The sound velocity was fixed on 1,450m/s. The transducer depth was 6.5 m; 100 velocity measurements were made at 5-m intervals starting 24-m below the surface. Every ping was recorded as raw ensemble data (.ENR). Also, 60 seconds and 300 seconds averaged data were recorded as short-term average (.STA) and long-term average (.LTA) data, respectively. Major parameters are listed in Table 6.3.2.1.

(4) Preliminary results

Current vectors averaged over 30 minutes are plotted along the ship track for two near surface layers (Figure 6.3.2.1).

(5) Data archives

The data obtained during this cruise will be submitted to the JAMSTEC and will be opened to the public via "R/V Mirai Data Web Page" in the JAMSTEC home page under JAMSTEC data policy.

(6) Remarks

The observation was not conducted in the EEZ of Russian Federation.

Table 6.3.2.1 Major parameters

Bottom-Track Commands

BP = 001	Bottom Tracking ON/Pings per Ensemble 4 Aug. 2006 11:10UTC – 9 Aug. 0:56UTC 19 Aug. 21:57UTC – 20 Aug. 0:00UTC
BP = 000	Bottom Tracking OFF 1 Aug. 13:17UTC – 4 Aug. 11:09UTC 10 Aug. 4:45UTC – 16 Aug. 2:00UTC 17 Aug. 14:17UTC – 19 Aug. 21:56UTC
BA = 020	The minimum value for a valid bottom detection (0 – 255 Counts)
BC = 200	The minimum correlation magnitude for valid velocity data (0 – 255 Counts)
BM = 4	Bottom-Track mode (4 or 5)
BX = 7000	Maximum Tracking Depth (0 – 9999 decimeter)

Environmental Sensor Commands

EA = +00000	Heading Alignment (1/100 deg)
EB = +00000	Heading Bias (1/100 deg)
EC = 1450	Sound Velocity (1400 – 1600m/s)
ED = 00065	Transducer Depth (0 - 65535 dm)
EF = +0001	Pitch/Roll Divisor/Multiplier (pos/neg) [1/99 - 99]
EH = 00000	Heading (1/100 deg)
ES = 35	Salinity (0-40 pp thousand)
ET = 0000	Sea Water Temperature (-5.00 – +40.00 degC)
EX = 00000	Coord Transform (Xform:Type; Tilts; 3Bm; Map)
EZ = 0020001	Sensor Source (C;D;H;P;R;S;T) C(0): Sound velocity calculate using Fixed value (EC) D(0): Manual ED H(2): External synchro P(0), R(0): Manual EP, ER (0 degree) S(0): Manual ES T(1): Internal transducer sensor

Timing Commands

TE = 00:00:02.00	Time per Ensemble (hrs:min:sec.sec/100)
TP = 00:02.00	Time per Ping (min:sec.sec/100)

Water-Track Commands

WA = 255	False Target Threshold (Max) (0-255 counts)
WB = 0	Mode 1 Bandwidth Control (0=Wid,1=Med,2=Nar)
WC = 064	Low Correlation Threshold (0-255)
WD = 111 111 110	Data Out (V;C;A PG;St;Vsum Vsum^2;#G;P0)
WE = 5000	Error Velocity Threshold (0-5000 mm/s)
WF = 1200	Blank After Transmit (cm)
WG = 001	Percent Good Minimum (0-100%)
WM = 1	Profiling Mode (1-8)
WN = 100	Number of depth cells (1-128)
WP = 00001	Pings per Ensemble (0-16384)
WS = 0500	Depth Cell Size (cm)
WV = 999	Mode 1 Ambiguity Velocity (cm/s radial)

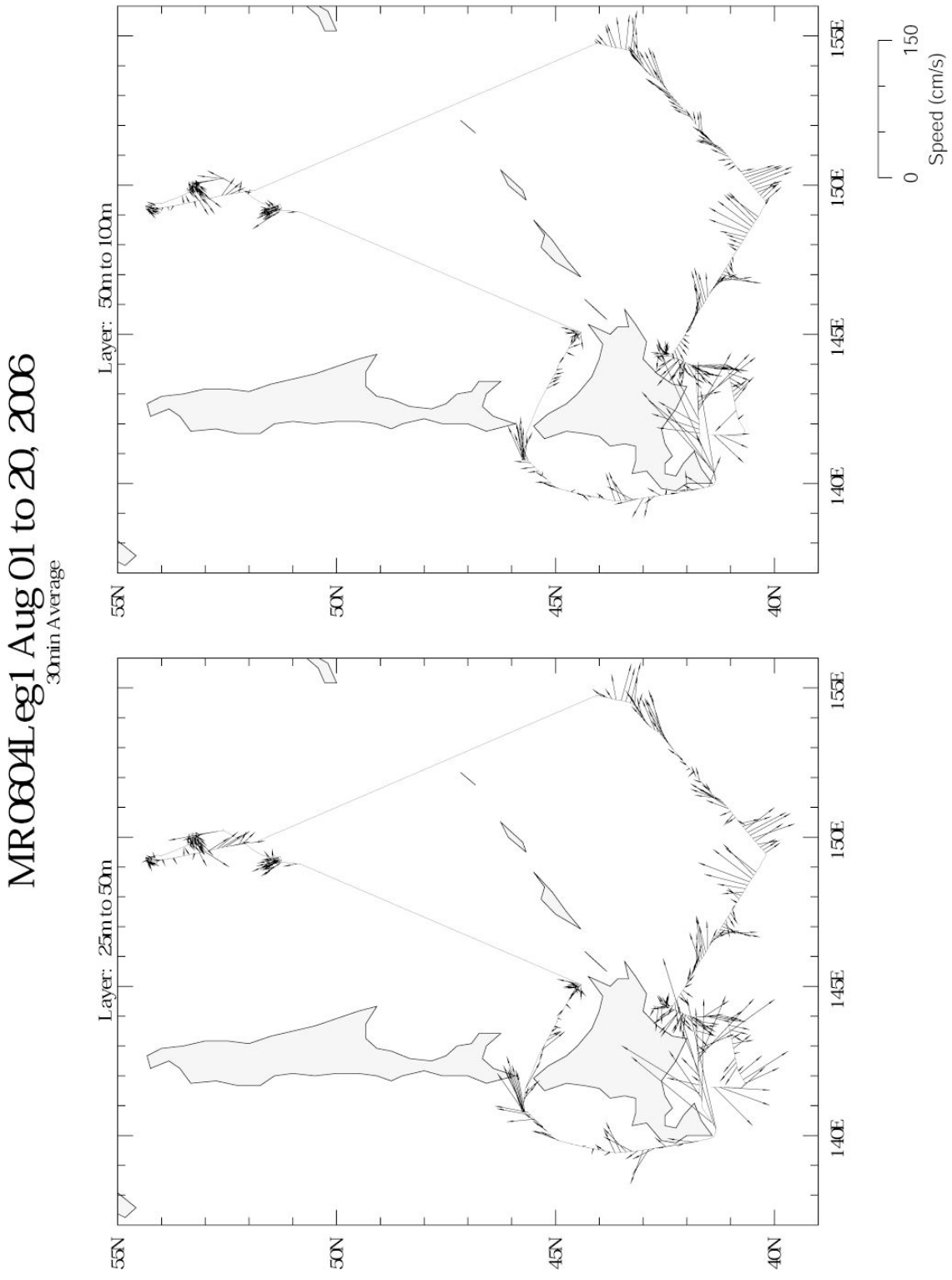

Figure 6.3.2.1 Current vectors plotted along the ship track for the near surface layers.

6.3.3 CTD hydrocast and water sampling

(1) Personnel

Leg.1: Hiroshi Matsunaga (Marine Works Japan Co. Ltd.): Operation leader
Tetsuya Tanaka (Marine Works Japan Co. Ltd.)

Leg.2: Tomoyuki Takamori (Marine Works Japan Co. Ltd.): Operation leader
Naoko Takahashi (Marine Works Japan Co. Ltd.)

(2) Objectives

Investigation of oceanic structure and water sampling.

(3) Measured parameters

Temperature, conductivity, dissolved oxygen, fluorescence

(4) Instruments and Methods

4-1 Overview of the equipment

The CTD system, SBE 911plus system (Sea-Bird Electronics, Inc., USA), is a real time data system with the CTD data transmitted from a SBE 9plus underwater unit via a conducting cable to the SBE 11plus deck unit. The SBE 11plus deck unit is a rack-mountable interface which supplies DC power to the underwater unit, decodes the serial data stream, formats the data under microprocessor control, and passes the data to a companion computer. The serial data from the underwater unit is sent to the deck unit in RS-232 NRZ format using a 34560 Hz carrier-modulated differential-phase-shift-keying (DPSK) telemetry link. The deck unit decodes the serial data and sends them to a personal computer (Hewlett Packard Vectra VL, Intel(r) Celeron(tm), Microsoft Windows98 2nd edition) to display, at the same time, to storage in a disk file using SBE SEASOFT software.

The SBE 911pus system acquires data from primary, secondary and auxiliary sensors in the form of binary numbers corresponding to the frequency or voltage outputs from those sensors at 24 samples per second. The calculations required to convert from raw data to engineering units of the parameters are performed by the SBE SEASOFT in real-time. The same calculations can be carried out after the observation using data stored in a disk file.

The SBE 911plus system controls the 36-position SBE 32 Carousel Water Sampler. The Carousel accepts 12-litre Niskin-X water sample bottles (General Oceanics, Inc., USA). Bottles were fired through the RS-232C modem connector on the back of the SBE 11plus deck unit while acquiring real time data. The 12-litre Niskin-X water sample bottle is equipped externally with two stainless steel springs. The external springs are ideal for applications such as the trace metal analysis because the inside of the sampler is free from contaminants from springs.

4-2 Detail of sensors

The system used in this cruise is summarized as follows:

Under water unit:	SBE, Inc., SBE 9plus, S/N 0357
Temperature sensor:	SBE, Inc., SBE 03-04/F, S/N 031359
Conductivity sensor:	SBE, Inc., SBE 04C, S/N 041172

Oxygen sensor:	SBE, Inc., SBE 43, S/N 430205
Pump:	SBE, Inc., SBE 5T, S/N 053293
Altimeter:	Benthos, Inc, PSA-916T, S/N 1157
Fluorometer:	Seapoint sensors,Inc, S/N 2579
Deck unit:	SBE, Inc., SBE 11plus, S/N 11P9833-0344
Carousel Water Sampler:	SBE, Inc., SBE 32, S/N 3227443-0278
Water sample bottle:	General Oceanics, Inc., 12-litre Niskin-X

4-3 Data processing

SEASOFT consists of modular menu driven routines for acquisition, display, processing, and archiving of oceanographic data acquired with SBE equipment, and is designed to work with a compatible personal computer. Raw data are acquired from instruments and are stored as unmodified data. The conversion module DATCNV uses the instrument configuration and calibration coefficients to create a converted engineering unit data file that is operated on by all SEASOFT post processing modules. Each SEASOFT module that modifies the converted data file adds proper information to the header of the converted file permitting tracking of how the various oceanographic parameters were obtained. The converted data is stored in rows and columns of ASCII numbers. The last data column is a flag field used to mark scans as good or bad.

The SEASOFT-Win32 (Ver. 5.27b) was used for processing the CTD data. Descriptions and settings of the parameters for the SEASOFT were written as follows.

DATCNV converted the raw data to scan number, pressure, depth, time elapsed, temperature, conductivity, oxygen voltage, altitude, desent rate, modulo error count and pump status. DATCNV also extracted bottle information where scans were marked with the bottle confirm bit during acquisition. The duration was set to 3.0 seconds, and the offset was set to 0.0 seconds.

ROSSUM created a summary of the bottle data. The bottle position, date, time were output as the first two columns. Oxigen, Salinity, sigma-theta and potential temperature were averaged over 3.0 seconds.

ALIGNCTD converted the time-sequence of oxygen sensor outputs into the pressure sequence to ensure that all calculations were made using measurements from the same parcel of water. For a SBE 9plus CTD with the ducted temperature and conductivity sensors and a 3000 rpm pump, the typical net advance of the conductivity relative to the temperature is 0.073 seconds. So, the SBE 11plus deck unit S/N 11P9833-0344 was set to advance the primary conductivity for 1.73 scans (1.75/24 = 0.073 seconds). Oxygen data are also systematically delayed with respect to depth mainly because of the long time constant of the oxygen sensor and of an additional delay from the transit time of water in the pumped plumbing line. This delay was compensated by 6 seconds advancing oxygen sensor output (oxygen voltage) relative to the pressure.

WILDEDIT marked extreme outliers in the data files. The first pass of WILDEDIT obtained an accurate estimate of the true standard deviation of the data. The data were read in blocks of 1000 scans. Data greater than 10 standard deviations were flagged. The second pass computed a standard deviation over the same 1000

scans excluding the flagged values. Values greater than 20 standard deviations were marked bad. This process was applied to pressure, depth, temperatur, conductivity, oxygen voltage, altitude, decent rate and oxygen outputs.

CELLTM used a recursive filter to remove conductivity cell thermal mass effects from the measured conductivity. Typical values used were thermal anomaly amplitude alpha = 0.03 and the time constant 1/beta = 7.0.

FILTER performed a low pass filter on pressure with a time constant of 0.15 seconds. In order to produce zero phase lag (no time shift) the filter runs forward first then backwards.

WFILTER performed a median filter to remove spikes in the fluorescence data.. A median value was determined from a window of 49 scans.

SECTION selected a time span of data based on scan number in order to reduce a file size. The minimum number was set to be the starting time when the CTD package was beneath the sea-surface after activation of the pump. The maximum number was set to be the end time when the package came up from the surface.

LOOPEDIT marked scans where the CTD was moving less than the minimum velocity of 0.0 m/s (traveling backwards due to ship roll).

DERIVE was used to compute oxygen.

BINAVG averaged the data into 1 m depth bins. The center value of the first bin was set equal to the bin size. The bin minimum and maximum values are the center value plus and minus half the bin size. Scans with pressures greater than the minimum and less than or equal to the maximum were averaged. Scans were interpolated so that a data record exists every m.

DERIVE was re-used to compute salinity, sigma-theta and potential temperature

SPLIT was used to split data into the down cast and the up cast.

(5) Preliminary Results

Total 10 and 31 casts of CTD measurements have been carried out in Leg1 and 2, respectively (see table 6.3.3.1). Vertical profile of temperature, salinity, oxygen, fluorescence with pressure are shown in Figure 6.3.3.1 – 10 for leg.1, and Figure6.3.3.11-41 for leg.2.

We also compared CTD-salinity and Bottle-salinity, CTD-oxygen and Bottle-oxygen. It was all bottle data that used for comparison. The results are shown in Figure.6.3.3.42-,43 and table 6-3-2.

(6) Data archive

All raw and processed data files will be submitted to the Data Management Office (DMO) and will be opened to public via “R/V MIRAI Data Web Page” in the JAMSTEC web site.

Table.6.3.3.1 CTD/ water sampling casts

MR06-04Leg1 CTD Cast Table

STNNBR	CASTNO	Date(UTC)	Time(UTC)		Start Position		Sample	CTD data file name	Remarks
		yyyy/mm/dd	Start	End	Latitude	Longitude			
1	1	2006/8/2	1:09	2:13	42-27.52N	144-17.40E	Routine	S01M01	
2	1	2006/8/4	0:40	1:31	41-51.85N	143-56.53E	Large Volume	S02M01	
2	1	2006/8/4	4:07	5:11	41-51.40N	143-56.72E	Routine	S02M02	
3	1	2006/8/6	1:53	2:41	45-45.13N	140-40.12E	Large Volume	S03M01	
3	2	2006/8/7	0:03	0:55	45-45.44N	140-47.06E	Routine	S03M02	
4	1	2006/8/7-8	23:59	0:55	44-31.63N	145-00.34E	Large Volume	S04M01	
4	2	2006/8/8	3:07	4:14	44-31.73N	144-59.62E	Routine	S04M02	
7	1	2006/8/10-11	23:57	1:05	51-16.43N	149-12.40E	Routine	S07M01	
6	1	2006/8/12-13	23:47	0:52	53-16.71N	150-04.68E	Routine	S06M01	
5	1	2006/8/14-15	23:37	0:32	54-19.15N	149-15.93E	Routine	S05M01	

MR06-04Leg2 CTD Cast Table

STNNBR	CASTNO	Date(UTC)	Time(UTC)		Start Position		Sample	CTD data file name	Remarks
		yyyy/mm/dd	Start	End	Latitude	Longitude			
15	1	2006/8/31	16:37	17:02	70-00.02N	168-00.00W	Large Volume		
15	2	2006/8/31	18:05	18:23	69-59.98N	168-00.00W	Routine		
14	1	2006/9/1	0:54	1:12	71-00.04N	165-59.87W	Routine		
13	1	2006/9/2	0:43	1:04	71-59.99N	165-59.91W	Routine		
12EX	1	2006/9/2	16:28	16:57	72-36.01N	166-59.98W	Large Volume		
12EX	2	2006/9/2	17:52	18:13	72-35.98N	166-00.26W	Routine		
13	2	2006/9/3	0:29	0:55	72-00.00N	165-59.99W	Large Volume		
12	1	2006/9/3	16:28	16:54	72-25.89N	166-57.75W	Large Volume		
12	2	2006/9/3	18:05	18:24	72-25.87N	166-57.95W	Routine		
16	1	2006/9/5	16:28	16:46	68-30.00N	167-59.98W	Routine		
17	1	2006/9/6	16:22	16:38	66-59.97N	167-00.01W	Routine		
18	1	2006/9/7	19:00	19:14	63-59.87N	168-59.93W	Routine		
19	1	2006/9/8	1:21	1:46	63-00.39N	167-29.58W	Large Volume		
19	2	2006/9/8	2:28	2:42	63-00.03N	167-30.00W	Routine		
20	1	2006/9/8	16:25	16:40	62-00.06N	169-00.06W	Routine		
20	2	2006/9/8	17:37	17:51	62-00.09N	168-59.93W	Routine		
21	1	2006/9/9	16:22	16:42	62-00.06N	172-00.07W	Routine		
22	1	2006/9/10	1:51	2:20	61-59.61N	176-00.12W	Routine		
23	1	2006/9/10	22:46	23:41	60-09.55N	179-27.83W	Large Volume		
23	2	2006/9/11	0:46	1:49	60-09.61N	179-28.05W	Routine		
24	1	2006/9/11	22:01	22:59	60-15.71N	179-25.30W	Routine		
24	2	2006/9/13	0:42	1:35	60-15.84N	179-25.15W	Large Volume		
26	1	2006/9/13	16:31	17:05	60-00.01N	175-59.96W	Routine		
27	1	2006/9/14	2:39	3:06	59-59.85N	171-59.94W	Routine		
28	1	2006/9/14	16:32	17:00	60-00.01N	168-59.98W	Routine		
29	1	2006/9/15	1:21	1:48	58-30.00N	167-30.03W	Large Volume		
29	2	2006/9/15	2:31	2:50	58-29.95N	167-30.12W	Routine		
30	1	2006/9/16	18:25	18:54	58-30.00N	172-00.02N	Routine		
31	1	2006/9/17	1:25	1:51	58-22.95N	169-59.84W	Routine		
32	1	2006/9/17	16:24	16:51	57-00.01N	167-30.03W	Routine		
33	1	2006/9/18	2:13	2:43	55-46.33N	166-13.38W	Routine		

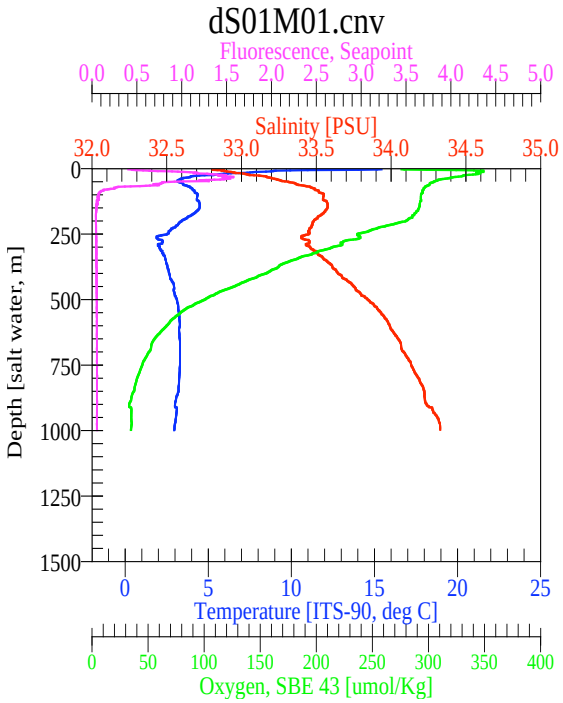

Fig.6.3.3.1

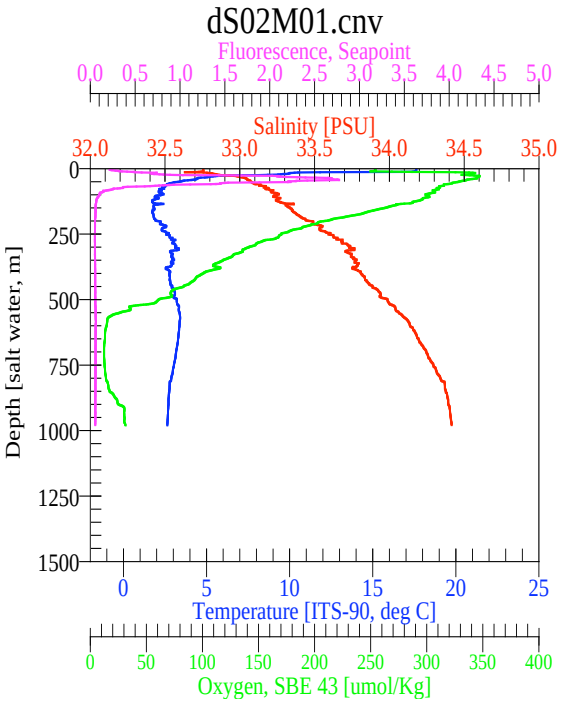

Fig.6.3.3.2

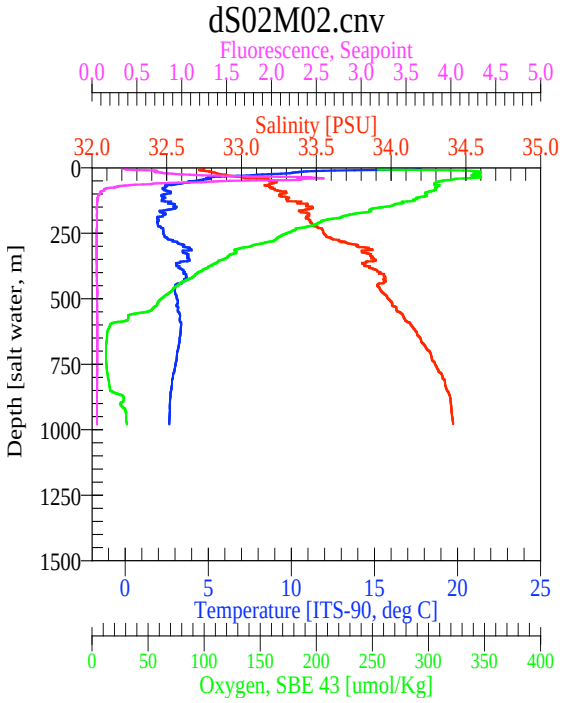

Fig.6.3.3.3

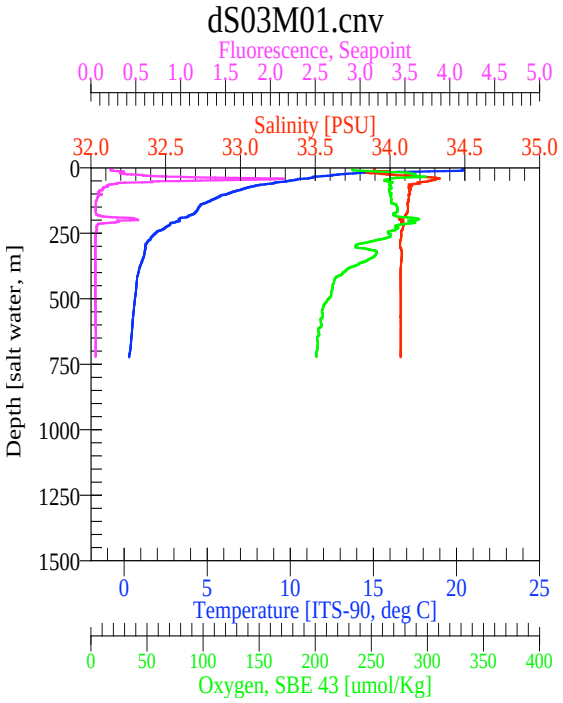

Fig.6.3.3.4

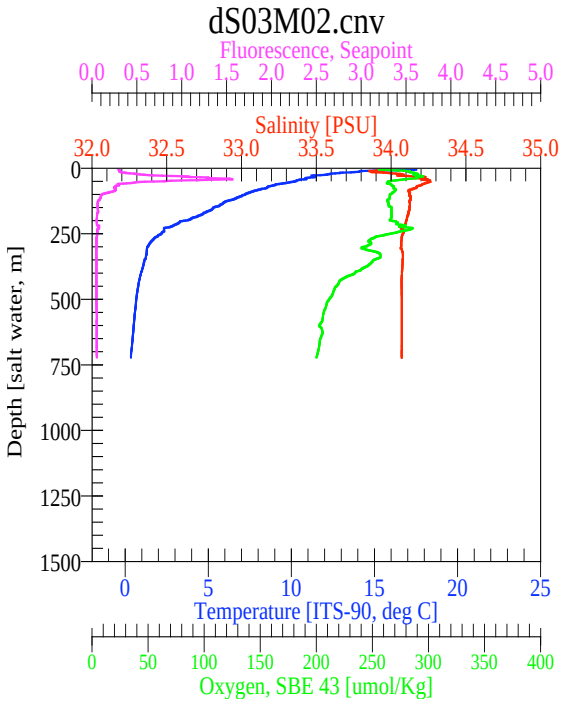

Fig.6.3.3.5

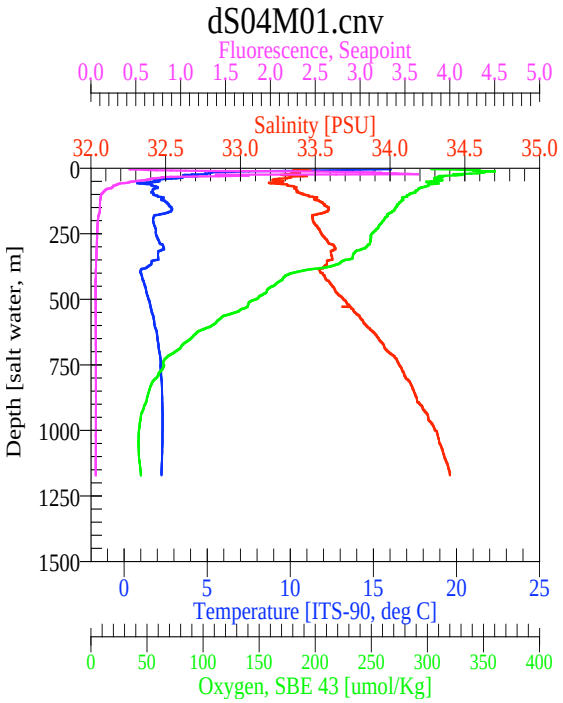

Fig.6.3.3.6

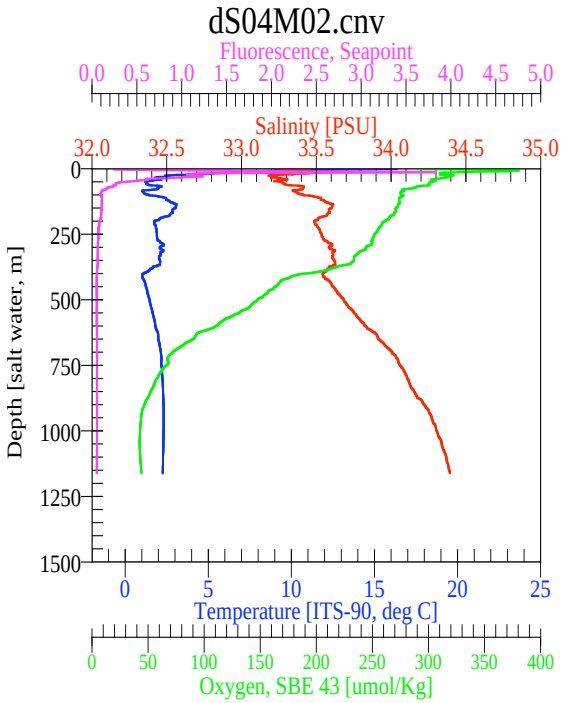

Fig.6.3.3.7

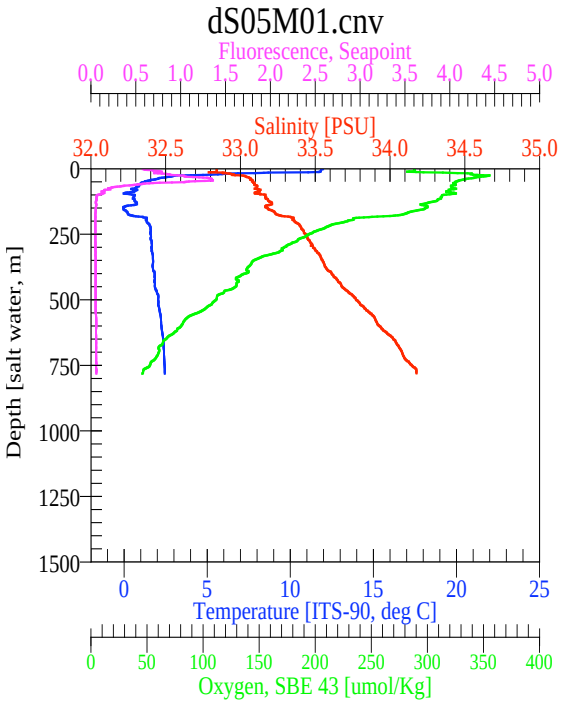

Fig.6.3.3.8

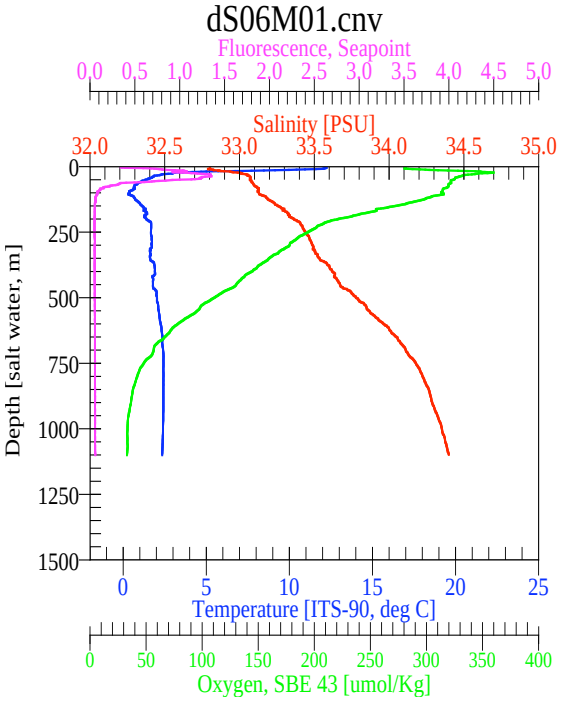

Fig.6.3.3.9

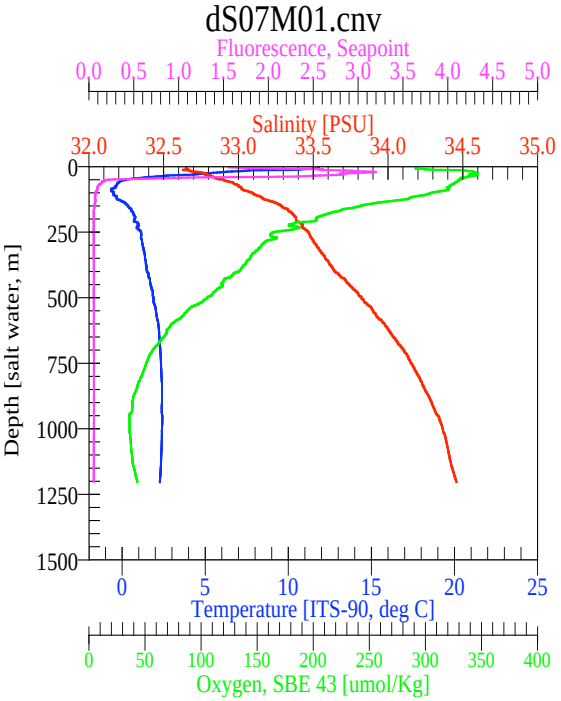

Fig.6.3.3.10

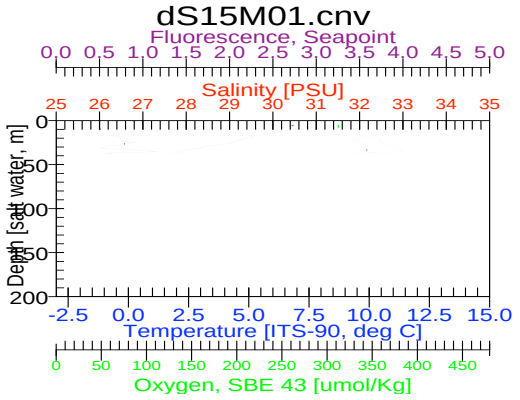

Fig.6.3.3.11

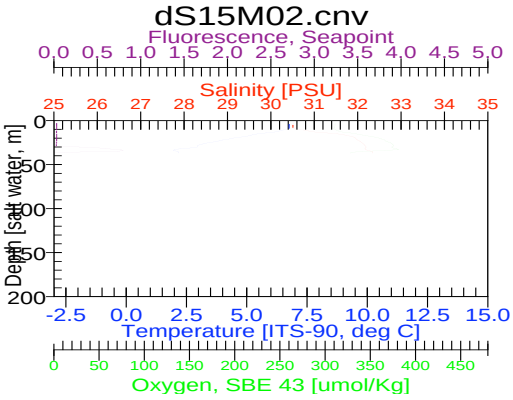

Fig.6.3.3.12

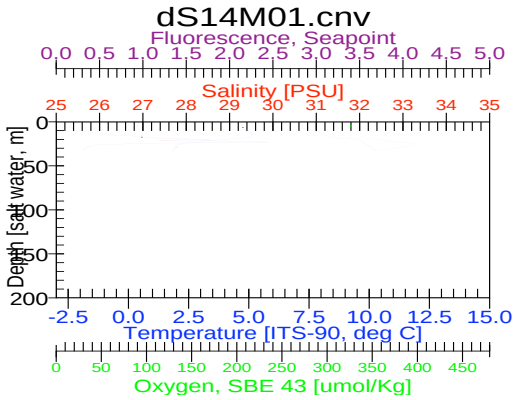

Fig.6.3.3.13

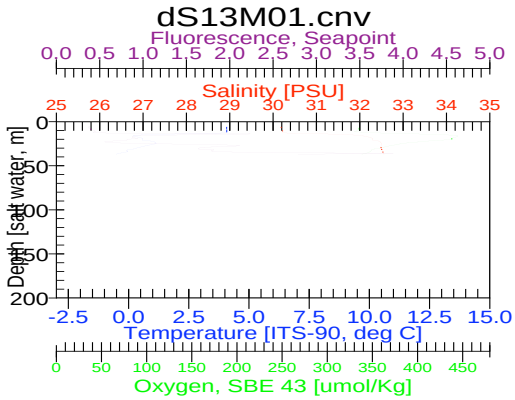

Fig.6.3.3.14

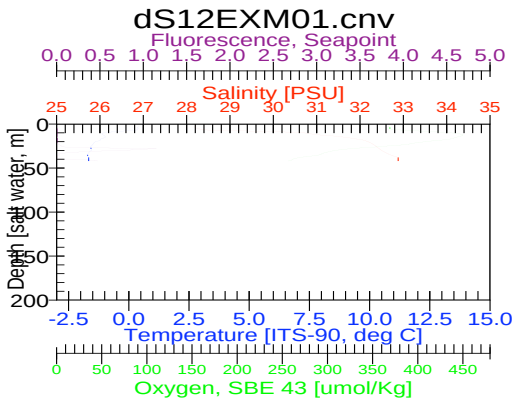

Fig. 6.3.3.15

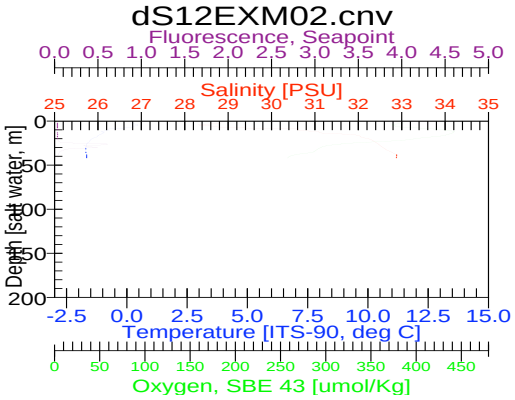

Fig. 6.3.3.16

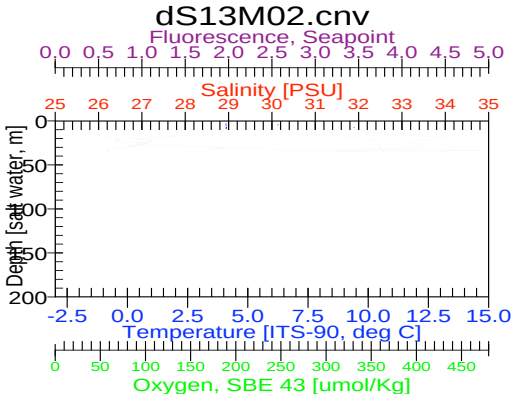

Fig. 6.3.3.17

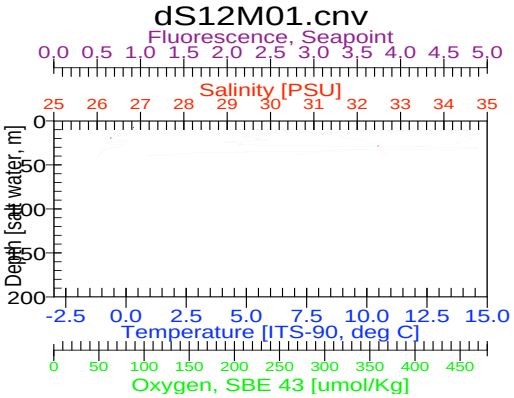

Fig. 6.3.3.18

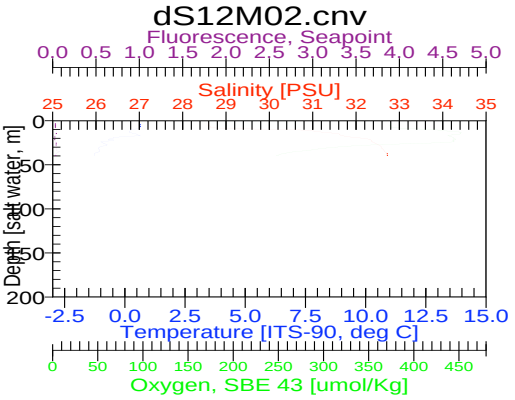

Fig. 6.3.3.19

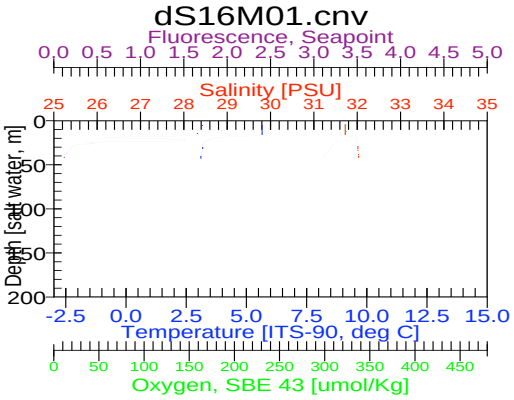

Fig. 6.3.3.20

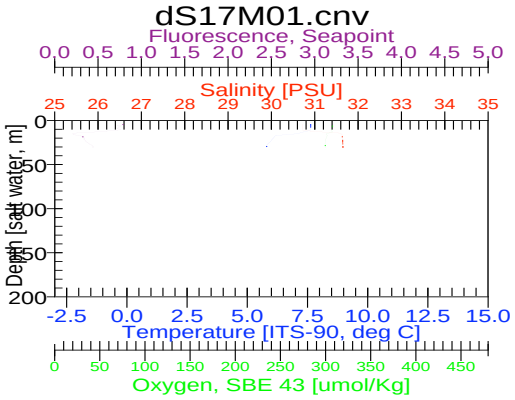

Fig. 6.3.3.21

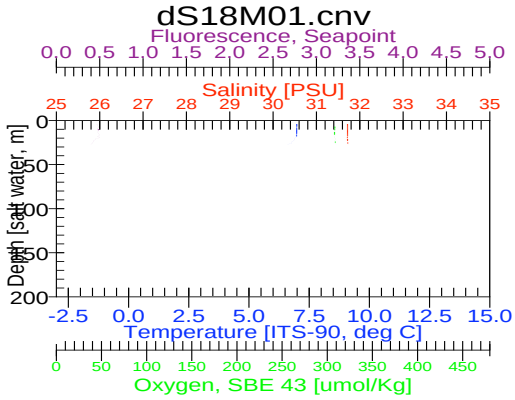

Fig. 6.3.3.22

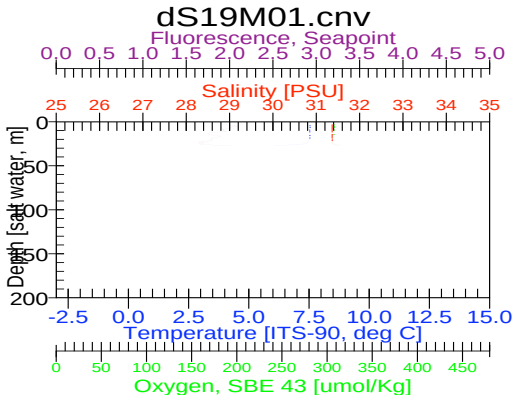

Fig. 6.3.3.23

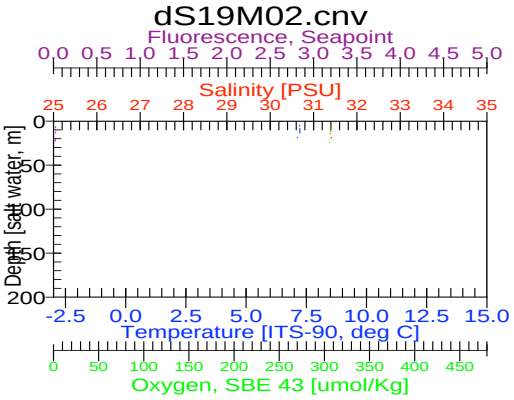

Fig. 6.3.3.24

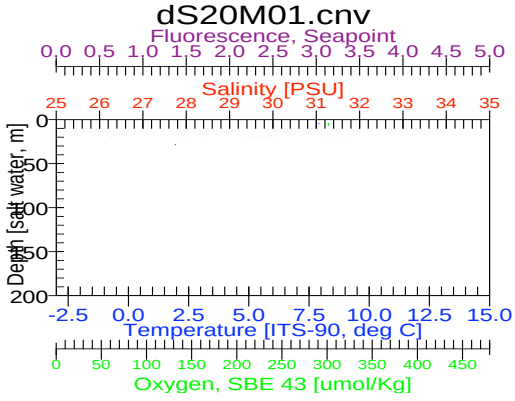

Fig. 6.3.3.25

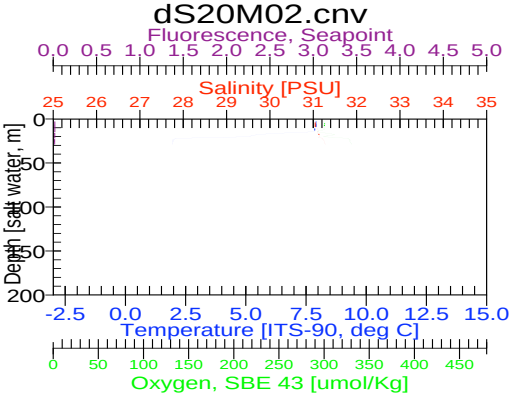

Fig. 6.3.3.26

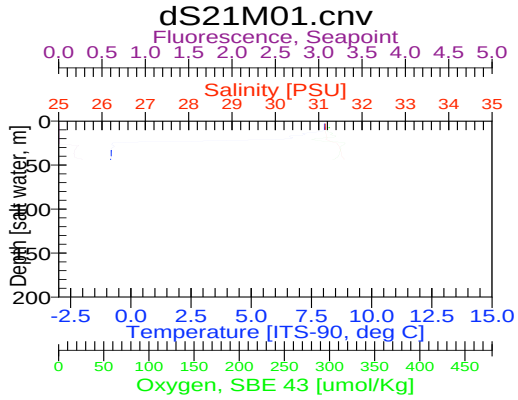

Fig. 6.3.3.27

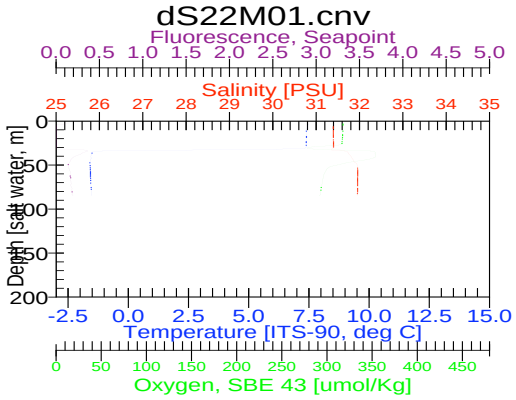

Fig. 6.3.3.28

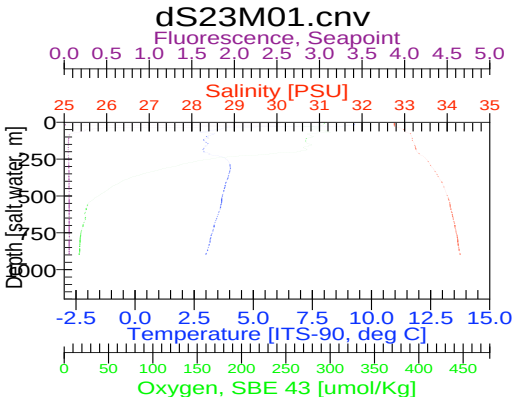

Fig. 6.3.3.29

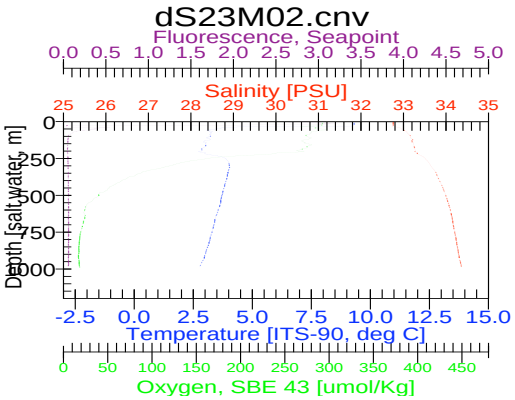

Fig. 6.3.3.30

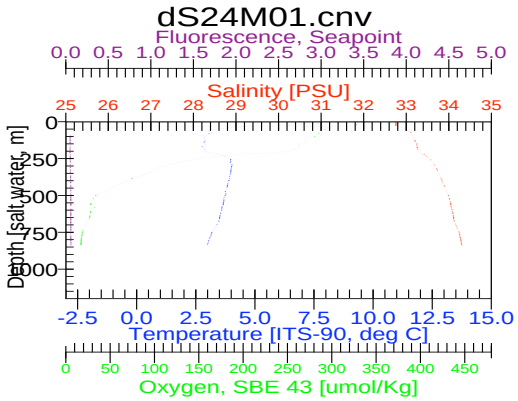

Fig. 6.3.3.31

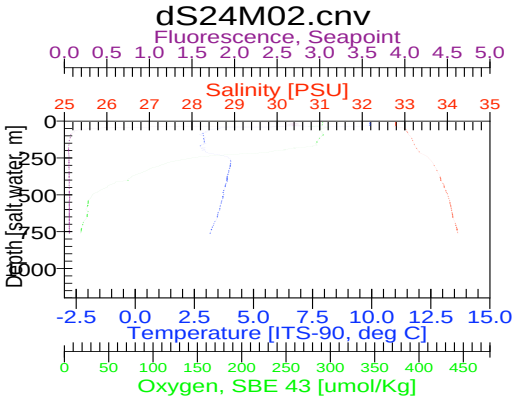

Fig. 6.3.3.32

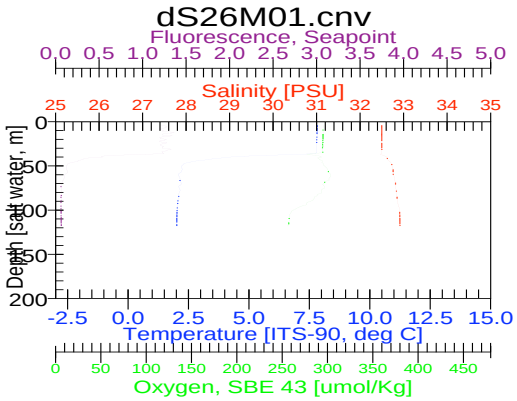

Fig. 6.3.3.33

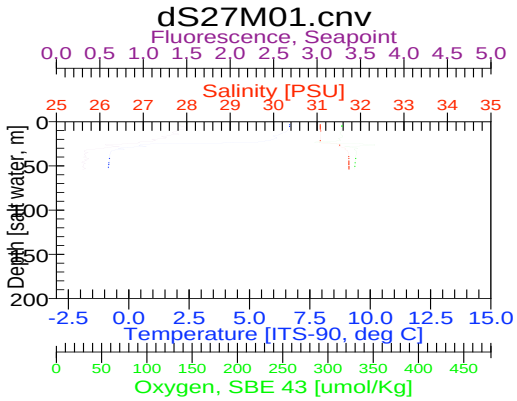

Fig. 6.3.3.34

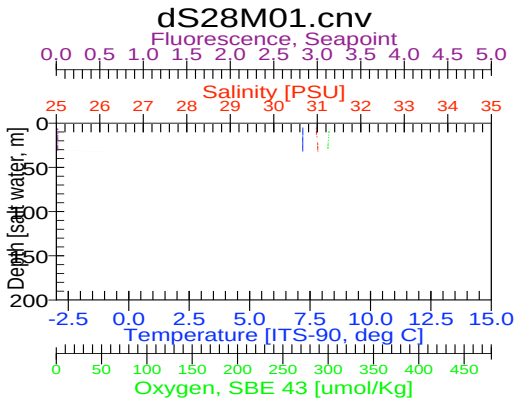

Fig. 6.3.3.35

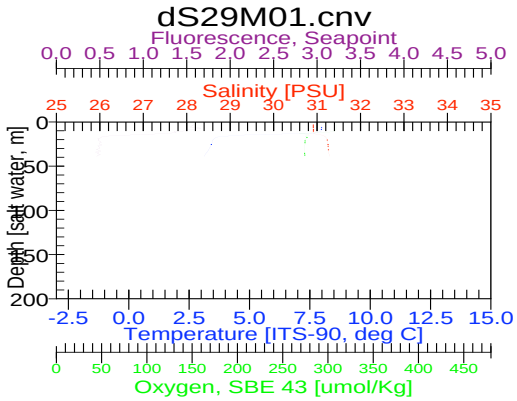

Fig. 6.3.3.36

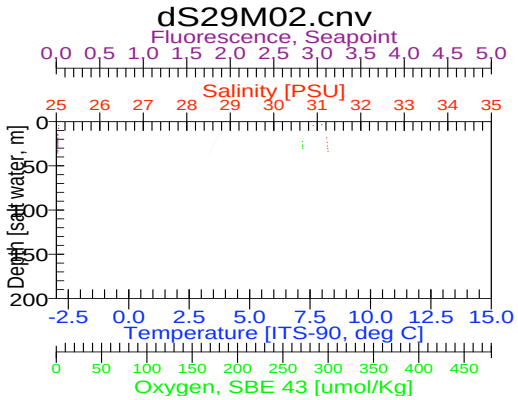

Fig. 6.3.3.37

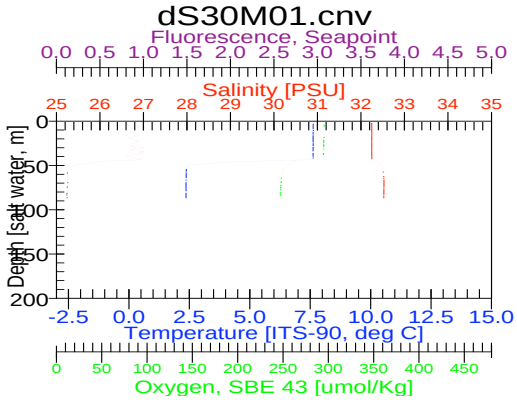

Fig. 6.3.3.38

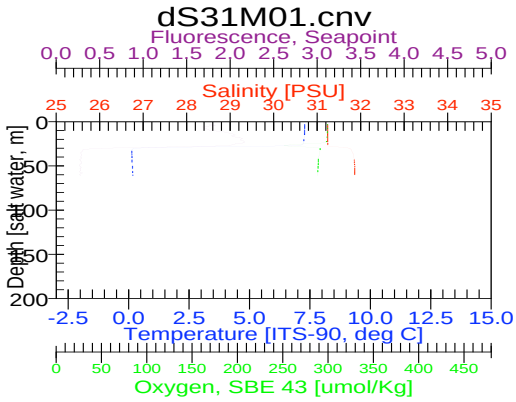

Fig. 6.3.3.39

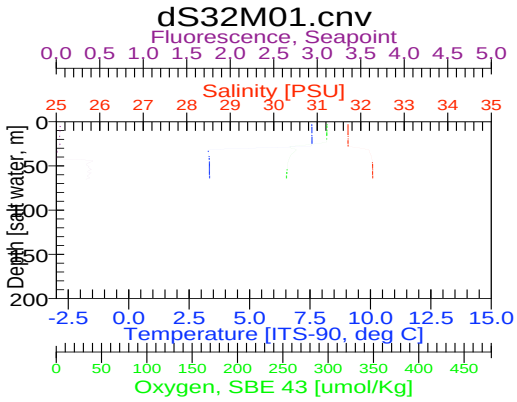

Fig. 6.3.3.40

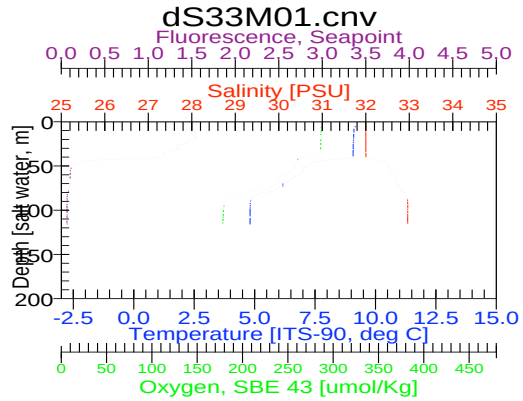

Fig. 6.3.3.41

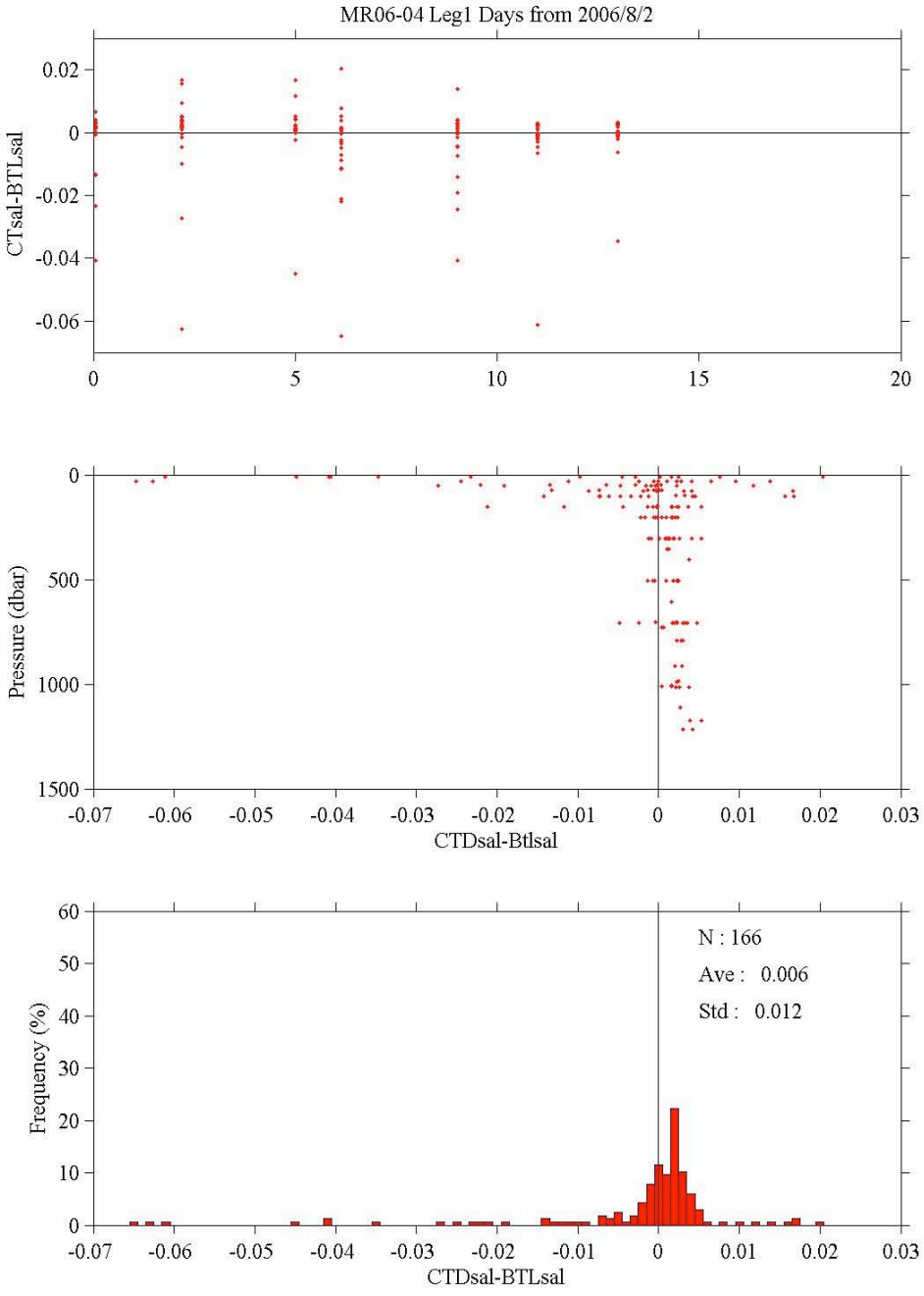
MR06-04 Leg1 Days from 2006/8/2
CTsal-BTLsal
0.02
0
-0.02
-0.04
-0.06
0
5
10
15
20
Pressure (dbar)
0
500
1000
1500
-0.07
-0.06
-0.05
-0.04
-0.03
-0.02
-0.01
0
0.01
0.02
0.03
CTDsal-Btlsal
Frequency (%)
60
50
40
30
20
10
0
N : 166
Ave : 0.006
Std : 0.012
CTDsal-BTLsal

Fig. 6.3.3.42

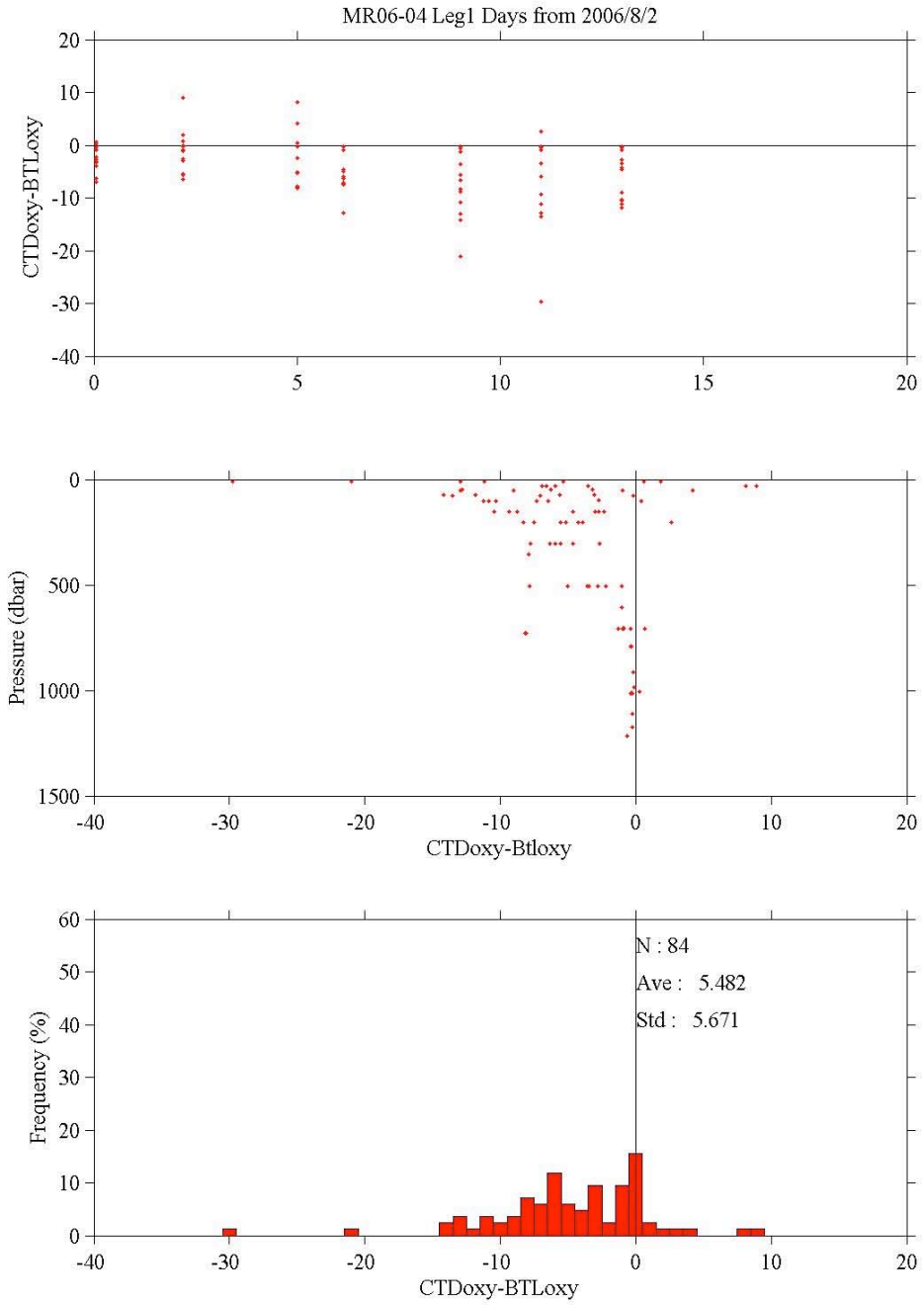
MR06-04 Leg1 Days from 2006/8/2
CTDoxy-BTLoxy
Pressure (dbar)
CTDoxy-Btloxy
Frequency (%)
CTDoxy-BTLoxy
N : 84
Ave : 5.482
Std : 5.671

Fig. 6.3.3.43

Table. 6.3.3.2 Comparison of oxygen data between CTD sensor detection and bottle water.

Leg.1	Number	Absolute average	Standard deviation
CTDsal – Btlsal	166	0.006	0.012
CTDoxy - Btloxy	84	5.482	5.671

Leg.2	Number	Absolute average	Standard deviation
CTDsal – Btlsal	191	0.003	0.005
CTDoxy - Btloxy	110	4.956	6.803

6.4 Chemical Oceanographic Observation

6.4.1. Salinity

(1) Personnel

Leg.1: Tatsuya Tanaka (Marine Works Japan Co. Ltd.) : Operation Leader
Hiroshi Matsunaga (Marine Works Japan Co. Ltd.)
Leg.2: Naoko Takahashi (Marine Works Japan Co. Ltd.) : Operation reader

(2) Objectives

To measure bottle salinity obtained by CTD casts, bucket sampling and EPCS.

(3) Measure parameters

Salinity of sampled seawater

(4) Instruments and Methods

4-1 Salinity Sample Collection

Seawater samples were collected with 12 liter Niskin-X bottles (Among 36 bottles, 12 bottles were coated with Teflon and others were not so), a bucket, and EPCS. The salinity sample bottle of the 250ml brown glass bottle was used to collect the sample water. The sample bottle was sealed with a plastic insert thimble and a screw cap. Basically, each bottle was rinsed three times with the sample water, and was filled with sample water to the bottle shoulder. From Station S23 to 33, each bottle was rinsed once with the sample water because we used the bottles that were washed and dried. Its inner cap and thimble were also thoroughly rinsed. The bottle was stored more than 24 hours (12 hours during leg.2) in 'AUTOSAL ROOM' before the salinity measurement.

4-2 Instruments and Methods

The salinity analysis was carried out on R/V MIRAI during the cruise of MR06-04 Leg1 using the salinometer (Model 8400B "AUTOSAL" ; Guildline Instruments Ltd.: S/N 62827), with additional peristaltic-type intake pump (Ocean Scientific International, Ltd.). We also used two pairs of precision digital thermometers (Model 9540 ; Guildline Instruments Ltd.). One thermometer monitored an ambient temperature and the other monitored a bath temperature.

The specifications of AUTOSAL salinometer and thermometer are shown as follows ;

Salinometer (Model 8400B "AUTOSAL" ; Guildline Instruments Ltd.)

Measurement Range	:	0.005 to 42 (PSU)
Accuracy	:	Better than ±0.002 (PSU) over 24 hours without restandardization
Maximum Resolution	:	Better than ±0.0002 (PSU) at 35 (PSU)

Thermometer (Model 9540 ; Guildline Instruments Ltd.)

Measurement Range	:	-180 to +240 deg C
Resolution	:	0.001
Limits of error ±deg C	:	0.01 (24 hours @ 23 deg C ±1 deg C)
Repeatability	:	±2 least significant digits

The measurement system was almost same as Aoyama et al. (2002). The salinometer was operated in the air-conditioned ship's laboratory at a bath temperature of 24 deg C. An ambient temperature

varied from approximately 19 deg C to 24 deg C, while a bath temperature is very stable and varied within +/- 0.002 deg C on rare occasion. We measured sub-standard seawater and confirmed that the salinometer was stable before the routine measurement of the day. The measurement for each sample was done with a double conductivity ratio that is defined as median of 31 times reading of the salinometer. Data collection was started in 25 second after filling sample to the cell during Leg.1. From station S15 to 32, the reading of salinometer was started 20 seconds after sample was filled to the cell and at the station S33, the reading salinometer was started 5 seconds after filling sample to the cell. It took about 15 second to collect 31 readings by a personal computer. Data were taken for the ranging from sixth to eighth filling of the cell. In case the difference between the double conductivity ratio of these two fillings is smaller than 0.00002, the average value of these double conductivity ratio was used to calculate the bottle salinity with the algorithm for practical salinity scale, 1978 (UNESCO, 1981). If the difference was greater than or equal to 0.00003, we measured next filling of the cell. In case of the double conductivity ratio of eighth or ninth filling did not satisfy the criteria above, we measured tenth and eleventh filling of the cell and the median of the double conductivity ratios of five fillings are used to calculate the bottle salinity.

The measurement was conducted about 12 hours per day (typically from 8:00 to 20:00) during Leg.1 and 8 hours during Leg.2, respectively and the cell was cleaned with soap or thin-ethanol or both after the measurement of the day. We measured totally 216 and 328 samples during legs.1 and 2, respectively.

The type and number of samples are shown as follows ;

Table 6.4.1-1: Type and number of samples

Type of samples	Number of samples (Leg.1)	Number of Samples (Leg.2)
Samples for CTD and Bucket	201	298
Samples for EPCS	15	30
Total	216	328

4-3 Standard Seawater

Standardization control of the salinometer (serial number: 62827) was set to 508 for Leg.1 and 406 for Leg.2 and all the measurements were done by this setting. We used IAPSO Standard Seawater (SSW) batch P147 which conductivity ratio was 0.99982 (double conductivity ratio is 1.99964) as the standard for salinity. And we measured the SSW in order to correct the measured salinity every station. We totally measured 22 and 32 bottles during Legs. 1 and 2, respectively.

The specifications of SSW used in this cruise are shown as follows ;

Standard seawater (SSW)

batch	:	P147
conductivity ratio	:	0.99982
salinity	:	34.993
preparation date	:	6-Jun.-2006

4-4 Sub-Standard Seawater

We also used sub-standard seawater which was obtained from 2,500-m depth in MR06-02 cruise filtered by Millipore filter (pore size of 0.45 μm), which was stored in a 20 liter polyethylene container and stirred for at least 24 hours before measuring. It was measured every six or eight samples in order to check the drift of the salinometer. During the whole measurements, there was no detectable

sudden drift of the salinometer.

(5) Preliminary Results

5-1 Replicate Samples

We took 28 and 48 pairs of replicate samples during Legs.1 and 2, respectively. Figures 6.4.1.1 and 6.4.1.2 show the histograms of the absolute difference between replicate samples. There were 24 questionable measurements of replicate samples during Leg.2. For Leg.1, the average and the standard deviation of the absolute deference of replicate samples were respectively 0.00018 and 0.00015 in salinity. For Leg.2, the standard deviation of the absolute deference of replicate samples was 0.007 in salinity.

5-2 Standard Seawater

The average and standard deviation of SSW were respectively 34.9923 and 0.0009 in salinity. After correction for the double conductivity ratio every station, the average and standard deviation were respectively 34.9929 and 0.0002 in salinity.

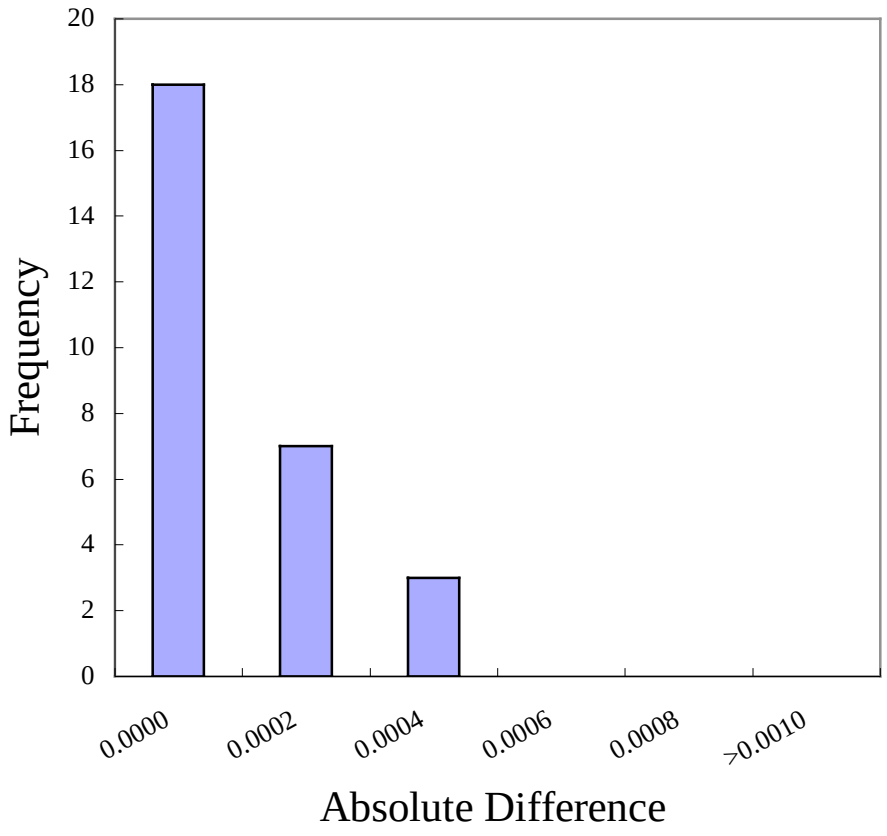

Fig. 6.4.1.1 The histogram of absolute difference between replicate samples during Leg.1

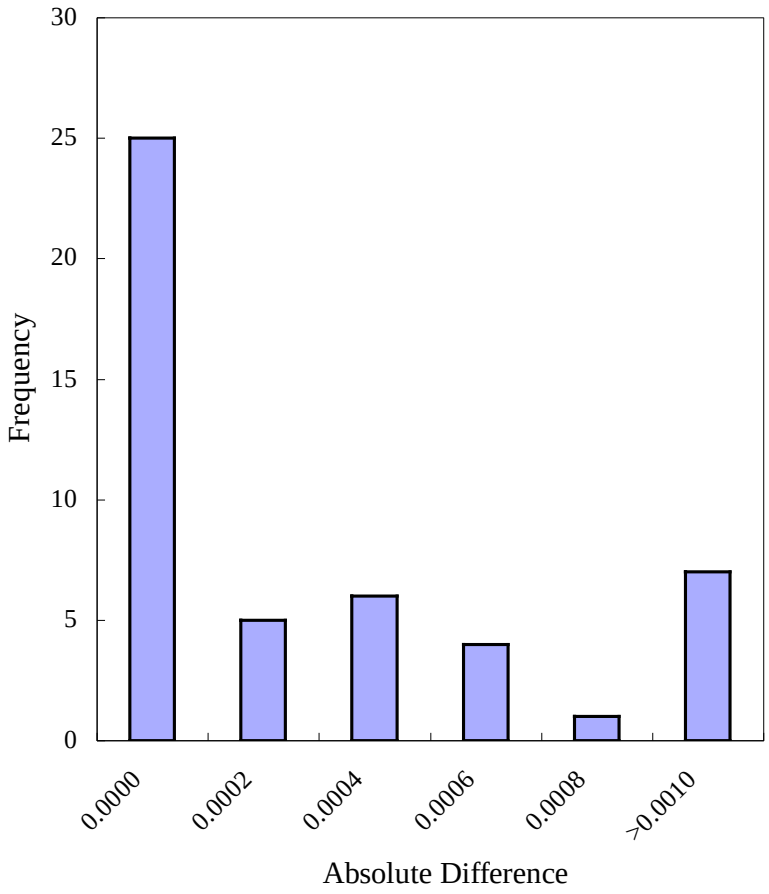

Fig. 6.4.1.2 The histogram of absolute difference between replicate samples during Leg.2

(6) Data Archives

All data will be submitted to JAMSTEC Data Management Office (DMO) and is currently under its control.

(7) References

Aoyama, M., T. Joyce, T. Kawano and Y. Takatsuki : Standard seawater comparison up to P129. Deep-Sea Research, I, Vol. 49, 1103～1114, 2002

UNESCO : Tenth report of the Joint Panel on Oceanographic Tables and Standards. UNESCO Technical Papers in Marine Science, 36, 25 pp., 1981

6.4.2 Sea surface monitoring

(1) Personnel

Leg.1: Keisuke Wataki (Marine Works Japan Co. Ltd.)

Leg2: Kimiko Nishijima (Marine Works Japan Co. Ltd.)

(2) Objectives

To measure salinity, temperature, dissolved oxygen, and fluorescence of near-sea surface water.

(3) Measured parameters

Salinity, temperature, dissolved oxygen, and fluorescence of near-sea surface water.

(4) Instruments and Methods

The Continuous Sea Surface Water Monitoring System (Nippon Kaiyo Co. Ltd.) has five kind of sensors and can automatically measure salinity, temperature (two systems), dissolved oxygen and fluorescence in near-sea surface water continuously, every 1-minute. Salinity is calculated by conductivity on the basis of PSS78. This system is located in the “sea surface monitoring laboratory” on R/V MIRAI. This system is connected to shipboard LAN-system. Measured data is stored in a hard disk of PC every 1-minute together with time and position of ship, and displayed in the data management PC machine.

Near-surface water was continuously pumped up to the laboratory and flowed into the Continuous Sea Surface Water Monitoring System through a vinyl-chloride pipe. The flow rate for the system is controlled by several valves and was 12L/min except with fluorometer (about 0.3L/min). The flow rate is measured with two flow meters.

Specification of the each sensor in this system of listed below.

a) Temperature and Conductivity sensor

SEACAT THERMOSALINOGRAPH

Model: SBE-21, SEA-BIRD ELECTRONICS, INC.

Serial number: 2126391-2641

Measurement range: Temperature -5 to +35℃, Conductivity 0 to 6.5 S m-1

Accuracy: Temperature 0.01℃ 6month-1,Conductivity 0.001 S m-1 month-1

Resolution: Temperatures 0.001℃, Conductivity 0.0001 S m-1

b) Bottom of ship thermometer

Model: SBE 3S, SEA-BIRD ELECTRONICS, INC.

Serial number: 032175

Measurement range: -5 to +35℃

Resolution: ±0.001℃

Stability: 0.002℃ year-1

c) Dissolved oxygen sensor

Model: 2127A, HACH ULTRA ANALYTICS JAPAN, INC.
Serial number: 44733
Measurement range: 0 to 14 ppm
Accuracy: ±1% at 5℃ of correction range
Stability: 1% month-1

d) Fluorometer

Model: 10-AU-005, TURNER DESIGNS
Serial number: 5562 FRXX
Detection limit: 5 ppt or less for chlorophyll a
Stability: 0.5% month-1 of full scale

e) Flow meter

Model: EMARG2W, Aichi Watch Electronics LTD.
Serial number: 8672
Measurement range: 0 to 30 l min-1
Accuracy: ±1%
Stability: ±1% day-1

The monitoring Periods (UTC) during this cruise are listed below.

Leg.1:

Start : 2006/08/01 11:31 Stop : 2006/08/08 23:58
Start : 2006/08/10 05:46 Stop : 2006/08/16 01:05
Start : 2006/08/17 15:30 Stop : 2006/08/19 05:59

Leg.2:

Start : 2006/08/21 11:17 Stop : 2006/08/28 13:58
Start : 2006/08/28 19:19 Stop : 2006/08/30 19:19
Start : 2006/08/30 21:14 Stop : 2006/09/07 00:19
Start : 2006/09/07 02:44 Stop : 2006/09/19 14:49
Start : 2006/09/19 20:30 Stop : 2006/09/27 22:52

(5) Preliminary Result

Preliminary data of temperature (Bottom of ship thermometer), salinity, dissolved oxygen, fluorescence at sea surface between this cruise are shown in Fig.6.4.2.1~8. We collected to compare salinity sensor and bottle data for onetime per day, Dissolve Oxygen sensor and bottle data for everystation. They are shown in Fig.6.4.2.9~16. All the salinity samples were analyzed by the Guildline 8400B, dissolve oxygen samples were analyzed by the KIMOTO DOT-01.

(6) Data archive

The data were stored on a magnetic optical disk, which will be submitted to the Data Management Office (DMO) JAMSTEC, and will be opened to public via "R/V MIRAI Data Web Page" in JAMSTEC homepage.

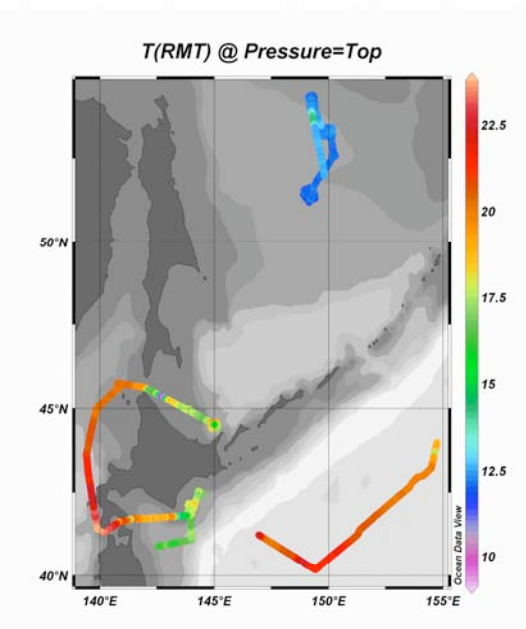

Fig.6.4.2.1 Contour line of Temperature (Leg.1).

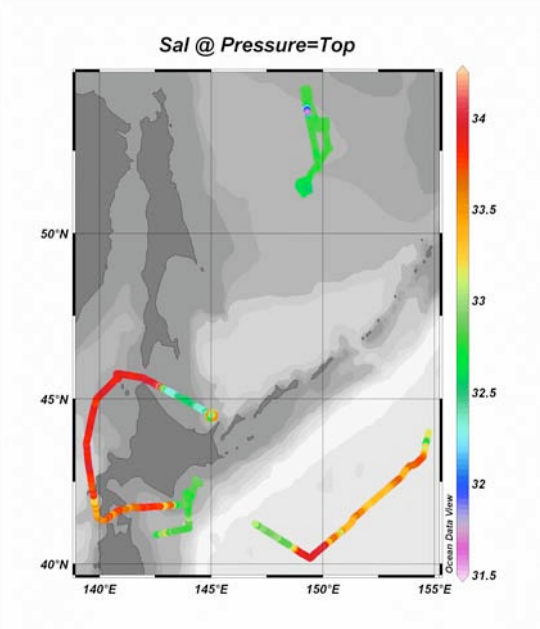

Fig.6.4.2.2 Contour line of salinity (Leg.1)

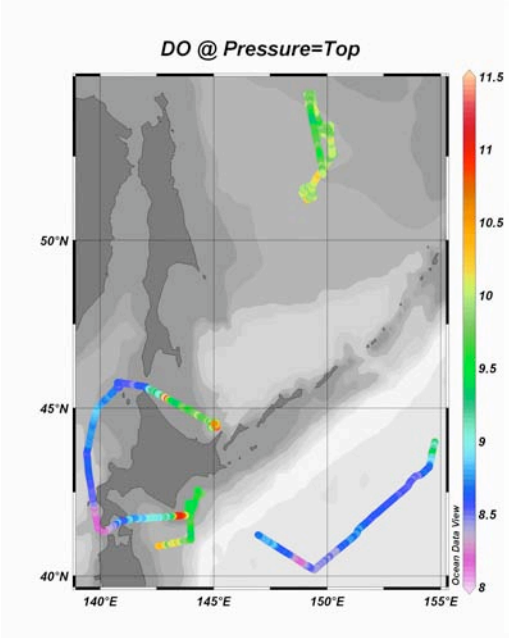

Fig.6.4.2.3 Contour line of dissolved oxygen (Leg.1)

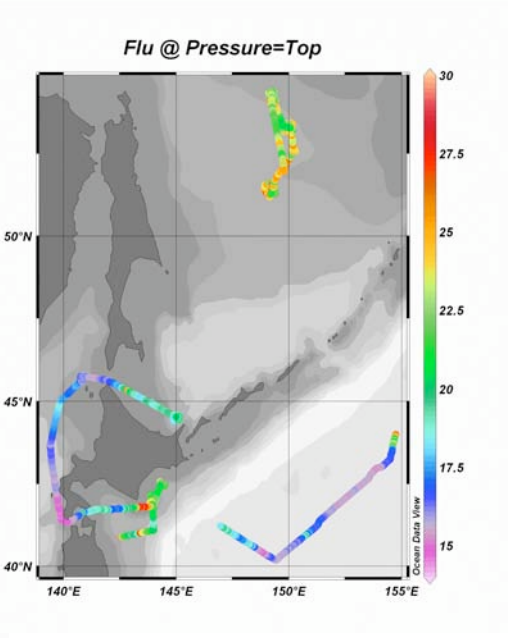

Fig.6.4.2.4 Contour line of fluorescence (Leg.1).

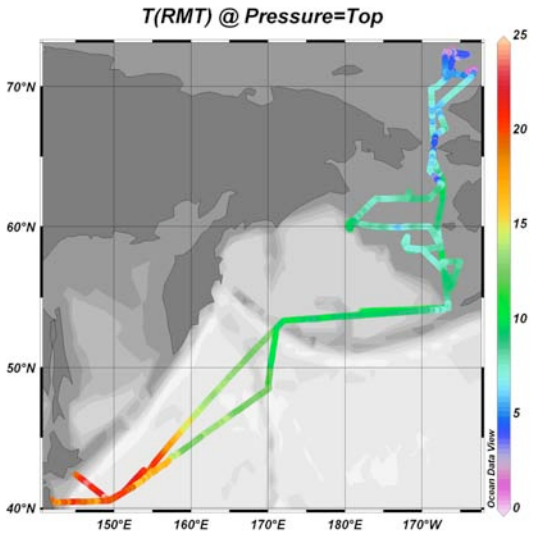

Fig.6.4.2.5 Contour line of Temperature (Leg.2).

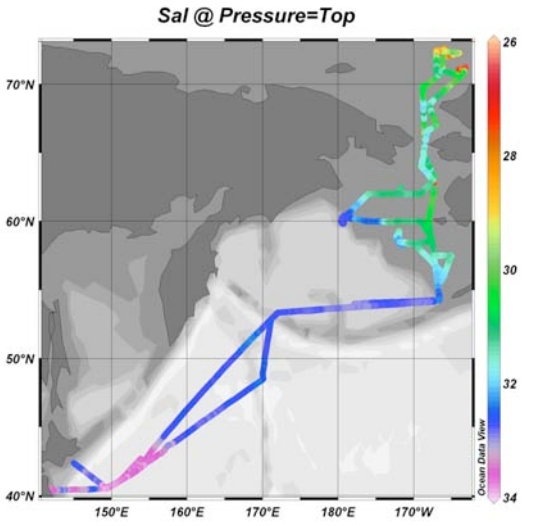

Fig.6.4.2.6 Contour line of salinity (Leg.2)

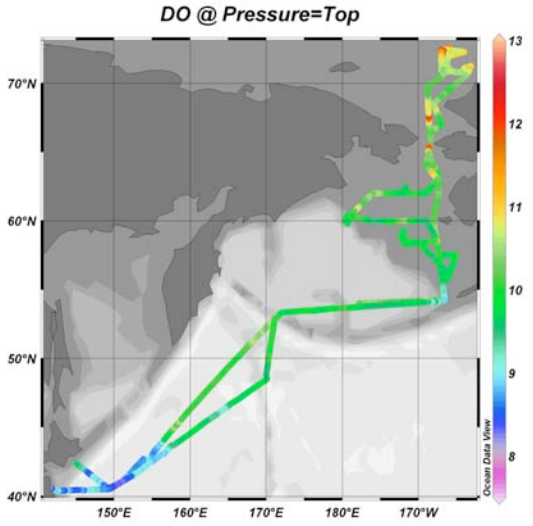

Fig.6.4.2.7 Contour line of dissolved oxygen (Leg.2)

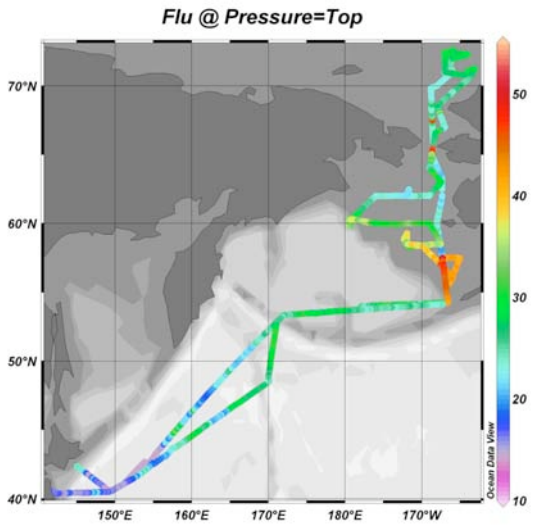

Fig.6.4.2.8 Contour line of fluorescence (Leg.2).

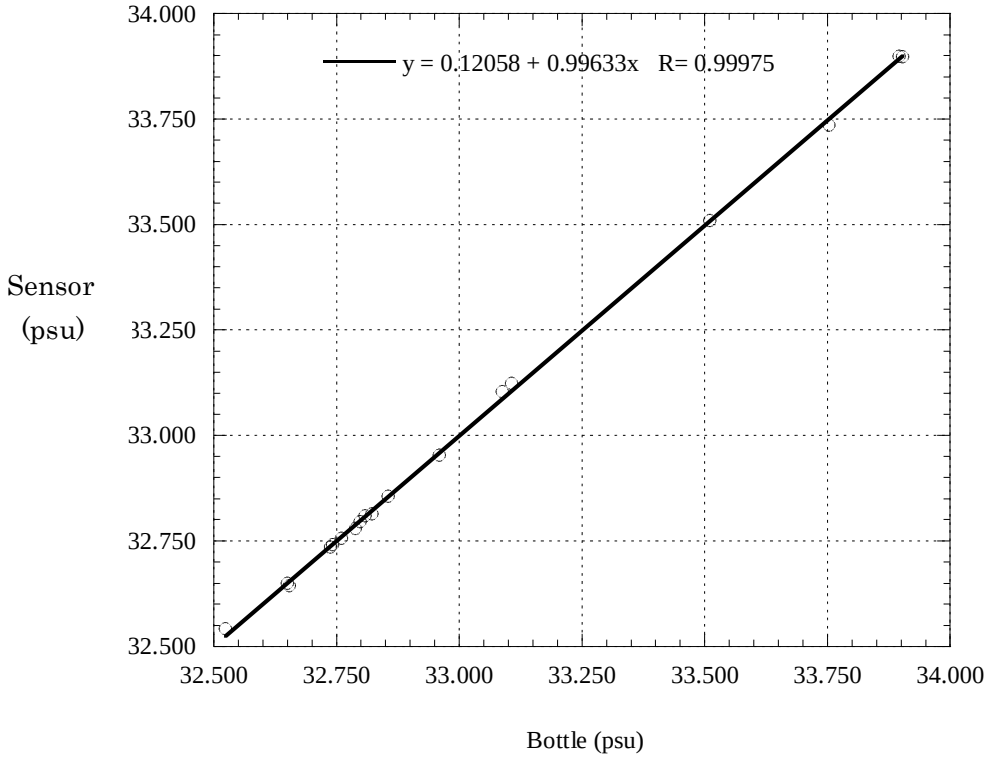

Fig.6.4.2.9 Comparison between salinity sensor and bottle data (Leg.1)

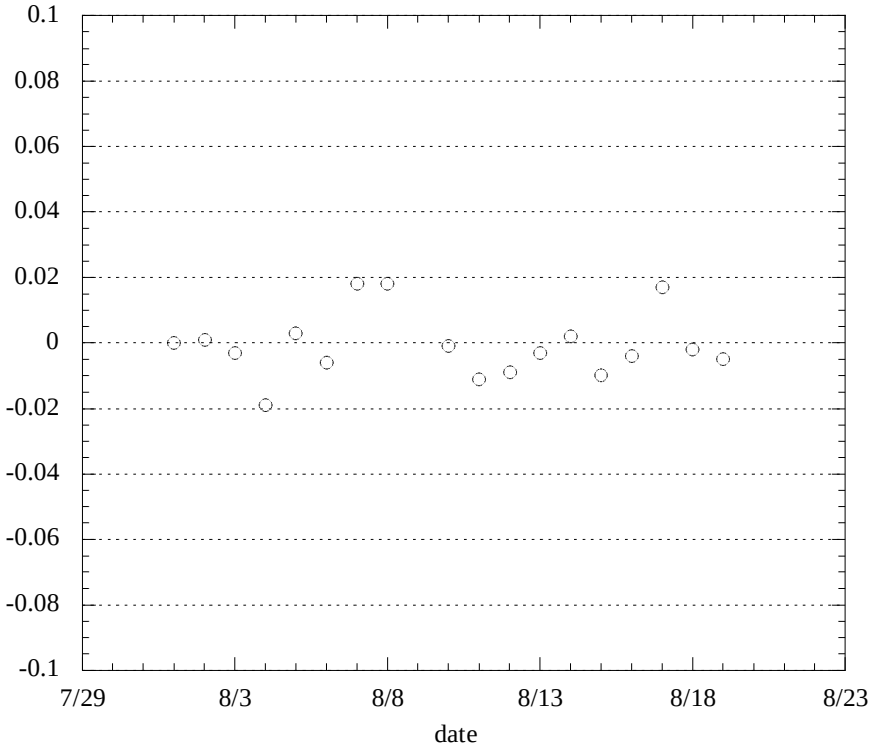

Fig.6.4.2.10 Difference in value between salinity sensor and bottle data (Leg.1).

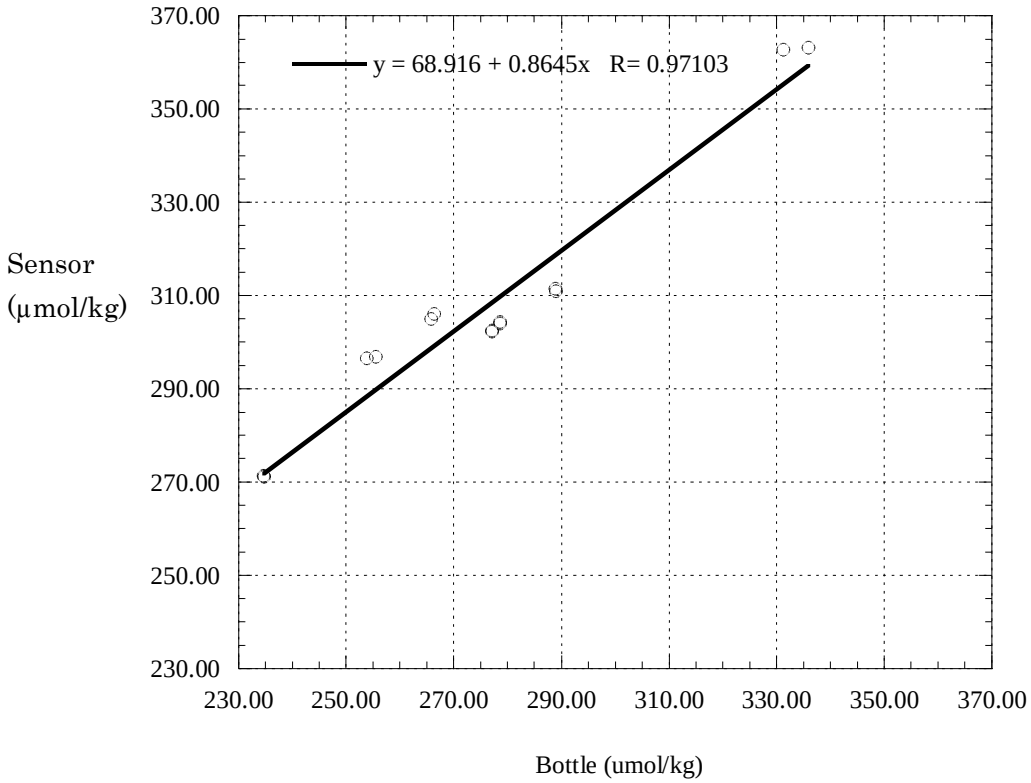

Fig.6.4.2.11 Comparison between dissolved oxygen sensor and bottle data (Leg.1).

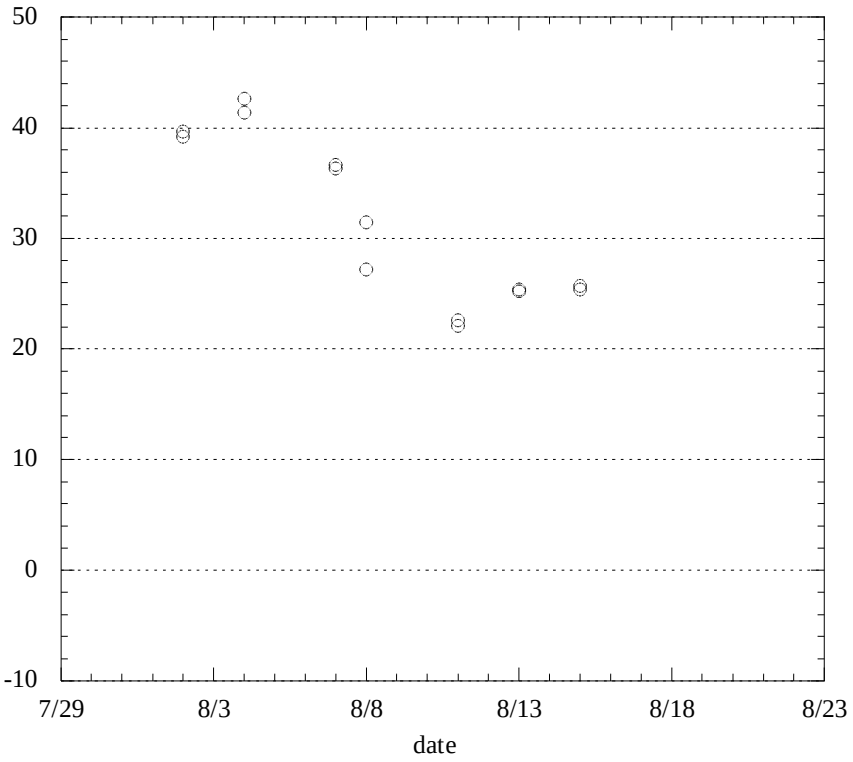

Fig.6.4.2.12 Difference in value between dissolved oxygen sensor and bottle data (Leg.1).

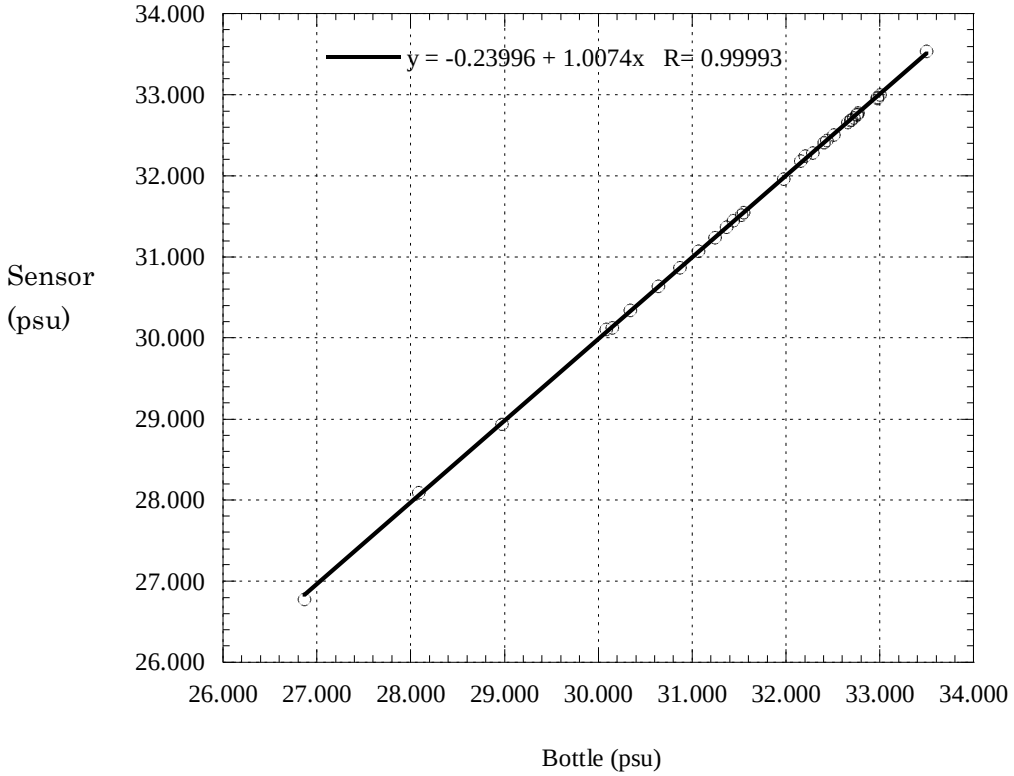

Fig.6.4.2.13 Comparison between salinity sensor and bottle data (Leg.2)

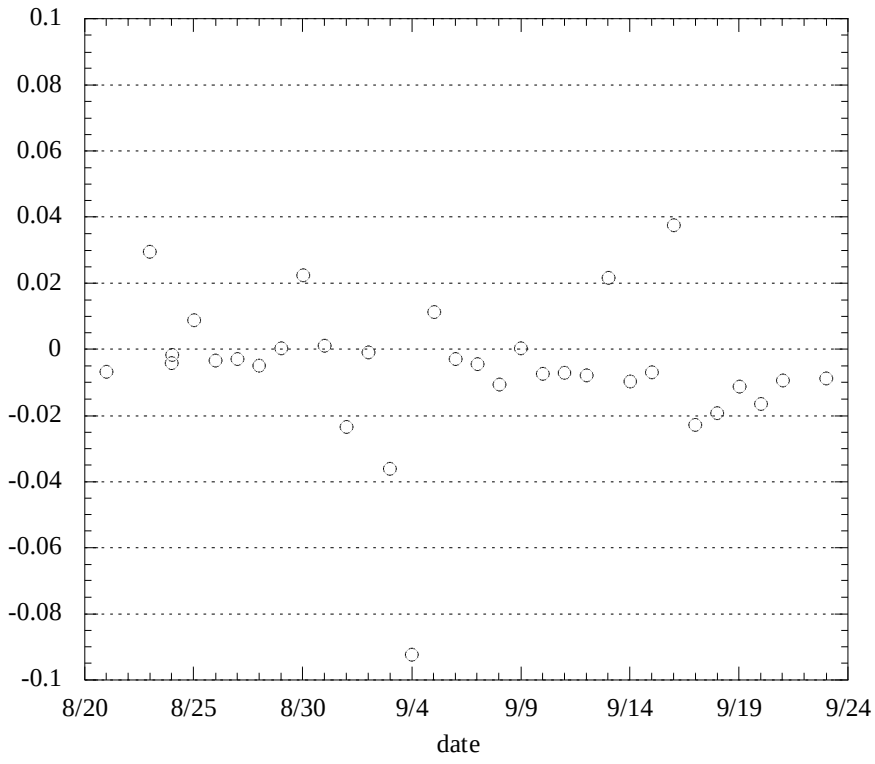

Fig.6.4.2.14 Difference in value between salinity sensor and bottle data (Leg.2).

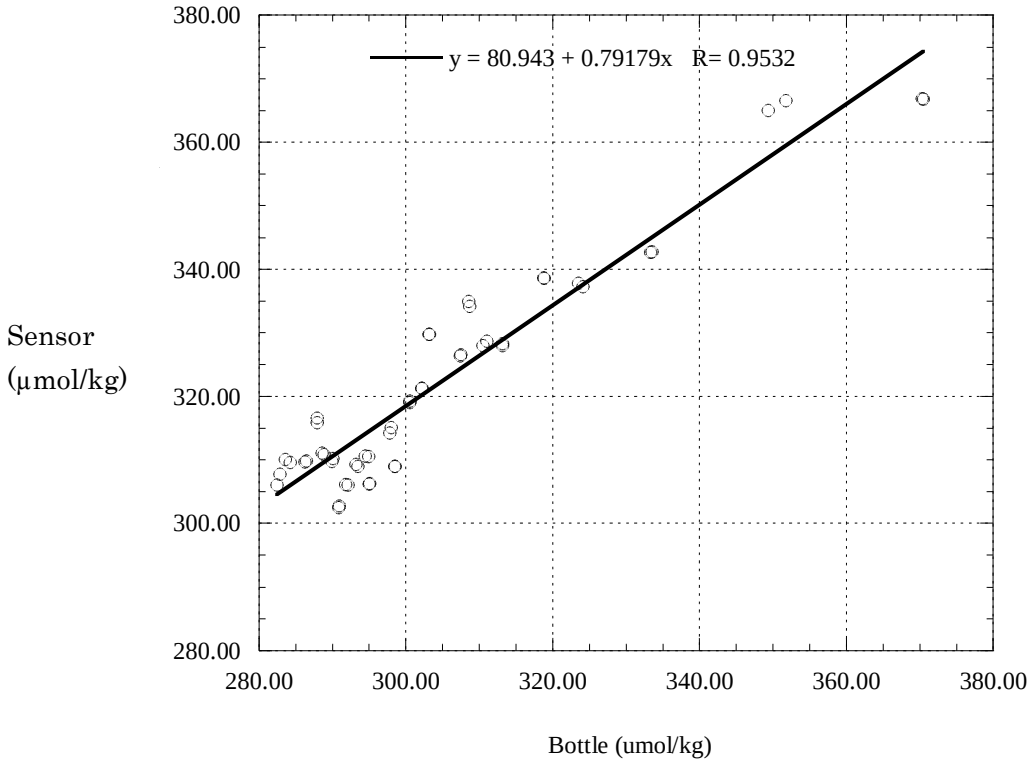

Fig.6.4.2.15 Comparison between dissolved oxygen sensor and bottle data (Leg.2).

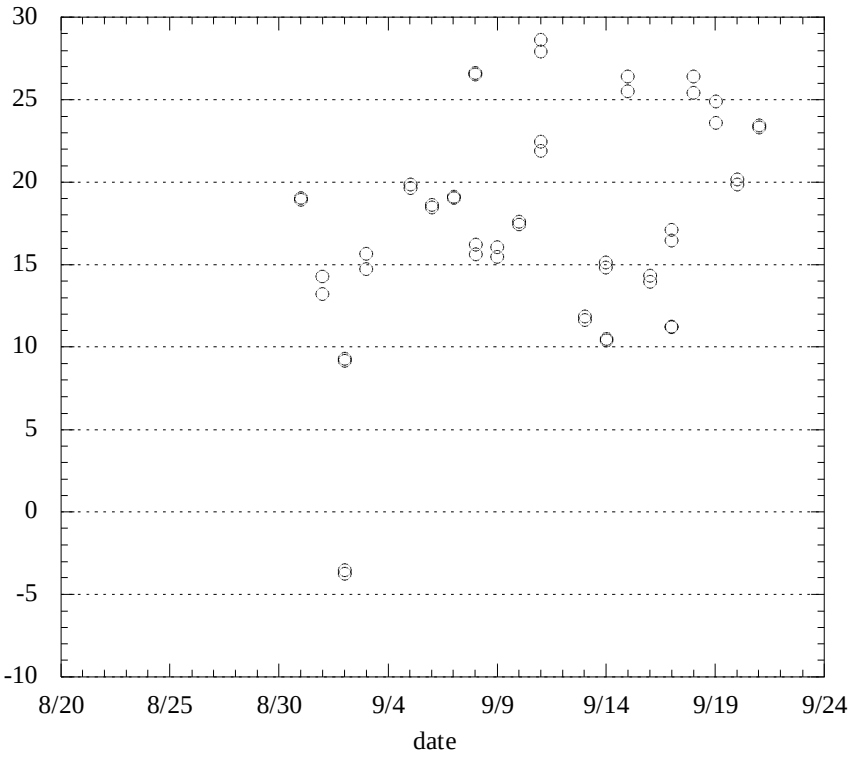

Fig.6.4.2.16 Difference in value between dissolved oxygen sensor and bottle data (Leg.2).

6.4.3 Dissolved oxygen measurement

(1) Personnel

Leg.1: Keisuke Wataki (Marine Works Japan Co. Ltd.)

Leg2: Kimiko Nishijima (Marine Works Japan Co. Ltd.)

(2) Objectives

Determination of dissolved oxygen in seawater by Winkler titration.

(3) Measured parameters

Dissolved oxygen of sampled seawater

(4) Instruments and Methods

4-1 Reagents

Pickling Reagent I: Manganous chloride solution (3M)

Pickling Reagent II: Sodium hydroxide (8M) / sodium iodide solution (4M)

Sulfuric acid solution (5M)

Sodium thiosulfate (0.025M)

Potassium iodate (0.001667M)

4-2 Instruments:

Burette for sodium thiosulfate;

APB-510 manufactured by Kyoto Electronic Co. Ltd. / 10 cm^3 of titration vessel

Burette for potassium iodate;

APB-410 manufactured by Kyoto Electronic Co. Ltd. / 20 cm^3 of titration vessel

Detector and Software; Automatic photometric titrator manufactured by Kimoto Electronic Co. Ltd.

4-3 Sampling

Following procedure is based on the WHP Operations and Methods (Dickson, 1996). Seawater samples were collected with Niskin bottle attached to the CTD-system. Seawater for oxygen measurement was transferred from Niskin sampler bottle to a volume calibrated flask (ca. 100 cm^3). Three times volume of the flask of seawater was overflowed. Temperature was measured by digital thermometer during the overflowing. Then two reagent solutions (Reagent I, II) of 0.5 cm^3 each were added immediately into the sample flask and the stopper was inserted carefully into the flask. The sample flask was then shaken vigorously to mix the contents and to disperse the precipitate finely throughout. After the precipitate has settled at least halfway down the flask, the flask was shaken again vigorously to disperse the precipitate. The sample flasks containing pickled samples were stored in a laboratory until they were titrated.

4-4 Sample measurement

At least two hours after the re-shaking, the pickled samples were measured on board. A magnetic stirrer bar and 1 cm^3 sulfuric acid solution were added into the sample flask and stirring began. Samples

were titrated by sodium thiosulfate solution whose morality was determined by potassium iodate solution. Temperature of sodium thiosulfate during titration was recorded by a digital thermometer. During this cruise we measured dissolved oxygen concentration using two sets of the titration apparatus (DOT-1 and DOT-2). Dissolved oxygen concentration (μmol kg^{-1}) was calculated by sample temperature during seawater sampling, salinity of the sample, and titrated volume of sodium thiosulfate solution without the blank.

4-5 Standardization and determination of the blank

Concentration of sodium thiosulfate titrant (ca. 0.025M) was determined by potassium iodate solution. Pure potassium iodate was dried in an oven at 130°C. 1.7835 g potassium iodate weighed out accurately was dissolved in deionized water and diluted to final volume of 5 dm^3 in a calibrated volumetric flask (0.001667M). 10 cm^3 of the standard potassium iodate solution was added to a flask using a calibrated dispenser. Then 90 cm^3 of deionized water, 1 cm^3 of sulfuric acid solution, and 0.5 cm^3 of pickling reagent solution II and I were added into the flask in order. Amount of sodium thiosulfate titrated gave the morality of sodium thiosulfate titrant.

The blank from the presence of redox species apart from oxygen in the reagents was determined as follows. 1 cm^3 of the standard potassium iodate solution was added to a flask using a calibrated dispenser. Then 100 cm^3 of deionized water, 1 cm^3 of sulfuric acid solution, and 0.5 cm^3 of pickling reagent solution II and I were added into the flask in order. Just after titration of the first potassium iodate, a further 1 cm^3 of standard potassium iodate was added and titrated. The blank was determined by difference between the first and second titrated volumes of the sodium thiosulfate. The oxygen in the pickling reagents I (0.5 cm^3) and II (0.5 cm^3) were assumed to be 3.8 x 10^{-8} mol (Dickson, 1996).

Table 6.4.3-1 shows results of the standardization and the blank determination during this cruise.

Table 6.4.3.1 Results of the standardization and the blank determinations during this cruise.

Date	KIO_3		DOT-1 (cm^3)			DOT-3 (cm^3)			Samples
(UTC)	#	bottle	$Na_2S_2O_3$	E.P.	blank	$Na_2S_2O_3$	E.P.	blank	(Stations)
2006/08/01	4	20060419-04-06	20060729-1	3.958	-0.010	20060729-2	3.952	-0.009	S01,S02
2006/08/07		20060419-04-07	20060729-1	3.956	-0.009	20060729-2	3.949	-0.010	S03,S04
2006/08/10		20060419-04-08	20060729-1	3.958	-0.012	20060729-2	3.951	-0.010	S07,S06
2006/08/14		20060419-04-09	20060729-1	3.956	-0.009	20060729-2	3.950	-0.011	S05
2006/09/03	5	20060419-05-05	20060825-2	3.959	-0.011	20060825-3	3.958	-0.010	S15,S14,S13,S12EX
2006/09/08		20060419-05-06	20060825-2	3.960	-0.010	20060825-3	3.957	-0.010	S12,S16,S17
2006/09/09		20060419-05-06	20060825-2	3.958	-0.012	20060825-3	3.956	-0.010	S18,S19,S20
2006/09/13		20060419-05-07	20060825-2	3.959	-0.009	20060825-3	3.957	-0.010	S21,S22,S23,S24
2006/09/16		20060419-05-08	20060914-1	3.960	-0.011	20060914-2	3.959	-0.010	S26,S27,S28,S29
2006/09/19		20060419-05-09	20060914-1	3.963	-0.011	20060914-2	3.962	-0.010	S30,S31,S32,S33

Batch number of the KIO_3 standard solution.

4-6 Reproducibility of sample measurement

Replicate samples were taken at every CTD cast; usually these were 5 - 10 % of seawater samples of each cast during this cruise. Results of the replicate samples were shown in Table 6.4.3-2 and this

histogram shown in Fig.6.4.3-1. The standard deviation was calculated by a procedure (SOP23) in DOE (1994).

Table 6.4.3.2 Results of the replicate sample measurements

Number of replicate sample pairs	Oxygen concentration (µmol/kg)
	Standard Deviation.
36	0.162

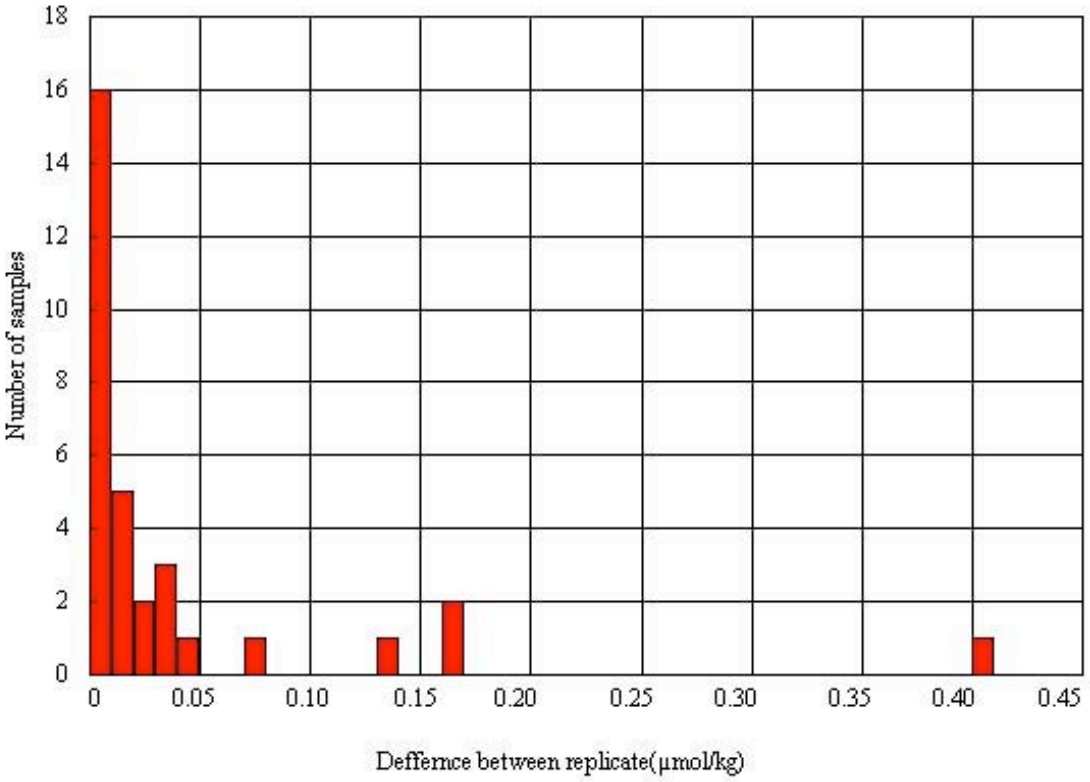

Fig 6.4.3.1 Results of the replicate sample measurements

(5) Preliminary Result

During this cruise, we measured oxygen concentration in 260 seawater samples at 30 stations. Concentrations of Dissolved oxygen in vertical section (Leg.2) shown in Fig. 6.4.3.2.

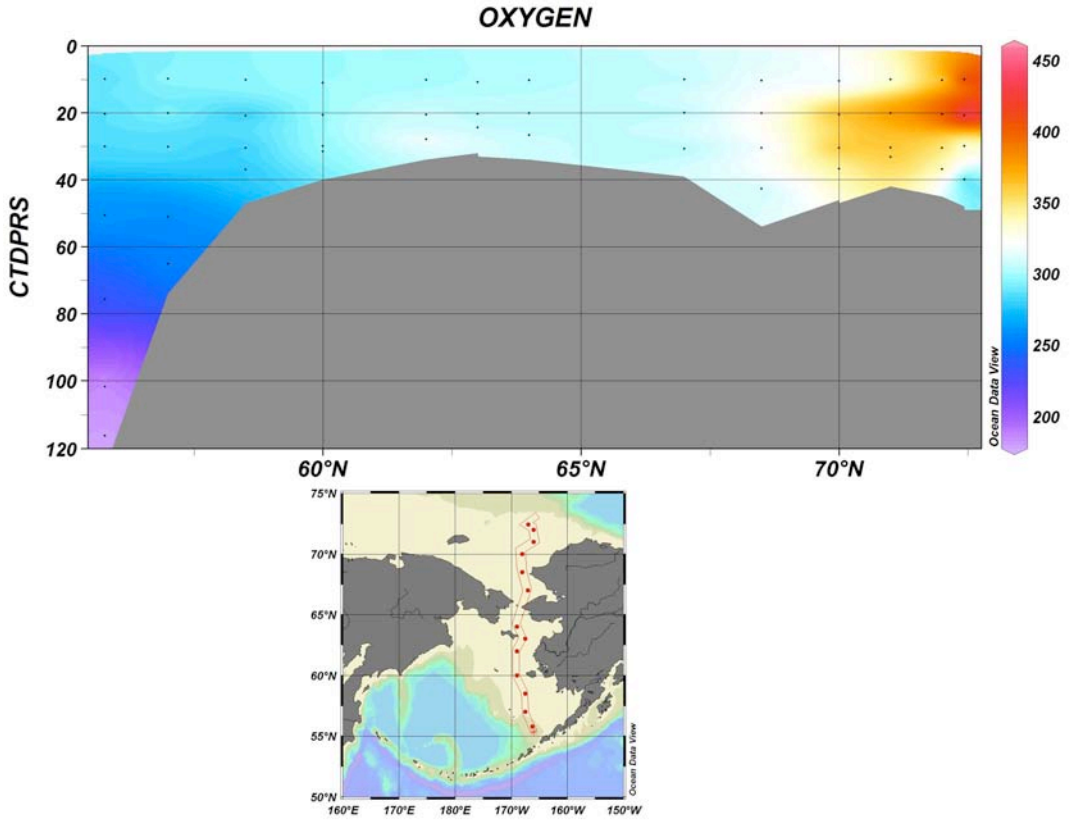

Fig 6.4.3.2 Vertical section of Dissolved oxygen.

(6) Data archive

All data will be submitted to JAMSTEC Data Management Office (DMO) and is currently under its control.

(7) Referencess

Dickson, A. (1996) Dissolved Oxygen, in WHP Operations and Methods, Woods Hole, pp1-13.

DOE (1994) Handbook of methods for the analysis of the various parameters of the carbon dioxide system in sea water; version 2. A.G. Dickson and C. Goyet (eds), ORNL/CDIAC-74.

Emerson, S, S. Mecking and J.Abell (2001) The biological pump in the subtropical North Pacific Ocean: nutrient sources, redfield ratios, and recent changes. Global Biogeochem. Cycles, 15, 535-554.

Watanabe, Y. W., T. Ono, A. Shimamoto, T. Sugimoto, M. Wakita and S. Watanabe (2001) Probability of a reduction in the formation rate of subsurface water in the North Pacific during the 1980s and 1990s. Geophys. Res. Letts., 28, 3298-3292.

6.4.4 Nutrients measurement

(1) Personnel

Leg.1: Ayumi Takeuchi, Junji Matsushita (Marine Works Japan Co. Ltd)

Leg.2: Kenichiro Sato, Takayoshi Seike (Marine Works Japan Co. Ltd)

(2) Objectives

The vertical and horizontal distributions of the nutrients are one of the most important factors on the primary production. During this cruise, nutrient (nitrate, nitrite, silicate, phosphate and ammonia) measurements give us the important information on the mechanism of the primary production or seawater circulation.

(3) Measured Parameters

Nitrate, Nitrite, Silicate, Phosphate, Ammonia.

(4) Instruments and Methods

Nutrient analysis was performed on the BRAN+LUEBBE TRAACS 800 system. The laboratory temperature was maintained ranging of 22-24 deg C.

4-1Measured Parameters

Nitrate + nitrite and nitrite were analyzed according to the modification method of Grasshoff (1970). The sample nitrate was reduced to nitrite in a cadmium tube inside of which was coated with metallic copper. The sample stream with its equivalent nitrite was treated with an acidic, sulfanilamide reagent and the nitrite formed nitrous acid, which reacted with the sulfanilamide to produce a diazonium ion. N1-Naphthylethylene-diamine added to the sample stream then couples with the diazonium ion to produce a red, azo dye. With reduction of the nitrate to nitrite, both nitrate and nitrite reacted and were measured. In the case that reduction is not done, only nitrite is reacted and can be detected. Thus, for the nitrite analysis, no reduction was performed and the alkaline buffer was not necessary. For nitrate, absorbance of 550 nm by azo dye in analysis was measured using a 3 cm length cell for Nitrate and 5 cm length cell for Nitrite.

The silicate (Although silicic acid is correct, we use silicate because a term of silicate is widely used as the name of Si nutrient in chemical oceanographic community) method is analogous to that described for phosphate. The method used is essentially that of Grasshoff et al. (1983), wherein silicomolybdic acid is first formed from the silicic acid in the sample and added molybdic acid; then the silicomolybdic acid is reduced to silicomolybdous acid, or "molybdenum blue,"

using L-ascorbic acid as the reductant. Absorbance of 630 nm by silicomolybdous acid in analysis is measured using a 3 cm length cell.

The phosphate analysis is a modification of the procedure of Murphy and Riley (1962). Molybdic acid is added to the seawater sample to form phosphomolybdic acid, which is in turn reduced to phosphomolybdous acid using L-ascorbic acid as the reductant. Absorbance of 880 nm by phosphomolybdous acid in analysis is measured using a 5 cm length cell.

Ammonia in seawater is mixed with an alkaline solution containing EDTA, ammonia as gas state is formed from seawater. The ammonia (gas) is absorbed in sulfuric acid solution by way of 0.5 μm pore size membrane filter (ADVANTEC PTFE) at the dialyzer attached to analytical system. The ammonia absorbed in acid solution is determined by coupling with phenol and hypochlorite solution to from an indophenol blue compound. Absorbance of 630 nm by indophenol blue compound in analysis is measured using a 3 cm length cell.

4-2 Nutrients Standard

Silicate standard solution, the silicate primary standard, was obtained from Merck, Ltd.. This standard solution, traceable to SRM from NIST was 1000 mg per litter. Since this solution is alkaline solution of 0.5 M NaOH, an aliquot of 40ml solution were diluted to 500 ml together with an aliquot of 20 ml of 1M HCl. Primary standard for nitrate (KNO_3) and phosphate (KH_2PO_4) were obtained from Merck, Ltd. and nitrite ($NaNO_2$) and ammonia ($(NH_4)_2SO_4$) were obtained from Wako Pure Chemical Industries, Ltd..

4-3 Sampling Procedures

Samples were drawn into virgin 10 ml polyacrylates vials that were rinsed three times before sampling without sample drawing tubes. Sets of 5 different concentrations for nitrate, nitrite, silicate, phosphate and 4 different concentrations for ammonia of the shipboard standards were analyzed at beginning and end of each group of analysis. We used 6 different concentrations for silicate (Stn. 06) and ammonia (Stn. 12), because the concentration of the samples exceeded the higher concentration of the standard solutions we normally use. The standard solutions of highest concentration were measured every 6–7 samples and were used to evaluate precision of nutrients analysis during the cruise. We also used reference material for nutrients in seawater, RMNS (KANSO Co., Ltd., lots AU), for every 2 or 3 runs to secure comparability on nutrient analysis throughout the cruise.

4-4 Low Nutrients Sea Water (LNSW)

Surface water having low nutrient concentration was taken and filtered using 0.45 mm pore size

membrane filter. This water is stored in 20-liter cubitainer with paper box. The concentrations of nutrient of this water were measured carefully in April 2006.

(5) Preliminary Results

Analytical precisions were 0.05% (55 mM) for nitrate, 0.07% (1.2 mM) for nitrite, 0.04% (171mM) for silicate, 0.09% (3.6 mM) for phosphate and 0.27% (4.0 mM) for ammonia in terms of median of precision, respectively. Results of RMNS analysis are shown in Tables 6.4.4.1 for the station's comparability. Concentrations of nitrate, nitrite, silicate, phosphate, ammonia in vertical section (Leg. 2) shown in Fig. 6.4.4.1.

(6) Data archives

All data will be submitted to JAMSTEC Data Management Office (DMO) and is currently under its control.

(7) References

Grasshoff, K. (1970), Technicon paper, 691-57.

Grasshoff, K., Ehrhardt, M., Kremling K. et al. (1983), Methods of seawater analysis. 2nd rev. Weinheim: Verlag Chemie, Germany, West.

Murphy, J., and Riley, J.P. (1962), Analytica chim. Acta 27, 31-36.

Table 6.4.4.1 Results of RMNS Lot. AU analysis in this cruise.

mmol/kg

	serial	Stn.	NO_3	NO_2	SiO_2	PO_4	NH_4
RM-AU	332	01	29.84	0.02	66.55	2.156	0.90
RM-AU	590	01	29.89	0.01	66.42	2.162	0.57
RM-AU	332	02	29.91	0.02	66.52	2.158	0.91
RM-AU	826	03	29.91	0.03	66.54	2.156	0.87
RM-AU	826	04	29.91	0.03	66.54	2.162	0.85
RM-AU	826	07	29.98	0.02	66.60	2.170	0.87
RM-AU	642	06	29.91	0.02	66.74	2.182	0.87
RM-AU	642	06_SiO2	—	—	66.46	—	—
RM-AU	642	05	29.89	0.02	66.63	2.183	0.84
RM-AU	330	15	29.89	0.03	66.53	2.173	0.90
RM-AU	600	15	29.87	0.04	66.67	2.176	0.93
RM-AU	330	14	29.86	0.03	66.50	2.173	0.92
RM-AU	600	14	29.93	0.04	66.55	2.175	1.01
RM-AU	7	13	29.78	0.03	66.32	2.175	0.88
RM-AU	330	13	29.85	0.03	66.44	2.181	0.91
RM-AU	7	12ex	29.83	0.03	66.26	2.178	0.89
RM-AU	330	12ex	29.85	0.03	66.27	2.182	0.96
RM-AU	660	12	29.84	0.03	66.48	2.163	0.83
RM-AU	7	12	29.83	0.03	66.49	2.172	0.84
RM-AU	660	16	29.96	0.03	66.54	2.172	0.87
RM-AU	7	16	29.99	0.03	66.67	2.173	0.88
RM-AU	660	17	29.99	0.03	66.75	2.169	0.90
RM-AU	7	17	30.07	0.03	66.88	2.172	0.91
RM-AU	978	18	29.84	0.02	66.56	2.174	0.87
RM-AU	660	18	29.94	0.03	66.54	2.184	0.87
RM-AU	978	19	30.00	0.03	66.57	2.177	0.88
RM-AU	660	19	30.04	0.03	66.59	2.179	0.89
RM-AU	978	20	29.97	0.03	66.60	2.172	0.90
RM-AU	660	20	29.95	0.04	66.64	2.177	0.93
RM-AU	978	21	29.82	0.03	66.29	2.169	0.91
RM-AU	978	22	29.82	0.03	66.29	2.169	0.90
RM-AU	681	23	29.77	0.03	66.30	2.168	0.88

RM-AU	978	23	29.83	0.03	66.33	2.171	0.88
RM-AU	681	24	29.88	0.03	66.55	2.170	0.86
RM-AU	978	24	29.87	0.03	66.48	2.178	0.89
RM-AU	681	26	29.82	0.02	66.51	2.173	0.88
RM-AU	978	26	29.77	0.03	66.58	2.174	0.89
RM-AU	681	27	29.80	0.03	66.45	2.183	0.88
RM-AU	19	28	29.84	0.03	66.43	2.175	0.85
RM-AU	681	28	29.80	0.03	66.45	2.183	0.87
RM-AU	19	29	29.82	0.04	66.46	2.181	0.86
RM-AU	681	29	29.84	0.03	66.56	2.184	0.89
RM-AU	19	30	29.93	0.03	66.46	2.173	0.88
RM-AU	681	30	29.96	0.03	66.60	2.184	0.93
RM-AU	653	31	29.85	0.02	66.38	2.171	0.89
RM-AU	19	31	30.03	0.03	66.38	2.170	0.97
RM-AU	653	32	29.85	0.02	66.38	2.171	0.87
RM-AU	19	32	30.03	0.03	66.38	2.170	0.86
RM-AU	653	33	29.85	0.02	66.38	2.171	0.88
RM-AU	19	33	30.03	0.03	66.38	2.170	0.88

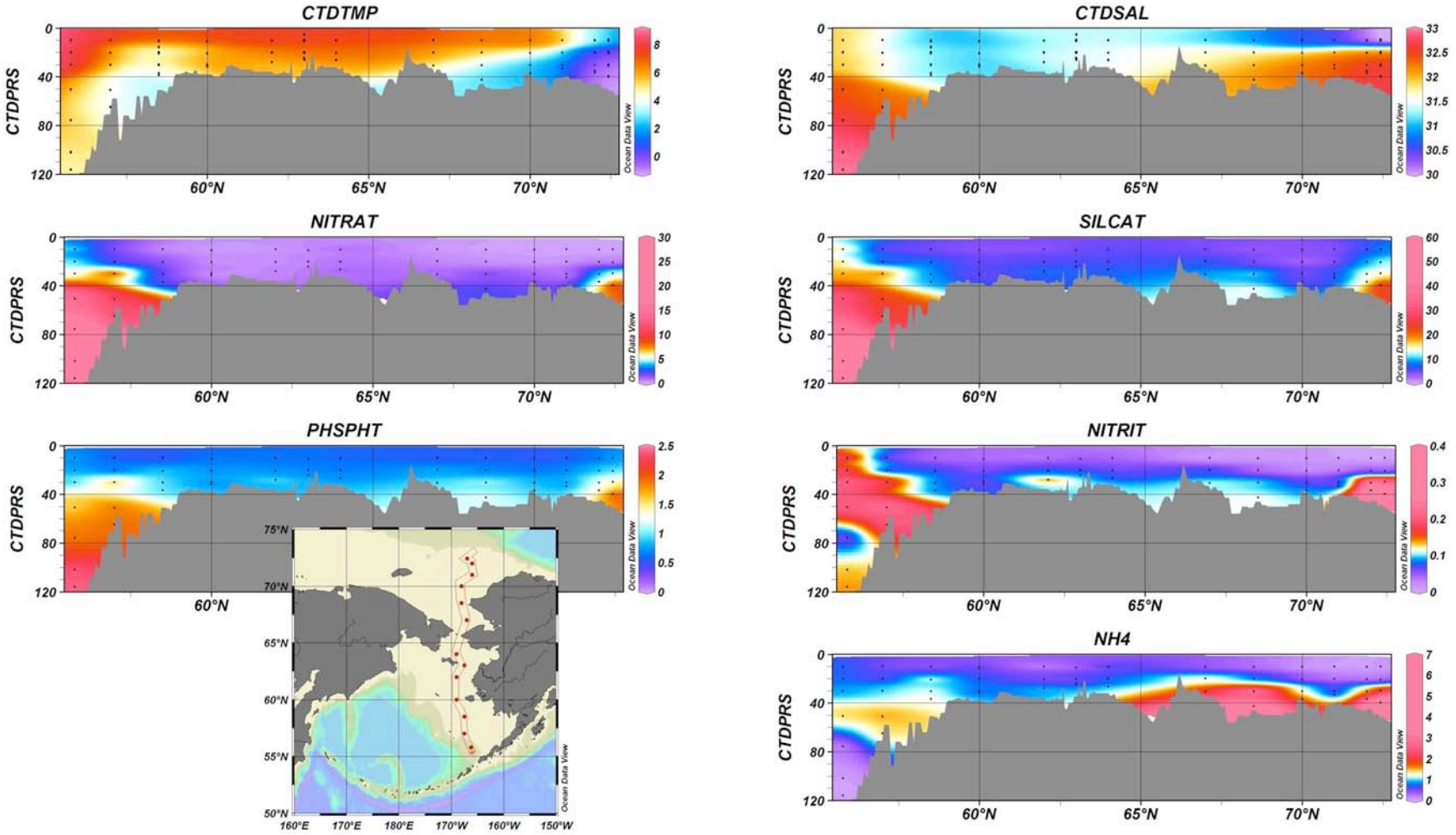

Fig. 6.4.4.1 Vertical sections (Leg. 2) of CTD temperature, CTD salinity and nutrients concentration (nitrate, nitrite, silicate, phosphate, ammonia).

6.4.5 Partial pressure of CO_2 (pCO_2) and carbonate system in seawater

6.4.5.1 Partial pressure of CO_2 (pCO_2)

(1) Personnel

Leg.1: Masaki Moro, Mikio Kitada , Hideki Yamamoto (Marine Works Japan Co. Ltd)

Leg.2: Mikio Kitada, Fuyuki Shibata, Ayaka Hatsuyama (Marine Works Japan Co. Ltd)

(2) Objectives

Since global warming has become a serious environmental crisis world-widely, studies on the green house gas such as CO_2 are drawing high attention. As the ocean plays an important roll in buffering the increase of atmospheric CO_2, studies on the exchange of CO_2 between the atmosphere and the seawater becomes highly important in order to predict the phenomenon that is likely to happen in the future.

When CO_2 dissolves in water, chemical reaction takes place and CO_2 alters its appearance into several species. Unfortunately, the concentrations of the individual species of CO_2 system in solution cannot be measured directly. Instead, the concentration of CO_2 system in the water could be estimated by measuring 2 parameters out of 4, which is total alkalinity (TA), total dissolved inorganic carbon (DIC), pH and pCO_2 (DOE, 1994). Here, we report on board measurements of pCO_2 in the North Pacific, including the Okhotsk, the Bering and the Chukchi Seas during MR06-04 cruise.

(3) Measured Parameters

Partial pressure of CO_2 in the atmosphere and surface seawater

(4) Instruments and Methods

Concentrations of CO_2 in the atmosphere and the sea surface were measured continuously during the cruise using an automatic system with a non-dispersive infrared (NDIR) analyzer (BINOS^{TM}). The automatic system was operated by on one and a half hour cycle. In one cycle, standard gasses, marine air and air in a headspace of an equilibrator were analyzed subsequently. The concentrations of the standard gasses used for the analysis were 289.75, 349.00, 393.75 and 439.73 ppm. The standard gasses will be recalibrated after the cruise.

The marine air taken from the bow was introduced into the NDIR by passing through a mass flow controller (controlling the air flow rate at about 0.5 L/min), a cooling unit, a Perma-pure dryer (GL Sciences Inc.) and a desiccant holder containing $Mg(ClO_4)_2$.

A fixed volume of the marine air taken from the bow was equilibrated with a stream of seawater that flowed at a rate of 5-6L/min in the equilibrator. The air in the equilibrator was circulated with a pump at 0.7-0.8L/min in a closed loop passing through two cooling units, a Perma-pure dryer (GL Science Inc.) and a desiccant holder containing $Mg(ClO_4)_2$.

(5) Results

Figures 6.4.5.1.1 and 6.4.5.1.2 show the results of measuring the CO_2 concentration (xCO_2) of ambient air samples and the seawater samples. The followings are the periods and the reasons for the lack of data from the analysis during the cruise (The periods appear in UTC).

8/9 00:37 - 8/10 05:17 Stopped the system during the passage of the Russian EEZ.

8/12 12:15 - 8/12 12:26 Stopped the system in order to adjust the 0 point of the NDIR.

8/16 01:04 - 8/17 15:11 Stopped the system during the passage of the Russian EEZ.

During the leg.2, it is found that the ocean acted as a source for atmospheric CO_2 during the former period of the cruise. However, it acted as a sink for atmospheric CO_2 during the latter period.

(6) Data Archive

All data will be submitted to JAMSTEC Data Management Office (DMO) and is currently under its control.

(7) References

Manual on Oceanographic Observation Part 1 (1999), Japan Meteorological Agency

DOE (1994), Handbook of methods for the analysis of the various parameters of the carbon dioxide system in sea water; version 2, A. G. Dickson & C. Goyet, Eds., ORNS/CDIAC-74.

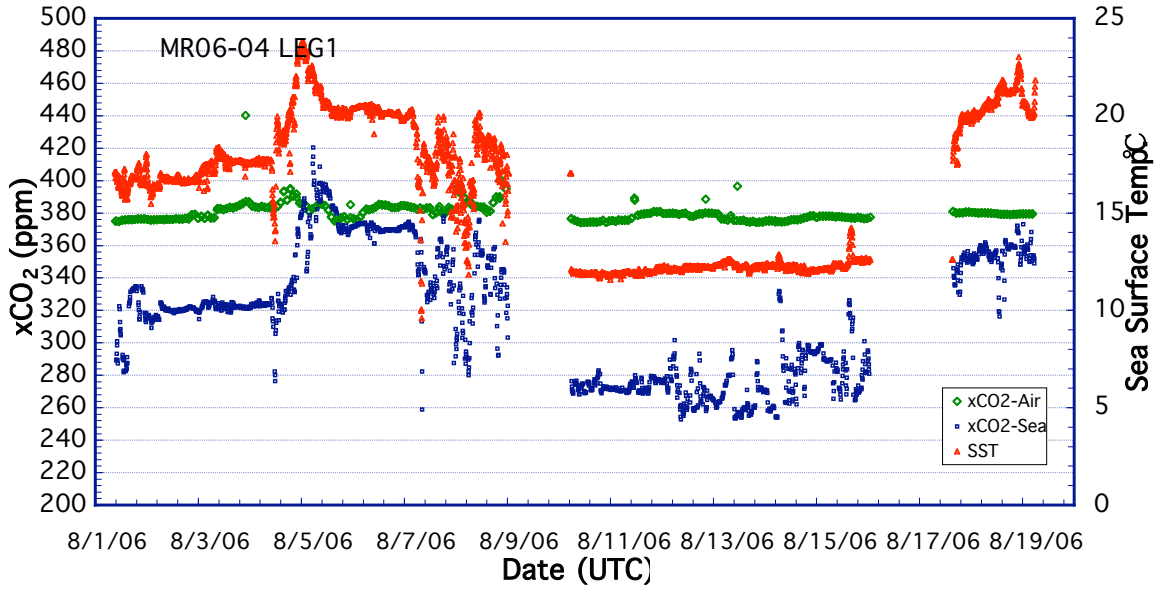

Fig. 6.4.5.1.1 Temporal changes of mole fraction of CO_2 (xCO_2) in atmosphere (green) and surface seawater (blue), and SST (red) during the leg.1.

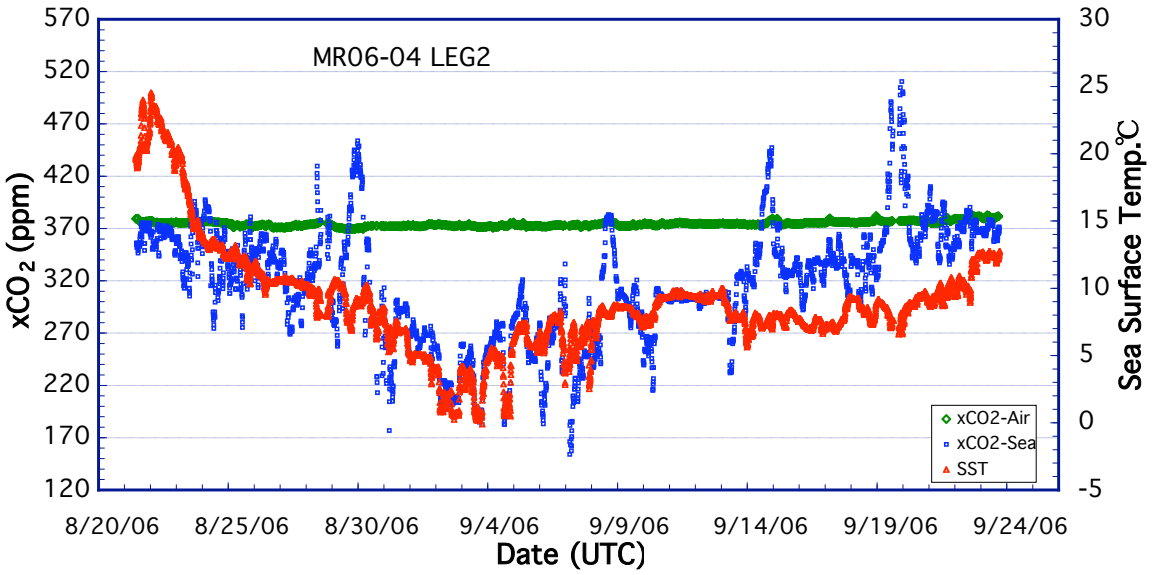

Fig. 6.4.5.1.2 Temporal changes of mole fraction of CO_2 (xCO_2) in atmosphere (green) and surface seawater (blue), and SST (red) during the leg.2.

6.4.5.2 Dissolved inorganic carbon (DIC)

(1) Personnel

Leg.1: Masaki Moro, Mikio Kitada, Hideki Yamamoto (Marine Works Japan Co. Ltd)

Leg.2: Mikio Kitada, Fuyuki Shibata, Ayaka Hatsuyama (Marine Works Japan Co. Ltd)

(2) Objectives

Since global warming is becoming an environmental issue world-widely, studies on the green house gas such as CO_2 are drawing high attention. As the ocean plays an important roll in buffering the increase of atmospheric CO_2, studies on the exchange of CO_2 between the atmosphere and the sea becomes highly important in order to predict the phenomenon that is likely to happen in the future.

When CO_2 dissolves in water, chemical reaction takes place and CO_2 alters its appearance into several species. Unfortunately, the concentrations of the individual species of CO_2 system in solution cannot be measured directly. Instead, the concentration of CO_2 system in the water could be estimated by measuring 2 parameters out of 4, which is total alkalinity (TA), total dissolved inorganic carbon (DIC), pH and pCO_2 (DOE, 1994). Here, we report on board measurements of DIC in the North Pacific including the Okhotsk Sea, and the Bering Sea and Arctic Ocean during MR06-04 cruise.

(3) Measured Parameters

Dissolved inorganic carbon

(4) Instruments and Methods

4-1 Seawater sampling

Sea-water samples were collected in 12L Niskin bottles from different depths at 7 and 22 stations during Legs.1 and 2, respectively. From the Niskin bottles, a part of seawater was each collected in a 250ml glass bottle. The glass bottle was previously soaked in 5% non-phosphoric acid detergent (pH13) solution at least 3 hours and was rinsed by fresh water for 5 times and Milli-Q deionized water for 3 times. When the sea-water was sub-sampled, a silicon sampling tube was used to introduce to the glass bottle calmly without bubbling. The sea-water was gently put on the bottom of the glass bottle and was overflowed during 20 seconds taking care of not leaving any bubbles in the bottle. After the sub-sampling of seawater finished, the glass bottles were transferred to the laboratory. Prior to the analysis, 3ml of the sample (1% of the bottle volume) was removed from the glass bottle in order to make a headspace. The samples were then poisoned with 100μl of over saturated solution of mercury chloride within one hour after the sub-sampling. The poisoned samples were sealed using grease (Apiezon M grease) and a stopper-clip. The samples were stored in a refrigerator under approximately 5 ˚C until measurement.

4-2 DIC measurement

The Model 5012 coulometer (Carbon Dioxide Coulometer, UIC Inc.) equipped with an automated sampling and CO_2 extraction system controlled by a computer (JANS, Inc.) was used for DIC measurement. The analytical cycle was composed of three measuring components of 70ml of standard CO_2 gas (2% CO_2 - N_2 gas), 2ml of 10%-phosphoric acid solution and six seawater samples. The standard CO_2 gas was measured to confirm the constancy of the calibration factor during the run and phosphoric acid was measured for acid blank correction.

Approximately 20ml of seawater was introduced into a receptacle from the glass bottle and was mixed with 2ml of 10%-phosphoric acid. The carbon dioxide gas evolving from the chemical reaction was purged by nitrogen gas (carbon dioxide free) for 12 minutes at the flow rate of 140ml/min. and was absorbed into an electrolyte solution. In the electrolyte solution, acids formed by the reaction between the solution and the absorbed carbon dioxide were titrated with hydrogen ions in the coulometer and the counts of the titration were stored in the computer.

Prior to the analysis of seawater, a calibration factor (slope) was calculated by measuring a series of sodium carbonate solutions (0~2.5mM) and this calibration factor was applied to all data acquired throughout the cruise. The concentration of a reference material KRM (batch AA: KANSO) was certified by measuring a Certified Reference Material (CRM batch 75: Scripps Institution of Oceanography) with the same electrolyte solution. For every electrolyte solution, KRM was measured each time to adjust the slope. Another reference material QRM (QRM batch Q14: JAMSTEC) was also measured in the beginning and the end of the measurements for one set of electrolyte solution in order to calibrate the inclination of the outcome during the run. The electrolyte solution was changed every 50 samples.

(5) Results

A duplicate measurement was made on every ninth seawater sample and the difference between each pair of analyses was plotted on a range control chart (see Figures 6.4.5.2.1, and 6.4.5.2.2). The average of the differences were 1.0 μmol/kg (n=14) for leg.1 and 0.6 μmol/kg (n=21) for leg.2. The standard deviation during the leg.1 and leg.2 were 0.9 μmol/kg and 0.5 μmol/kg, respectively and the measurement was accurate enough according to DOE (1994).

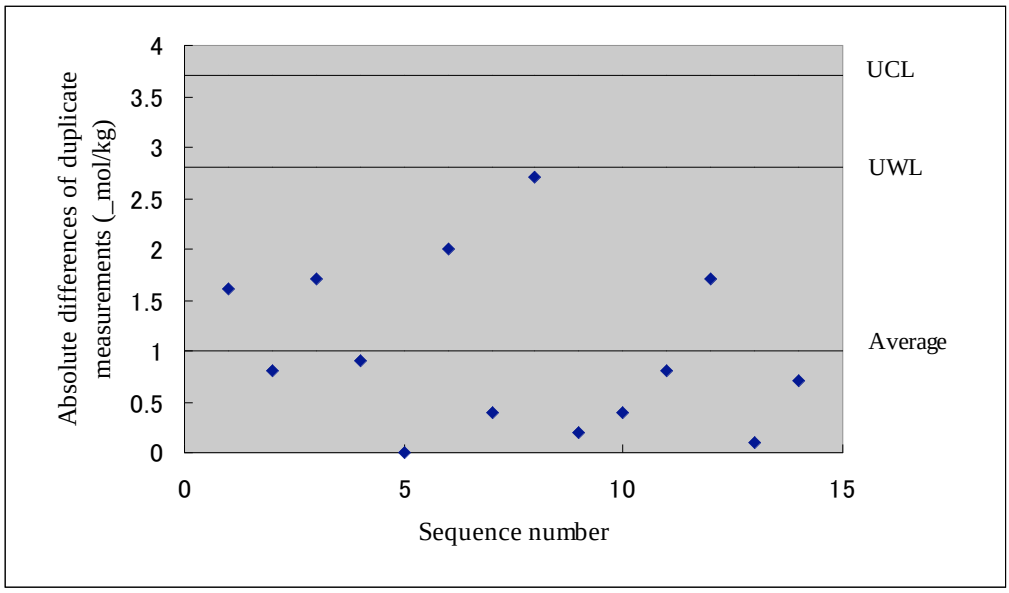

Figure 6.4.5.2.1 Range control chart of the absolute differences of duplicate measurements carried out in the measurement of DIC during the leg. 1 MR06-04 cruise.

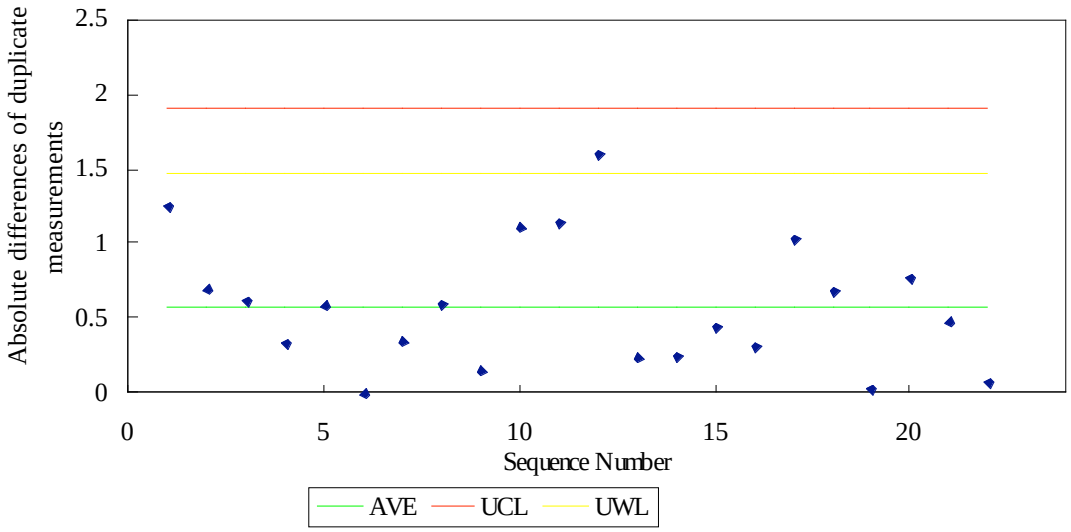

Figure 6.4.5.2.2 Range control chart of the absolute differences of duplicate measurements carried out in the measurement of DIC during the leg. 2 MR06-04 cruise.

(6) Data Archive

All data will be submitted to JAMSTEC Data Management Office (DMO) and is currently under its control.

(7) References

DOE (1994), Handbook of methods for the analysis of the various parameters of the carbon dioxide system in sea water; version 2, A. G. Dickson & C. Goyet, Eds., ORNS/CDIAC-74

Ishii M. Inoue Y.H., Matsueda H. (2000), Coulometric of Radiocarbon for the Carbon Dioxide in the Atmosphere and for the Total Inorganic Carbon in Seawater, TECHNICAL REPORTS OF THE METEOROLOGICAL RESERCH INSTITUTE No.41

6.4.5.3 Total Alkalinity

(1) Personnel

Leg.1: Mikio Kitada, Masaki Moro, Hideki Yamamoto (Marine Works Japan Co. Ltd)

Leg.2: Fuyuki Shibata, Mikio Kitada, Ayaka Hatsuyama (Marine Works Japan Co. Ltd)

(2) Objectives

When CO_2 dissolves in water, chemical reaction takes place and CO_2 alters its appearance into several species. Unfortunately, the concentrations of the individual species of CO_2 system in solution cannot be measured directly. Instead, the concentration of CO_2 system in the water could be estimated by measuring 2 parameters out of 4, which is total alkalinity (TA), total dissolved inorganic carbon (DIC), pH and pCO_2 (DOE, 1994). Here, we report on board measurements of TA in the North Pacific, the Okhotsk Sea, Bering Sea and the Arctic Ocean during MR06-04 cruise.

(3) Measured Parameters

Total alkalinity

(4) Instruments and Methods

4-1 Seawater sampling

Seawater samples were collected by 12L Niskin bottles at 7 and 22 stations during the Leg.1 and the Leg.2, respectively. Seawater was sub-sampled in a 125ml glass bottle that was previously soaked in 5% non-phosphoric acid detergent solution (pH13) at least 3 hours and was rinsed by fresh water for 5 times and Milli-Q deionized water for 3 times. A silicon sampling tube was connected to the Niskin bottle when the sampling was carried out. The seawater was gently put on the bottom, and was overflowed for 10 seconds with taking care not to leave any bubbles in the bottle. After sub-sampling finished, the glass bottles were moved to the laboratory. The bottles were put in the water bath under 25 ˚C till the titration.

4-2 Seawater analysis

The 50ml of seawater was sub-sampled in a 100ml tall beaker with a Knudsen pipette. The titration carried out adding the hydrochloric acid (0.05M) to seawater past carbonic acid point with a set of electrodes used to measure electromotive force at 25 ˚C. After titration, the data of acid volume utilized by titration and electromotive force and seawater temperature pipetted were calculated to total alkalinity.

The titration system composed of a titration manager (Radiometer, TIM900), an auto-burette (Radiometer, ABU901), a pH glass electrode (pHG201) and reference electrode (Radiometer, REF201), a thermometer (Radiometer, T201) and a computer installed burette operation software (Lab Soft, Tim Talk9).

At the first of all, the calibration factor (acid concentration) was calculated by measuring a series of

sodium carbonate solutions (0.5~2.5mM) and this calibration factor was applied to all data acquired throughout the cruise. By measuring House Reference Material (HRM: batch Q14) before and after the measurements of all samples were measured, the factor was calibrated. During every run, filtered seawater measurement was carried out before samples ware measured.

(5) Preliminary results

A replicate analysis was made on every 4th seawater sample and the difference between each pair of analyses was plotted on a range control chart (see Figures 6.4.5.3.1 and 6.4.5.3.2). The average of the difference were 1.1 μmol/kg (N=11 pairs) for the Leg.1 and 1.2μmol/kg (n=21 pairs) for the Leg.2, respectively. The standard deviation was 0.8 μmol/kg for the Leg.1 and 1.1μmol/kg for the Leg.2 and the analysis was accurate enough according to DOE (1994).

(6) Data Archive

All data will be submitted to JAMSTEC Data Management Office (DMO) and is currently under its control.

(7) Reference

DOE (1994), Handbook of methods for the analysis of the various parameters of the carbon dioxide system in sea water; version 2, A. G. Dickson & C. Goyet, Eds., ORNS/CDIAC-74.

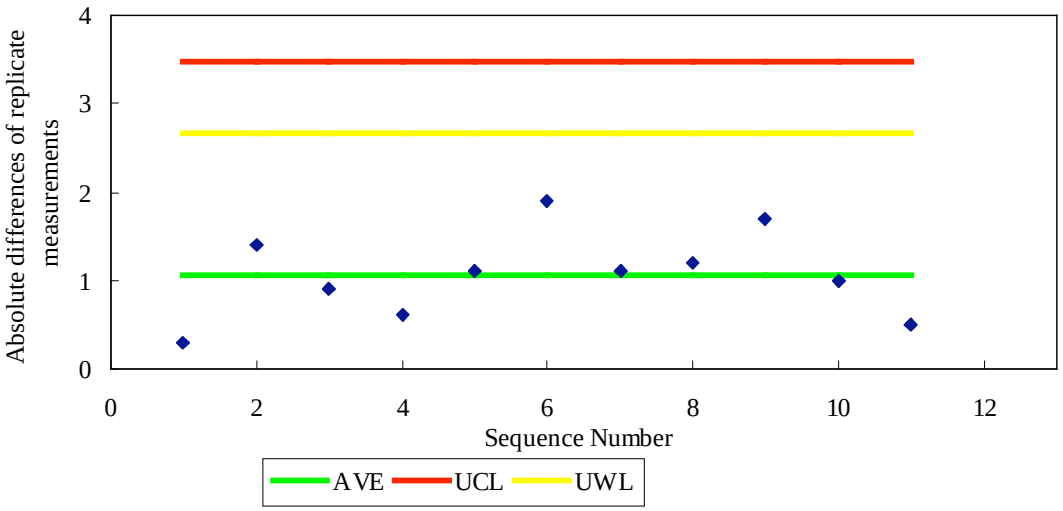

Figure 6.4.5.3.1 Range control chart of the absolute differences of replicate measurements carried out in the analysis of TA during the MR06-04 Leg.1 cruise.

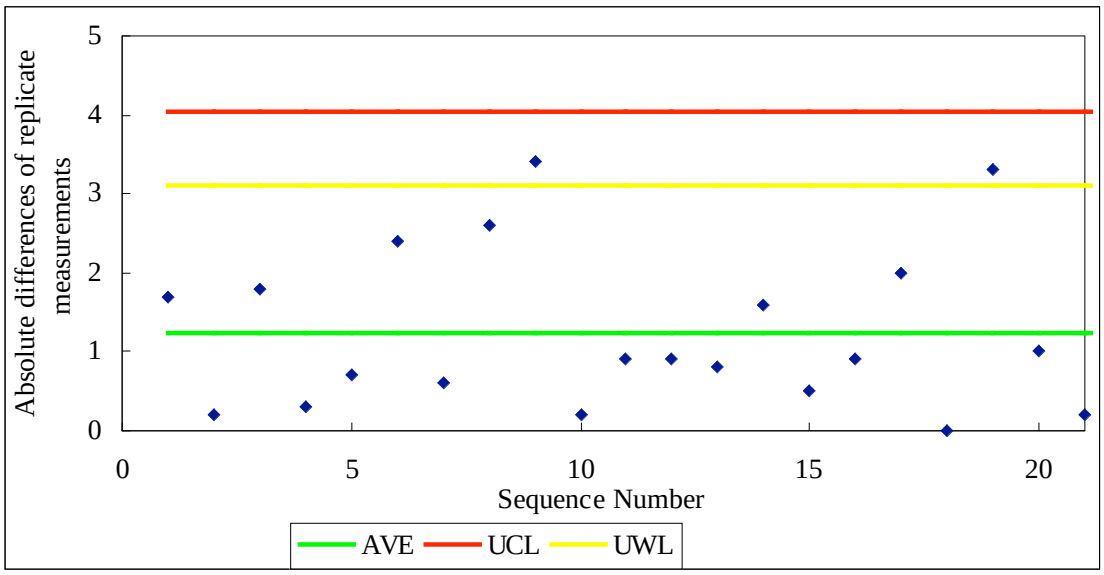

Figure 6.4.5.3.2 Range control chart of the absolute differences of replicate measurements carried out in the analysis of TA during the MR06-04 Leg.2 cruise.

6.4.5.4 Total hydrogen ion concentration scale (pH)

(1) Personnel

Leg.1: Mikio Kitada, Masaki Moro, Hideki Yamamoto (Marine Works Japan Co. Ltd)

Leg.2: Fuyuki Shibata, Mikio Kitada, Ayaka Hatsuyama (Marine Works Japan Co. Ltd)

(2) Objectives

To understand the carbonate system in the seawater, we measured four parameters of CO_2 system in solution (alkalinity, total dissolved inorganic carbon, total hydrogen ion concentration scale (pH) and pCO_2) throughout the cruise. When more than two of the four parameters are measured, the concentration of CO_2 system in the water could be estimated (DOE, 1994). Here, we report on board measurements of pH in the North Pacific, the Okhotsk Sea, the Bering Sea and the Arctic Ocean during MR06-04 cruise.

(3) Measured Parameters

pH (Total hydrogen ion concentration scale)

(4) Instruments and Methods

4-1 Seawater sampling

Seawater samples were collected by 12L Niskin bottles at 7 and 22 stations during the Leg.1 and Leg.2, respectively. Seawater was sub-sampled in a 125ml glass bottle that was previously soaked in 5% non-phosphoric acid detergent solution (pH13) at least 3 hours and was rinsed by fresh water for 5 times and Milli-Q deionized water for 3 times. A silicon sampling tube was used when the sub-sampling was carried out. The seawater was gently put on the bottom of the glass bottle, was overflowed for 10 seconds with taking care not to leave any bubbles in the bottle. After sub-sampling finished, the glass bottles were moved to the laboratory. The glass bottles were put in the water bath under 25℃ till the measurement.

4-2 Seawater analysis

Total hydrogen ion concentration scale (pH; $-\log[H^+]$) of the seawater was measured potentiometrically in the closed glass bottle at the temperature 25℃ (pH_{25}). Value of pH determined experimentally from sequential measurements of the electromotive force (the e.m.f.) of electrode cell in a standard buffer that the value of pH is known (defined) and in the seawater sample (Ag, AgCl | solution of KCl || test solution | H+ -glass –electrode). The e.m.f. of the glass / reference electrode cell was measured with a pH / Ion meter (Radiometer PHM240). Separate glass (Radiometer pHG201) and reference (Radiometer REF201) electrodes were used. To inhibit the exchange of CO_2 between seawater sample and the atmosphere during pH measurement, closed glass bottle was used. The temperature during pH measurement was monitored with temperature sensor (Radiometer T201) and controlled to 25℃ within ±0.1℃.

The TRIS (Lot=060413-1, 060413-2: pH=8.0906 pH units at 25℃, Delvalls and Dickson, 1998) and AMP (Lot=060802-1: pH=6.7839 pH units at 25℃, DOE, 1994) in the authentic seawater (Total hydrogen scale) were used to calibrate the electrodes.

The pH_T of seawater sample (pH_{samp}) is calculated from the following expression:

$$pH_{samp} = pH_{TRIS} + (E_{TRIS} - E_{samp}) / ER \qquad (1)$$

where, electrode response "ER" is calculated as follows:

$$ER = (E_{AMP} - E_{TRIS}) / (pH_{TRIS} - pH_{AMP}) \qquad (2)$$

(5) Preliminary results

A replicate analysis was made on every 2nd or 4th or 6th seawater sample and the difference between each pair of analyses was plotted on a range control charts (see Figures 6.4.5.4.1 and 6.4.5.4.2). The average of the difference was 0.001 pH units (n=14 pairs for the Leg.1, and n=22 pairs for the Leg.2). The standard deviation was 0.001 pH units, and the analysis was accurate enough according to DOE (1994).

(6) Data Archive

All data will be submitted to JAMSTEC Data Management Office (DMO) and is currently under its control.

(7) References

DOE (1994), Handbook of methods for the analysis of the various parameters of the carbon dioxide system in sea water; version 2, A. G. Dickson & C. Goyet, Eds., ORNS/CDIAC-74

DelValls, T. A. and Dickson, A. G., (1998) The pH of buffers based on 2-amino-2-hydroxymethyl-1,3-propanediol ('tris') in synthetic sea water. Deep-Sea Research I 45, 1541-1554.

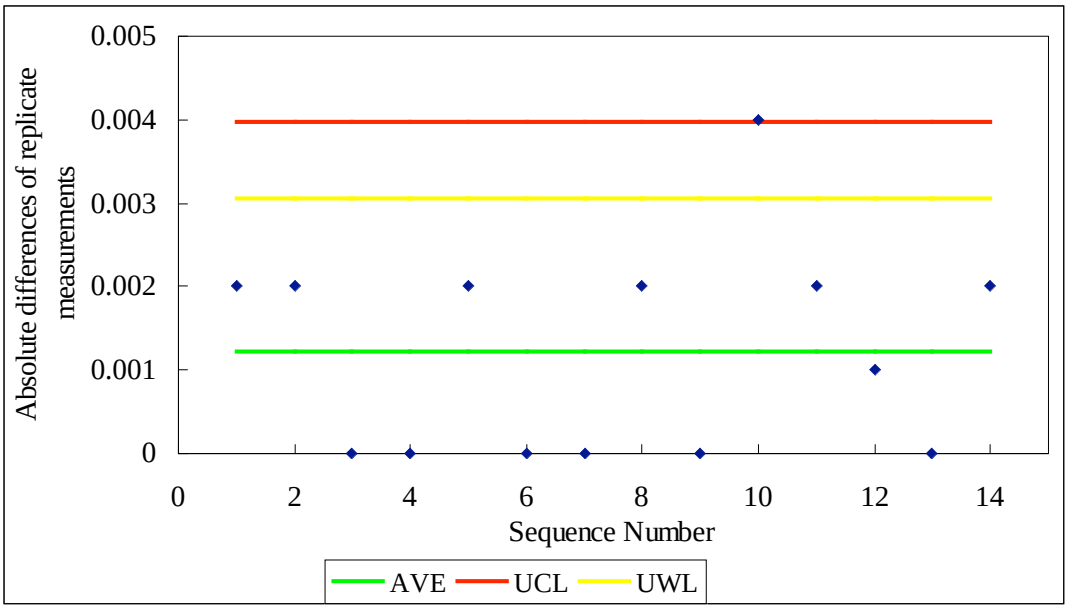

Figure 6.4.5.4.1 Range control chart of the absolute differences of replicate measurements carried out in the analysis of pH during the MR06-04 Leg.1 cruise.

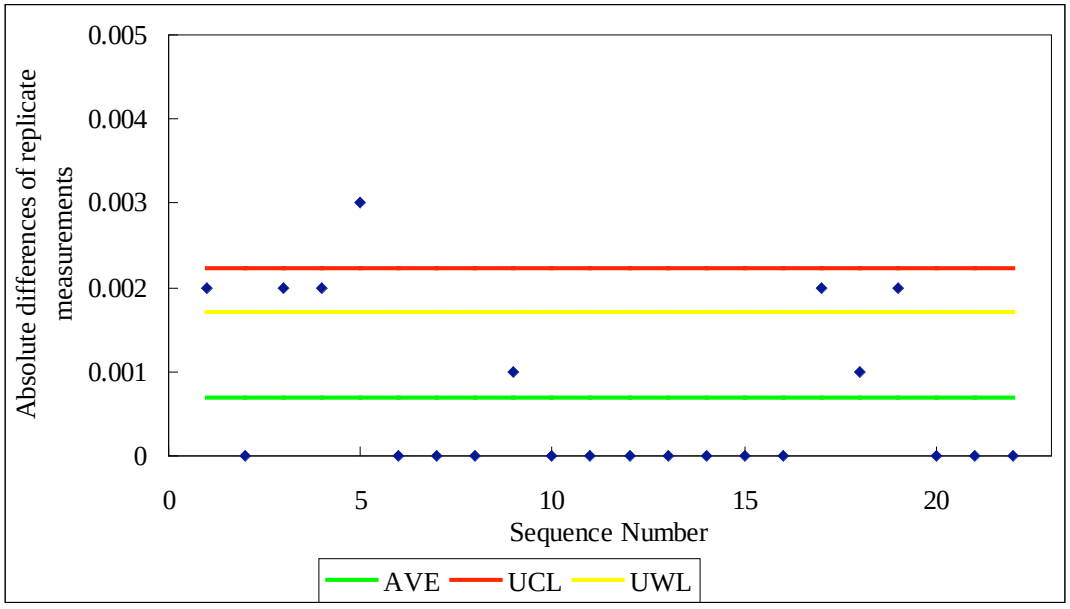

Figure 6.4.5.4.2 Range control chart of the absolute differences of replicate measurements carried out in the analysis of pH during the MR06-04 Leg.2 cruise.

6.4.6 Rare Earth Elements

6.4.6.1 Dissolved Rare Earth Elements measurements

(1) Personnel

Harumi Murayama (University of Toyama) Leg.1

Jing Zhang (University of Toyama) on shore

(2) Introduction

Recently, it was suggested that the deep convection system of the Sea of Japan is weaken, and increasing of potential temperature is reported as a characteristic of the bottom water. In this study, observing northern of Japan Sea and the Sea of Okhotsk, using the dissolved oxygen, nutrients, salinity, Rare Earth Elements (REEs) and oxygen isotope ratio, to clarify the detail of the deep convection system of the Sea of Japan.

In addition, The North Pacific is an upwelling area of oceanic circulation as well as an important area with high level of primary productivity. However, it is known that part of North Pacific is characterized by high nutrients and low chlorophyll (HNLC). Recently, coccolithophorids were observed in HNLC areas. To clarify the causes of coccolithophorids' appearance, it is an important to understand the details regarding abyssal circulation.

(3) Objectives

The objectives of this study to clarify and investigate oceanic general circulation in North Pacific by the REEs, nutrients and oxygen isotope ($\delta^{18}O$) .

(4) Inventory Information for the Sampling

4-1 REEs

A total of 98 seawater samples, about one liter for each sample, were collected from 7 stations (Table 6.4.6.1.1) for dissolved REEs determination of seawater in Okhotsk Sea and Japan Sea , using standard CTD/X-NISKIN bottles, clean bucket for surface water, and multiple core for bottom water. All seawater samples (1 liter) were filtered immediately through 0.1-μm membrane filters after being collected. The residues and filters were stored in a refrigerator, and the filtrate sample was acidified to pH<1.6 for measurements on land performed with ICP mass spectrometers immediately afterwards.

4-2 Nutrients

Seawater samples about 20 ml were collected at each station (Table 6.4.6.1.1) for nutrients.

4-3 Oxygen isotope ($\delta^{18}O$)

Seawater samples about 100 ml were collected at each station (Table 6.4.6.1.1) for oxygen isotope

($\delta^{18}O$).

(5) Data Archive

All of the raw and processed data on the seawater and sediment will be submitted to the JAMSTEC Data Management Office (DMO) as soon as the analysis is completed, and will remain under its control.

Table 6.4.6.1.1. Sample locations and descriptions for REEs, nutrients oxygen isotope concentration collected by NISKIN-X.

Station name	REEs	Nutrients	Oxygen Isotope ($\delta^{18}O$)
St.1	14	2	14
St.2	14	2	14
St.3	13	3	13
St.4	14	3	14
St.5	13	3	13
St.6	14	3	14
St.7	14	3	14

6.4.6.2 Circulation pattern in Arctic Ocean by chemical tracers

(1) Personnel

Ajit Kumar Mandal (Toyama University) Leg.2

Jing Zhang (Toyama University) on shore

(2) Introduction

In the Arctic Ocean, the 1 degree Fahrenheit (0.6 degree Celsius) rise in temperature over last century should have caused a corresponding increase in Arctic river discharge. The freshwater influx into the oceans continues to rise, it could have a large-scale impact on ocean circulation patterns in the North Atlantic. The influx could slow down or shut off the North Atlantic Deep water (NADW) formation, the driving factor behind the convey or belt current known as thermohaline circulation, which brings large amounts of warm water to the North Atlantic region.

(3) Objectives

In this study, water samples were collected from the Chukchi Sea and Bering Sea. The objective of this study is to clarify the circulation by using strontium and oxygen isotopes of seawater–which is difficult to achieve by using salinity and/or sea water temperature.

Due to the simplicity and predictability of their chemical systematics, rare earth elements (REEs) have been receiving increased attention in marine geochemistry, and recent studies indicate that the REEs, especially the ratios of their shale normalized pattern and their neighboring trivalent HREEs (heavy REEs), are particularly useful as tracers of different water masses.

Inventory information for the sampling

The samples for oxygen isotope ($\delta^{18}O$) and strontium isotope ($^{87}Sr/^{86}Sr$) compositions, and rare earth element concentration were collected for analysis. The nutrients in all surface and deep sea water samples were analyzed on board. The other chemical components will be determined at our laboratory of Toyama University after the expedition.

3-1 Oxygen and strontium isotopes

About 100 ml of 177 samples for oxygen and strontium isotopes were collected. They will be analyzed for oxygen by IRMS (Isotope Ratio Mass Spectrometry) and strontium isotope composition by TIMS (thermal ionization mass spectrometry) respectively.

3-2 REEs

Total of 177 seawaters, about one liter for each sample, were collected from 22 stations for dissolved REE determination of sea water in Arctic Ocean, with standard CTD/Niskin-Rosette and X-NISKIN bottles. Immediately after collection, all seawater samples (1 liter) were filtered through 0.1-µm

membrane filters. The residues and filters were stored in a refrigerator, and the filtrate was acidified to pH<1.6 for measurements on land performed with ICP mass spectrometers.

(4) Data Archive

All of the raw and processed data on the seawater will be submitted to the JAMSTEC Data Management Office (DMO) as soon as analysis is completed and will remain under its control.

6.5 Biogeochemical Observations in the sea-water

6.5.1 Particulate nutrients, Calcium carbonate and Chlorophyll a

(1) Personnel

Yoko Kishi (Tokai Univ.) Leg.1-2
Hisashi Narita (Tokai Univ.) Leg.2

(2) Introduction

The subarctic Pacific is one of the most productive areas among the world's oceans. However, the eastern North subarctic Pacific (i.e. Alaskan Gyre: AG) is known the high-nutrient low-chlorophyll (HNLC) due to Fe limitation, because of the dust flux from atmosphere is decreased west to east and small phytoplankton are dominate. Recently, the western North Pacific (i.e. e. Western Subarctic Gyre: WSG) is also known the HNLC during summer season, although the high chlorophyll *a* concentrations have been observed during spring bloom. Therefore, some works have reported that coccolithophorids (*Emiliania huxleyi*) were present in significant numbers in surface water during summer to fall in the WSG, where diatoms were dominated during spring to summer. Coccolithophorids are one of the main groups of calcifying organisms in the marine environment, and *E. huxleyi* is the most common coccoithophorid and is one of the species, which has a worldwide distribution, and it has the capacity to occur massive blooms. Thus, the present of *E. huxleyi* in the WSG can contribute to primary production or export production, which is the oceanic carbon cycle, with the present of a distinct spring bloom. Therefore, *E. huxleyi* may influence the global climate system, because CO_2 was released from the ocean surface during calcification by this organism and dimethylsulfonio-propionate (DMSP), which is the precursor of dimethyl-sufide (DMS), are more produced by this species. Here, we measure particulate nutriments, calcium carbonate and Chollopyll *a* to evaluate the contributions of diatom and coccolithophorids account for chlorophyll biomass during late summer in the subarctic Pacific and marginal sea, such as the Japan sea, Sea of Okhotsk, the Bering Sea including shelf area and the Arctic Ocean.

(3) Method

3-1 Measurement of particulate and Dissolved Organic nutrients, calcium carbonate and chlorophyll a concentrations

Water samples were collected from upper 300 m water depth at all hydrocast stations, using CTD systems attached with Niskin-X Sampler of 12 L capacity. In addition, surface seawater samples were collected in the Sea Surface Water navigation during this cruise.

Particulate nutrients and calcium carbonate samples were collected into a 2 L of dark polyethylene bottles and filtered onto 0.5 μm hydrophilic PTFE (polytetrafluoroethylene) membrane fitter (ADVANTEC MFS, Inc.) and grass fiber filter (Whatman GF/F), respectivly. The filter after filtration was stored under –85 °C in a freezer until analysis. Particulate matters were digested by alkaline potassium persulfate solution. Nutrient concentrations in those and surface water determined using an auto analyzer in the on-shore laboratory. Calcium carbonate concentrations were determined by a coulometer in the on-shore laboratory.

Chlorophyll *a* samples were also collected in 2 L of dark polyethylene bottles and carried out size fraction with nuclepore filter (with the pore size in 2, 5 and 10 μm) and grass fiber filter (Whatman GF/F), appling to vacuum less than 100 mmHg. Filtering volume were ~250 ml for GF/F filter, ~150

ml for 2 μm, ~500 ml for 5 μm and ~1,000 ml for 10 μm of nuclepore filter. Filtered samples were extracted in 7 ml of N, N-dimethylformamide (DMF) and stored keeping in cold (-20 °C) and dark condition until analysis. Chlorophyll *a* concentrations measured onboard by the welschmeyer method with a Turner designs Fluorometer.

3-2 Expected results and future works

Chlorophyll *a* concentrations and its size distributions show large variations in each study area. Chlorophyll *a* concentrations observed in the Bering Sea were 3~4 times higher than that in the subarctic Pacific and the other marginal sea. There was a higher abundant of > 10 μm fraction corresponding higher concentration of chlorophyll *a* in the Bering Sea, while the > 5 μm fraction were always abundant than < 2 μm fraction. These findings are a difference of phytoplankton community due to differences of chemical and physical environment during summer season in each study area.

In future, particulate nutrients and calcium carbonate will be analyzed as direct information for a difference of phytoplankton community. The difference of biogeochemical processes in each study area will be discussed according to chlorophyll a, particulate nutrients and calcium carbonate data including nutrients and hydrographic data.

6.5.2 Alkenone biomarker observations

(1) Personnel

Naomi Harada (IORGC, JAMSTEC)

Miyako Sato (IORGC, JAMSTEC)

Kyung Eun Lee (Korea Maritime University)

(2) Objectives

The alkenone unsaturation indices, U^{K}_{37} that is derived from the relative abundance of methyl alkenones with 37 carbon atoms and 2, 3 or 4 double bonds, have been proposed as a proxy measure of water temperature ($U^{K'}_{37} = C_{37:2}/ (C_{37:2} + C_{37:3})$. In order to make alkenone be more robust paleo-thermometer, characteristics of alkenone particles produced in modern surface ocean should be cleared. Thus, we collected the water samples to gather the alkenone particles in this cruise.

(3) Instruments and Methods

Suspended particles were collected as sea water samples at the same station as the sediment core and in the Japan/East Sea, Okhotsk Sea, and the Bering Sea during the R/V MIRAI cruise MR06-04 (1 August to 29 September 2006). Seawater samples 9–10 L in volume were corrected from water depths of upper 100m and filtered through GF/F filters on board to obtain the suspended particles. The GF/F filters were frozen under the -30 ˚C during the cruise. The alkenone analysis will be done on land.

(4) Results

For alkenone analysis of suspended particles, 30 and 59 water samples were collected during leg.1 and leg.2 respectively. At the *Emiliania huxleyi* bloom area found in this cruise on the continental shelf of the Bering Sea, surface water was also collected from underway sea surface observation system.

(5) Data archives

All the data will be published within the moratorium period and will be submitted to JAMSTEC Data Management Office (DMO) as a publication.

6.5.3 Biogeochemical cycle observations

(1) Personnel

Fumiko Nakagawa, Toyoho Ishimura (Division of Natural History Sciences, Faculty of Science, Hokkaido University) Leg.1

Akinari Hirota, (Division of Natural History Sciences, Faculty of Science, Hokkaido University) Leg.1-2

Akira Ijiri, Daisuke D. Komatsu, Satoru Ohkubo (Division of Natural History Sciences, Faculty of Science, Hokkaido University) Leg.2

Sohiko Kameyama, Tomoyuki Ohya, Yuta Konno, Keisuke Furumochi, Urumu Tsunogai (Division of Natural History Sciences, Faculty of Science, Hokkaido University on shore)

(2) Introduction

The goal of our study is to understand the cycling of the bioactive elements (carbon and nitrogen) in the ocean, in order to determine the role of the ocean in global climate change (Figure 6.3.5.1). Our study is especially focused on the atmospheric trace gases, which play important roles in climate changes: such as global warming, stratospheric ozone depletion, and atmospheric photochemistry. We determine the distribution of trace gases (methane, nitrous oxide, non-methane hydrocarbons, carbon monoxide, and hydrogen) in water column. Their stable isotopic compositions ($\delta^{13}C$, $\delta^{15}N$, $\delta^{18}O$) will be analyzed to clarify the production and consumption processes of these gases.

In addition to the trace gas studies, stable isotope study for dissolved organic matter (DOM) in seawater is perform for two reasons: (1) DOM is one of the earth's largest bioactive reservoirs of carbon and (2) DOM is considered as major precursor of some of the trace gases such as non-methane hydrocarbons and carbon monoxide. We also make a challenge on a real-time measurement for nitrogen (N_2) and oxygen (O_2) which is important parameter to understand biological activities during this cruise.

It is well known that the distribution of nitrogen (mostly nitrate) often regulates the productivity in most of the oceans. Since the production and consumption process of the important trace gases are linked to biological activity in the oceans, we examine the distribution and stable isotopic compositions ($\delta^{15}N$, $\delta^{17}O$, $\delta^{18}O$) of

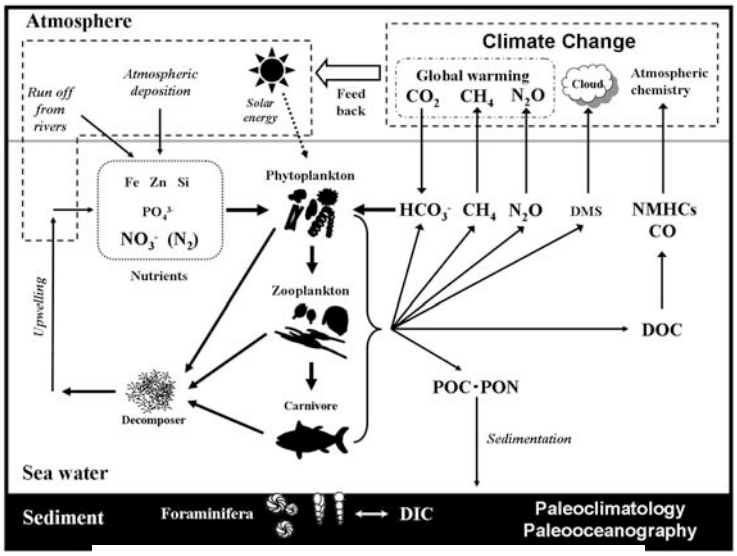

Figure 6.5.3.1 Schematic diagram of our study

nitrate and nitrite to understand their cycle in the oceans.

Our interest is also expanded to paleoenvironmental studies. We believe that our newly developed technique for stable carbon and oxygen isotopic measurements of individual foraminiferal shells, will give us new insights into paleoenvironmental studies.

(3) Sampling of Dissolved methane and nitrous oxide

Both CH_4 and N_2O are important greenhouse gases together with CO_2. They are produced in anoxic microenvironments of some zooplankton species and/or of sinking particles such as fecal pellets and emitted from the surface ocean. In this study, we examined the distribution and stable isotopic compositions of dissolved CH_4 and N_2O in seawater to clarify the processes of trace gas production/consumption.

Seawater sampling was carried out at 31 stations (Stn.1-2: western Pacific Ocean, Stn.3: Japan Sea, Stn.4-7: Sea of Okhotsk, Stn.12-16: Arctic Ocean, Stn.18-33: Bering Sea) on the R/V *Mirai* (JAMSTEC) during a KH-06-04 cruise (Leg 1 and Leg 2). Seawater samples were collected with a 36-port Rosette multi-sampler (12L Niskin bottles) attached to a CTD system. Seawater was slowly transferred into glass vials (ca. 120-mL) via a Tygon tube (6 mm i.d.). The vials were treated by adding 0.5-mL of saturated $HgCl_2$ solution as a preservative, and stored in the dark until the stable isotopic measurements of dissolved gases (CO_2, CH_4 and N_2O). Concentration and stable isotopic compositions ($\delta^{13}C$, $\delta^{18}O$, and $\delta^{15}N$) of these gases will be measured by using continuous-flow isotope mass spectrometry after the cruise.

(4) Method of Nonmethane hydrocarbons (NMHC's) measurement

4-1 Dissolved non-methane hydrocarbons

Nonmethane hydrocarbons (NMHC's), together with carbon monoxide (CO) and methane (CH_4), highly reacts with hydroxyl radical in the troposphere so that they strongly affect the oxidizing capacity of the atmosphere. Growing atmospheric concentrations of these trace gases by increased anthropogenic emissions deplete hydroxyl radicals in the troposphere, affecting atmospheric chemistry, and cause climate change. In this study, we determine the mixing ratios and $\delta^{13}C$ values of dissolved NMHCs and CH_3Cl in the high latitudinal seawater. Seawater sampling was carried out at 4 stations during Leg 1 and 15 stations during Leg 2 (Table 6.5.3.1). Seawater samples were collected with a 36-port Rosette multi-sampler (12L Niskin bottles) attached to a CTD system. The sample was introduced into pre-evacuated ca. 2.7 L glass bottle up to 2.2 L so as to extract dissolved volatiles into vacuum headspace during the step of sample introduction. Then sampled seawater was purged with ultra-pure helium bubble flow (300 ml min^{-1}) for 30 min. while stirring a Teflon coating magnetic stirrer bar vigorously for further extraction of volatiles still dissolved in seawater. All ultra-pure helium used in our measurements was obtained by passing 99.99995% helium through a 4mm i.d. column packed with molecular sieve 5A held at liquid nitrogen temperature just prior

Table 6.5.3.1 Sampling sites, sampling depth (m), and the volume of seawater sample for dissolved NMHCs.

< Leg. 1 >											
Depth	**10 m**	**20 m**	**30 m**	**50 m**	**75 m**	**100 m**	**150 m**	**200 m**	**300 m**	**500 m**	**B-50**
Stn. 1	**2.09 L**			**1.47 L**		**2.10 L**		**2.06 L**		**2.00 L**	**1.95 L**
Stn. 3	**2.02 L**			**2.07 L**		**2.00 L**		**2.01 L**	**2.32 L**	**(350 m)**	**2.31 L**
Stn. 4		**2.15 L**		**2.02 L**							
Stn. 5	**2.17 L**			**2.10 L**		**2.08 L**				**2.16 L**	**2.23 L**
< Leg. 2 >											
Depth	**10 m**	**20 m**	**30 m**	**50 m**	**75 m**	**100 m**	**150 m**	**200 m**	**300 m**	**500 m**	**B-50**
Stn. 15	**2.40 L**	**2.40 L**	**2.40 L**	**2.40 L**							
Stn. 13	**2.40 L**	**2.40 L**		**2.40 L**	**(36 m)**						
Stn. 12	**2.40 L**	**2.40 L**	**2.40 L**	**2.40 L**	**(41 m)**						
Stn. 12EX	**2.40 L**	**2.40 L**	**2.40 L**	**2.40 L**							
Stn. 16	**2.40 L**	**2.40 L**	**2.40 L**	**2.40 L**	**(45 m)**						
Stn. 17	**2.40 L**	**2.40 L**		**2.40 L**	**(39 m)**						
Stn. 18	**2.40 L**	**2.40 L**	**2.40 L**	**(26 m)**							
Stn. 19	**2.40 L**	**2.40 L**	**2.40 L**	**(23 m)**							
Stn. 20	**2.40 L**	**2.40 L**	**2.40 L**	**(27 m)**							
Stn. 21	**2.40 L**	**2.40 L**	**2.40 L**	**2.40 L**	**(42 m)**						
Stn. 22	**2.40 L**			**2.40 L**		**2.40 L**	**(84 m)**				
Stn. 23			**2.40 L**	**2.40 L**	**2.40 L**	**2.40 L**					
Stn. 24	**2.40 L**			**2.40 L**			**2.40 L**	**2.40 L**	**2.40 L**		
Stn. 26	**2.40 L**		**2.40 L**	**2.40 L**	**2.40 L**	**2.40 L**					
Stn. 27	**2.40 L**										

to use. After the volatiles extracted from seawater together with helium flow was dried by passing them through cold-trap (4mm i.d., 0°C) and $Mg(ClO_4)_2$ (approximately 50g, 8-24 mesh; Wako Pure Chemical Industries, Ltd., Osaka, Japan), NMHCs and methyl chloride was gathered onto the first pre-concentration trap (7mm i.d.) packed with quartz glass wool held at liquid nitrogen temperature together with CO_2 while the other major dissolved gases (N_2, O_2, Ar, and CH_4) passes through the trap. After the extraction, non-condensable helium atmosphere in the first pre-concentration trap was evacuated using a rotary vacuum pump and the gathered NMHCs and methyl chloride with CO_2 matrix in the first pre-concentration trap were liberated and transferred to the second pre-concentration trap (glass ampoule) bottom of which was held at liquid nitrogen temperature. After the perfect transport, inlet of the ampoule was flame-sealed for long storage of NMHCs and methyl chloride in the ampoule, together with CO_2. After the cruise, we will measure the mixing ratios and stable isotopic compositions of NMHCs by using an isotope-ratio-monitoring gas chromatography/mass spectrometry system in our laboratory.

4-2 Atmospheric non-methane hydrocarbons

In order to determine the mixing ratios and $\delta^{13}C$ values of NMHCs and CH_3Cl in the high latitudinal atmosphere, 14 times maritime air sampling was performed over the Bering Sea and Pacific Ocean between 71°N and 40°N on board (Table 6.5.3.2). All samples were collected using evacuated stainless steel canisters, 6L fused silica lined canisters (Silico-can, Restek) in both of which NMHCs and CH_3Cl was stable for more than six months. Sampling time and other sampling conditions were carefully

chosen to minimize all possible contamination from the ship itself.

Table 6.5.3.2 Sampling time and location for atmospheric NMHCs measurement

Sampling time		Sampling location	
Local time	UTC	Latitude	Longitude
2006/9/1 12:44	2006/9/1 20:44	N 71.32	W 166.15
2006/9/2 14:10	2006/9/2 22:10	N 72.21	W 165.59
2006/9/5 0:00	2006/9/5 8:00	N 69.20	W 166.23
2006/9/6 11:43	2006/9/6 19:43	N 66.51	W 167.23
2006/9/7 12:49	2006/9/7 20:49	N 63.45	W 168.36
2006/9/14 10:04	2006/9/14 18:04	N 59.54	W 168.54
2006/9/17 10:18	2006/9/17 18:18	N 56.48	W 167.11
2006/9/20 7:30	2006/9/21 22:30	N 53.58	W 171.46
2006/9/21 18:37	2006/9/21 8:37	N 53.23	E 173.27
2006/9/22 9:08	2006/9/21 22:08	N 51.04	E 170.35
2006/9/22 20:52	2006/9/23 9:52	N 48.33	E 170.05
2006/9/23 22:16	2006/9/24 10:16	N 45.59	E 163.38
2006/9/24 23:28	2006/9/25 10:28	N 43.04	E 156.32
2006/9/1 12:44	2006/9/1 20:44	N 40.11	E 150.04

(5) Results

5-1 Dissolved hydrogen and carbon monoxide

Onboard measurement of dissolved hydrogen and carbon monoxide was carried out during a KH-06-04 cruise (only Leg 2). Dissolved hydrogen and carbon monoxide concentrations were measured by using analytical system connected to Trace Reduction Gas Detector (TRD) on board (Konno in prep.). 200 ml of sea water was transferred into a pre-evacuated glass bottle (250 ml) from the Niskin bottle,

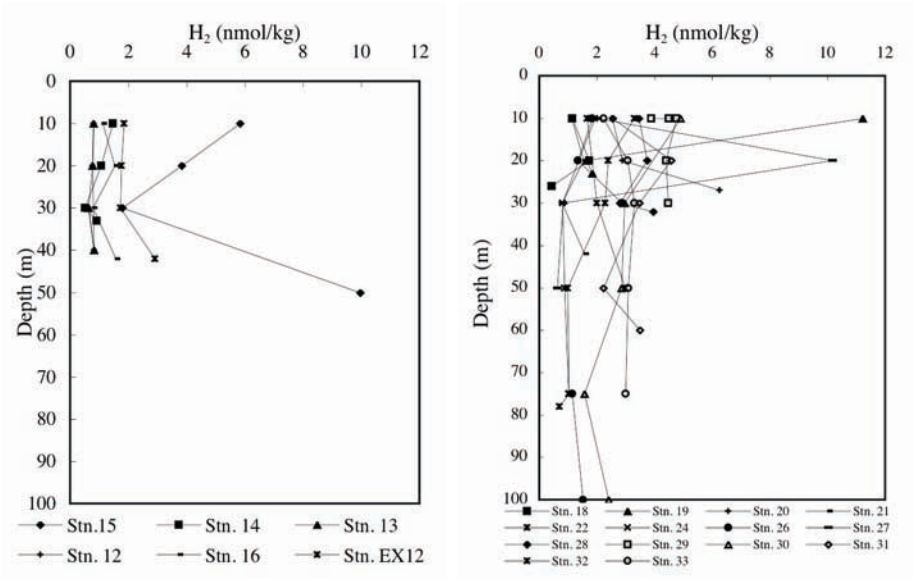

Figure 6.5.3.2. Hydrogen concentrations in the Arctic Ocean Sites (left) and in the Bering Sea Sites (right)

leaving 50 ml of headspace, and kept standing at 20°C for 30 min to complete the equilibration between aqueous and gaseous phases. The headspace gas was then introduced into the analytical system to measure its hydrogen and carbon monoxide concentrations.

The concentrations of hydrogen in the Arctic Ocean Sites (Stn. 12~16) and the Bering Sea Sites (Stn. 18 ~ Stn.33) are shown in Figure 6.5.3.2. The concentrations of dissolved hydrogen at all sites were above saturation (>0.4 nmol/kg). The concentrations were high in surface water above 30 m. The highest concentration (11.2 nmol/kg) was observed in 10 m depth at Stn. 19 located on the estuary of the Yukon River. The concentrations of carbon monoxide in the Arctic Ocean Sites (Stn. 12~16) and the Bering Sea Sites (Stn. 18 ~ Stn.33) were shown in Figure 6.5.3.3. The highest concentration was observed in 10 m depth at Stn. 12.

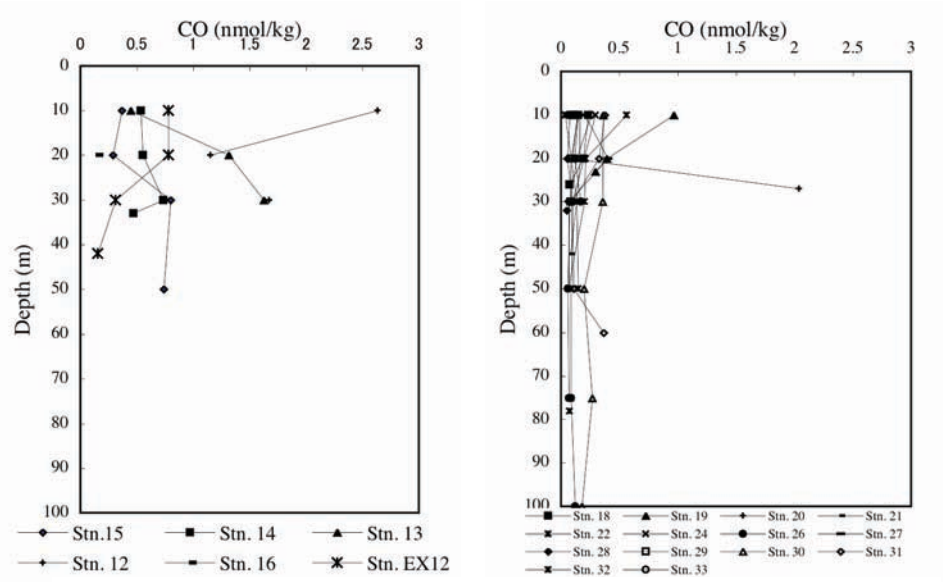

Figure 6.5.3.3. CO concentrations in the Arctic Ocean Sites (left) and in the Bering Sea Sites (right)

5-2 Nutrients and dissolved organic matter

In many ecosystems, the bioavailability of fixed nitrogen regulates productivity and controls the overall biodiversity of the system. So it is important to identify sources and resolve fates of nitrate in order to understand nitrogen cycling and the effect of human activity upon cycle. In this study, we will measure two nitrogen isotopes and three oxygen isotopes of nitrate to identify their sources (Figure 6.5.3.4).

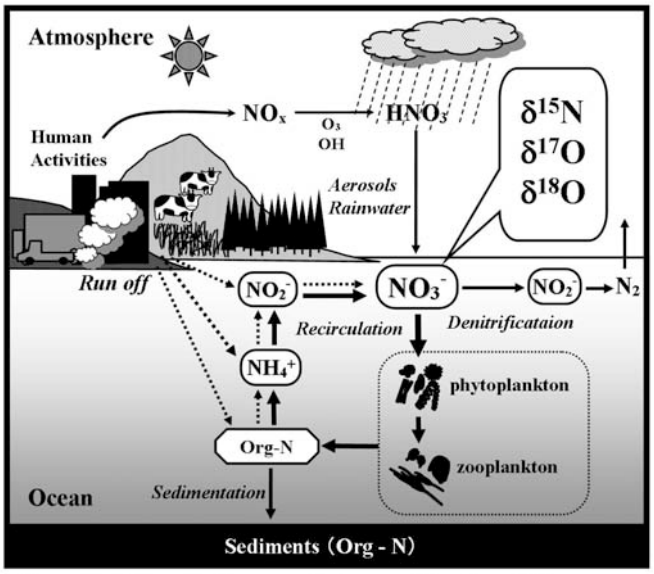

Figure 4 Schematic diagram of nitrogen (nitrate) cycle in seawater

Figure 6.5.3.4 Schematic diagram of nitrogen (nitrate) cycle in seawater

Water samples for analyses of nutrients and organic matters were obtained in all hydrocast stations (31 stations; Stn.1-2: western Pacific Ocean, Stn.3: Japan Sea, Stn.4-7: Sea of Okhotsk, Stn.12-16: Arctic Ocean, Stn.18-33: Bering Sea) on the R/V *Mirai* (JAMSTEC) during a KH-06-04 cruise (Leg 1 and Leg 2). Seawater samples were collected with a 36-port Rosette multi-sampler (12L Niskin bottles) attached to a CTD system. 1.3 liters per sample were filtered by using all glass devices through precombusted Whatman glass-fiber membranes (GF/F ~0.7mm) rinsed with the sample. Filtered samples were collected in J-bottle and glass vials for nutrients and organic matters analyses, respectively, and then freezed for preservation. $\delta^{15}N$, $\delta^{18}O$ and $\delta^{17}O$ of nitrate, and $\delta^{13}C$ and $\delta^{15}N$ of dissolved organic matters will be quantified.

5-3 Isotopic compositions of individual foraminiferal shell

For more than 50 years, stable carbon and oxygen isotopic compositions ($\delta^{13}C$ and $\delta^{18}O$) of calcium carbonate, especially foraminiferal shells, have been used for paleoenvironmental studies because their variations in isotopic compositions are useful for estimating paleoenvironments, such as global sea level changes, paleotemperature, global deep-sea circulation, and huge methane release events from the seafloor. In general, isotopic values of foraminiferal shells are determined through several factors, such as isotopic compositions of sea / bottom water, temperature, and vital effects. By quantifying the detailed relationship between the isotopic compositions of shells and ecological factors, we will be able to broaden the range of application of foraminifera as paleoenvironmental tracers. In addition, we can apply them in new foraminiferal studies, such as evaluating the extent of bioturbation at the sediment surface, or reconstructing paleo-seasonal climate variations, and estimations of biogeochemical circulations. In this study, we are going to estimate the ecology of small foraminifera using their isotopic dispersion in the same species sampled at the same depth at the same station. The

results are expected to be very useful for choosing appropriate paleoindicators in future paleoenvironmental studies.

To determine the dispersion of the $\delta^{13}C$ and $\delta^{18}O$ values that might exist within each individual small foraminiferal shell of the same species sampled at the same depth at the same station, surface sediment samples were collected during a cruise of the MR06-04 (see table 3 about the sampling stations). The sediment, collected by a multiple-corer, was subsampled and used for the individual foraminiferal analysis. Prior to isotopic analysis, the sediment was stained with 0.5% Rose-Bengal solution for at least 1 week to distinguish the living from the dead foraminifera. Then, the samples were washed and sieved at 63 μm using 50 °C water and oven-dried at 40 °C before being chosen for isotopic analysis. To determine the stable carbon and oxygen isotopic compositions of individual small foraminifera, we employed the analytical system using continuous-flow isotope ratio mass spectrometry (CF-IRMS) described by Ishimura et al. (2004). By using this system, we can determine stable carbon and oxygen isotopic compositions of as little as 0.2 micrograms of $CaCO_3$, within external standard deviations of 0.10 ‰ for $\delta^{13}C$ and 0.18 ‰ for $\delta^{18}O$.

Talble 6.5.3.3 Sampling stations for isotopic study of ingividual foraminifera

Leg.1 MC samples for foraminiferal study

station	core length (cm)	stained (cm)	non-stained (cm)
1	28	0-20	20-28
2	27	0-20	20-27
3	23	0-23	-
4	42	0-42	-
5	26	0-10	10-26
6	39	0-20/26-27	20-26/27-39
7	31	0-20	20-31

Leg.2 MC samples for foraminiferal study

station	core length (cm)	stained (cm)	non-stained (cm)
12	20.5	0-10	10-20.5
12EX	31.6	0-10	10-31.6
14	8.5	0-8.8	-
16	26	0-10	10-26.0
18	16	0-10	10-16.0
19	16	0-10	10-16.0
20	10.5	0-10	-
21	20	0-10	10-20
22	23	0-10	10-23
23	21.5	0-10	10-21.5
24	14.5	0-10	10-14.5
25	16.5	0-10	10-16.5
26	20.3	0-10	10-20.3
29	16	0-10	10-16
30	22		0-22.0
31	20.5	0-10	0-20.5
33		0-10	10-

Reference

Ishimura, T., Tsunogai, U., and Gamo, T., Stable carbon and oxygen isotopic determination of sub-microgram quantities of CaCO3 to analyze individual foraminiferal shells. Rapid Communications in Mass Spectrometry. 18. pp 2883-2888. DOI: 10.1002/rcm.1701. 2004.

6.6 Biological Oceanographic Observations

6.6.1 Ecology of living foraminifera

(1) Personnel

Katsunori Kimoto (IORGC, JAMSTSEC) Leg.1

Takuya Itaki (Univ. Tokyo) Leg.1,2

Takashi Toyofuku (IFREE/JAMSTEC) Leg.2

Kota Katsuki (Shimane Univ.) Leg.2

Atsushi Kurasawa (Hokkaido Univ / IFREE, JAMSTEC) Leg.1

(2) Objectives

Oceanic microplankton is one of the group of marine Protista, and they are fundamental components of oceanic material cycles and food-web. Especially, the unicellular organisms, such as foraminifera, radiolarians and diatoms are very common in the water column and they build a hard-skeletons made from calcareous and/or silicates. After they died, their hard skeletal shells sink down and are preserved in the deep-sea sediments. Therefore their secreted shells are good indicator for estimating paleo-sea surface environmental conditions.

It is known that such skeleton-bearing microplankton make habitats in wide range of environments in the surface water, however, their distribution, abundances, and genetic diversity in the water column are poorly documented. Especially in high latitude area, basic data of ecology of skeleton-bearing plankton is lacking prominently. In this study, we collected planktic foraminifers, radiolarian and diatom samples used the multi-depth plankton net (Closing net) from the water column at the Sea of Okhotsk, western Pacific, Bering Sea, Arctic Sea and its adjacent area, and try to make general view of their habitat and ecology. This study will be contributed to make blueprint for reconstructing the paleo-sea surface environmental conditions in the high latitude oceans in the northern hemisphere.

(3) Equipments and Sampling strategy

The closing net (Rigosha, co. ltd.) was used for multiple-depth plankton sampling in this study. The closing net is a kind of vertical-towing plankton sampler and it can close the mouth at the any depth by the messenger actions. Fundamental specification of this plankton net is shown in Figure 6.6.1.1. Flow meter was also used in this study. Details of sampling stations and data for collection were listed in Table 6.6.1.1.

Fundamental strategy for sampling by closing net is as follows:

1) Closing net was lowered from starboard side of R/V Mirai by vinyl-coated wire to avoid the oil contamination. The lowering speed of wire was at 1.0 m /sec.

2) After closing net reached at the bottom of target water depth, it was pulled up from bottom to top water depth where we targeted. At this moment, pulling up speed of wire was at 0.5 m /sec.

3) Messenger (1.5 kg weight) was through out to close the net mouth at the given water depth.

4) After the releaser activated, closing net was pulled up to the deck at 1.0 m wire speed.

5) Samples were collected used 0.2 μm filtered seawater on the deck.

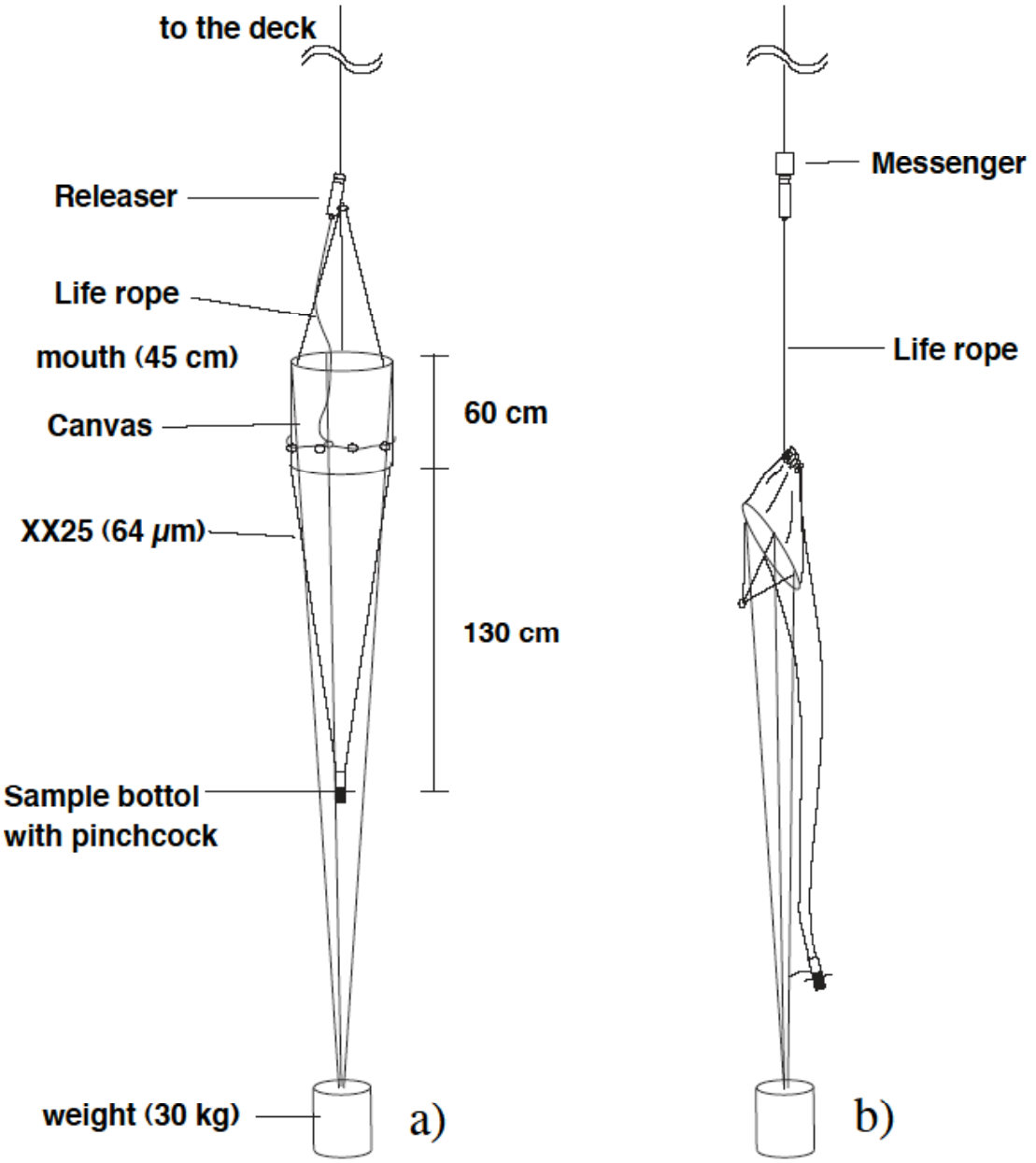

Figure 6.6.1.1 Schematic illustration of the closing net. a) Before closing; b) After closing

(4) Shipboard treatments

Plankton net experiments was performed at all observation stations in Leg 1. For microfossil assemblages, they were fixed by alkali- buffered formaline (pH = 8.2) immediately and were diluted to be 5 % concentration of formaline in the laboratory. After that, they were kept in the refrigerator. For DNA

analysis, samples were sorted under a stereo-microscope immediately after collection, Isolated specimens were cleaned with filtered seawater using fine brush in order to remove microorganisms from the test surface. Cleaned specimens were transferred on the faunal slides and dried at room temperature. The dried specimens were stored in refrigerator at -80°C. The extraction of DNA and further molecular biological analysis were carried out after the cruise.

(5) Analytical items

All plankton samples were shared for following analysis.

1) Phylogenetic diversity of living planktic foraminifers (IFREE, JAMSTEC)

2) Faunal analysis of planktic foraminifers, radioralians, and diatoms (IORGC, JAMSTEC, University of Tokyo, and Shimane University)

3) Trace metal analysis incorporating planktic foraminiferal shells (IORGC, JAMSTEC)

4) Measurements of metabolic activity of surface planktons (Hokkaido University)

5) Stable isotopic analysis of individual planktic foraminifers (Hokkaido University)

Table 6.6.1.1 Plankton sampling log during MR06-04

Station	Researcher	Target	Date	Latitude			Longitude			Start	Wire angle	Wire out	Messenger Throw		Net closed			Flow Meter				End	Filtered	Net type	Remarks
		depth (m)		(°)	(')		(°)	(')		Time	(°)	(m)	(Wire angle)	(Wire out)	(Time)	(Wire out)	(arrival count)	(no.)	(read)	(read / m)	(%)	Time	distance (m)		
Leg. 1																									
St. 1	Test	500-0	2.Aug	42	28.18	N	144	17.40	E	11:34	10	500						3034	5290	11	100	11:56	500	45 cm without net	
	Test	200-0										200						3034	2110	11	100		200		
	Test	50-0										50						3034	567	11	100		50		
	Test	50-0										50						3034	553	11	10.9		50		
St. 1	Kurasawa	200-100	2.Aug	42	28.59	N	144	17.49	E	12:28	10	200	10	100	12:38	100						12:38		45 cm 100 µm	Net changed
		100-50								12:50	10	100	10	50	12:56	50						12:58			
		50-25								13:03	8	50	15	25	13:07	25						13:09			
		25-0								13:14	5	25										13:18			
	Kimoto	200-150								13:45	24	219	5	169	13:54	147		3034	709	10	90.3	13:58	72	75 cm 63 µm	Net changed
		150-100								14:09	0	150	10	113	14:16	100		3034	500	10	91.7	14:19	50		
		100-50								14:37	6	100	15	56	14:43	49		3034	680	13	122.3	14:45	51		
		50-20								14:48	17	54	5	20	14:54	18		3034	321	9	81.8	14:55	36		
		20-0								15:00	5	20						3034	227	11	104.1	15:02	20		
St. 2	Kurasawa	200-0	4.Aug	42	52.12	N	143	7.21	E	14:42	0	200										14:55		45 cm 100 µm	Net changed
	Kimoto	20-0								15:02	0	20										15:05		75 cm 63 µm	Net changed, No sampled
		20-0 (1)								15:10															
		50-20								15:35	9	50	9	25	15:38	21		3034	388	13	122.7	15:40	29	45 cm 63 µm	Net changed
		100-50								15:51	30	100	3	60	15:57	51		3034	408	8	76.4	15:58	49		
		150-100								16:02	20	160	15	124	16:09	113		3034	438	9	85.5	16:12	47		
		200-150								16:16	10	203	10	172	16:22	154		3034	255	5	47.7	16:25	49		
		300-200								16:29	7	303	17	248	16:39	220		3034	1555 (555?)	7	61.3	16:44	83		
		500-300								16:48	35	603	35	430	17:08	no tention		3034	8			17:18			No sampled
		500-300								17:55	5	500	3	354	18:12	300		3034	1909 (909?)	5	41.7	18:19	200		
		20-0 (2)								18:26	0	20						3034	90	5	41.3	18:29	20		
St. 3	Kurasawa	200-100	6.Aug	45	45.47	N	140	47.06	E	14:57	15	200	15	100	15:07	100						15:10	100	45 cm 100 µm	
		100-60								15:15	18	100	20	60	15:20	60						15:22	40		
		60-25								15:26	10	60	25	15	15:29	25						15:31	35		
		25-0								15:35	0	25										15:37	25		
		200-0		45	45.60	N	140	48.15	E	15:41	15	200										15:51	200		
	Nakagawa	200-60								15:56	5	200	15	75	16:05	65	13	3034	808 (1808?)	6	54.9	16:07	135	45 cm 63 µm	Net changed
										Break time 10 min															
		60-25								16:17	0	60	0	31	16:20	27	7.7	3034	215	7	59.8	16:21	33		
		25-0								16:24	0	25						3034	65	3	23.9	16:27	25		
	Kimoto	20-0		45	45.61	N	140	49.41	E	16:29	0	20						3034	85 (?)	4	39.0	16:31	20		
		50-20								16:35	0	50	0	25	16:38	23		3034	300	11	101.9	16:39	27		
		100-50 (1)								16:43	0	100	5	56	16:47	54		3034	428	9	85.4	16:49	46		
		100-50 (2)								16:52	5	100	10	62	16:56	55	15.3	3034	425	9	86.6	16:58	45		
										Break time 30 min															
		150-100		45	45.51	N	140	50.46	E	17:34	0	150	5	119	17:40	110	29.9	3034	168	4	38.5	17:44	40		
		200-150								17:48	7	200	10	170	17:55	147.6		3034	415	8	72.7	17:58	52.4		
		300-200								18:03	15	310	25	254	18:13	no tention		3034	8			18:19			No sampled
		300-200		45	45.92	N	140	51.43	E	18:39	40	354	40	307	18:51	269	83	3034	1743 (743?)	9	80.2	18:59	85		
		500-300		45	44.89	N	140	52.14	E	19:07	30	577	25	383	19:28	336	97	3034	1895	8	72.1	19:37	241		
		700-500								19:42	20	>700	20	624	20.02	554	150	3034	760			20:15			Touched with sea-floor (W.D. 670 m)
St. 4	Kurasawa	200-100	8 Aug.	44	31.88	N	144	59.26	E	13:29	10	200	5	100	13:39	100	30					13:42	100	45 cm 100 µm	
		100-50								13:45	5	100	0	50	13:51	50	13					13:50	50		
		50-25								13:56	5	50	0	25	14:00	25	7.8					14:02	25		Messenger changed
		25-0								14:04	10	25										14:07	25		
	Kimoto	20-0								14:12	5	20						3034	37	2	17.0	14:14	20	45 cm 63 µm	Net changed
		50-20								14:17	5	50	5	25	14:20	21		3034	33	1	10.4	14:23	29		
		100-50								14:26	0	100	0	60	14:30	52		3034	225	5	43.0	14:32	48		

Table 6.6.1.1 Plankton sampling log during MR06-04

Station	Researcher	Target	Date	Latitude			Longitude			Start	Wire angle	Wire out	Messenger Throw	Net closed			Flow Meter				End	Filtered	Net type	Remarks
		depth (m)		(°)	(')		(°)	(')		Time	(°)	(m)	(Wire angle)	(Wire out)	(Time)	(Wire out)	(arrival count)	(no.)	(read)	(read / m)	(%)	Time	distance (m)		
		150-100								14:36	10	152	10	121	14:41	107		3034	28	1	5.7	14:44	45		Sampled very few plankton
		200-150		44	31.92	N	144	59.17	E	14:48	12	204	10	180	14:54	160	45	3034	5	0	1.0	14:58	44		Sampled very few plankton
		Break time15 min																						
		500-200								15:19	15	515	15	242	15:37	214	62	3034	393	1	12.0	15:45	301		
		1000-500								15:53	10	1015	12	600	16:22	533	145	3034	1060	2	20.2	16:35	482		
	Nakagawa	25-0								16:39	0	25						3034	18	1	6.6	16:41	25		
	Kimoto	200-100								16:44	10	203	5	119	16:52	105		3034	50	1	4.7	16:55	98		
St. 7	Kurasawa	200-100	11 Aug.	51	16.57	N	149	12.55	E	12:22	15	200	20	100	12:33	100	34					12:36	100	45 cm 100 µm	
		100-50								12:39	10	100	10	50	12:46	50	15					12:47	50		
		50-25								12:51	10	50	10	25	12:53	25	9					12:55	25		
		25-0								12:58	0	25										13:01	25		
	Kimoto	20-0		51	16.74	N	149	12.88	E	13:05	0	23						3034	33	1	13.2	13:07	23	45 cm 63 µm	Net changed
		50-20								13:10	5	50	5	25	13:14	21	8	3034	77	3	24.4	13:15	29		
		100-50								13:18	20	106	20	65	13:22	56	18.6	3034	293	6	53.8	13:24	50		
		150-100								13:27	15	155	10	121	13:33	103	35.7	3034	433	8	76.4	13:36	52		
		200-150		51	16.87	N	149	12.99	E	13:39	10	203	10	174	13:44	150		3034	56	1	9.7	13:44	53		
		300-200								13:52	5	300	10	242	14:00	210	67	3034	613	7	62.5	14:05	90		
		500-300								14:08	30	577	25	377	14:29	321	99	3034	1580	6	56.6	14:34	256		
		1000-500								14:38	7	1008	13	624	15:11	534	169	3034	103	0	2.0	15:24	474		
St. 6	Test	100-0	13 Aug.							12:09		100						2887/3355/3250/1132/1169			100	12:17	100	75 cm without net	
		100-0								12:18		100						2887/3355/3530/2310/2360			100	12:26	100		
		100-0								12:27		100						2887/3355/3764/3412/3490			100	12:35	100		
	Kurasawa	200-100		53	16.80	N	150	4.74	E	12:36	13	219	24	109	12:47	109						12:50	110	45 cm 100 µm	Net changed
		100-50								12:53	25	110	25	55	13:00	55						13:02	55		
		50-25								13:05	15	50	15	25	13:08	25						13:10	25		
		25-0								13:12	26	25										13:15	25		
	Kimoto	20-0		53	16.88	N	150	5.15	E	13:19	1	20						2887	215	11	98.6	13:22	20	45 cm 63 µm	Net changed
		50-20								13:26	20	50	20	27	13:29	23		2887	261	10	88.7	13:30	27		
		100-50								13:33	10	100	10	60	13:37	51		2887	423	9	79.2	13:39	49		
	Nakagawa	60-0								13:52	10	60						2887	212	4	32.4	13:57	60		
		200-60		53	17.04	N	150	5.45	E	14:00	19	213	15	74	14:09	63		2887	152	1	9.3	14:11	150		
	Kimoto	150-100								14:15	20	150	15	126	14:19	110		2887	200	5	45.9	14:22	40		
		200-150								14:25	26	223	26	195	14:32	166		2887	113	2	18.2	14:35	57		
		Short break due to XBT obserbation																						
		300-200 (1)								14:44	32	354	30	272	14:53	234	78	2887	20	0	1.5	14:58	120		Sampled very few plankton
		300-200 (2)		53	17.12	N	150	6.14	E	15:03	8	300	8	236	15:12	204	64	2887	36	0	3.4	15:16	96		
		500-300								15:20	10	508	6	354	15:34	305	94	2887	209	1	9.4	15:41	203		
		1000-500								15:45	20	1064	15	606	16:21	519	165	2887	1618	3	27.2	16:33	545		
St. 5	Kurasawa	200-0	15 Aug.	54	19.62	N	149	16.21	E	9:46	10	200										9:58	200	45 cm 100 µm	
	Kimoto	20-0								10:03	0	20						2887	135	7	61.9	10:06	20	45 cm 63 µm	Net changed
		50-20								10:11	8	50	8	24	10:14	20	7	2887	120	4	36.7	10:15	30		
		100-50								10:18	4	100	6	58	10:23	50		2887	310	6	56.9	10:25	50		
		150-100		54	19.87	N	149	16.30	E	10:28	10	150	10	118	10:34	100		2887	269	5	49.4	10:36	50		
		200-150								10:41	9	203	9	173	10:46	147	54	2887	145	3	23.8	10:50	56		
		300-200 (1)								10:54	15	310	15	237	11:03	204	64	2887	115	1	10.0	11:08	106		
		750-500								11:21	25	800	30	662	11:32	571	179	2887	205	1	8.2	11:45	229		Water depth: 803 m
		500-300		54	18.86	N	149	16.09	E	15:12	10	508	0	346	15:30	300	90	2887	53	0	2.3	15:35	208		
		300-200 (2)								15:41	5	300	0	231	15:48	200	62	2887	50	1	4.6	15:53	100		
	Nakagawa	150-0								15:56	15	150						2887	195	1	11.9	16:06	150		

6.6.2 Planktonic foraminifera: Genetic diversity of planktonic foraminifera in the Sea of Japan, the Sea of Okhotsk, the Bering Sea, northern Northwest Pacific and Chukchi Sea: Its relationship to Quaternary paleoenvironmental changes.

(1) Personnel

Atsushi Kurasawa[*1*2], Masashi Tsuchiya[*1], Takashi Toyofuku[*1], Kate Darling[*3], Michael Kucera[*4], Christopher Wade[*5], Hidetaka Nomaki[*1], Kazuhiko Fujita[*6], Hiroshi Nishi[*2], Hiroshi Kitazato[*1]

[*1]: IFREE, JAMSTEC

[*2]: Graduate School of Science, Hokkaido University

[*3]: School of Geosciences, Science and Engineering at the University of Edinburgh

[*4]: Dept. Geology, Royal Holloway, Univ. of London

[*5]: Genetics at. The University of Nottingham

[*6]: Faculty of Science, Ryukyu University

(2) Objective

The aim of this study is to reveal genetic diversity of planktonic foraminifera to understand relations among genotypes, ecology, and morphology with oceanography and environmental change histories. In this MR06-04 cruise, our research topic is focused on (I) genetic diversity of planktonic foraminifera in marginal seas, and its relationship to open sea populations, and (II) genetic diversity in boundary area between the North Pacific and the Arctic sea, and inter-oceanic gene flow of planktonic foraminifera between these two oceans.

Planktonic foraminifera are one of the major marine carbonates producer have calcareous tests. Planktonic foraminifera exist in various oceanographic conditions, from polar to equatorial, and from surface to deep water in relation to water masses, surface and deep water current, that lives from past and Modern Ocean. Planktonic foraminifera are useful materials for reconstruct such oceanic environment, and thus, these have important rolls in global carbon and calcium circulation in the ocean. The other hand, the regional distribution of foraminiferal assemblage should be controlled by such oceanographic environments as temperature, salinity and primary productivity. In a word, foraminiferal assemblage and oceanographic environments have a close relationship with each other.

The problems are arisen from recent molecular phylogenetic studies that demonstrated high genetic variability existed within a species. These genotypes respectively distributed in each oceanic environment, and it is not always represent a relationship between assemblage and ocean environments in a species level. For instance, high intra-species genetic diversities of foraminifera that was not expected

from traditional morphological studies are reported (Huber *et al.*, 1997; Darling *et al.*,1999, 2000; Stewart et al., 2001; Tsuchiya et al., 2000; de Vargas *et al.*, 1999). All morphospecies studied so far include multiple genotypes, and these genotypes appeared to be differed in environmental preferences (Bauch *et al.* 2003). Then the intra-species genetic diversity and their difference of habitat is important problem for paleoceanographic studies. The paleo-environmental information derived from planktonic foraminifera may have been based on ecologically distinct populations and therefore contain significant noise (Darling *et al.* 2000). In order to deal with this problem, the genetic diversity of planktonic foraminifera and its relations to physical and chemical environments should be clarify. Molecular biological study may also give us important information about evolution on planktonic foraminifera in the oceans, such as inter-oceanic gene flows, speciation between open sea and marginal seas, and the correlation among paleoceanographic changes, geologic events and genetic isolations.

To reveal the correlations between the geographic isolation in ocean and the distributions of genotype, we planned to investigate the genetic diversity of planktonic foraminifera both in Pacific Ocean and in its marginal seas. It is considered that the geographical isolation plays important role for marine organisms speciation. Since there are few apparent barriers in ocean that prevent the migrations of marine organisms, what makes the population in ocean isolated from others and how the isolated populations are distributed is not yet fully understood. Because marginal seas are partially enclosed circumstances, these seas may give geographical isolation opportunity to marine planktonic organisms. Therefore, marginal seas are good appropriate place to study how geographical isolation affects the speciation of planktonic foraminifera. There are several marginal seas adjacent to the Northwest Pacific. Though there are oceanic currents that flow into marginal seas, the marginal seas have their own characteristic environment. For instance, the surface water in the Japan Sea is affected by both Tsushima current from East China Sea and Liman Current from the Sea of Okhotsk while the deep water is well isolated by shallow sill depth. The Sea of Okhotsk is known as the lowest latitude zone in the world where the seasonal sea ice covers the sea. Revealing the genetic diversity in marginal seas would give us information about formation of gene pools in semi-enclosed environment.

The gene flow of planktonic foraminifera between the North Pacific and the Arctic sea is another significant issue. In order to reveal the genetic diversity in the boundary area of major oceans, we sampled the planktonic foraminifera in the Bering Sea and the Chukchi Sea. The lacks of apparent barrier in oceans and the conceivable inter-oceanic geneflows have been a basis of the idea of cosmopolitan species of planktonic foraminifera. Recent molecular phylogenic studies of planktonic foraminifera, however, suggest that there are multiple genotypes in single morphospecies and they are distributed widely and some particular genotypes are reported from both the Pacific and the Atlantic oceans. The

inter-oceanic variation of genotype is not yet well understood and we do not know how the global genetic exchanges that causes global distributions of the genotype work. In order to clarify the inter-oceanic geneflow mechanism, we need to reveal the genetic diversity in boundary of two oceans. Since the Bering Sea and the Arctic Sea are located north of Aleutian Islands and the Bering Strait is connected to the Chukchi Sea. The genetic diversity of this area should be an essential knowledge when comparing the North Pacific and the North Atlantic populations. There is oceanic current that flows through the Bering Strait today, but during the last glacial maximum, the Bering Strait was closed and the water flow through the strait was blocked completely and the gene flow via the Bering Strait was also prevented. The genetic diversity in the Bering Sea and the Chukchi Sea might reflect this geological event. The genetic diversity of planktonic foraminifera is well studied in the Atlantic Ocean. The Arctic Sea lies between the North Pacific Ocean and the North Atlantic Ocean, therefore the arctic sea might be a pathway from the Pacific Ocean to the Atlantic Ocean.

In this study, we chose three morphospecies of planktonic foraminifera, *Globigerina bulloides, Turborotalita quinqueloba,* and *Neogloboquadrina pachyderma* as the main targets. They are bipolar species and widely adapted in middle to high latitude oceans. Chemical compositions, and isotopic ratios of these species are generally used as paleoceanographic proxies. The genetic studies of these species have just started in Atlantic Ocean, but wide area research has not yet been carried out in the Northwest Pacific Ocean and especially adjacent marginal seas. Therefore, this study will be the first report about regional genetic variation of planktonic foraminiferal populations in this region.

(3) Method

Living planktonic foraminifera were collected by both plankton net method and pumping method for molecular biological study, morphological observation. Planktonic foraminifera are identified and sorted under stereomicroscopes. The number of total sorted individuals and target species, *Globigerina bulloides, Turborotalita quinqueloba, and Neogloboquadrina pachyderma*, are counted. Ethanol-fixed bulk samples were also taken for species composition, chemical and stable isotope analysis.

Morphology of the tests will be observed using a SEM after this cruise. DNA extractions, PCR, and sequencings of SSU rDNA will be carried out using the same individuals as SEM observation. DNA was extracted from a single individual specimen to clarify the genotype-morphotype relation.

3-1 Plankton net sampling

Planktonic foraminifera were collected using a NORPAC net system (XX13: 100μm mesh) with closing mechanism. The plankton net towing was carried out. (see also 6.6.1 in this cruise report).

Sampling depth was divided into up to 4 layers (0-25 m, 25-50 m, 50-100 m, 100-200 m: depths were modified at some stations to reflect the water profiles) and the NORPAC net was towed 4 times at each station for our research purpose. Collected samples were stored in plastic bottles and kept at 4 ℃ until sample sorting.

3-2 Pumping methods

Pumping methods were carried out for collecting planktonic animals in surface water (depth=4 m). Samples were collected by filtering surface water from surface water supply in the laboratory. Pumping methods were carried out for 63 times during navigation (Table 6.6.2.1). Sampling location, sampling time, water temperature, and number of sorted specimens were recorded. A Filtering apparatus (100 μm mesh) was used to filter planktonic foraminifera (Fig. 6.6.2.1). The apparatus was connected to seawater supply and placed in a bucket. Some parts of these samples are stored with 70% EtOH-sea water to analyze the assemblage compositions of both planktonic foraminifera and radiolaria (see also 6.6.1 in this cruise report).

3-3 Sorting and sample storage

Planktonic foraminifera were sorted using stereomicroscopes. Sorted individual specimen were cleaned with a fine writing brush to remove associated microorganisms and transferred to paper slides and air-dried. Air dried specimens are kept under –80 ℃ for molecular biological analysis. The residues of the plankton net samples were preserved with 70% ethanol to the assemblage analyze and chemical and stable isotopic measurements.

(4) Expected results

The species assemblages are considered to reflect the property of the water mass and the distribution of populations are under influence of the environment. Different species assemblages observed in the samples suggest various environments in sampling stations of this cruise. And the results of molecular phylogenic study might suggest the existence of the endemic populations in a single morphospecies.

(5) Future plan and data archive

We are planning to continue the genetic analysis and to carry out morphological observations with scanning electron microscope (SEM) and chemical and isotopic measurement on foraminifera specimens. These studies will examine genotype-morphotype correlations and reveal possible

genotype-specific vital effects, which affect chemical and isotopic compositions of the tests. The phylogenic tree will be obtained by molecular phylogenic analysis, and the genetic relationship should be compared with detailed morphological characters. The geochemical signals of calcareous hard tissue will be connected with both species-specific ecology and environmental factors. All data will be submitted to JAMSTEC Data Management Office (DMO).

References

Bauch et al. (2003), Palaeoceanographic implications of genetic variation in living North Atlantic *Neogloboquadrina pachyderma*, Nature 424, 299-302.

Darling et al. (1999), The diversity and distribution of modern planktic foraminiferal SSU rRNA genotypes and their potential as tracers of present and past ocean circulations. Paleoceanography 14 (3), 3-12.

Darling et al. (2000), Molecular evidence for genetic mixing of Arctic and Antarctic subpolar populations of planktonic foraminifers. Nature 404, 43-47.

Huber et al. (1997), Cryptic speciation in the living planktonic foraminifer *Globigerinella siphonifera* (d'Orbigny). Paleobiology 23(1), 33-62.

Stewart et al. (2001), Genotypic variability in subarctic Atlantic planktic foraminifera. Marine Micropaleontology. 43, 143-153.

Tsuchiya et al., (2000), Phylogenic relationships among species of Glabratellidae (Foraminifera) inferred from ribosomal DNA sequences: Comparison with morphological and reproductive data. Micropaleontology, Vol. 46, Supplement 1: Advances in the Biology of Foraminifera, 13-20

de Vargas et al. (1999), Molecular evidence of cryptic speciation in planktonic foraminifers and their relation to oceanic provinces. Proc. Natl. Acad. Sci. 96, 2864-2868.

Figure 6.6.2.1 Surface water filtration (left) and the filtration apparatus (right)

Table 6.6.2.1. Pumping method sampling sample list.

	Start					End						
Date	Time (UTC)	Latitude	Longitude	Temp.(°C)	Salinity	Time (UTC)	Latitude	Longitude	Temp.(°C)	Salinity	DNA	Assemblages
Leg. 1												
4-Aug	22:10	41-26,0578	140-26,2970	22.853	33.739	23:15	41-19.8554	140-12.3071	23.313	33.660	x	
5-Aug	3:05	42-05.2434	139-43.6902	22.030	33.779	4:05	42-20.1579	139-39.8442	22.316	33.708	x	
5-Aug	9:04	43-36.3002	139-25.0999	21.487	33.918	11:19	44-09.91	139-34.0242	20.711	33.880	x	
Leg. 2												
22-Aug	6:00	40-48.14330N	150-12.40860E	23.090	33.350	8:00	40-58.74270N	150-49.04650E	22.170	33.340	x	x
23-Aug	1:30:00	43-19.94580N	155-25.73300E	20.340	33.500	4:45	43-53.10020N	156-16.04340E	19.560	33.210	x	
23-Aug	4:45	43-53.10020N	156-16.04340E	19.560	33.210	7:45	44-19.94150N	156-56.87250E	17.860	32.850	x	x
24-Aug	3:00	47-38.89990N	162-10.17370E	13.430	32.717	6:00	48-08.91860N	163-00.68240E	12.900	32.670	x	
24-Aug	6:00	48-08.91860N	163-00.68240E	12.900	32.670	7:48	48-26.87950N	163-31.04380E	13.450	32.770		x
25-Aug	0:05	51-13.02060N	168-11.45980E	12.283	32.391	1:05	51-23.55150N	168-28.66690E	12.510	32.340	x	
25-Aug	1:05	51-23.55150N	168-28.66690E	12.510	32.340	4:00	51-53.21600N	169-22.58760E	12.170	32.560		x
25-Aug	23:15	53-30.86110N	176-06.82920E	11.290	32.740	1:15	53-32.56670N	176-48.80170E	11.997	32.735		x
26-Aug	1:15	53-32.56670N	176-48.80170E	11.997	32.735	4:10	53-35.62000N	177-46.46230E	11.158	32.899	x	
26-Aug	22:30	54-00.86400N	177-09.99130W	10.630	33.022	23:30	54-01.58230N	176-54.94220W	10.620	33.040	x	
26-Aug	23:30	54-01.58230N	176-54.94220W	10.620	33.040	3:00	54-02.62160N	176-00.79660W	10.550	32.980		x
27-Aug	20:00	54-08.08510N	171-19.80140W	10.513	32.594	21:15	54-07.58830N	170-55.44710W	10.085	32.790	x	
28-Aug	20:10	54-29.32870N	166-36.46190W	8.525	32.587	21:29	54-49.11620N	166-42.60270W	8.476	32.395	x	
28-Aug	21:29	54-49.11620N	166-42.60270W	8.476	32.395	23:40	55-25.1486	166-48.489	9.999	31.934		x
29-Aug	21:15	60-29.60530N	167-53.57090W	8.834	30.613	22:15	60-43.09820N	167-47.75310W	9.173	30.611		
29-Aug	22:50	60-50.89160N	167-44.88450W	9.233	30.468	23:50	61-04.10230N	167-39.79980W	8.836	30.434		
30-Aug	6:00	62-27.89550N	167-21.42150W	9.409	31.219	8:00	62-56.15420N	167-21.31550W	10.210	27.558	x	
30-Aug	20:00	*65-35N*	*168-31W*	*8.1*	*30.07*	22:00	66-06.31250N	168-32.07380W	8.489	29.833		x
30-Aug	22:00	66-06.31250N	168-32.07380W	8.489	29.833	23:30	66-27.44380N	168-33.84660W	8.270	29.250	x	
31-Aug	20:00	70-08.72620N	167-44.03740W	6.997	30.245	21:30	70-27.42770N	167-05.49460W	6.528	30.169	x	
31-Aug	21:30	70-27.42770N	167-05.49460W	6.528	30.169	23:00	70-42.84510N	166-34.98060W	5.184	31.462		x
31-Aug	23:00	70-42.84510N	166-34.98060W	5.184	31.462	1:30	71-00.45480N	165-58.03350W	5.102	31.142	x	
1-Sep	20:00	71-20.11500N	166-17.36480W	2.912	29.944	22:00	71-50.70430N	166-06.68020W	4.057	30.248		
2-Sep	1:00	72-00.09080N	165-59.81160W	4.110	30.187	3:30	72-26.94260N	165-59.80390W	1.031	28.660	x	
2-Sep	3:30	72-26.94260N	165-59.80390W	1.031	28.660	7:00	72-30.95010N	166-00.03780W	1.005	28.644	-	-
2-Sep	21:30	72-31.52190N	165-58.15740W	1.692	28.295	0:00	72-00.05810N	165-59.85050W	4.123	30.132	-	-
3-Sep	23:00	71-41.71270N	166-59.03460W	4.599	30.745	1:00	71-21.56850N	166-58.39090W	4.964	31.191	-	-
4-Sep	3:00	71-01.27140N	166-58.12230W	5.315	31.089	4:00	70-56.84070N	166-28.85830W	5.327	31.117		x
4-Sep	18:00	71-12.84080N	163-14.83030W	1.404	26.212	20:00	71-08.98610N	163-12.92990W	1.455	26.857		x
5-Sep	0:00	70-29.41470N	163-54.68920W	6.121	30.478	1:00	70-20.90740N	164-12.52360W	6.389	30.530	x	
5-Sep	5:00	69-45.36200N	165-29.45350W	7.325	29.709	7:00	69-27.87780N	166-07.38020W	7.104	30.508	-	-
5-Sep	23:00	68-15.68030N	167-49.24920W	5.790	31.264	1:00	68-06.00010N	167-43.13780W	5.922	31.213		x
6-Sep	1:00	68-06.00010N	167-43.13780W	5.922	31.213	3:00	67-56.04850N	167-36.69110W	5.617	31.477	-	-
6-Sep	23:00	66-13.01160N	168-19.92230W	4.051	31.916	2:00	65-28N	168-33W	4.413	31.821		x
7-Sep	23:00	63-17.61870N	167-55.19960W	3.849	31.805	1:00	63-00.20090N	167-29.82050W	7.557	31.359		x
8-Sep	18:30	62-00.20930N	169-13.01380W	8.161	30.994	19:30	62-00.06510N	169-42.57600W	8.540	31.050	x	x
9-Sep	1:30	62-01.96840N	171-54.08100W	8.655	31.211	2:30	62-04.32260N	171-52.63990W	8.510	31.232	x	
9-Sep	18:45	62-00.20820N	172-47.01500W	8.157	31.053	20:45	62-00.04450N	173-48.09600W	7.697	31.075	-	-
10-Sep	4:00	61-43.16270N	176-31.92030W	7.273	31.531	5:00	61-32.03360N	176-52.30490W	7.724	31.725	-	-
13-Sep	19:30	59-59.16370N	175-07.46090W	8.072	32.456	21:30	59-57.86920N	174-08.99620W	7.805	32.250	-	-
14-Sep	17:30	59-59.56370N	169-00.23500W	7.224	30.964	18:30	59-47.18360N	168-47.08830W	7.477	30.946	x	
14-Sep	18:30	59-47.18360N	168-47.08830W	7.477	30.946	21:30	59-10.67070N	168-08.58990W	7.944	30.828		x
14-Sep	21:30	59-10.67070N	168-08.58990W	7.944	30.828	22:30	58-57.84140N	167-56.35710W	7.363	30.862	x	
15-Sep	20:30	58-34.07130N	172-05.38500W	8.004	32.268	22:30	58-40.83060N	172-12.24810W	7.700	35.239		x
16-Sep	0:30	58-47.11990N	172-17.69310W	7.751	32.282	2:00	58-51.23970N	172-18.77300W	7.599	32.209	x	
17-Sep	20:00	56-29.91110N	166-39.07000W	8.784	31.944	21:00	56-19.08920N	166-19.93940W	8.919	31.943	x	
18-Sep	22:00	56-57.48430N	167-11.36800W	7.850	31.771	0:00	56-31.21990N	167-05.60700W	8.870	31.978		x
19-Sep	3:00	55-56.25530N	166-57.41690W	8.938	32.047	5:00	55-33.66940N	166-52.62770W	8.880	32.085		x
19-Sep	21:30	54-07.52420N	167-36.52080W	6.888	32.688	22:30	54-06.27070N	167-59.55460W	8.184	32.928	x	
20-Sep	2:30	54-02.67460N	169-37.66550W	8.518	32.912	3:30	54-02.08720N	170-02.97210W	8.698	32.919	x	x
20-Sep	17:20	53-48.46930N	175-58.17890W	9.415	32.962	18:20	53-47.80850N	176-23.62740W	9.464	33.030	x	
20-Sep	20:00	53-45.83770N	177-05.71810W	9.409	32.989	21:00	53-44.84550N	177-30.91900W	9.410	33.009	x	x
20-Sep	22:00	53-43.17120N	177-55.79290W	9.512	32.974	23:00	53-41.94520N	178-21.38890W	8.976	33.001	x	x
21-Sep	0:40	53-40.07490N	179-04.13550W	8.802	33.013	1:40	53-39.28430N	179-29.85400W	8.915	32.978	x	
21-Sep	19:00	53-23.18710N	173-16.97250E	10.049	32.768	20:00	53-22.58610N	172-51.78310E	10.387	32.712	x	x
21-Sep	21:00	53-21.10470N	172-27.52890E	10.590	32.737	22:00	53-20.13130N	172-02.65370E	10.148	32.690	x	x
22-Sep	0:45	52-58.49100N	171-21.44600E	9.383	32.712	1:45	52-50.66120N	171-07.04370E	9.854	32.679	x	x
22-Sep	2:40	52-38.54540N	171-02.60120E	9.510	32.719	4:00	52-19.03730N	170-57.50350E	10.850	32.507	x	x
22-Sep	19:50	48-46.48580N	170-00.96390E	11.424	32.584	20:55	48-32.37950N	170-05.14270E	12.408	32.489	x	x
22-Sep	7:00	47-47.14430N	168-13.39870E	12.561	32.647	8:00	47-39.79340N	167-54.51370E	12.730	32.669	x	x

6.6.3. Emissions of trace gases from marine planktons

(1) Personnel

Daisuke D. Komatsu[1], Fumiko Nakagawa[1], Toyoho Ishimura[1], Keisuke Furumochi[1], Sohiko Kameyama[1]

[1]Department of Natural History, Hokkaido University

(2) Objective

While oceanic emissions of volatile trace gases such as hydrogen, methane, nitrous oxide and non-methane hydrocarbons (NMHCs) have considerable impacts on atmospheric chemistry, the production processes of trace gases in seawater are not clarified as yet. Clarifying the production processes of these trace gases in seawater is essential for estimating more reliable global emission of them to atmosphere, as well as their possible future variations. The stable isotopic compositions such as $\delta^{13}C$ and $\delta^{15}N$ of trace gases can be a useful tool for understanding their production mechanisms; such as the origin and/or the pathways of production or degradation of these gases in seawater. Trace gases in seawater are thought to be produced through complex processes including both abiological (photochemical oxidation of DOC) and biological (direct emission from phytoplankton). In this study, we plan to clarify and quantify the relationship between phytoplankton density and trace gases production by using their stable isotopic compositions.

(3) Methods

In order to determine the stable isotopic compositions of trace gases emitted from marine planktons, plankton culture experiments were performed at several stations. All living marine planktons collected by plankton net were cultured in several ca. 120cc glass vials filled by filtered surface seawater collected at the same station. The glass vials were kept at sea surface temperature in the culture system on board and 1 ml of saturated $HgCl_2$ solution (6 %wt) was slowly added as a preservative after a certain culture time. We analyzed the concentration of H_2 and CO by using TRD detector and extracted NMHCs and methyl chloride by using our extraction system (see section 6.5.3) on board. Other glass vials for analysis both the mixing ratios and stable isotopic compositions of methane and nitrous oxide were stored in the light-resistant container and kept at 4°C until onshore analysis.

(4) Future Plan and Data Archives

The data of the emissions of methane, nitrous oxide, H_2, CO, and NMHCs obtained in this cruise will be analyzed to clarify and quantify the relationship between phytoplankton density and trace gases production by using their stable isotopic compositions. In addition, we are going to estimate the ecology of small planktonic foraminifera using their isotopic dispersion ($\delta^{13}C$ and $\delta^{18}O$) in the same species sampled at the same depth at the same station. These results are also expected to be useful information for future paleoenvironmental studies.

Table 6.6.3.1. Summary of culture experiments marine planktons

Date	Stn.	Depth interval	methane		nitrous oxide		NMHCs, hydrogen, CO	
			culture time (h)	number	culture time (h)	number	culture time (h)	number
2006/8/6 18:00	3	0-25	0	2	0	2	0	2
			14	2	14	2	14	2
			38	2	38	2	38	2
		25-60	0	2	0	2	0	2
			14	2	14	2	14	2
			38	2	38	2	38	2
		60-200	0	2	0	2	0	2
			14	2	14	2	14	2
			38	2	38	2	38	2
2006/8/8 17:00	4	0-25					0	2
							16	2
							27	2
2006/8/8 17:00	5	0-150	0	2	0	2	0	2
			20	2	20	2	20	2
2006/8/13 14:00	6	0-60	0	2	0	2		
			21	2	21	2		
			71	2	71	2		
		60-200	0	2	0	2		
			21	2	21	2		
			71	2	71	2		
2006/9/1 10:30	14	0-20	0	1	0	1	0	1
			12	1	12	1	12	1
			24	1	24	1	24	1
		20-35	0	1	0	1	0	1
			12	1	12	1	12	1
			24	1	24	1	24	1
2006/9/2 13:30	12EX	0-40	0	1	0	1	0	1
			12	1	12	1	12	1
			24	1	24	1	24	1
2006/9/5 11:00	16	0-40	0	1	0	1	0	1
			6	1	6	1	6	1
			12	1	12	1	12	1
2006/9/6 10:30	17	0-40					0	4
							9	4
2006/9/7 13:30	18	0-25	0	1	0	1	0	1
			9	1	9	1	9	1
			24	1	24	1	24	1
2006/9/7 20:30	19	0-25	0	1	0	1	0	1
			13.5	1	13.5	1	13.5	1
			24	1	24	1	24	1
2006/9/11 0:30	23	0-20	0	1	0	1	0	1
			12	1	12	1	12	1
			no Hg	1	24	1	no Hg	1
		20-50	0	1	0	1	0	1
			12	1	12	1	12	1
			no Hg	1	24	1	no Hg	1
		50-200	0	1	0	1	0	1
			12	1	12	1	12	1
			no Hg	1	24	1	no Hg	1
2006/9/14 12:00	28	0-30	0	1	0	1	0	2
			6	1	6	1	6	2
			34	1	34	1	34	2
			60	1	60	1	60	2
			no Hg	1	no Hg	1	no Hg	2
2006/9/16 15:00	30	0-20	0	1	0	1	0	1
			16	1	16	1	16	1
			28	1	28	1	28	1
							no Hg	1
		20-50	0	1	0	1	0	1
			16	1	16	1	16	1
			28	1	28	1	28	1
							no Hg	1
		50-80	0	1	0	1	0	1
			16	1	16	1	16	1
			28	1	28	1	28	1
							no Hg	1
		control	0	1	0	1	0	1
			16	1	16	1	16	1
			28	1	28	1	28	1
							no Hg	1
2006/9/16 21:00	31	0-20	0	1	0	1	0	1
			12	1	12	1	12	1
			24	1	24	1	24	1
			no Hg	1	no Hg	1	no Hg	1
		20-50	0	1	0	1	0	1
			12	1	12	1	12	1
			24	1	24	1	24	1
			no Hg	1	no Hg	1	no Hg	1
		50-80	0	1	0	1	0	1
			12	1	12	1	12	1
			24	1	24	1	24	1
			no Hg	1	no Hg	1	no Hg	1
2006/9/17 23:00	33	0-40	0	1	0	1	0	1
			12	1	12	1	12	1
			34	2	34	2	34	2
			no Hg	1	no Hg	1	no Hg	1
		40-80	0	1	0	1	0	1
			12	1	12	1	12	1
			34	2	34	2	34	2
			no Hg	1	no Hg	1	no Hg	1
		80-110	0	1	0	1	0	1
			12	1	12	1	12	1
			34	2	34	2	34	2
			no Hg	1	no Hg	1	no Hg	1
		0-110	0	1	0	1	0	1
			12	2	12	2	12	2
			34	2	34	2	34	2
			no Hg	2	no Hg	2	no Hg	2
		control	0	1	0	1	0	1
			34	2	34	2	34	2
			no Hg	2	no Hg	2	no Hg	2

6.6.4 Microplankton studies in the Japan Sea, Sea of Okhotsk and northwestern Pacific

(1) Personnel

Ryoko Ohira, (Leg.1; Dept. of Earth & Environmental Sciences, Faculty of Science, Yamagata University)

Susumu Konno (Leg.2; Dept. of Earth & Environmental Sciences, Faculty of Science, Yamagata University)

Richard W. Jordan (on shore: Dept. of Earth & Environmental Sciences, Faculty of Science, Yamagata University)

(2) Objectives

The main aims of this project are to:

1) study the microplankton communities in the surface waters along continuous transects so as to understand the biogeographic distributions of individual species and the effects of oceanographic features like straits, harbours, sea-ice, algal blooms, and oceanic frontal systems,

2) study the vertical distribution of microplankton communities in order to understand the ecologic preferences and seasonal cycles of individual species,

3) study in detail the taxonomy of various microplankton groups and to compile photographic catalogues (identification guides) for publication and laboratory use.

(3) Methods

Surface water samples were obtained during Leg 1 using the shipboard seawater supply for research use on a regular basis, 3-4 times a day when the ship was steaming (i.e. not on station) and more often when traveling through island passes. About 1-4 l of seawater were collected in plastic bottles with the following information recorded at the same time as sampling: the date and time (GMT), coordinates, and those parameters (such as temperature, salinity, and chlorophyll) being continuously recorded by instruments connected to the seawater supply. In total, 31 samples were collected using this method during Legs. 1 and 2 (see Tables 6.6.4.1 and 6.6.4.2) of MR06-04.

Vertical samples were obtained from shallow and deep hydrocasts at 7 and 22 stations during Leg. 1 and 2, respectively, with about 3-8 depths sampled during each cast. About 4 l of seawater were collected in plastic bottles after the CTD rig had returned to the ship. A bucket sample was also taken to represent 0 m. In total 63 and 126 samples were collected using this method during Legs 1 and 2, of MR06-04 (see Tables 6.6.4.1 and 6.6.4.2).

Water samples collected using these methods were then filtered through 47 mm (0.45 μm porosity) HA-type Millipore polycarbonate filters using an Eyela A3-S aspirator and 3 filter holder manifold system. The filters were then air dried (but not washed) and then sealed in plastic petrislides.

Later, the filters will be washed briefly in distilled water and air dried again. A 3 x 3 mm portion of each filter will be cut out and mounted onto an aluminum SEM stub, coated with Pt/Pd in an Eiko IB-3 ion sputter coater, and observed in a Hitachi S-2250N SEM.

Table 6.6.4.1: MR06-04 Leg 1 water sample list of surface water

Sample	Date	Lat. (˚N)	Long. (˚E)
OS-001	8/1/2006	40.697	141.831
OS-002	8/1/2006	41.046	143.714
OS-003	8/1/2006	41.705	143.969
OS-004	8/3/2006	42.444	144.291
OS-005	8/3/2006	42.132	143.87
OS-006	8/4/2006	41.794	143.436
OS-007	8/4/2006	41.667	141.238
OS-008	8/4/2006	41.656	140.955
OS-009	8/4/2006	41.43	140.431
OS-010	8/4/2006	41.347	140.1
OS-011	8/5/2006	42.261	139.681
OS-012	8/5/2006	43.511	139.435
OS-013	8/5/2006	45.076	139.973
OS-014	8/7/2006	45.642	141.927
OS-015	8/7/2006	45.14	143.34
OS-016	8/7/2006	44.59	144.814
OS-017	8/10/2006	51.066	149.136
OS-018	8/11/2006	51.48	148.979
OS-019	8/11/2006	51.47	149.325
OS-020	8/11/2006	52.426	150.097
OS-021	8/11/2006	53.213	150.1
OS-022	8/14/2006	54.109	149.405
OS-023	8/15/2006	53.436	149.392
OS-024	8/15/2006	52.689	149.632
OS-025	8/15/2006	52.2	149.756
OS-026	8/16/2006	51.928	149.819
OS-027	8/17/2006	43. 698	154.63
OS-028	8/18/2006	42.2	152.832
OS-029	8/18/2006	41.483	151.537
OS-030	8/19/2006	40.87	147.785
OS-031	8/19/2006	41.19	147.033

Table 6.6.4.2: MR06-04 Leg 2 water sample list of surface water

Station	Date	Lat		Long	

Station	Date	Lat.		Long	
KS-037	8/25/2006	53.1424	N	171.6449	E
KS-038	8/25/2006	53.1919	N	171.7393	E
KS-039	8/25/2006	53.4361	N	174.4189	E
KS-040	8/25/2006	53.5071	N	175.9035	E
KS-041	8/26/2006	53.5851	N	177.6331	E
KS-042	8/26/2006	53.6705	N	179.5717	E
KS-043	8/26/2006	53.817	N	177.9974	W
KS-044	8/26/2006	54.0007	N	177.7281	W
KS-045	8/27/2006	54.0447	N	176.3914	W
KS-046	8/27/2006	54.0759	N	174.5477	W
KS-047	8/27/2006	54.1167	N	172.6713	W
KS-048	8/27/2006	54.1226	N	172.0207	W
KS-049	8/27/2006	54.1403	N	171.1491	W
KS-050	8/28/2006	54.1861	N	169.583	W
KS-051	8/28/2006	54.2065	N	168.7351	W
KS-052	8/28/2006	54.2315	N	167.836	W
KS-054	8/28/2006	54.8229	N	166.7106	W
KS-055	8/29/2006	55.8702	N	166.9349	W
KS-056	8/29/2006	56.6382	N	167.0917	W
KS-057	8/29/2006	57.517	N	167.3186	W
KS-058	8/29/2006	59.4503	N	167.8736	W
KS-059	8/29/2006	59.8472	N	167.9883	W
KS-060	8/29/2006	60.3104	N	167.9765	W
KS-061	8/29/2006	60.9958	N	167.7175	W
KS-062	8/30/2006	61.5348	N	167.4909	W
KS-063	8/30/2006	62.1998	N	167.3589	W
KS-064	8/30/2006	62.8045	N	167.3531	W
KS-065	8/30/2006	62.864	N	167.3541	W
KS-066	8/30/2006	64.8084	N	168.5763	W
KS-067	8/30/2006	65.0725	N	168.6459	W
KS-072	8/31/2006	67.4277	N	168.6266	W
KS-073	8/31/2006	67.4953	N	168.6301	W
KS-074	8/31/2006	67.5308	N	168.633	W
KS-075	8/31/2006	67.5703	N	168.6383	W
KS-076	8/31/2006	68.3639	N	168.7396	W
KS-077	9/4/2006	71.227	N	163.3074	W
KS-078	9/4/2006	71.0909	N	163.2452	W

Station	Date	Lat		Long	
KS-079	9/4/2006	70.6858	N	163.6172	W
KS-080	9/5/2006	70.2017	N	164.5374	W
KS-081	9/5/2006	69.2956	N	166.4705	W
KS-082	9/5/2006	68.4098	N	167.9082	W
KS-083	9/6/2006	68.0125	N	167.664	W
KS-084	9/6/2006	67.9725	N	167.6379	W
KS-085	9/6/2006	67.9372	N	167.6137	W
KS-086	9/6/2006	67.5953	N	167.3768	W
KS-087	9/6/2006	66.6639	N	167.9396	W
KS-088	9/7/2006	65.9406	N	168.4081	W
KS-098	9/7/2006	65.3779	N	168.5843	W
KS-099	9/7/2006	65.3576	N	168.5906	W
KS-100	9/7/2006	65.0801	N	168.689	W
KS-101	9/7/2006	63.674	N	168.4909	W
KS-102	9/8/2006	62.6453	N	167.9909	W
KS-103	9/8/2006	61.9913	N	170.9851	W
KS-104	9/9/2006	62.131	N	171.8596	W
KS-105	9/9/2006	62.2622	N	171.7752	W
KS-106	9/9/2006	61.9954	N	175.4706	W
KS-107	9/10/2006	61.147	N	177.5805	W
KS-108	9/12/2006	60.0746	N	179.4637	W
KS-109	9/13/2006	60.2038	N	178.1649	W
KS-110	9/14/2006	59.9408	N	172.8304	W
KS-111	9/15/2006	58.3962	N	169.9631	W
KS-112	9/15/2006	58.5727	N	172.0961	W
KS-113	9/16/2006	58.8679	N	172.3057	W
KS-114	9/16/2006	58.9151	N	172.2808	W
KS-115	9/16/2006	59.159	N	171.9387	W
KS-116	9/16/2006	58.5251	N	172.0211	W
KS-117	9/16/2006	58.4621	N	171.3787	W
KS-118	9/16/2006	58.4201	N	170.6127	W
KS-119	9/17/2006	58.0419	N	169.3783	W
KS-120	9/17/2006	57.4311	N	168.2281	W
KS-121	9/17/2006	56.3941	N	166.4687	W
KS-122	9/18/2006	55.918	N	166.1383	W
KS-123	9/18/2006	56.128	N	165.9846	W
KS-124	9/18/2006	56.972	N	165.3833	W

Station	Date	Lat.		Long.	
KS-125	9/18/2006	57.4999	N	166.3266	W
KS-126	9/18/2006	57.4919	N	167.106	W
KS-127	9/18/2006	57.4233	N	167.336	W
KS-128	9/18/2006	57.3826	N	167.3219	W
KS-129	9/18/2006	57.1652	N	167.2435	W
KS-130	9/19/2006	56.4437	N	167.0761	W
KS-131	9/19/2006	56.1257	N	166.9964	W
KS-132	9/19/2006	55.4708	N	166.8588	W
KS-133	9/20/2006	54.0666	N	169.1939	W
KS-134	9/20/2006	53.9815	N	171.4122	W
KS-135	9/20/2006	53.9568	N	171.9346	W
KS-136	9/20/2006	53.8068	N	176.0119	W
KS-137	9/20/2006	53.7235	N	177.8671	W
KS-138	9/21/2006	53.6519	N	179.5899	W
KS-139	9/21/2006	53.6298	N	179.2362	E
KS-140	9/21/2006	53.5294	N	177.2402	E
KS-141	9/21/2006	53.3949	N	173.6788	E
KS-142	9/21/2006	53.3895	N	173.4666	E
KS-143	9/21/2006	53.3864	N	173.2759	E
KS-144	9/21/2006	53.3836	N	173.0004	E
KS-145	9/21/2006	53.3734	N	172.8161	E
KS-146	9/21/2006	53.361	N	172.6342	E
KS-147	9/21/2006	53.3508	N	172.432	E
KS-148	9/21/2006	53.346	N	172.2976	E
KS-149	9/21/2006	53.3422	N	172.1837	E
KS-150	9/21/2006	53.3377	N	172.0865	E
KS-151	9/21/2006	53.3207	N	171.9994	E
KS-152	9/21/2006	53.2904	N	171.9451	E
KS-153	9/21/2006	53.2517	N	171.8748	E
KS-154	9/21/2006	53.2137	N	171.805	E
KS-155	9/21/2006	53.0129	N	171.4297	E
KS-156	9/22/2006	52.9833	N	171.3735	E
KS-157	9/22/2006	52.9558	N	171.3216	E
KS-158	9/22/2006	52.9233	N	171.2613	E
KS-159	9/22/2006	52.8901	N	171.2008	E
KS-160	9/22/2006	52.8595	N	171.1452	E
KS-161	9/22/2006	52.6506	N	171.0459	E

Station	Date	Lat		Long	
KS-162	9/22/2006	52.1464	N	170.9206	E
KS-163	9/22/2006	48.7788	N	170.0149	E
KS-164	9/22/2006	48.535	N	170.102	E
KS-165	9/22/2006	48.3243	N	169.6712	E
KS-166	9/23/2006	48.0249	N	168.8625	E
KS-167	9/23/2006	47.3419	N	167.11	E
KS-168	9/23/2006	46.8942	N	165.9265	E
KS-169	9/23/2006	46.2707	N	164.3299	E
KS-170	9/24/2006	45.7307	N	162.9618	E
KS-171	9/24/2006	45.2109	N	161.5937	E
KS-172	9/24/2006	44.4932	N	159.8754	E
KS-173	9/24/2006	43.2908	N	156.9975	E
KS-174	9/25/2006	42.9087	N	155.992	E
KS-175	9/25/2006	42.5791	N	154.9414	E
KS-176	9/25/2006	41.2019	N	151.5378	E
KS-177	9/26/2006	40.8539	N	150.5152	E
KS-178	9/26/2006	40.5041	N	149.277	E
KS-179	9/26/2006	40.469	N	147.5958	E

6.6.5 *Distribution of Siliceous phytoplankton in sea-surface water in the Chukchi and the eastern Bering Seas*

(1) Personnel

Kota Katsuki[1], Jonaotaro Onodera[2] and Kozo Takahashi[2]

1. Shimane University, Research Center for Coastal Lagoon Environments
2. Kyushu University, Graduate School of Sciences, Department of Earth and Planetary Science

(2) Objectives

Silicoflagellates constitute minor primary producer groups in the Ocean, though they sometimes dominate the microplankton group in coastal and estuarine waters. It has been reported about the ecology of silicoflagellate that its assemblage variation and growth rate can be used as an indicator of water temperature and salinity (e.g., Onodera and Takahashi, 2005). The aberrant skeleton's frequency of silicofragellates reflects the fluctuation in salinity (Shitanaka, 1983). On the other hand, as far as the sea-ice environment such as the Arctic Ocean is concerned, little information on its influence on the distribution of silicoflagellates and their ecology has been available (e.g., Booth and Horner, 1997). Thus, the present research purpose is to characterize the relationship between silicofragellates distribution/ecology and sea-ice environmental conditions. Another aim of the study on the silicoflagellates assemblage distribution is to consolidate our basic understanding of the related research fields such as paleoenvironmental construction based on marine sediment. These researches will provide us with appreciation of past sea-ice cover areas.

(3) Methods

The samples were obtained from sea waters in the Chukchi Sea and the eastern Bering Sea (Figure 6.6.6.1) using buckets, a shipboard pump, and CTD Rosette bottles. Sea surface water samples were taken by buckets and a shipboard pump (5 m depth). CTD samples were collected at 3-7 discrete depths from the surface to 10 m up from the bottom except for Station 24. In the St. 24, CTD samples were obtained seven discrete depths (10, 30, 50, 75, 100, 150, 200 m). They were collected at scattering points in the Chukchi Sea and the eastern Bering Sea during 25 August - 17 September 2006. Two to three milliliters of the samples were passed through Gelman R membrane filter of 47 mm diameter with nominal pore size of 0.45 μm. The filtered samples were desalted with distilled water and dried for one day. After MR06-04 is completed, the filtered samples will be permanently mounted on microslides with Canada Balsam and will be examined in the shore laboratory at Kyushu Univ. and/or Shimane Univ. for

further analysis.

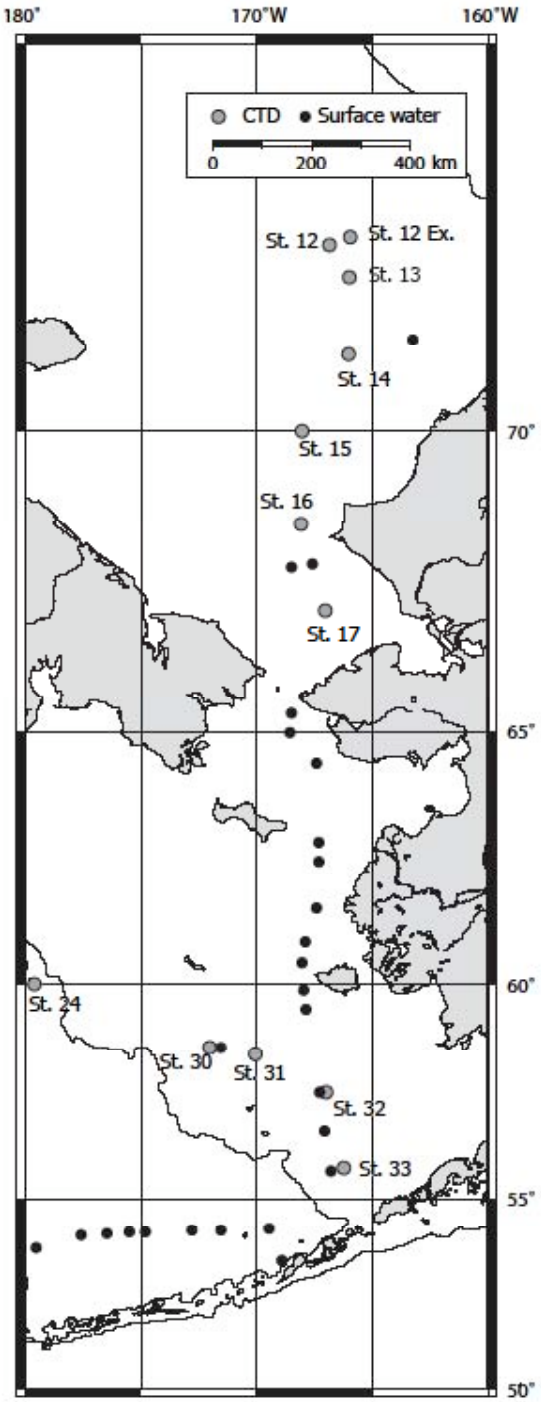

Figure 6.6.5.1 Plankton sampling sites

Table 6.6.5.1 Plankton sampling positions

Underway Samples

Date	Time[LST]	Longtitude	Latitude
2006/8/26	4:02	53°41.96N	179°31.71W
	12:18	54°00.11N	177°27.55W
	16:26	54°02.68N	176°24.85W
	20:03	54°03.15N	175°29.66W
	23:51	54°04.33N	174°48.12W
2006/8/27	7:41	54°06.82N	172°44.19W
	11:57	54°08.06N	171°20.64W
	17:49	54°11.37N	169°28.25W
	20:10	53°12.22N	168°52.85W
2006/8/28	17:11	55°43.54N	166°53.98W
	20:54	56°37.03N	167°05.43W
2006/8/29	0:40	57°32.21N	167°19.37W
	8:27	59°21.38N	167°50.71W
	10:30	59°50.93N	167°59.34W
	13:04	60°27.27N	167°54.67W
	15:12	60°55.85N	167°42.98W
	18:05	61°33.43N	167°28.95W
	22:43	62°38.29N	167°21.19W
	23:42	62°51.84N	167°21.25W
2006/8/30	8:07	64°43.81N	167°30.65W
	9:41	65°05.18N	168°38.77W
	20:31	67°39.38N	168°38.94W
2006/9/4	8:14	71°13.38N	163°17.82W
2006/9/5	18:37	67°58.097N	167°38.11W
2006/9/6	19:37	65°22.55N	168°35.14W
2006/9/16	14:58	58°26.87N	171°37.83W

CTD Samples

Site	Date	Latitude	Longtitude
15	2006/8/31	70°00.00N	168°00.00W
	Depth: 0(Backet), 10, 20, 30, 38 (m)		
14	2006/9/1	71°00.00N	165°59.80W
	Depth: 0(Backet), 10, 20, 30, 33 (m)		
13	2006/9/1	72°00.00N	165°59.80W
	Depth: 0(Backet), 10, 20, 30, 36 (m)		
12 ex.	2006/9/2	72°36.11N	165°59.90W
	Depth: 0(Backet), 10, 20, 30, 42 (m)		
12	2006/9/3	72°26.00N	166°58.00W
	Depth: 0(Backet), 10, 20, 30, 41 (m)		
16	2006/9/3	68°30.00N	168°00.00W
	Depth: 0(Backet), 10, 20, 30, 42 (m)		
17	2006/9/3	67°00.00N	167°00.00W
	Depth: 0(Backet), 10, 20, 30 (m)		
24	2006/9/11	60°15.60N	179°58.60W
	Depth: 0(Backet), 10, 30, 50, 75, 100, 150, 200 (m)		
30	2006/9/16	58°30.00N	172°00.00W
	Depth: 0(Backet), 10, 20,30, 50, 75, 90 (m)		
31	2006/9/16	58°23.00N	170°00.00W
	Depth: 0(Backet), 10, 20, 30, 50, 60 (m)		
32	2006/9/17	57°00.00N	167°30.00W
	Depth: 0(Backet), 10, 20, 30, 50, 60 (m)		
33	2006/9/17	55°46.50N	166°13.50W
	Depth: 0(Backet), 10, 20, 30, 50, 75, 100, 116 (m)		

Table. 1

6.7 Microbiological observations in the sea-water and sediment

(1) Personnel

Masao Uchida (IORGC, JAMSTEC) on shore

Motoo Utsumi (Tsukuba University) Leg.2

(2) Objectives

Marine microbes, especially bacteria, are large and essential components of food webs and elemental cycles in the oceans. Marine bacteria include the two deepest divisions, or domains, Bacteria and Archaea. These domains are identified by genetic distance in the composition of the 16S rRNA gene (Woose et al. 1990). Marine bacteria are morphologically simple: microscopic rods, spheres and filaments generally less than 1-2 μm in size, but bacteria are highly diverse in terms of both taxonomy and metabolism. There are many different varieties of bacteria existing in the oceans, but it has been long noted a discrepancy of several orders of magnitude between the number of bacterial cells that can be seen in the oceans by direct count (by epifluorescence microscopy) and the number of colonies that appear on agar plates (e.g. Jannasch and Jones, 1959).

In terms of carbon cycling, one of the most important activities of bacteria in marine systems is aerobic heterotrophy. Heterotrophic bacteria served primarily as a pathway for regeneration of organic nitrogen, phosphorus, and other bioactive elements, and represented a shunt of carbon and energy from the main phytoplankton-based food web. In addition, it is reported that nonthermophilic archaea represent up to 40% of the free-living prokaryotic community in the water column of the world's oceans (ex. Delong, 1992), and some of their population is chemoautotrophy (ex. Pearson et al. 2001). Therefore, it is important to study the relationship between carbon cycling and bacterial community structure in the sea-water column and sediment. The key aim of this study is to analyze the relationship between community structures of microorganisms and dissolved organic carbon cycling in the sea-water column and sediments. The objectives of this study are as follow: 1) collect large volume of sea-water samples for measuring stable isotope ratio of POC and bacterial cell membrane lipids, 2) collect mega volume of surface sea-water for measuring radioactive isotope ratio of POC and bacterial cell membrane lipids, 3) collect surface sediment core samples to analyze the relationship between bacterial community structure and physicochemical environment factors.

(3) Methods

3-1 Large volume filtration

To study diversity of bacteria community and stable isotope ratio of POC and bacterial cell membrane lipids, we filtered 10-100 L sea-water at each sampling station (Tables 6.7.1 and 6.7.2). Water samples were collected from different depths with Niskin water samplers (12 L, General Oceanic) and immediately transferred to 20 L plastic canteens. Each water sample was filtered with glass fiber filters (Whatman GF/F, with a operational pore size of 0.7 μm, 125 mm in diameter) on board. The filters were

frozen at -30°C during the cruise. To count the population density of bacteria, same water samples (100 mL) were fixed with formalin (final concentration in the sample was 3.6%) immediately and stored at -80°C.

3-2 Mega volume filtration

To study diversity of bacteria community, radioactive isotope ratio of POC and bacterial cell membrane lipid, we filtered c.a. 100,000 L surface sea-water during the cruise.

3-3 Surface sediment collection

To study vertical diversity of bacteria community in the surface sediments, we collected surface sediment cores with Multiple Core Sampler at the stations. Sediment samples were continuously sliced at every 2.2 cm in thickness throughout the cores on board, and collected in plastic bags. All sediment samples were frozen at -30 °C during the cruise.

References

Delong, E.F. (1992) *Proc. Natl. Acad. Sci. USA* 89: 5685-5689.

Jannasch, H. W., and Jones, G. E. (1959) *Limnol. Oceanogr.* 4:128-139.

Pearson, A., McNichol, A.P., Bentitez-Nelson, B.C., Hayes, J.M. and Eglinton, T.I. (2001) *Geochim. Cosmochim. Acta* 65: 3123-3137.

Woese, C. R., Kandler, O., and Wheelis, M. L. (1990) *Proc. Natl. Acad. Sci. USA* 87:4576-4579.

Table 6.7.1. List of filtrated sea-water samples during MR06-04 Leg.1.

date	2006/8/4
station No.	2
depth (m)	filtrated vol. (L)
50	65.3
100	65.9
300	74.8
500	54.2
b-50	64.7

date	2006/8/6
station No.	3
depth (m)	filtrated vol. (L)
50	10.6
100	10.4
300	10.2
500	10.6

date	2006/8/8
station	4
depth (m)	filtrated vol. (L)
50	67.4
100	64.5
300	74.0
500	51.8
b-50	60.9

Table 6.7.2. List of filtrated sea-water samples during MR06-04 Leg.2.

date	2006/8/31
station No.	15
depth (m)	filtrated vol. (L)
10	142
38	140

date	2006/9/2
station No.	12ex
depth (m)	filtrated vol. (L)
8	90.5
15	89
42	90

date	2006/9/2
station No.	13
depth (m)	filtrated vol. (L)
10	89.5
20	87.5
35	91

date	2006/9/3
station No.	12
depth (m)	filtrated vol. (L)
10	102.2
20	95.6
30	100
39	101

date	2006/9/7
station No.	19
depth (m)	filtrated vol. (L)
5	102.8
10	103.4
20	102.9
25	103.9

date	2006/9/9
station No.	22
depth (m)	filtrated vol. (L)
10	18
50	26.6
75	28.7
84	36

date	2006/9/10
station No.	23
depth (m)	filtrated vol. (L)
SW	57
50	85.2
100	80.2
300	81
500	82.4
900	94

date	2006/9/10
station No.	23
depth (m)	filtrated vol. (L)
SW	57
50	85.2
100	80.2
300	81
500	82.4
900	94

date	2006/9/10
station No.	23
depth (m)	filtrated vol. (L)
10	18.8
200	15
700	13.2
990	14.5

date	2006/9/11
station No.	24
depth (m)	filtrated vol. (L)
SW	56.8
10	20.8
30	21.5
50	21.5
75	21.5
100	21.5
200	13
700	20.5

date	2006/9/12
station No.	24
depth (m)	filtrated vol. (L)
50	79.4
100	80.2
300	79.8
500	79.3
750	93.1

date	2006/9/13
station No.	26
depth (m)	filtrated vol. (L)
10	22.2
20	23
30	22
50	21.8
75	22
100	22.4
114	22.4

840	13.4

date	2006/9/13
station No.	27
depth (m)	filtrated vol. (L)
10	45.5
20	45.5
30	44.5
50	37.5
53	45

date	2006/9/14
station No.	28
depth (m)	filtrated vol. (L)
10	67.2
20	63.8
30	67
31	86

date	2006/9/14
station No.	29
depth (m)	filtrated vol. (L)
10	81.2
15	76
20	80.4
30	82
38	93.4

date	2006/9/16
station No.	30
depth (m)	filtrated vol. (L)
10	37.8
20	38
30	37.8
50	38
75	34
86	45.2

date	2006/9/16
station No.	31
depth (m)	filtrated vol. (L)
10	45.2
20	45.4
30	44.7
50	44.5
60	44.3

date	2006/9/17
station No.	32
depth (m)	filtrated vol. (L)
10	45.2
20	44.2
30	45.2
50	45
64	44.8

date	2006/9/17
station No.	33
depth (m)	filtrated vol. (L)
10	26.5
20	25.6
30	23.6
50	35.6
75	32
100	41
116	39.2

6.8 Sediment Observations

6.8.1 Site survey (bathymetry and sediment structure) observations

(1) Personnel

Naomi Harada (JAMSTEC); Principal Investigator	- Leg1, 2 -
Katsunori Kimoto (JAMSTEC)	- Leg1 -
Tatsuhiko Sakamoto (JAMSTEC)	- Leg1 -
Kouichi Iijima (JAMSTEC)	- Leg1, 2 -
Gorbarenko Sergey A. (Pacific Oceanological Institute)	- Leg1 -
Takuya Itaki (Tokyo University)	- Leg1, 2 -
Satoshi Okumura (Global Ocean Development Inc.; GODI)	- Leg1 -
Souitchiro Sueyoshi (GODI)	- Leg1 -
Kazuho Yoshida (GODI)	- Leg1, 2 -
Kazuya Yamashita (GODI)	- Leg1 -
Shin'ya Okumura (GODI)	- Leg2 -
Wataru Tokunaga (GODI)	- Leg2 -
Ryo Ohyama (GODI)	- Leg2 -

(2) Objective

Site survey was conducted using the Multi Narrow Beam Echo Sounding system (MNBES), SEABEAM 2112.004 (SeaBeam Instruments Inc.) on R/V MIRAI. Sub Bottom Profiler (SBP) is an add-on option to the “SEABEAM 2100”. SBP subsystem collected vertical sediments information.

(3) Measured parameters

System configuration, performance and data acquisition of SEABEAM 2100.004 system showed “6.9.3 Swath Bathymetry”.

(4) Preliminary results

Survey maps for Stations No.1 to No.7 (Fig 6.8.1.1, 6.8.1.4 to 6.8.1.8) at Leg1 and Station No.23 to No.25 (Fig 6.8.1.12) at Leg2 were constructed for determination of coring points. Sub-Bottom profiles at coring sites were shown in Fig. 6.8.1.2, 6.8.1.3 to 6.8.1.11 and 6.8.1.13 to 6.8.1.22. Sediment coring was conducted at 33 stations using multiple corer, piston and gravity coring system. Geographic positions of cored locations listed Table 6.8.1.1 below.

Table 6.8.1.1 Positions of stations during MR06-04 cruise

Station	Latitude	Longitude	Depth [m]	Figure No.	Remarks
1	42-30.62N	144-19.75E	996	Fig. 6.8.1.1/.2	
2	41-52.00N	143-57.00E	1,046	Fig. 6.8.1.1/.3	
3	45-45.49N	140-47.02E	766	Fig. 6.8.1.4	
4	44-31.65N	145-00.25E	1,215	Fig. 6.8.1.5	
5	54-18.95N	149-16.05E	831	Fig. 6.8.1.6	
6	53-16.92N	150-04.71E	1,148	Fig. 6.8.1.7	
7	51-16.60N	149-12.57E	1,251	Fig. 6.8.1.8	
12	72-25.93N	166-57.81W	53	---	No survey
12ex	72-36.02N	165-59.96W	53	---	No survey
13	72-00.01N	165-59.99W	46	---	No survey
14	70-59.97N	166-59.85W	44	---	No survey
15	67-59.90N	167-59.96W	48	---	No survey
16	68-29.99N	168-00.01W	56	Fig. 6.8.1.9	
17	66-59.99N	166-59.95W	40	---	No survey
18	63-59.88N	168-59.97W	35	---	No survey
19	63-00.01N	167-29.94W	33	---	No survey
20	62-00.01N	169-00.04W	37	---	No survey
21	62-00.04N	172-00.02W	55	Fig. 6.8.1.10	
22	62-00.04N	176-00.02W	100	Fig. 6.8.1.11	
23	60-09.52N	179-27.81W	1,002	Fig. 6.8.1.12/.13	
24	60-15.71N	179-25.36W	852	Fig. 6.8.1.12/.14	
25	60-04.49N	179-27.77W	1,158	Fig. 6.8.1.12/.15	
26	60-00.00N	176-00.00W	133	Fig. 6.8.1.16	
27	60-00.02N	172-00.00W	68	Fig. 6.8.1.17	
28	60-00.00N	168-59.99W	43	---	No survey
29	58-29.99N	167-30.04W	50	Fig. 6.8.1.18	
30	58-30.01N	172-00.01W	101	Fig. 6.8.1.19	
31	58-22.99N	170-00.04W	74	Fig. 6.8.1.20	
32	57-00.01N	167-30.00W	78	Fig. 6.8.1.21	
33	55-46.42N	166-13.57W	130	Fig. 6.8.1.22	

Station No.1 & No.2

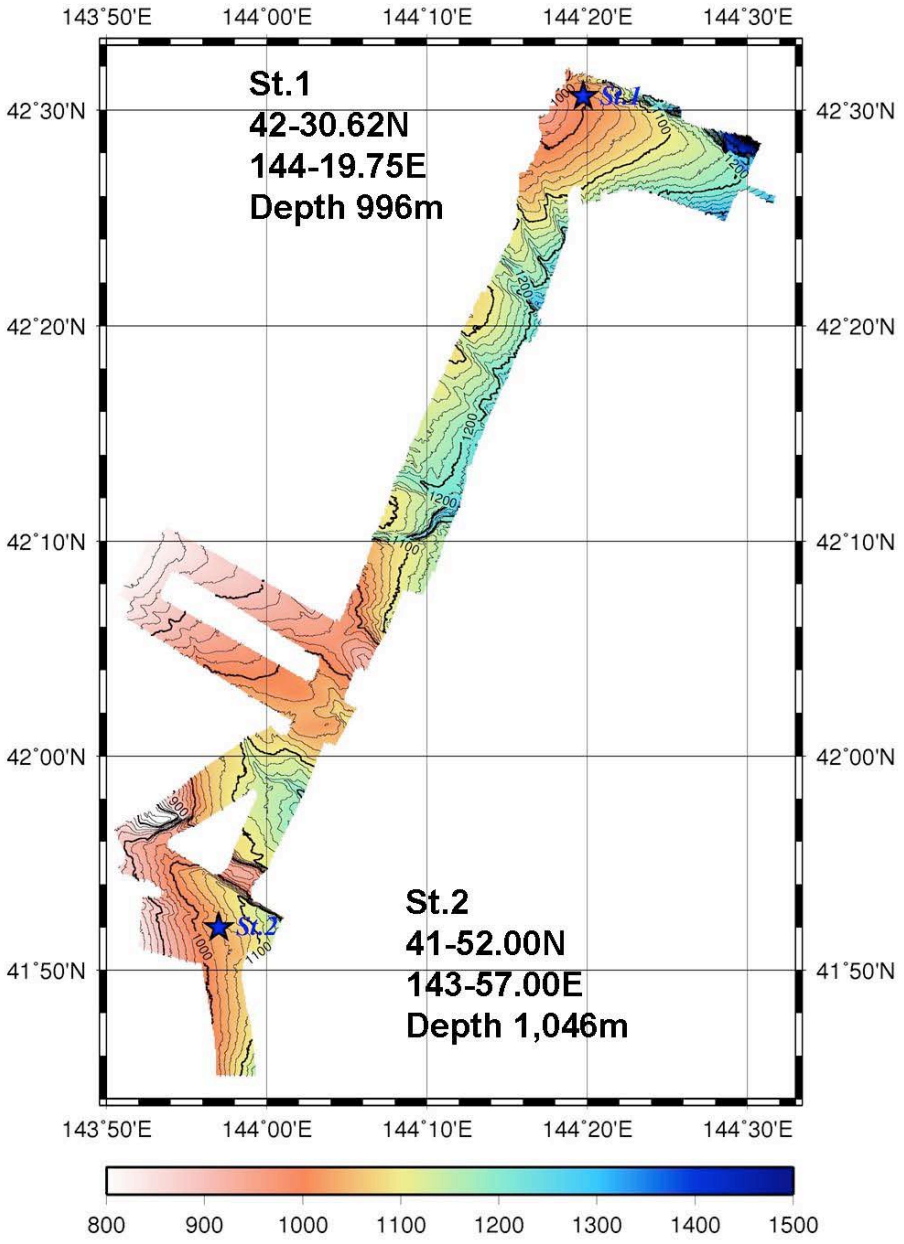

Fig. 6.8.1.1

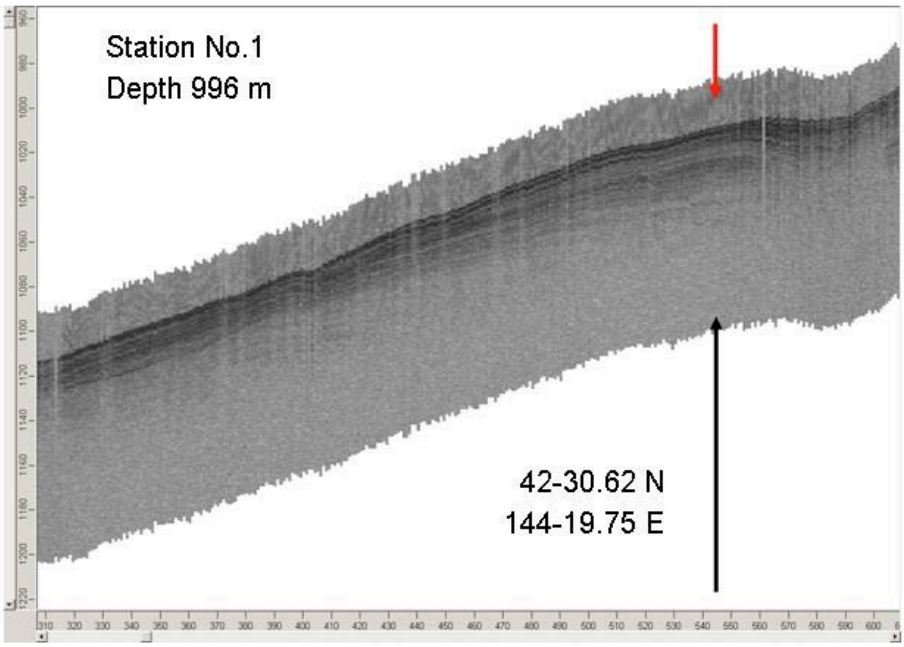

Fig 6.8.1.2

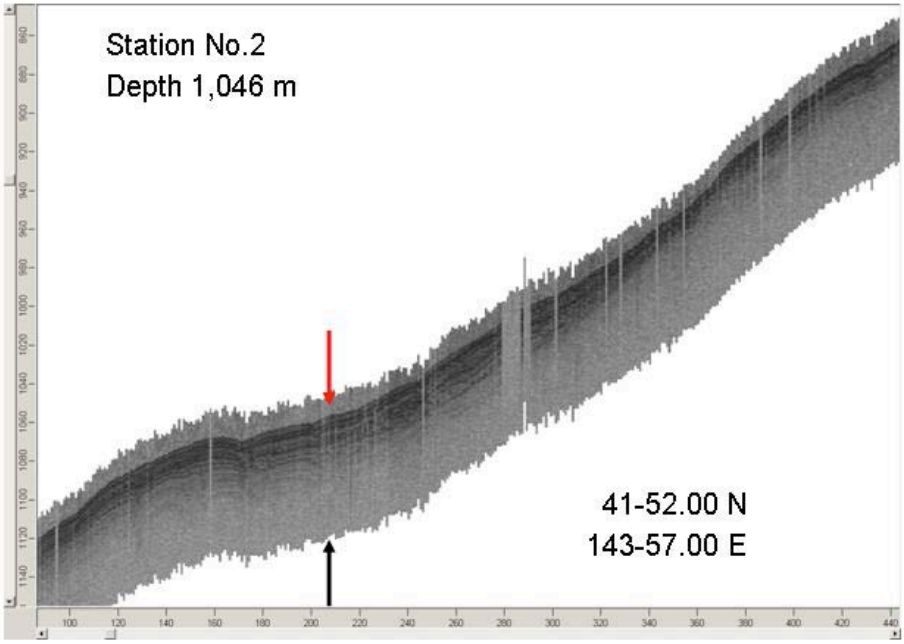

Fig. 6.8.1.3

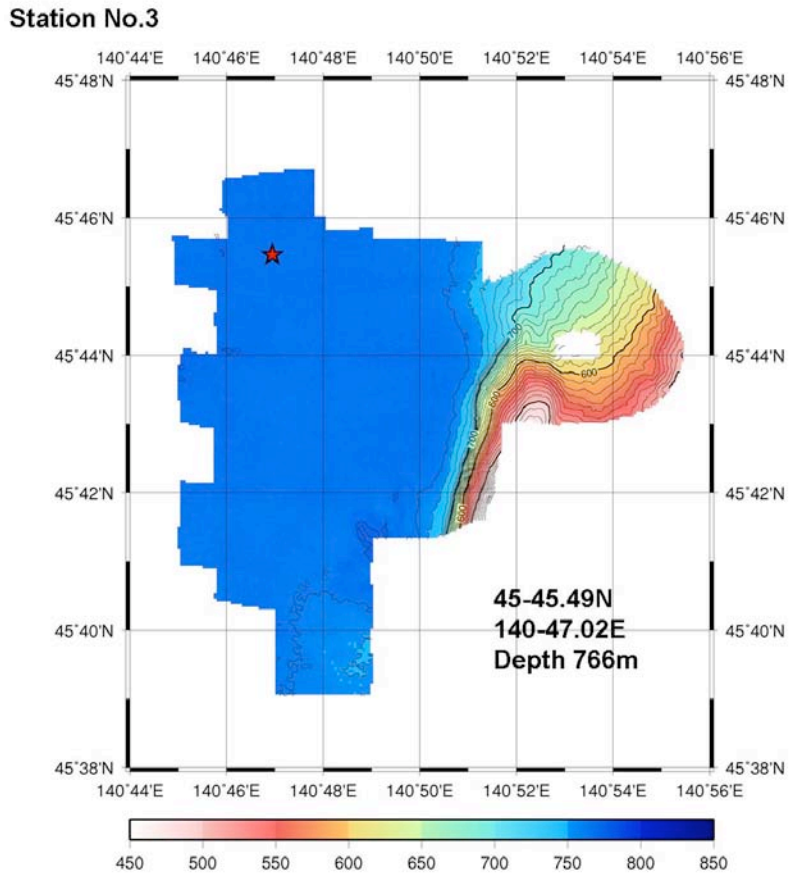
Station No.3
140°44'E
140°46'E
140°48'E
140°50'E
140°52'E
140°54'E
140°56'E
45°48'N
45°46'N
45°44'N
45°42'N
45°40'N
45°38'N
45-45.49N
140-47.02E
Depth 766m
450
500
550
600
650
700
750
800
850

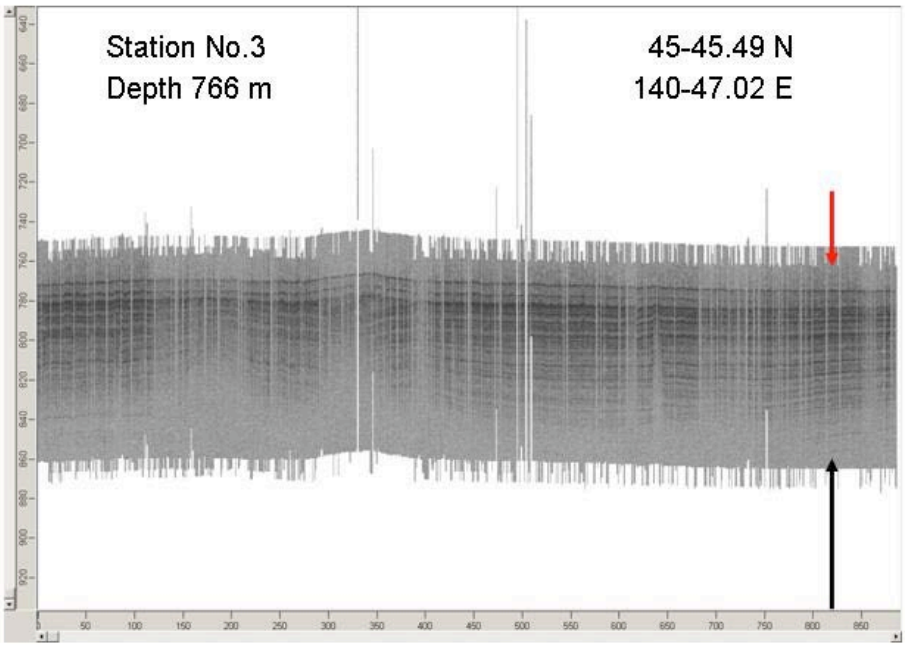
Station No.3
Depth 766 m
45-45.49 N
140-47.02 E

Fig. 6.8.1.4

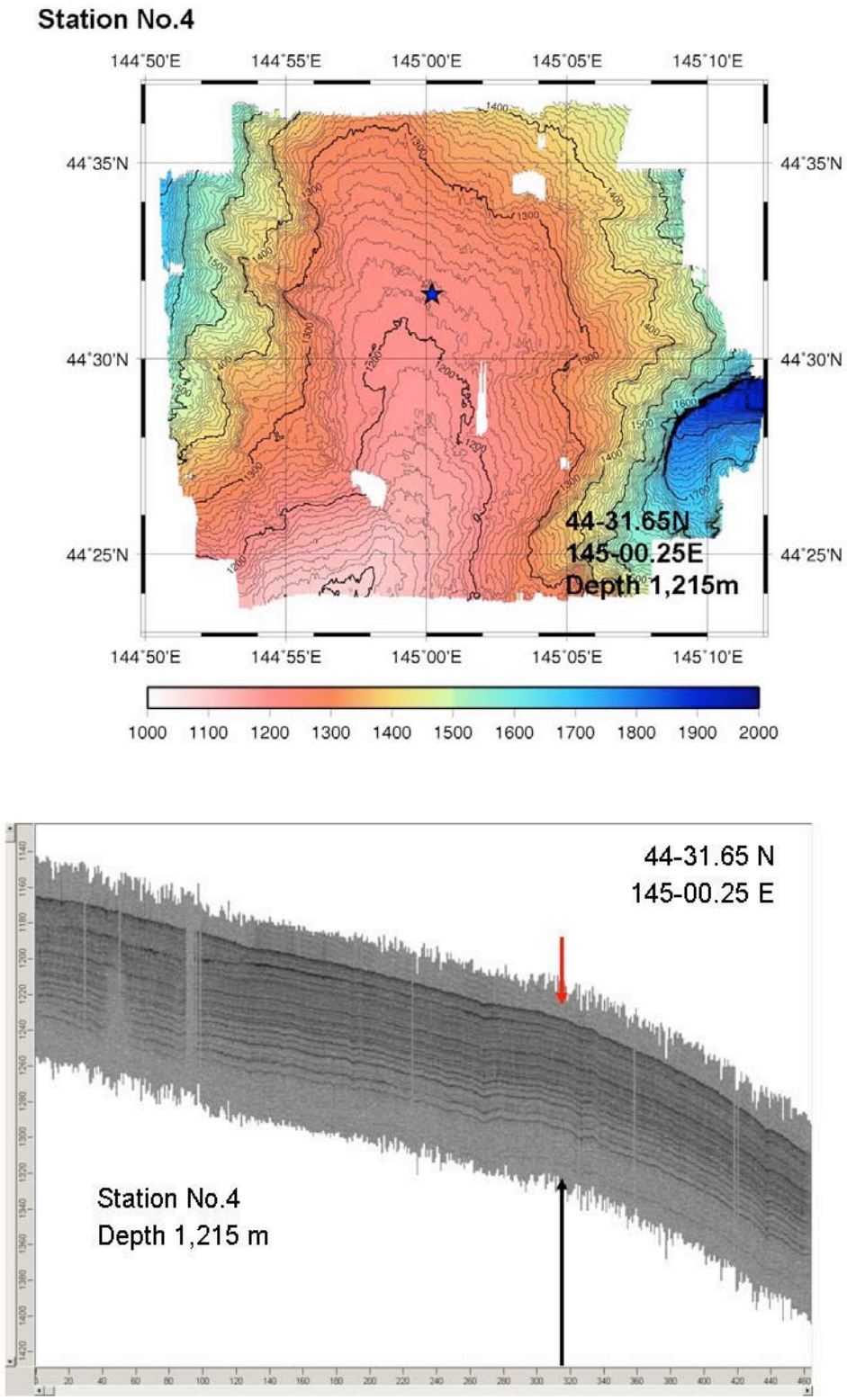
Station No.4
144°50'E
144°55'E
145°00'E
145°05'E
145°10'E
44°35'N
44°30'N
44°25'N
44-31.65N
145-00.25E
Depth 1,215m
1000 1100 1200 1300 1400 1500 1600 1700 1800 1900 2000
44-31.65 N
145-00.25 E
Station No.4
Depth 1,215 m

Fig. 6.8.1.5

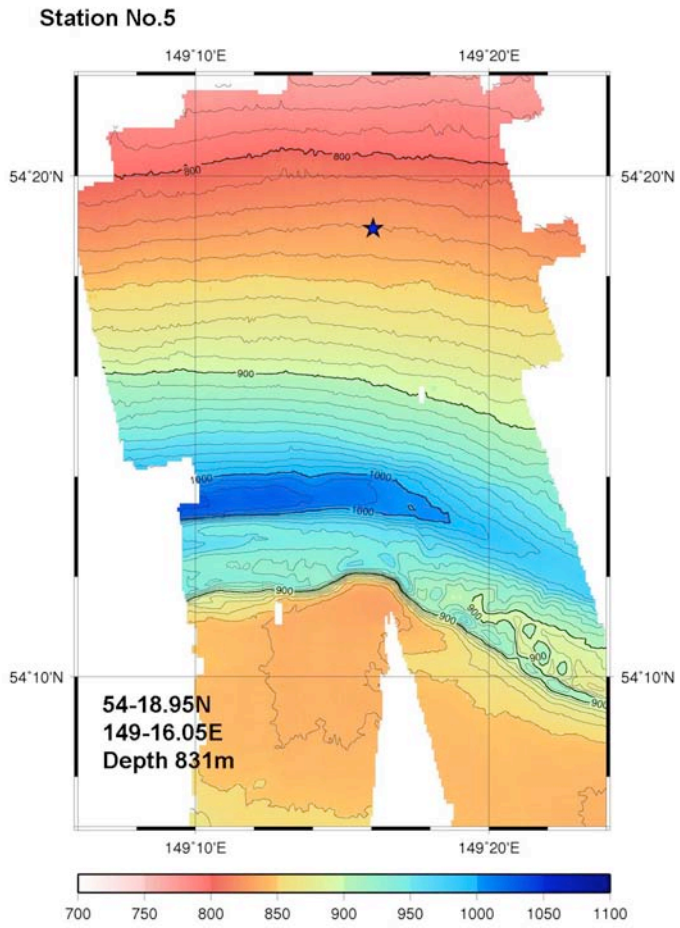
Station No.5
149°10'E
149°20'E
54°20'N
54°10'N
54-18.95N
149-16.05E
Depth 831m
700
750
800
850
900
950
1000
1050
1100

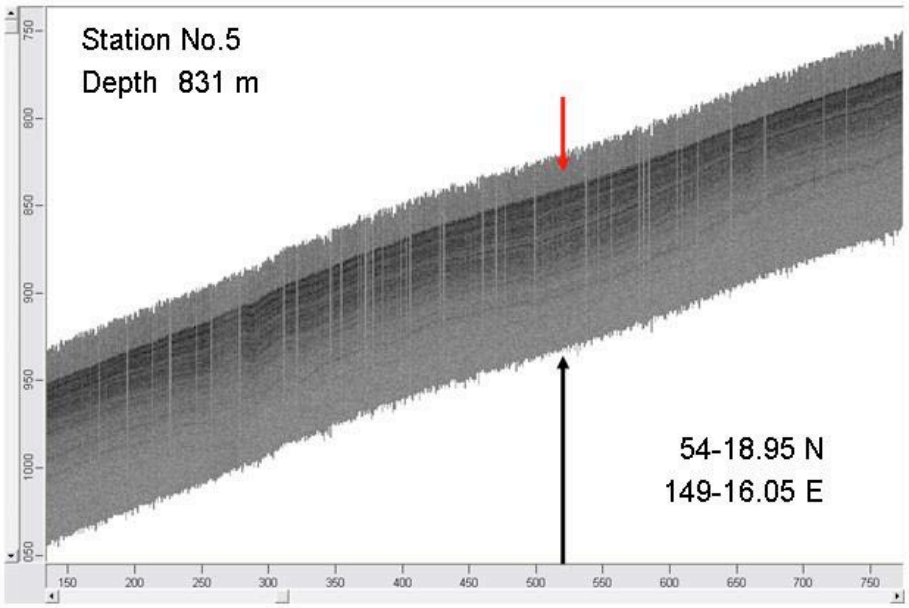
Station No.5
Depth 831 m
54-18.95 N
149-16.05 E
150
200
250
300
350
400
450
500
550
600
650
700
750

Fig. 6.8.1.6

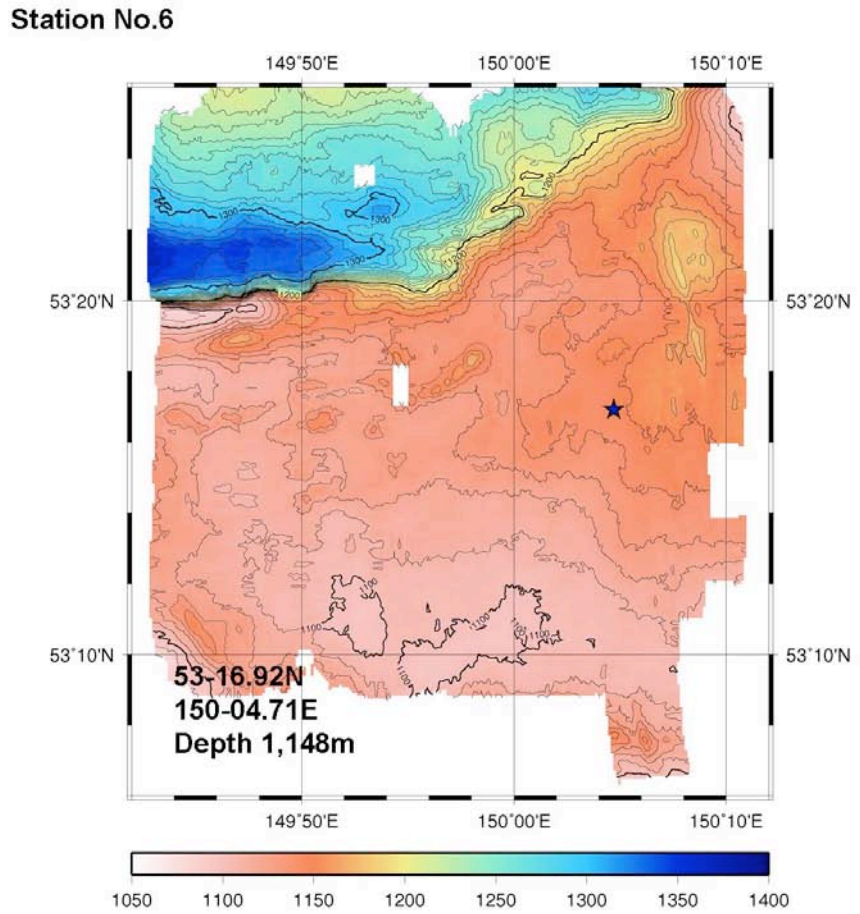
Station No.6
149°50'E
150°00'E
150°10'E
53°20'N
53°10'N
53-16.92N
150-04.71E
Depth 1,148m
1050
1100
1150
1200
1250
1300
1350
1400

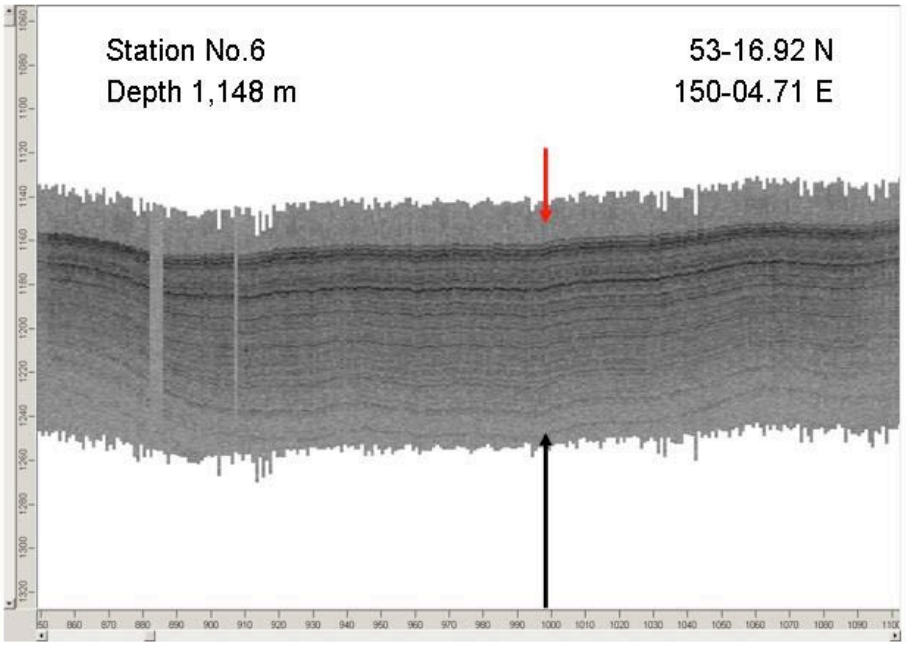
Station No.6
Depth 1,148 m
53-16.92 N
150-04.71 E

Fig. 6.8.1.7

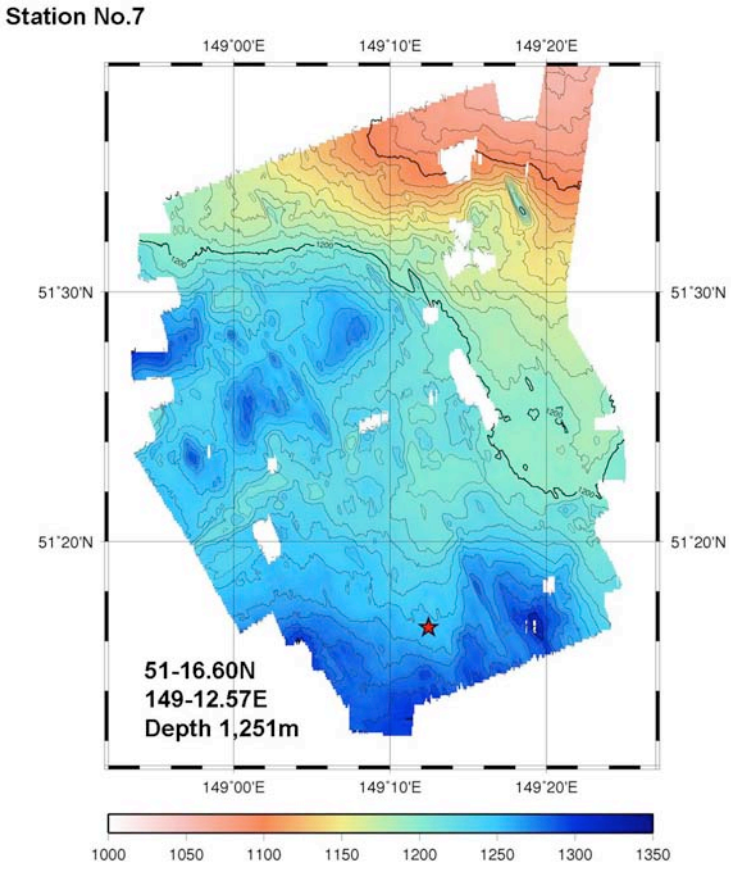
Station No.7
149°00'E
149°10'E
149°20'E
51°30'N
51°20'N
51-16.60N
149-12.57E
Depth 1,251m
1000
1050
1100
1150
1200
1250
1300
1350

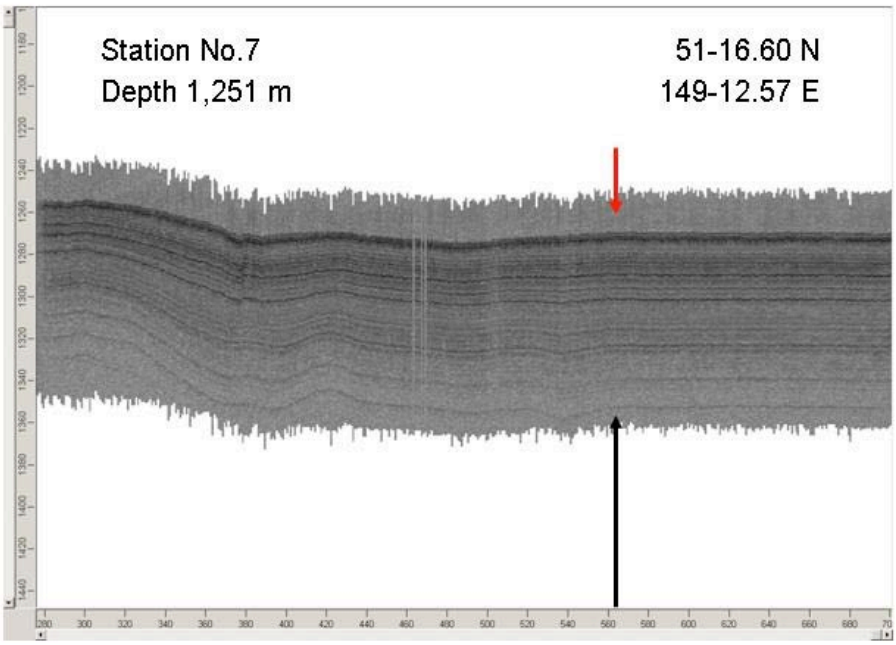
Station No.7
Depth 1,251 m
51-16.60 N
149-12.57 E

Fig. 6.8.1.8

Station No.16

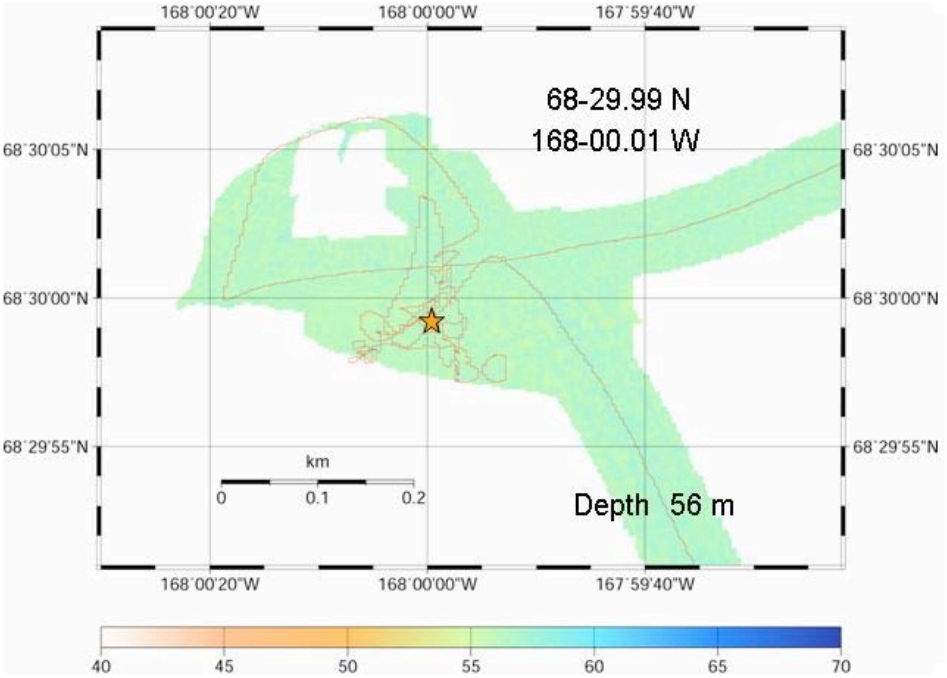

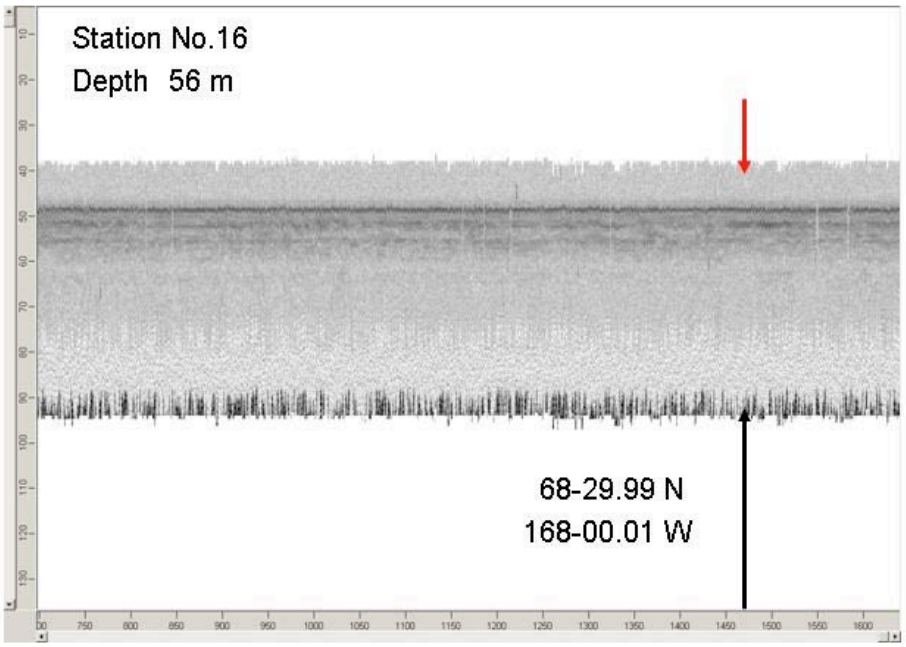

Fig. 6.8.1.9

Station No.21

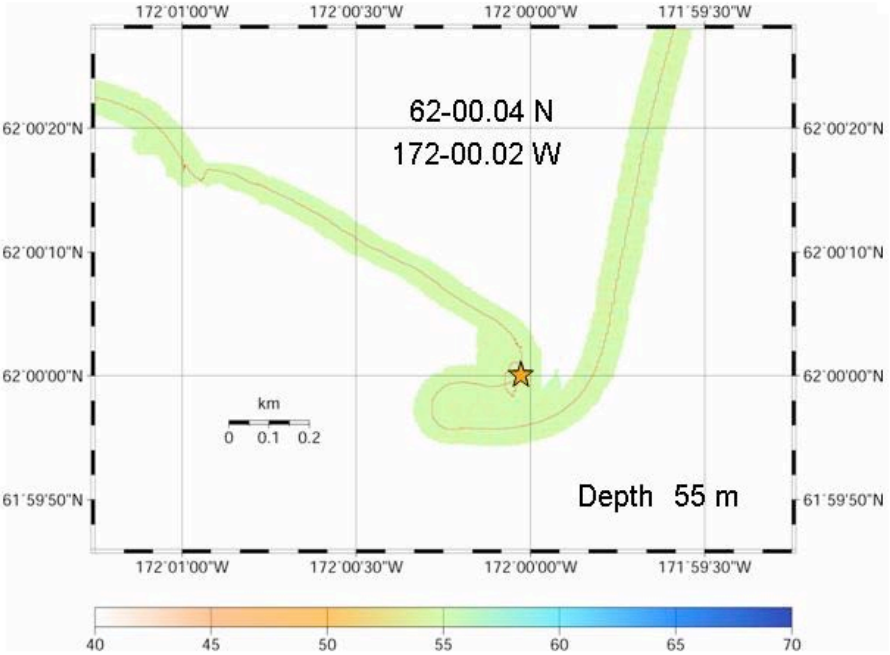

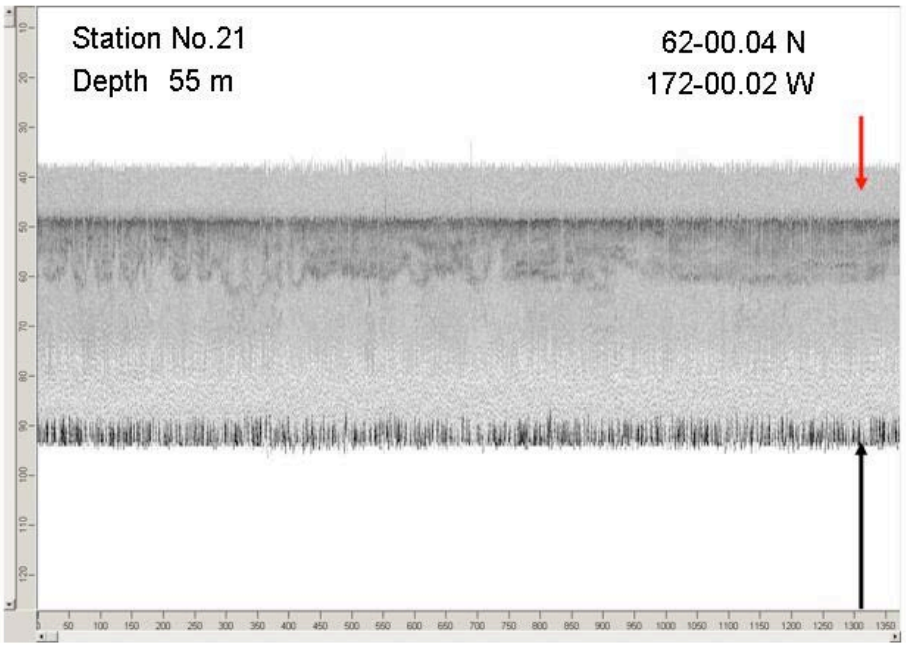

Fig. 6.8.1.10

Station No.22

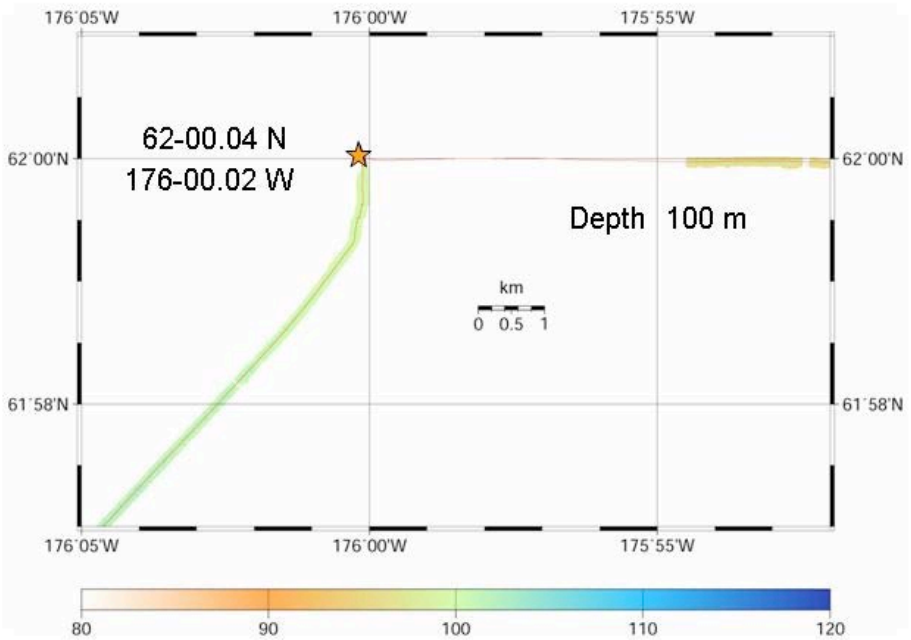

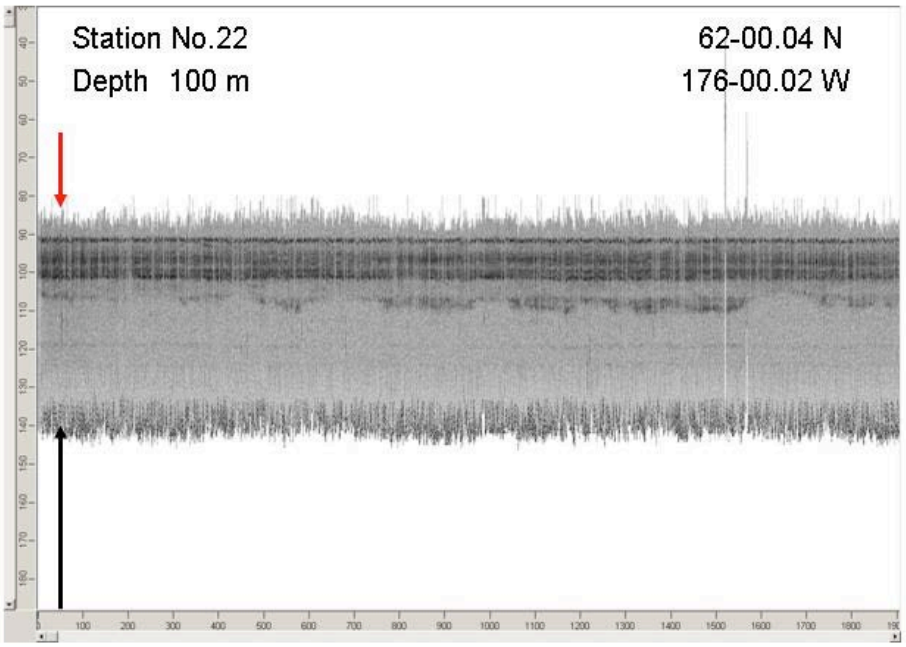

Fig. 6.8.1.11

Station No.23 & No.24 & No.25

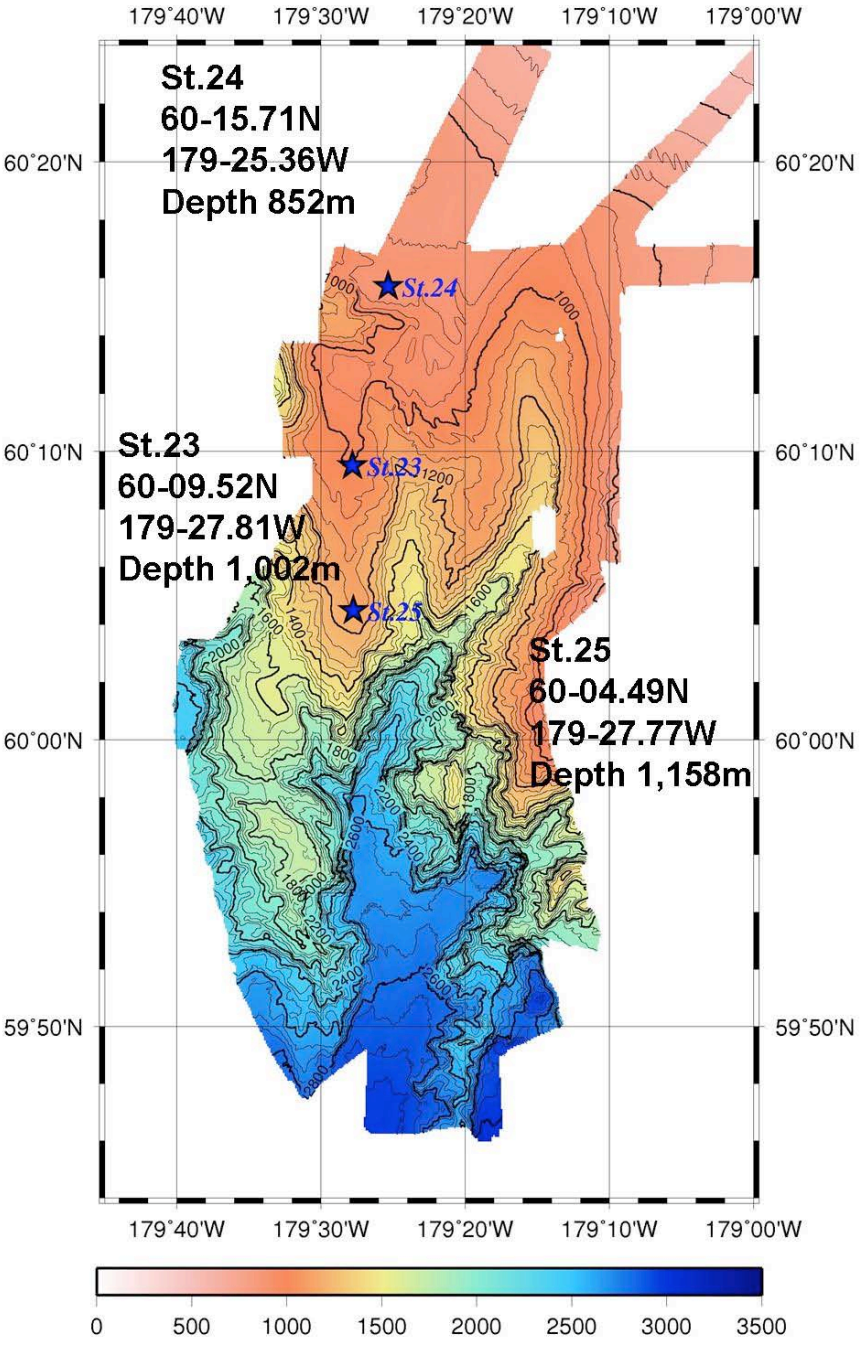

Fig. 6.8.1.12

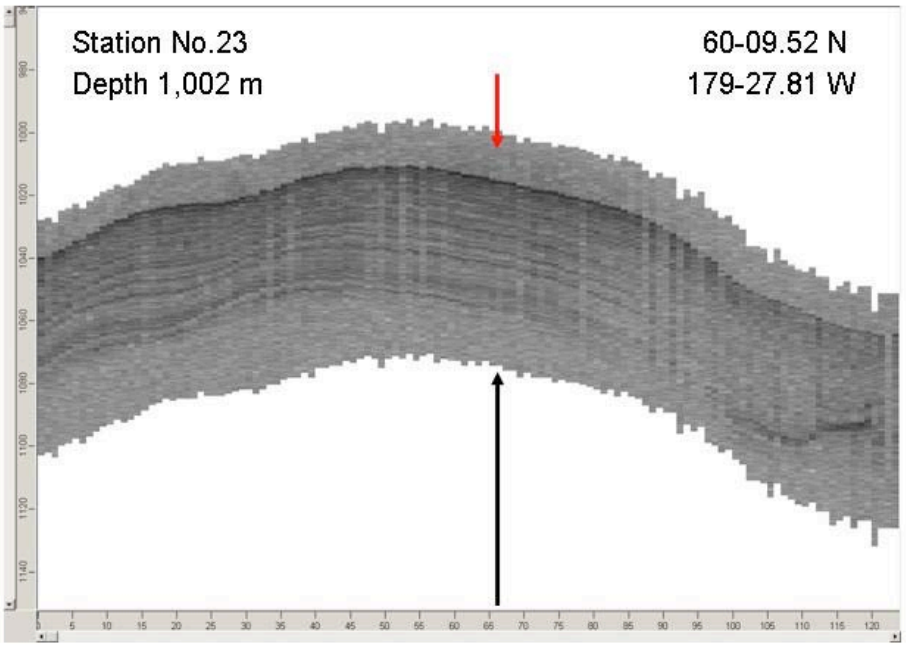

Fig. 6.8.1.13

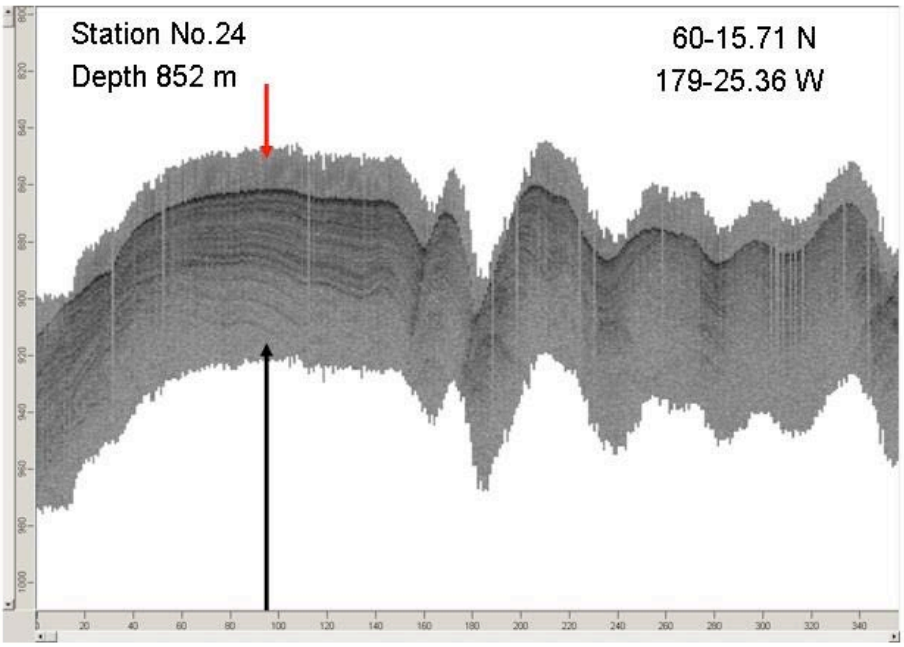

Fig. 6.8.1.14

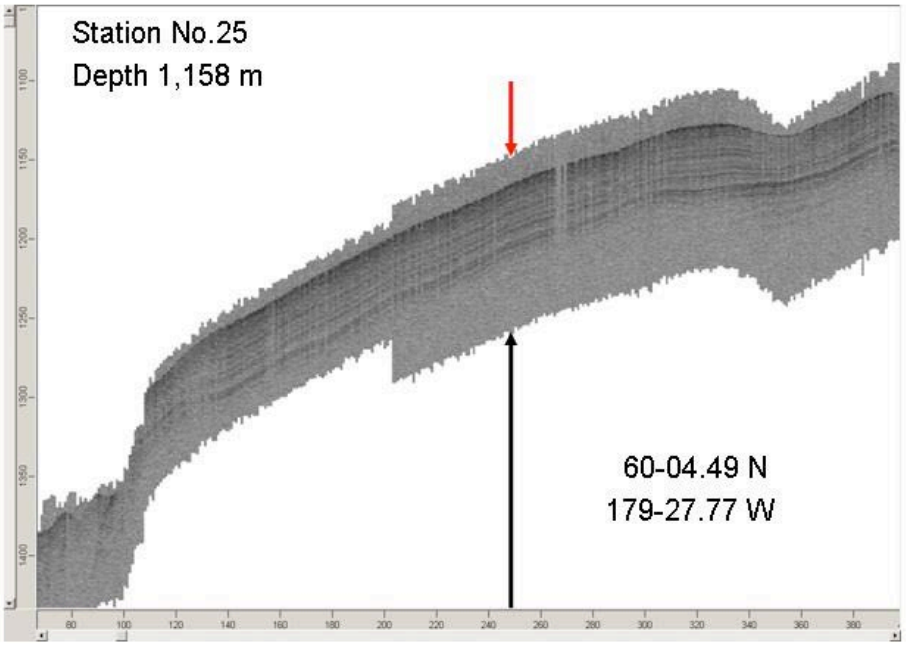

Fig. 6.8.1.15

Station No.26

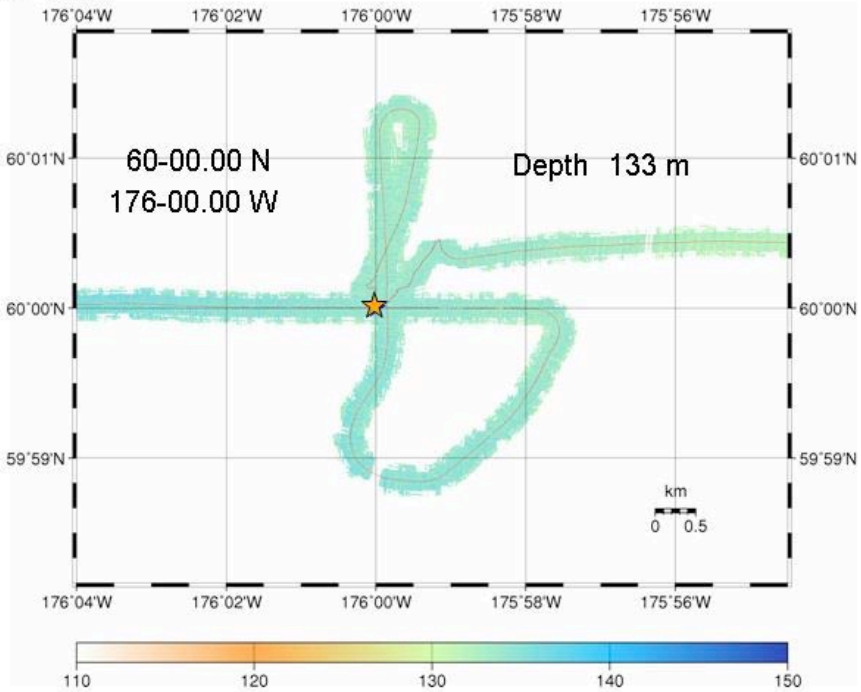

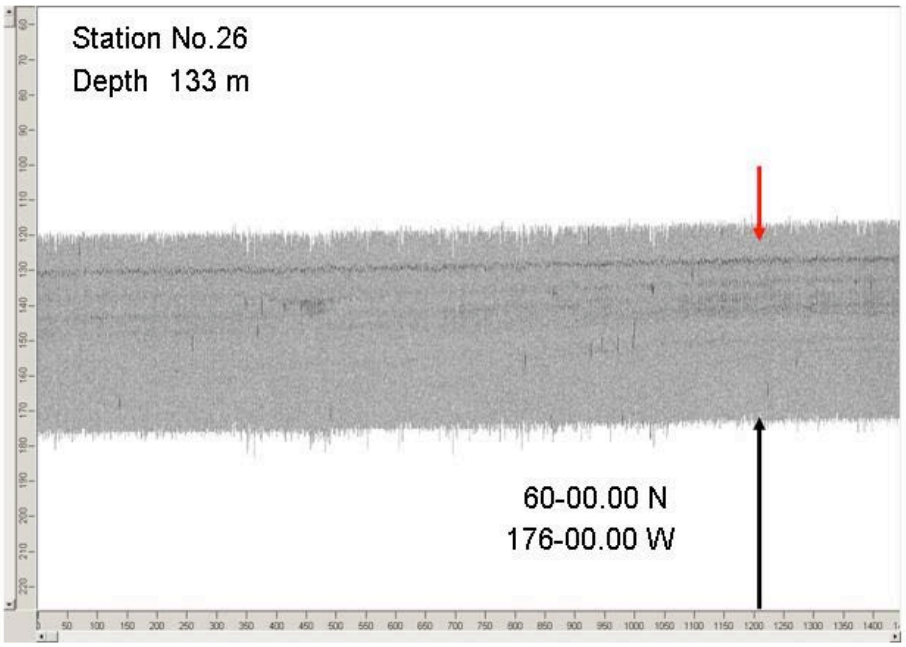

Fig. 6.8.1.16

Station No.27

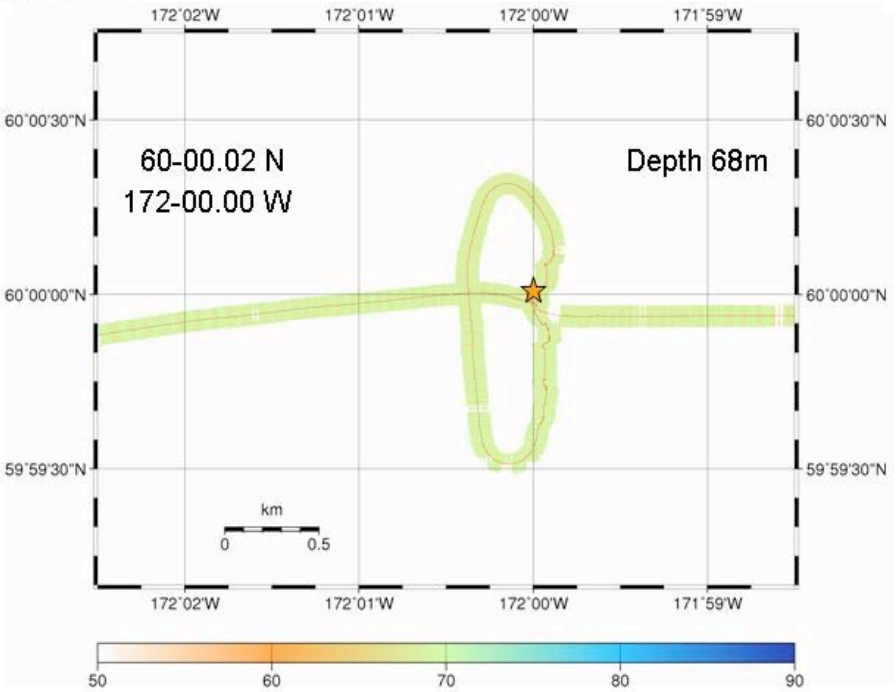

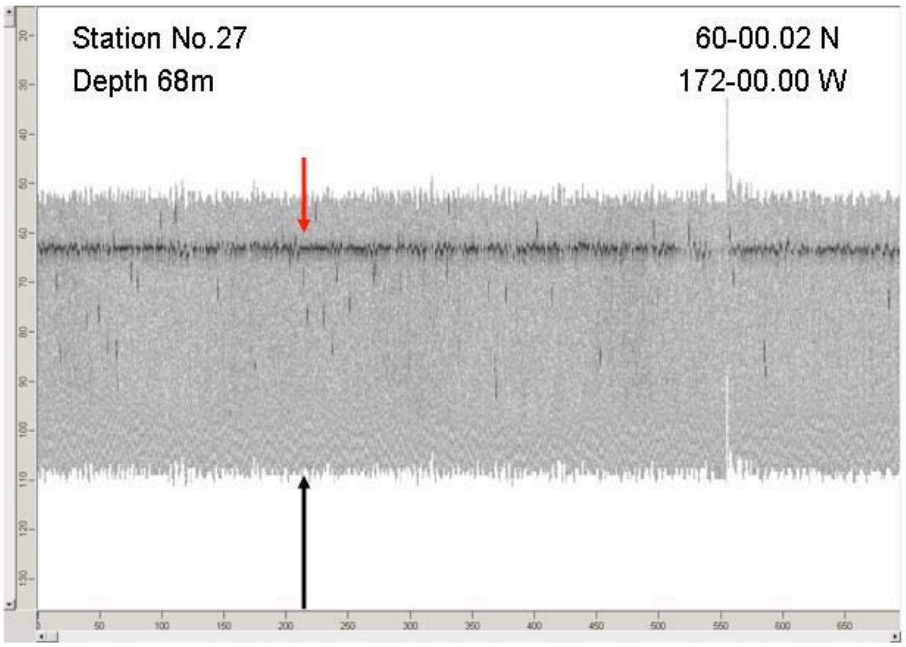

Fig. 6.8.1.17

Station No.29

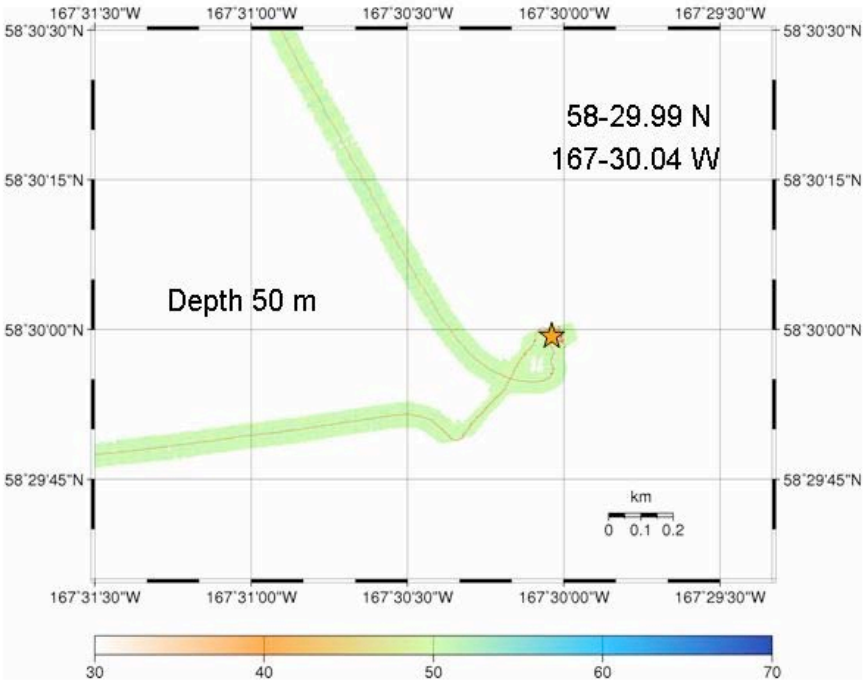

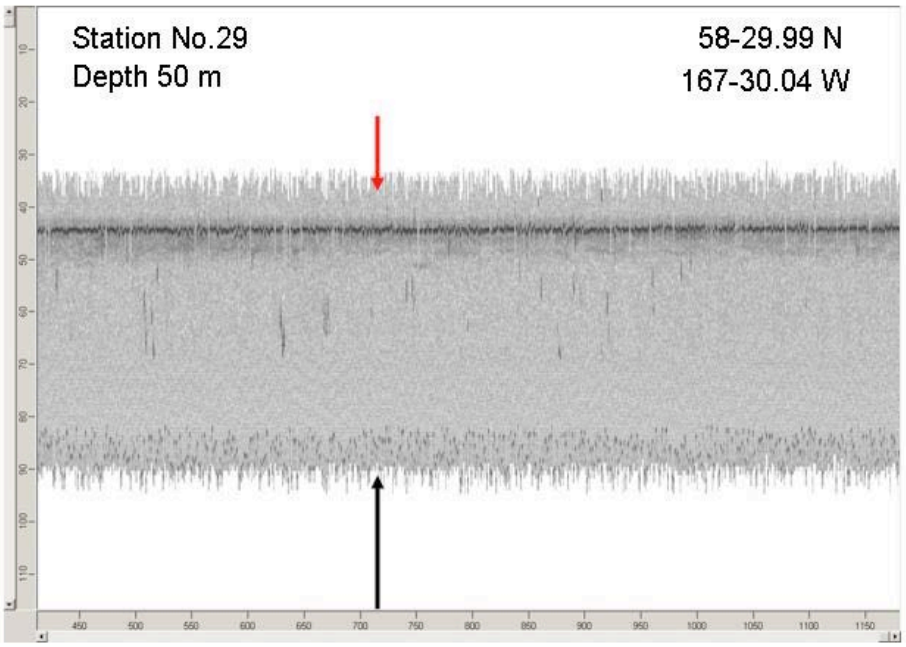

Fig. 6.8.1.18

Station No.30

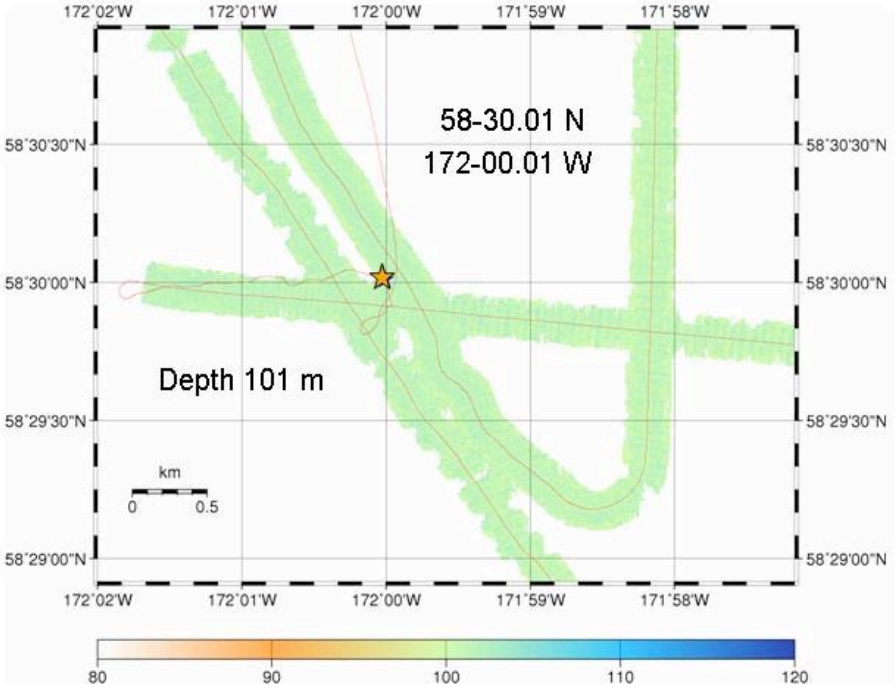

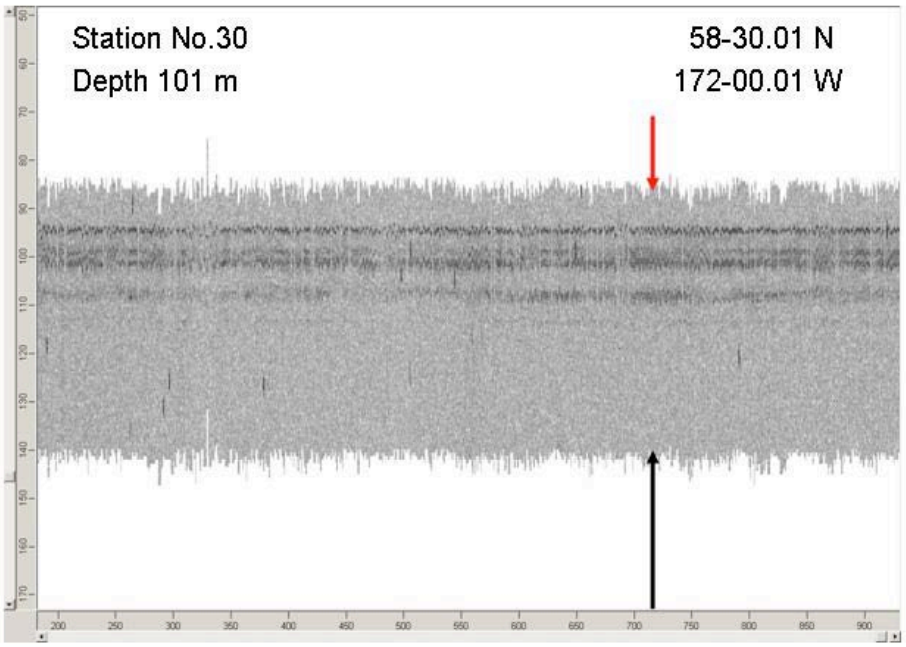

Fig. 6.8.1.19

Station No.31

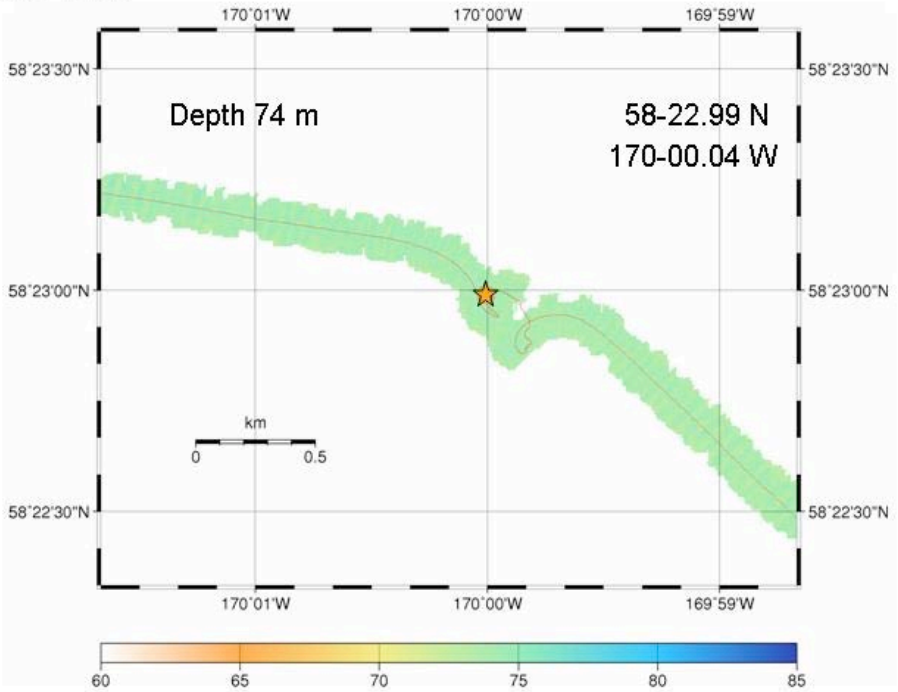

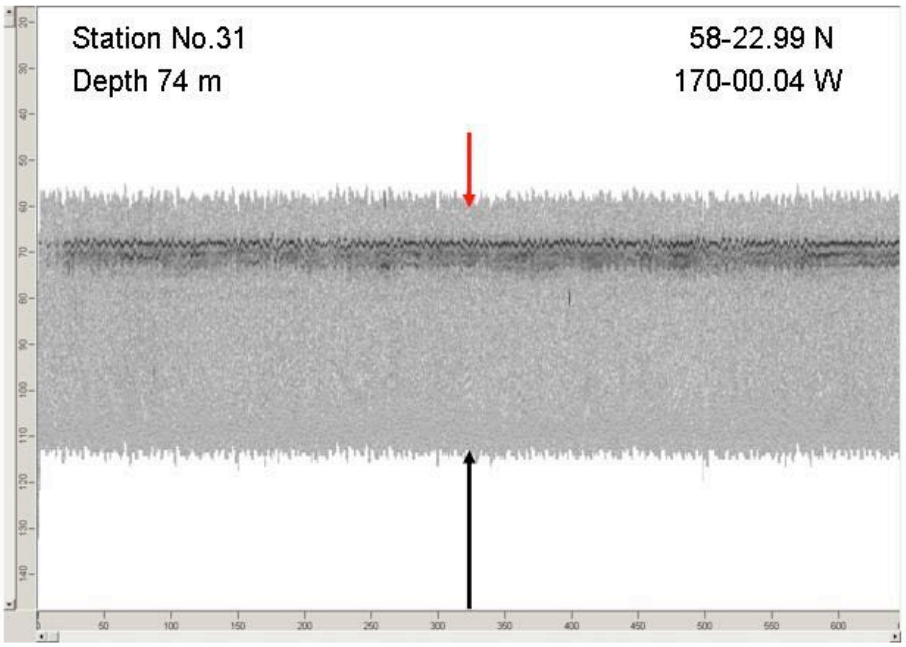

Fig. 6.8.1.20

Station No.32

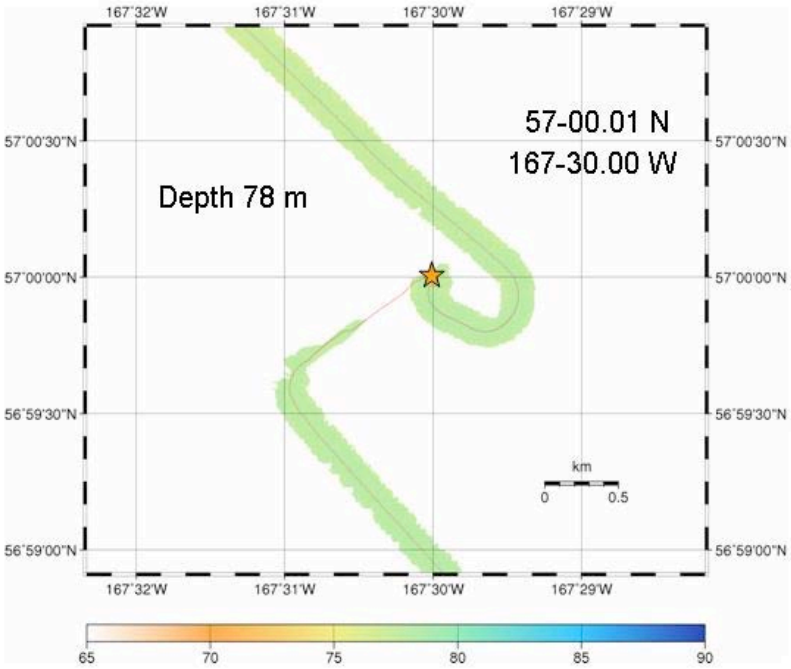

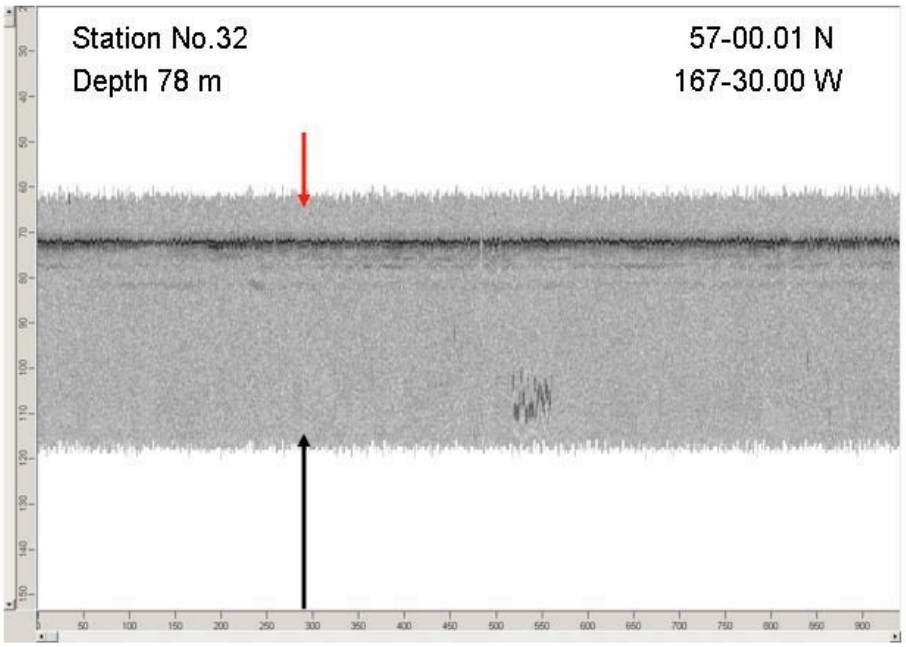

Fig. 6.8.1.21

Station No.33

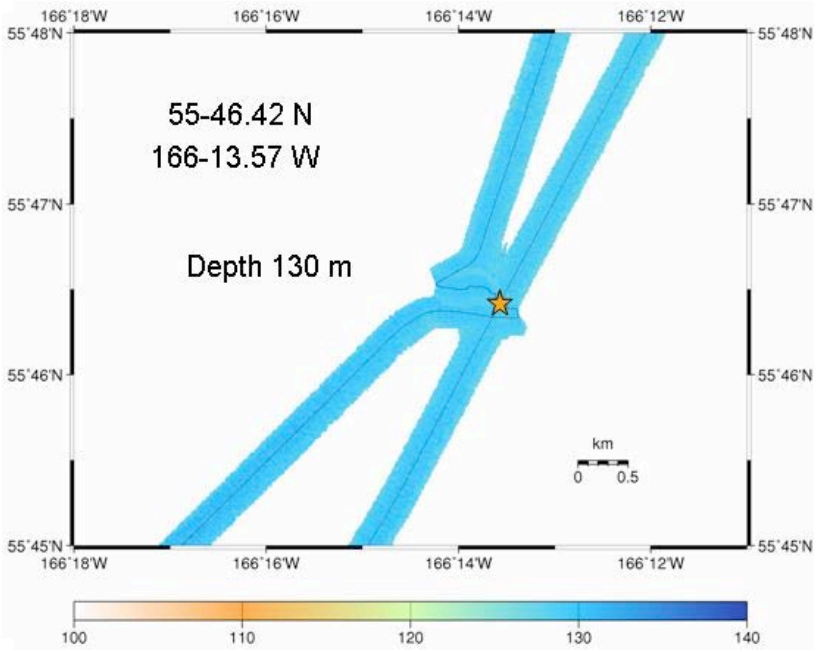

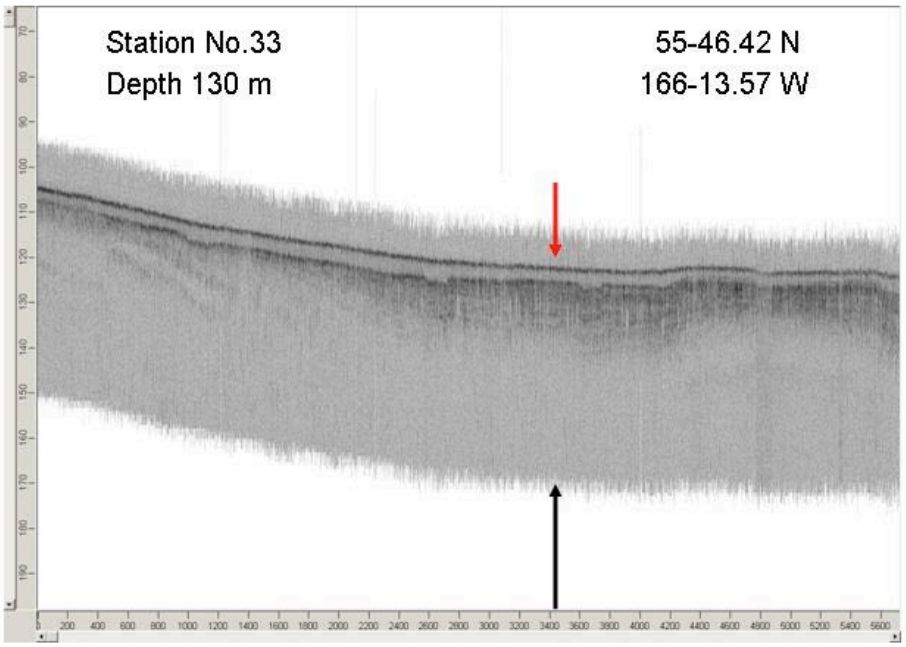

Fig. 6.8.1.22

6.8.2 Operation summary

(1) Personnel

Leg.1: Yutaka Matsuura (Operation Leader), Yusuke Sato, Hiroyuki Hayashi, Takami Mori (Marine Works Japan Ltd.)

Leg.2: Yutaka Matsuura (Operation Leader), Yusuke Sato, Yohei Taketomo, Yasushi Hashimoto (Marine Works Japan Ltd.)

(2) Objectives

Collection of sea floor sediment

(3) Instruments and method

3-1 Piston corer system (PC)

Piston corer system composed of 1.3t-weight, 5m-long aluminum barrel with polycarbonate liner tube and a pilot core sampler. The total weight of the system is approximately 1.5 ton. The length of the core barrel was 10m or 20m that was determined based on site survey data (bathymetry and sedimentation structure) derived from SeaBeam system onboard. We used a small type of multiple corer ("Ashura") as a trigger. The inner diameter (I.D.) of polycarbonate inner tube is 74mm. A compass with inclinometer was attached above the weight of the corer to examine the performance of the corer during operation.

In this cruise, we used three type pistons, Normal type, Short type and Rubber Plate Piston (RPP). The normal type piston composed of a stainless steel body and some biton O-rings (size: P63). The short type piston is different from the normal type piston regarding the length (4.5cm) only. The RPP composed of a stainless steel body and some rubber plates. At each station, we selected the most suitable piston among three type pistons according to the softness of sediment estimated by the data of sub-bottom profiler.

3-2 Gravity Corer (GC)

A Gravity corer produced by OYO Chishitsu Ltd. was used in this cruise. The GC system composed of a 500kg-weight, 1m-long stainless barrel with acrylic resin inner tube. In this cruise, 5m or 7m of the core barrel as a total length was selected by based on the site survey data. The inner diameter of acrylic resin is 115mm. At station 14, the Ashura type multiple corer was used as a trigger.

3-3 Multiple corer (MC)

A Multiple core sampler produced by Rigosha Co. was used for taking the surface sediment. This core sampler composed of a main body of 620kg-weight and 8 sub-core samplers (I.D. 74mm and length of 60cm).

3-4 Winch operation

During the operation of PC and MC under sea water, the speed of wire out was set to be 0.2 m/s at the beginning of operation, and then gradually increased to the maximum of 1.0 m/s. The wire out of corer system was stopped at the depth about 100 m above the sea floor for 3-5 minutes to reduce any pendulum motion of the system. If water depth was shallower than 100m, the wire out of corer system was not stopped. After the corer system became stable, the wire out was started again at the speed of 0.2-0.4 m/s, and we carefully watched a tension meter. When the corer system arrives at the bottom, the wire tension becomes immediately decrease due to reduction of the weight of corer system. After we confirmed the decrease of tension, the wire out was stopped and rewinding of the wire was started at a dead slow speed (~0.4m/s.). When the corer system leaves for the bottom, the wire tension indicates increase. After we confirmed that the wire tension increased, wire was in at the maximum speed.

The GC operation was almost same as the PC operation. The difference between GC and PC operations was the speed of wire out (1.0m/s) when the corer system was near the bottom.

(4) Result

4-1 Performance of the piston corer

In this cruise, we monitored the performance of the piston corer by a compass with inclinometer (APC-USB: Alec-electronics co., Ltd.). In many cases, when the piston corer plumbed down, the whole core barrel penetrated immediately into the sea floor (Fig.6.8.2.1). In the case of PC-01-B, the core barrel penetrated only 5m, and the core barrel bent. We also found that the piston corer inclined after the penetration in the case that core barrel bent (Fig.6.8.2.2). Details of coring position is shown in the Appendix01.

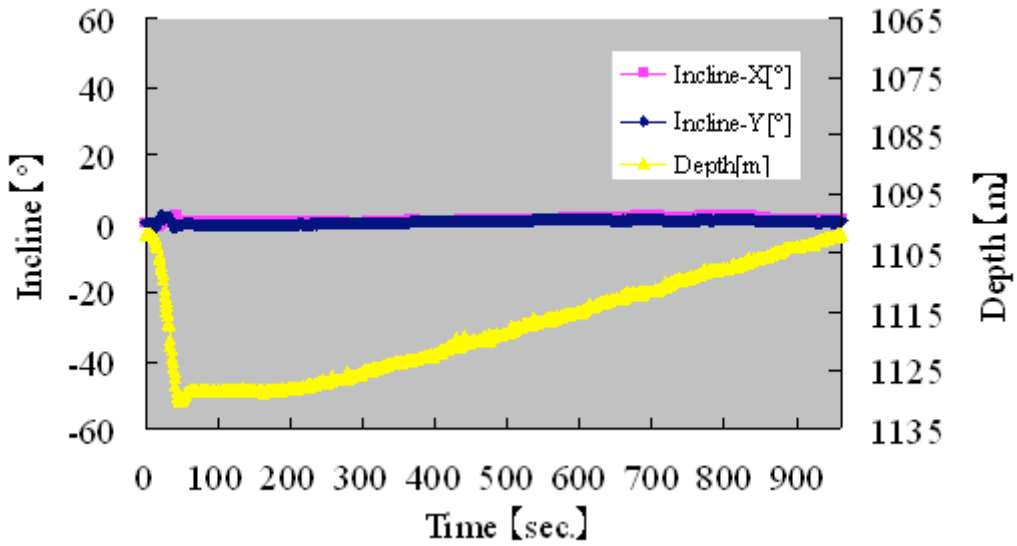

Figure 6.8.2.1 The performance when piston corer plumbed down and core barrel penetrated into sea floor (Core Name: PC-06-R).

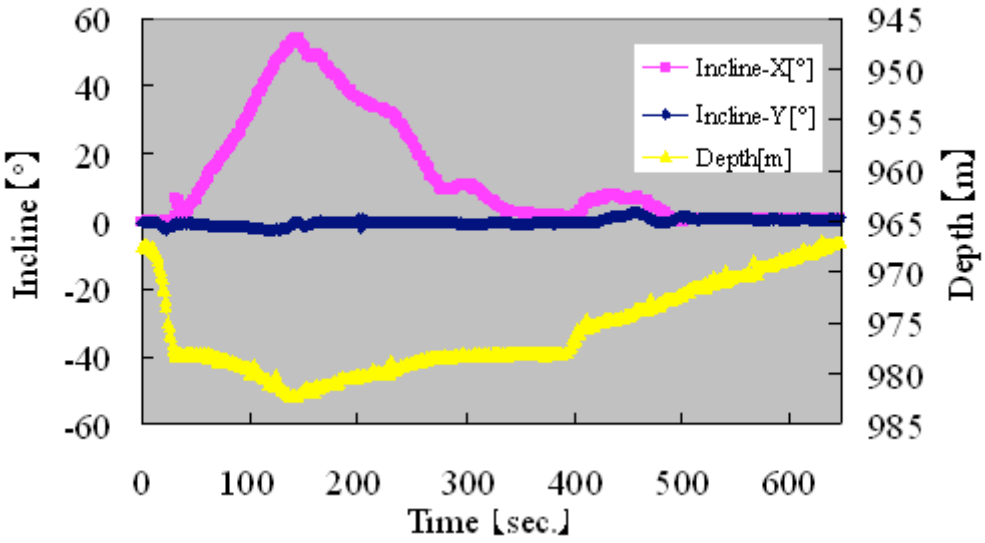

Figure 6.8.2.2 The performance when the core barrel of piston corer was bended (Core Name: PC-01-B).

6.8.3 Physical properties measurements

6.8.3.1 Multi-Sensor Core Logging

(1) Personnel

Kazuhiro Yoshida, Yuko Sagawa, Yusuke Sato (Marine Works Japan Co. Ltd)

(2) Objectives

To understand basic characteristics of marine sediment, physical properties (p-wave velocity, magnetic susceptibility, bulk density, colors, fine sedimentation structure, components of sediment) were measured onboard for piston, multiple and gravity core samples. Here, we reported Gamma-ray attenuation (GRA), P-wave amplitude and travel time, magnetic susceptibility (MS) by using the Multi-Sensor Core Logger.

(3) Measured parameters

Gamma-ray attenuation (GRA), P-wave amplitude and travel time, magnetic susceptibility (MS), Core diameter and temperature.

(4) Instruments and Method

The GRA, P-wave velocity (PWV), MS were measured by using GEOTEK multi-sensor core logger (MSCL). The assumption that the inside of the liner core tube were filled by only sediment and seawater was applied to calculate wet bulk density from the GRA value, PWV and fractional porosity (FP). Measurements of long cores (piston and gravity cores) were carried out every 2cm. Short cores (multiple and pilot cores) were measured on 1cm intervals. The temperature of sediment cores should be same as the room temperature. Therefore, piston, multiple and pilot cores were kept at the laboratory for 12 hours and gravity cores for 24 hours till the MSCL measurement. The GRA calibration assumes a two-phase (minerals and the interstitial water) system model between sediments and rocks. The working standard is a telescoping aluminum rod that 4 or 6 different thickness parts are mounted in a piece of core liner with distilled water. The GRA data of the working standard was used to make an equation to calculate the wet bulk density of sediment samples. Fractional porosity was also calculated directly from the data of bulk density.

The PWV of sediment can be simply calculated from P-wave travel time, core diameter and temperature. However, the travel time data includes the pulse travel time through the transducer faces with the pulse travel time through the liner. All time delays were deleted from the travel time data of the working standard. If the sediment is not completely filled in the inner tube, analytical data is not correct. For some gassy sediment cores, the state of sediment in inner tube was inadequate for taking the PWV data.

The MS was measured by Bartington MS2C system within the MSCL equipped with a loop sensor.

The loop sensor for piston, multiple and pilot cores has an internal diameter of 100 mm and has 140mm diameter for gravity core. The MS data were corrected by the bulk density data and estimated to be mass specific magnetic susceptibility. The unit switch should always be on SI. The MS was measured every 1 or 2cm of whole core with 1 second.

Light reminiscence analysis will be carried out on land to make an age model of sediment cores. Therefore, sediment cores for analysis of light luminescence were collected by using black inner tube to inhibit any lights. For black inner tube core samples collected in the leg.1, aluminum foil that is used as a cap of both ends of tube due to shut any light from outside was removed only during the MSCL measurement. During the Leg 2, a special cap composed of thin rubber board internally and black vinyl tape outside was used instead of aluminum foil, and thus both ends of sediment in black inner tube collected in the leg.2 was not damaged for light luminescence analysis during the MSCL measurement.

(5) Depth correction for sub cores

In electric files of Raw Data, the core length of each section is recorded as "Core Depth" and contains the length of end caps (2 or 4mm / one section). In electric files of Processed Data, the core length that the length of end cap was corrected from "Core Depth" is recorded as "Sub Bottom (SB) Depth". However, because MSCL measurement was carried out from the top of the inner core tube, the data of empty part (no sediment) would be included. Thus, the data of empty part was eliminated from Processed Data based on the PinPrick length that was firstly measured when the inner core tube was splitted into halves, and was most accurate. In addition, if the section length of MSCL measurement was different from that of PinPrick, the measurement interval of MSCL was corrected to become same section length as the PinPrick length. The length of sections having no MSCL data was added to "SB Depth". The raw data is compiled in the Appendix03 sediment info&data.

6.8.3.2 Sediment color

(1) Personnel

Ei Hatakeyama, Takami Mori (Marine Works Japan Co. Ltd)

(2) Objectives

To understand basic characteristics of marine sediment, physical properties (p-wave velocity, magnetic susceptibility, bulk density, colors, fine sedimentation structure, components of sediment) were measured onboard for piston, multiple and gravity core samples. Here, we reported color reflectance to recognize the characteristics of sediments such as lithology, oxic and anoxic condition, and abundances of carbonate, organic matter and inorganic compounds.

(3) Measured parameters

There are some different systems to quantify the color reflectance for soil and sediment measurements. The most common is the L*a*b* system, and is also referred to as the CIE (Commission International d'Eclairage) LAB system. It can be visualized as a cylindrical coordinate system in which the axis of the cylinder is the lightness variable L*ranging from 0 to 100 % (white and black), and the radii are the chromaticity variables a* and b*. Variable a* is the green (negative) to red (positive) axis, and variable b* is the blue (negative) to yellow (positive) axis. Spectral data can be used to estimate the abundance of certain components of sediments.

(4) Instruments and methods

Core color reflectance was measured by using the Minolta CM-2002 reflectance photospectrometer using 400 to 700nm in wavelengths. This is a compact and hand-held instrument, and can measure spectral reflectance of sediment surface with a scope of 8mm diameter. To ensure accuracy, the CM-2002 was used with a double-beam feedback system, monitoring the illumination on the specimen at the time of measurement and automatically compensating for any changes in the intensity or spectral distribution of the light. The Minolta CM-2002 has a switch that allows the specular component to be included (SCI) or excluded (SCE). The specular component inclusion (SCI) essentially includes glare and provides a better estimate of color as seen by the human eye. However, glare does not contribute to the spectrum reflected from the sediments. Thus, we used the switch to SCE. The SCE setting is the recommended mode of operation for sediments in which the light reflected at a certain angle (angle of specular reflection) is trapped and absorbed at the light trap position on the integration sphere.

Calibration was carried out using the zero and white calibration piece (Minolta CM-2002 standard accessories) without crystal clear polyethylene wrap before the measurement of core samples. The color of the sediment surface of a half core was measured on every 2-cm through crystal clear polyethylene

wrap.

Measurement parameters are displayed in the Table 6.8.3.2.1 and the raw data is compiled in the Appendix03 sediment info&data.

Table 6.8.3.2.1. Measurement parameters.

Instrument	Minolta Photospectrometer CM-2002
Illuminant	d/8 (SCE)
Light source	D_{65}
Viewing angle	10 degree
Color system	L*a*b* system

6.8.3.3 Photographs

(1) Personnel

Yutaka Matsuura, Tamami Ueno, Kazuhiro Yoshida, Takami Mori (Marine Works Japan Co. Ltd)

(2) Objectives

To understand basic characteristics of marine sediment, physical properties (p-wave velocity, magnetic susceptibility, bulk density, colors, fine sedimentation structure, components of sediment) were measured onboard for piston, multiple and gravity core samples. Here, we reported photographs to obtain visual information such as sediment structure, color, and components.

(3) Measured parameters

Photographs of surface sediment

(4) Instruments and Method

After splitting each section of piston, pilot and multiple cores into halves, photographs of section halves were taken by a Nikon single-lens digital camera. Shutter speed was selected on 1/10 and sensitivity ISO 400 was used. The photos are compiled in Appendix03 sediment info&data.

6.8.3.4 Soft-X ray photographs

(1) Personnel

Tamami Ueno, Kazuhiro Yoshida, Yohei Taketomo, Ei Hatakeyama (Marine Works Japan Co. Ltd)

(2) Objective

To understand basic characteristics of marine sediment, physical properties (p-wave velocity, magnetic susceptibility, bulk density, colors, fine sedimentation structure, components of sediment) were measured onboard for piston, multiple and gravity core samples. Here, we reported Soft-X ray photographs which to obtain information of invisible sedimentary microstructure of the cores.

(3) *Instruments and methods*

Sediment was sub-sampled by using an original plastic case (length of 200mm x thickness of 3mm x width of 7mm) from sediment halves. The voyage code, core number, section number, case number, and the position range (cm) printed on TEPURA was put on each case and sub-sampled plastic cases were tightly sealed to avoid exudation of pore water by using PARAFILM.

Soft-X ray photographs were taken by a device of SOFTEX PRO-TEST 150 on board. The energy level (voltage and ampere) and irradiation time of X ray were changed according to the result of test photographs of each sediment core section. The energy level ranged from 40 to 50KVp for voltage, from 2 to 3mA for ampere, and from 150 to 200 seconds for applying time of X ray.

All negative films of soft-X ray photograph were developed by a device FIP-1400 on board.

(4) Preliminary results

In this cruise, the total 963 sediment samples were sub-sampled in plastic cases from cores, and the total 221 negative films of soft-X ray photograph were taken and developed. The finishing touch of negative films was applied to be lighter than usual touch, because the negative films will be used for scanning in digital data.

6.9 Underway Geophysical Observations

6.9.1 Sea Surface Gravity

(1) Personnel

Takeshi Matsumoto (University of Ryukyu) : Principal Investigator	(Not on-board)
Satoshi Okumura (Global Ocean Development Inc., GODI)	- Leg1 -
Souichiro Sueyoshi (GODI)	- Leg1 -
Kazuho Yoshida (GODI)	- Leg1, 2 -
Kazuya Yamashita (GODI)	- Leg1 -
Shin'ya Okumura (GODI)	- Leg2 -
Wataru Tokunaga (GODI)	- Leg2 -
Ryo Ohyama (GODI)	- Leg2 -

(2) Introduction

The difference of local gravity is an important parameter in geophysics and geodesy. We collected gravity data at the sea surface during the MR06-04 cruise from Sekinehama on 31st July 2006 to Sekinehama on 29th September 2006, and called at ports Kushiro on 20th - 21st August, except for the EEZ of Russia and territorial waters of U.S.A.

(3) Parameters

Relative Gravity [CU: Counter Unit]
[mGal] = (coef1: 0.9946) * [CU] (120 seconds QC flitted)

(4) Data Acquisition

We have measured relative gravity using LaCoste and Romberg air-sea gravity meter S-116 (LaCoste and Romberg Gravity Meters, Inc.) during this cruise. To convert the relative gravity to absolute one, we measured gravity using portable gravity meter (Scintrex gravity meter CG-3M), at Sekinehama Port, Kushiro Port as reference points.

(5) Preliminary Results

Absolute gravity shown in Table 6.9.1.1

Table 6.9.1.1

No.	Gravity at Date	Level	Absolute L&R *2 U.T.C. Draft [mGal]	Sensor *1 [mGal]	Sea Port	Gravity [cm]	Gravity [cm]	[mGal]
#01	July/31		20:00		Sekinehama		980371.95	
	261		623		980372.80		12645.43	
#02	Aug/20		01:53		Kushiro	978302.30		161
		635		979742.30		12874.40		
#03	Sep/29		03:30		Sekinehama		980371.95	
	246		615		980372.75		12644.15	

*[1]: Gravity at Sensor = Absolute Gravity + Sea Level*0.3086/100 + (Draft-530)/100*0.0431
*[2]: LaCoste and Romberg air-sea gravity meter S-116

(6) Data Archives

Gravity data obtained during this cruise will be submitted to the JAMSTEC and archived

there.

(7) Remarks

We did not sample the data in the EEZ of Russia and territorial waters of U.S.A. as following terms.

01:13UTC, 09 Aug. - 04:40UTC, 10 Aug. (Russia EEZ)
02:00UTC, 16 Aug. - 15:17UTC, 18 Aug. (Russia EEZ)
14:00UTC - 19:10UTC, 28 Aug. (USA, territorial waters)
19:00UTC - 21:15UTC, 30 Aug. (USA, territorial waters)
00:20UTC - 02:45UTC, 07 Sep. (USA, territorial waters)
14:50UTC - 20:30UTC, 19 Sep. (USA, territorial waters)

GPS navigation data (Positions, SOG and COG) was invalid as following terms.

08:31:04UTC - 08:31:16UTC, 25 Aug.
08:43:42UTC - 08:48:52UTC, 25 Aug.
08:43:23UTC - 08:46:37UTC, 26 Aug.
12:10:03UTC - 12:10:09UTC, 28 Aug.
08:14:45UTC - 08:14:55UTC, 29 Aug.
08:15:29UTC - 08:16:07UTC, 29 Aug.
08:16:33UTC - 08:17:05UTC, 29 Aug.
08:18:19UTC - 08:18:33UTC, 29 Aug.
08:19:21UTC - 08:30:49UTC, 29 Aug.
22:27:38UTC - 22:38:15UTC, 08 Sep.
22:23:36UTC - 22:30:09UTC, 09 Sep.

We used No.1 Ship's gyro-compass, following period. (We always used No.2 Ship's gyro-compass for this cruise.)

09:54:51UTC - 12:07:01UTC, 05 Sep.

6.9.2 Sea Surface three-component magnetic field

(1) Personnel

Takeshi Matsumoto (University of Ryukyu) : Principal Investigator (Not on-board)
Satoshi Okumura (Global Ocean Development Inc., GODI) - Leg1 -
Souichiro Sueyoshi (GODI) - Leg1 -
Kazuho Yoshida (GODI) - Leg1, 2 -
Kazuya Yamashita (GODI) - Leg1 -
Shin'ya Okumura (GODI) - Leg2 -
Wataru Tokunaga (GODI) - Leg2 -
Ryo Ohyama (GODI) - Leg2 -

(2) Introduction

Measurements of magnetic force on the sea are required for the geophysical investigations of marine magnetic anomaly caused by magnetization in upper crustal structure. We measured geomagnetic field using a three-component magnetometer during the MR06-04 cruise from Sekinehama on 31st July 2006 to Sekinehama on 29th September 2006, and called at ports Kushiro on 20th - 21st August, except for the EEZ of Russia and territorial waters of U.S.A.

(3) Parameters

Three-component magnetic force [nT]
Ship's attitude [1/100 deg]

(4) Instruments on R/V MIRAI

A shipboard three-component magnetometer system (Tierra Tecnica SFG1214) is equipped on-board *R/V MIRAI*. Three-axes flux-gate sensors with ring-cored coils are fixed on the fore mast. Outputs of the sensors are digitized by a 20-bit A/D converter (1 nT/LSB), and sampled at 8 times per second. Ship's heading, pitch, and roll are measured utilizing a ring-laser gyro installed for controlling attitude of the Doppler radar Vertical Reference Unit (VRU). Ship's position (GPS) and speed data (COG) are taken from LAN every second.

(5) Preliminary Results

The results will be published after primary processing.

(6) Data Archives

Magnetic force data obtained during this cruise will be submitted to the JAMSTEC Data Management Division, and archived there.

(7) Remarks

1) We did not collect data in EEZ of Russia.
9 Aug. 00:56 UTC - 10 Aug. 04:37 UTC
16 Aug. 02:00 UTC - 17 Aug. 15:11 UTC

2) We did not collect data in territorial waters of U.S.A.
28 Aug. 14:00 UTC - 28 Aug. 19:10 UTC
30 Aug. 19:20 UTC - 30 Aug. 21:15 UTC
7 Sep. 00:20 UTC - 7 Sep. 02:45 UTC
19 Sep. 14:50 UTC - 19 Sep. 20:30 UTC

3) The following period, we did not collect data due to logging error.
17 Sep. 11:12:21 UTC - 17 Sep. 12:40:57 UTC

4) The following period, we did not collect data due to operation trouble.

17 Sep. 18:06:28 UTC - 17 Sep. 18:07:21 UTC

5) The following period, we used No.1 gyrocompass. (We usually used No.2 gyrocompass for this cruise.)

5 Sep. 09:54:51 UTC - 5 Sep. 12:07:01 UTC

6) For calibration of the ship's magnetic effect, we steered ship a pair of clockwise and anticlockwise rotation. The periods were follows;

4 Aug. 09:38 UTC - 10:01 UTC
6 Aug. 11:32 UTC - 11:53 UTC
8 Aug. 08:36 UTC - 08:55 UTC
11 Aug. 06:36 UTC - 06:56 UTC
15 Aug. 12:32 UTC - 12:58 UTC
23 Aug. 07:02 UTC - 07:23 UTC
27 Aug. 21:16 UTC - 21:37 UTC
1 Sep. 05:24 UTC - 05:47 UTC
2 Sep. 03:52 UTC - 04:11 UTC
4 Sep. 14:56 UTC - 15:15 UTC
5 Sep. 14:41 UTC - 15:03 UTC
8 Sep. 02:59 UTC - 03:20 UTC
12 Sep. 01:00 UTC - 01:24 UTC
14 Sep. 14:41 UTC - 15:04 UTC

7) The following period, ship's navigation data were invalid;

25 Aug. 08:31:04 UTC - 25 Aug. 08:31:16 UTC
25 Aug. 08:43:42 UTC - 25 Aug. 08:48:52 UTC
26 Aug. 08:43:23 UTC - 26 Aug. 08:46:37 UTC
28 Aug. 12:10:03UTC - 28 Aug. 12:10:09 UTC
29 Aug. 08:14:45 UTC - 29 Aug. 08:14:55 UTC
29 Aug. 08:15:29 UTC - 25 Aug. 08:16:07 UTC
29 Aug. 08:16:33 UTC - 29 Aug. 08:17:05 UTC
29 Aug. 08:18:19 UTC - 25 Aug. 08:18:33 UTC
29 Aug. 08:19:21 UTC - 29 Aug. 08:30:49 UTC
8 Sep. 22:27:38 UTC - 8 Sep. 22:38:15 UTC
9 Sep. 22:23:36 UTC - 9 Sep. 22:30:09 UTC

6.9.3 Swath Bathymetry

(1) Personnel

Takeshi Matsumoto (University of the Ryukyus) : Principal Investigator (Not on-board)
Satoshi Okumura (Global Ocean Development Inc. GODI) - Leg1 -
Souichiro Sueyoshi (GODI) - Leg1 -
Kazuho Yoshida (GODI) - Leg1, 2 -
Kazuya Yamashita (GODI) - Leg1 -
Shin'ya Okumura (GODI) - Leg2 -
Wataru Tokunaga (GODI) - Leg2 -
Ryo Ohyama (GODI) - Leg2 -

(2) Introduction

R/V MIRAI equipped a Multi Narrow Beam Echo Sounding system (MNBES), SEABEAM 2112.004 (SeaBeam Instruments Inc.). Sub Bottom Profiler (SBP) is an add-on option to the "SEABEAM 2100". SBP subsystem collects vertical sediments information.

The major objective of MNBES is site survey so that we have gathered necessary bathymetric and sub-sediment information around the core sampling points (see, 6.8.1 Site survey observation description). And also, the other objective is collecting continuous bathymetry data along ship's track to make a contribution to geological and geophysical investigations and global datasets.

(3) Data Acquisition

The "SEABEAM 2100" on R/V MIRAI was used for bathymetry mapping during the this cruise from Hachinohe on 1st August 2006 to Hachinohe on 28th September 2006, and called at ports Kushiro on 20th - 21st August, except for the EEZ of Russia and territorial waters of U.S.A.

To get accurate sound velocity of water column for ray-path correction of acoustic multibeam, we used Surface Sound Velocimeter (SSV) data at the surface (6.2m) sound velocity, and the others depth sound velocity calculated temperature and salinity profiles from XBT, XCTD and CTD data by the equation in Mackenzie (1981) during the cruise.

Table 6.9.3-1 listed system configuration and performance of SEABEAM 2112.004 system and SBP subsystem.

Table 6.9.3.1 System configuration and performance

SEABEAM 2112.004 (12kHz system)

Frequency:	12 kHz
Transmit beam width:	2 degree
Transmit power:	20 kW
Transmit pulse length:	3 to 20 msec.
Depth range:	100 to 11,000 m
Beam spacing:	1 degree athwart ship
Swath width:	150 degree (max) 120 degree to 4,500 m 100 degree to 6,000 m 90 degree to 11,000 m
Depth accuracy:	Within < 0.5% of depth or +/-1m, whichever is greater, over the entire swath. (Nadir beam has greater accuracy; typically within < 0.2% of depth or +/-1m, whichever is greater)

Sub-Bottom Profiler (4kHz system)

Frequency:	4 kHz
Transmit beam width:	5 degree
Sweep:	5 to 100 msec
Depth Penetration:	As much as 75 m (varies with bottom composition)
Resolution of sediments:	Under most condition within < tens-of-centimeters range (dependent upon depth and sediment type)

(4) Preliminary Results

The results will be published after primary processing.

(5) Data Archives

Bathymetry data obtained during this cruise will be submitted to the JAMSTEC and archived there.

(6) Remarks

We did not collect the data in the EEZ of Russia and territorial waters of U.S.A. as following terms.

01:13UTC, 09 Aug. - 04:40UTC, 10 Aug. (Russia EEZ)
02:00UTC, 16 Aug. - 15:17UTC, 18 Aug. (Russia EEZ)
14:00UTC - 19:10UTC, 28 Aug. (USA, territorial waters)
19:00UTC - 21:15UTC, 30 Aug. (USA, territorial waters)
00:20UTC - 02:45UTC, 07 Sep. (USA, territorial waters)
14:50UTC - 20:30UTC, 19 Sep. (USA, territorial waters)

GPS navigation data (Positions, SOG and COG) was invalid as following terms.

08:31:04UTC - 08:31:16UTC, 25 Aug.
08:43:42UTC - 08:48:52UTC, 25 Aug.
08:43:23UTC - 08:46:37UTC, 26 Aug.
12:10:03UTC - 12:10:09UTC, 28 Aug.
08:14:45UTC - 08:14:55UTC, 29 Aug.
08:15:29UTC - 08:16:07UTC, 29 Aug.
08:16:33UTC - 08:17:05UTC, 29 Aug.
08:18:19UTC - 08:18:33UTC, 29 Aug.
08:19:21UTC - 08:30:49UTC, 29 Aug.
22:27:38UTC - 22:38:15UTC, 08 Sep.
22:23:36UTC - 22:30:09UTC, 09 Sep.

6.10 Analytical plan on land

6.10.1 Past variations in the origin and grain size of detrital materials in the Bering and Chukchi Seas sediments and those association with atmospheric/ocean circulations.

(1) Personnel

Kana Nagashima（IORGC, JAMSTEC）

(2) Objectives of this study

Detrital materials in the sea sediments contain the information of both on land and in the ocean. Flux of detrital materials in the sediments derived from continental shelf seems to reflect the amount of river discharge, which may relate to the precipitation on land. Whereas the origin and grain size of detrital materials in the deep sea sediments mostly reflect direction and speed of bottom current of the ocean. Based on those ideas, our main purposes are as follows.

1) Examine the origin of North Pacific Intermediate Water (NPIW) during last glacial period through the grain size and origin of detrital materials in the depth-transect deep sea sediments recovered from the Bering Sea in order to reconstruct past variation in ocean circulation at North Pacific.

2) Reconstruct near-past variations in Yukon River discharge through the spatial distribution of detrital materials of Yukon River origin and its temporal variations using the sediments recovered from the Bering Sea in order to examine the variation of weather on land during the last several decades.

3) Examine the relative influx change of Pacific Summer Water (PSW; Coachman et al., 1975) to the Chukchi Sea during the last several decades based on the comparison of the origin and flux of detrital materials in the sediments recovered from the Chukchi Sea with those of the Bering Sea in order to examine the relationship between the water current from the North Pacific Ocean to the Arctic Ocean and sea ice distribution in the Arctic Ocean.

(3) Provenance study and grain size analysis

For the provenance study of detrital materials in the Bering/Chukchi Sea sediments, we will measure mineral and major element compositions of detrital materials in the samples of Bering/ Chukchi Sea sediments with XRD and XRF microscanner (Kido et al., 2006), respectively, and measure ESR (Electron Spin Resonance) signal intensity and crystallinity of quartz in the detrital materials with an X-band ESR spectrometer (JEOL, PX-2300) and XRD. Moreover, we will measure grain size distributions of detrital materials in the samples of those sea sediments using laser-diffraction-scattering grain size analyzer (Horiba LA-920).

6.10.2 Late Quaternary diatom taxonomy of Sea of Okhotsk, Chukchi Sea and Bering Sea sediments

(1) Personnel

Susumu Konno, Richard W. Jordan (Dept. of Earth & Environmental Sciences, Faculty of Science, Yamagata University)

(2) Objectives

The main aims of this project are to:

1) prepare a diatom catalogue (identification guide) for publication and laboratory use,

2) provide taxonomic support to those scientists working on palaeoenvironmental reconstruction.

(3) Methods

Sediment samples from piston, gravity and multiple cores intended for palaeoenvironmental reconstruction were subsampled for taxonomic studies. These samples will be acid-cleaned and prepared for LM and SEM observations using standard methodologies. Mountmedia-prepared slides will be observed with a Nikon Optiphot2-pol polarizing light microscope, while material mounted on aluminium EM stubs will be observed in a Hitachi S-2250N SEM. Specimens will be photographed using camera attachments.

6.10.3 Productivity changes during warming periods in the Okhotsk and Bering Seas

(1) Personnel

Yusuke Okazaki (IORGC, JAMSTEC)

Naomi Harada (IORGC, JAMSTEC)

(2) Objectives

In order to reconstruct productivity changes during warming periods in the late Quaternary in the Okhotsk and Bering Seas, We are planning to utilize following proxies in sediment cores: biogenic opal, total organic carbon (TOC), $CaCO_3$, $\delta^{13}C$, $\delta^{15}N$, diatom assemblages, and radiolarian assemblages. In particular, We have an interest in three warming periods with different timescale, i.e., (1) last 100 kyrs, (2) last deglaciation, and (3) past warm periods (marine isotope stages (MIS) 5e, 9, and 11).

2-1 last 100 kyrs (decadal variation)

Geochemical analysis (biogenic opal, TOC, $CaCO_3$, $\delta^{13}C$, $\delta^{15}N$) will be performed from thirteen multiple cores (Stations 18, 19, 20, 21, 22, 26, 27, 28, 29, 30, 31, 32 and 33) and one gravity core (Station 33) in eastern continental shelves of the Bering Sea. The aim of this work is to clarify recent productivity changes in decadal (e.g., Pacific Decadal Oscillation, Arctic Oscillation) timescales. We will collaborate with Drs. Itaki (radiolarians), Katsuki and Jordan (diatoms) to discuss plankton succession during the past 100 kyrs.

2-2 last deglaciation (centurial to millennial variation)

We will reconstruct centurial to millennial changes in productivity in the southwestern Okhotsk Sea based on geochemical parameters (biogenic opal, TOC, $CaCO_3$, $\delta^{13}C$, $\delta^{15}N$) and siliceous microplanktons (diatoms, radiolarians). Two piston cores obtained from the southern Okhotsk Sea (Station 4) will be appropriate for the purpose because of their estimated high sedimentation rates (~100 cm/kyr). Previous studies indicated that pronounced productivity increase event during the last deglaciation in the Okhotsk Sea (Seki et al., 2004; Okazaki et al., 2005). In the present study, we focus on the event and try to reconstruct its detail. In particular, we have an interest in productivity changes relating to submerged continental shelves with sea-level rise. This work will be cooperated with Dr. Jordan (taxonomy of diatom assemblages).

2-3 past warm periods (MIS 5e, 9, and 11)

Little is known about productivity during the interglacials such as MIS 5e, 9 and 11 in the Okhotsk Sea. Bottom ages of three piston cores (Stations 5, 6, and 7) collected in the central Okhotsk Sea were estimated to have reached into MIS 9 and MIS 11. Hence, we try to clarify productivity changes during MIS 5e, 9 and 11 employing geochemical parameters (biogenic opal, TOC, $CaCO_3$, $\delta^{13}C$, $\delta^{15}N$) and

siliceous microplanktons (diatoms, radiolarians). In the Okhotsk Sea, notable plankton succession was reported from the last glacial to the Holocene, i.e., (1) low productivity during the last glacial, (2) abundant coccolithophorids and intermediate water dwelling radiolarians during the last deglaciation, (3) abundant diatoms and subsurface dwelling radiolarians during the Holocene (Seki et al., 2004; Okazaki et al., 2005). We will investigate whether such kind of plankton successions were occurred or not during the past deglaciation events.

(3) List of analytical items in PC, GC and MC cores

PC03: diatoms

PC04: Opal, TOC, $CaCO_3$, $\delta^{13}C$, $\delta^{15}N$, diatoms, radiolarians

PC05: diatoms, radiolarians

PC06: Opal, TOC, $CaCO_3$, $\delta^{13}C$, $\delta^{15}N$, diatoms, radiolarians

PC07: Opal, TOC, $CaCO_3$, $\delta^{13}C$, $\delta^{15}N$, diatoms, radiolarians

GC33: Opal, TOC, $CaCO_3$, $\delta^{13}C$, $\delta^{15}N$

MC03: diatoms

MC04, MC06, MC07: TOC, $CaCO_3$, $\delta^{13}C$, $\delta^{15}N$, diatoms, radiolarians

MC05: diatoms, radiolarians

MC18, MC19, MC20, MC 21, MC 22, MC 26, MC 27, MC 28, MC 29, MC 30, MC 31, MC 32, MC 33: Opal, TOC, $CaCO_3$, $\delta^{13}C$, $\delta^{15}N$

(4) References

Okazaki, Y., K. Takahashi, K. Katsuki, A. Ono, J. Hori, T. Sakamoto, M. Uchida, Y. Shibata, M. Ikehara, and K. Aoki, Late Quaternary paleoceanographic changes in the southwestern part of the Okhotsk Sea: Based on analyses of geochemical, radiolarian, and diatom records, *Deep-Sea Research II* 52, 2332-2350, 2005.

Seki, O., M. Ikehara, K. Kawamura, T. Nakatsuka, K. Ohnishi, M. Wakatsuchi, H. Narita, and T. Sakamoto, Reconstruction of paleoproductivity in the Sea of Okhotsk over the last 30 kyr, *Paleoceanography* 19, PA1016, 2004

6.10.4 Reconstruction of the late Quaternary East Asian monsoon fluctuations

(1) Personnel

Ikehara, K. (Geological Survey of Japan, AIST)

Itaki, T. (University of Tokyo)

Khim, B.K. (Pusan National University, Korea)

Irino, T. (Hokkaido University)

Usami, K. (Kumamoto University)

(2) Objectives

Paleoenvironments of the Japan Sea have been influenced by the glacio-eustatic sea-level changes with 100-kys time-scale and the East Asian monsoonal climate changes with millennial time-scale. Furthermore, deep-sea sediments in the northern Japan Sea are thought to record both summer and winter monsoon fluctuations. Our objectives of this study are: (1) to reconstruct the late Quaternary paleoenvironmental changes in the northern Japan Sea, especially histories of seasonal sea-ice, and deep-water ventilation, and their relation to surface water environmental changes, and (2) to understand the late Quaternary East Asian summer and winter monsoon fluctuations and their relation to global climate changes.

(3) Analytical items

Sea-ice history: Ice-rafted debris, Deep-water ventilation: radiolarian and benthic foraminifera assemblages, Surface water properties: TOC, stable isotopes of organic matters, planktonic foraminifera and radiolarian assemblages, Mg/Ca ratio of planktonic foraminifera

6.10.5 Paleoceanographic reconstruction on the basis of siliceous microplankton assemblages from the Chukchi and the eastern Bering Seas

(1) Personnel

Kota Katsuki[1], Kozo Takahashi[2], Seiji Tanaka[2], and Jonaotaro Onodera[2]

1. Shimane University, Research Center for Coastal Lagoon Environments
2. Kyushu University, Graduate School of Sciences, Department of Earth and Planetary Science

(2) Objectives

Understanding the past global environment is essential for understanding the present global one. However, accumulation of the knowledge on the past environment is not sufficient enough in some areas of the earth such as the Arctic Ocean. Thus, the purpose of this research is to clarify the past environment of the Arctic Ocean and the marginal Sea. Toward this end, this study covers the following three objectives. The first one is to examine the effect of short-term climate cycle on the Arctic Ocean and the marginal Sea environment during the late Quaternary, in particular the Holocene. The second one is to clarify the impact of world wide human activity on global warming. Therefore, the high resolution analysis will be done over about the past several hundred years based on gravity and multiple cores analysis. These paleoenvironmental reconstructions will be carried out by the analysis of siliceous microplanktons such as diatom, radiolarian, and silicoflagellate assemblages. Siliceous microplanktons are well preserved in sediment than other microplanktons. Diatom and silicoflagellate are primary producers, which provide an useful information for understanding paleo-condition of sea surface environment. Radiolarians are siliceous microzooplankton, which inhabits various depths of the water column and exhibits high diversity. Therefore, radiolarian assemblages are useful environmental tracers, especially for intermediate water masses. The third purpose is to shed light on the relationship between the duration of sea-ice cover and the distribution of each siliceous microplankton. The data from siliceous microplankton assemblages in these areas give us information about their ecology and paleoenviromental changes during the late Quaternary.

(3) Measure Parameters

Diatom (Paleoenvironment) and silicoflagellate assemblages will be observed as follows: 14 multiple core sites (MC-12, 12 EX, 13, 14, 15, 16, 17, 18, 19, 20, 28, 29, 32, and 33), five gravity core sites (GC-12EX, 13, 14, and 16, 33), and three piston core sites (PC-23, 24, and 25). Radiolarian assemblage will be measured as follows: seven multiple core sites (MC-12, 12 EX, 13, 14, 15, 16, and 17), and four gravity core sites (GC-12EX, 13, 14, and 16) (Fig, 6.10.5.1).

(4) Samples and Methods

Sediment samples were continuously sliced every 2.2 cm in thickness throughout the core on

board, and we got about 5 cc sediment samples for analysis of siliceous microplankton assemblages. For diatom and silicoflagellate analysis, a freeze dried sample (2-5 mg) will be weighed and placed in a 200 ml beaker containing a hydrogen peroxide solution (10%, 20 m*l*) and hydrochloric acid (1-N, 3 m*l*), and heated on a hot plate for one hour. After the manipulation, Calgon® (hexametaphosphate, surfactant) solution will be added to the mixtures in order to disaggregate the sediments. The sample will be then filtered through a Gelman® membrane filter of 47 mm in diameter with a nominal pore size of 0.45 μm, rinsed with distilled water to remove salt, and dried in an oven overnight. The dried filter samples will be permanently mounted on microslides with Canada Balsam. For radiolarian analysis, freeze dried samples of 100 mg will be weighed. The procedure used for diatom and silicoflagellate will be applied to radiolarian sample processing, except that the size fraction should be carried out in the latter process. Each sample will be sieved through a stainless screen with 45 μm mesh before passed through a Gelman® membrane filter. Each sample will be permanently mounted on microslide with Canada Balsam. Observation under a light microscope will be conducted at least 300 shells per one sample.

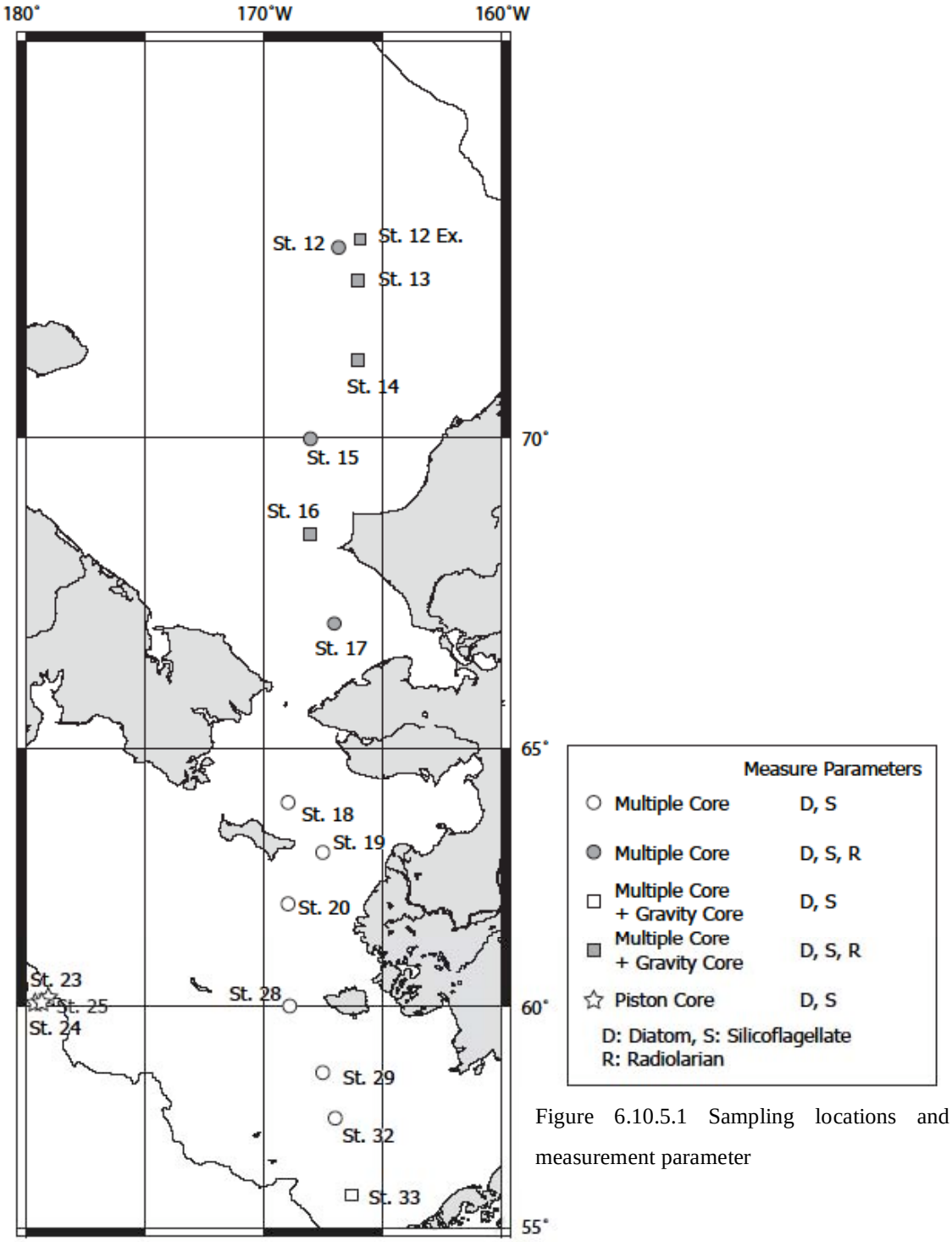

Figure 6.10.5.1 Sampling locations and measurement parameter

6.10.6 Provenance analysis by radiogenic isotopes of strontium and neodymium of core sediments in the Bering Strait and the Okhotsk Sea and paleoenvironmental reconstruction during the past 100 kyr

(1) Personnel

Fumi Takeuchi (Nagoya University)

Yoshihiro Asahara (Nagoya University)

(2) Objectives

Radiogenic isotopes such as strontium (Sr) and neodymium (Nd) in detritus of a marine sediment are useful tracers for identifying the geographical provenance of the detritus, and are the clue to reconstruct the atmosphere and ocean circulation (e.g. Dasch, 1969; Grousset et al., 1988; Nakai et al., 1993; Jones et al., 1994; Asahara et al., 1999). In this study, Sr and Nd isotopes of detrital fractions (silicate) in core sediments of the Bering Strait and the Okhotsk Sea will be investigated in order to reconstruct paleoenvironment in the high-latitude and Arctic area. Source region and flux of the terrigenous material in the Bering Strait and the Okhotsk Sea at the present day will be estimated by Sr and Nd isotopes of surface layers in core sediments. Then temporal changes of Sr and Nd isotopes of the terrigenous material in core sediments during the past 100 kyr will be investigated. Main focus is on isotopic characteristics during glacial and interglacial periods. Especially, the changes of material transport between the Chukchi Sea and the Bering Sea during glacial and interglacial periods will be compared. Dominant sources of the terrigenous materials in the Bering Sea and the Okhotsk Sea are the Yukon river and the Amur river, and the terrigenous material will also provide information on environment in the continents, Alaska and eastern Siberia.

Sediments from multiple cores, piston cores and gravity cores will be used for the analysis, which were obtained during the MR06-04 cruise of the R/V MIRAI from August to September 2006. Sediment samples were continuously sliced at every 1.0 cm (multiple core) or 2.2 cm (piston core and gravity core) in thickness throughout the cores on board, and 1 to 5g of sediment for each slice was taken for the isotopic analysis. On land, firstly, extraction procedure of detrital fractions in the sediments by chemical leaching will be established. In this study, extraction procedure aimed at ESR (electron spin resonance) analysis of detrital fractions in sediments will be applied in order to compare the Sr and Nd isotope data with ESR data. A combination of the radiogenic isotope data and the ESR data will get more detailed information on geographical provenance of the detritus and its transport process. Chemical preparation and isotopic measurement of Sr and Nd have already been set up at Nagoya University, Japan (Asahara et al., 1999). The Sr and Nd isotopes ($^{87}Sr/^{86}Sr$, $^{143}Nd/^{144}Nd$) for the samples will be measured by a sector-type thermal ionization mass spectrometer (VG Sector 54-30, GVI IsoProbe-T) at Nagoya University, Japan.

(3) References

Asahara, Y., Tanaka, T., Kamioka, H., Nishimura, A., Yamazaki, T., 1999. Provenance of the north Pacific sediments and process of source material transport as derived from Rb-Sr isotope systematics. Chem.Geol. 158, 271-291.

Dasch, E.J., 1969. Strontium isotopes in weathering profiles, deep sea sediments and sedimentary rocks. Geochim.Cosmochim.Acta 33, 1521-1552.

Grousset, F.E., Biscaye, P.E., Zindler, A., Prospero, J., Chester, R., 1988. Neodymium isotopes as tracers in marine sediments and aerosols: North Atlantic. Earth Planet. Sci. Lett. 87, 367-378.

Jones, C.E., Halliday, A.N., Rea, D.K., Owen, R.M., 1994. Neodymium isotopic variations in north Pacific modern silicate sediment and the insignificance of detrital REE contributions to seawater. Earth Planet. Sci. Lett. 127, 55-66.

Nakai, S., Halliday, A.N., Rea, D.K., 1993. Provenance of dust in the Pacific Ocean. Earth Planet. Sci. Lett. 119, 143-157.

6.10.7 Paleomagnetic and rock-magnetic study on sediment cores

(1) Personnel

Toshitsugu Yamazaki (Geological Survey of Japan, AIST)
Seiko Inoue (Graduate School of Life and Environmental Sciences, Tsukuba University)
Noriko Kawamura (Graduate school of human and environmental studies, Kyoto University)

(2) Objectives

A paleomagnetic and rock-magnetic study will be conducted on sediment cores taken by a piston corer and a multiple corer during the MR06-04 cruise. The purposes of the study is the following (2-1) and (2-2) for piston cores, and (2-3) for multiple cores.

2-1 High-resolution chronostratigraphy

Recent progress of relative paleointensity estimation from sediments has brought an important application as a high-resolution dating tool for marine sediments. Paleointensity variations are globally synchronous for a dipole component, and their resolution can be on the order of 1000 years in an ideal case, which is higher than the oxygen isotope stratigraphy. If relative paleointensity can be recovered successfully from the sediment cores of this cruise, it should be quite useful for inter-core correlation within and between the Okhotsk Sea and Bering Sea, and also for correlation with available records in other regions in the world including the Northwest Pacific, equatorial Pacific, and North Atlantic. The paleointensity-assisted stratigraphy would contribute to understand leads and lags of paleoclimatic events in different regions and a teleconnection of climatic changes.

2-2 Evaluation of the effect of lithological changes to paleointensity estimation

Recently, a possibility of the orbital forcing of the geomagnetic field has been argued among paleomagnetists. Occurrence of the Milankovitch orbital frequencies, ~40 kyr obliquity and ~100 kyr eccentricity, has been reported from paleointensity and inclination records. An argument against the orbital forcing hypothesis is that such orbital frequencies are artifact caused by contamination from paleoclimatically induced lithological changes of sediments; magnetic (and even non-magnetic) property changes of sediments might affect relative paleointensity estimation. To solve the problem, it is necessary to accumulate paleointensity records from sediments of various lithologies. In this purpose, the Okhotsk Sea is particularly important, because it belongs to a paleoceanographic regime quite different from the nearby Northwest Pacific; for example, biological productivity is higher at glacial-to-interglacial transitions and earliest interglacials in the Okhotsk Sea, whereas it is higher in glacials in the Northwest Pacific. On the other hand, paleointensity variations should be almost the same between the two regions

because they are nearby and effects of the non-dipole components should be similar. We will compare in detail paleointensity and magnetic properties of the Okhotsk Sea with those of the Northwest Pacific, where a regional paleointensity curve has already been established by our group.

2-3 Rock-magnetic changes during early diagenesis

Surface sediments, in particular those under high productivity provinces, are geochemically active, and magnetic properties can change during early diagenesis. To understand in detail the process of the rock magnetic changes has been an important topic for environmental rock magnetism, and it is also important to enhance reliability of paleomagnetic records. Using surface sediments taken by a multiple corer, we aim to reveal rock-magnetic processes together with geochemistry of sediments and interstitial waters including onboard measurements of pH, Eh, and dissolved oxygen.

For all three purposes mentioned above, we will carry out a suite of paleomagnetic and rock magnetic analyses including anisotropy of magnetic susceptibility, NRM (natural remanent magnetization) measurements, stepwise alternating-field demagnetization, ARM (anhysteretic remanent magnetization) and IRM (iso-thermal remanent magnetization) acquisition experiments, magnetic hysteresis measurements, and high- and low-temperature magnetic property measurements.

6.10.8 Foraminiferal assemblage analysis

(1) Personnel

Ken'ichi Ohkushi, Institute of Geology and Geoinformation, National Institute of Advanced Industrial Science and Technology (AIST), Tsukuba 305-8567, Japan

(2) Objectives

MR04-06 Leg. 1

To reconstruct millennial-scaled changes in intermediate water oxygenation off north Japan, last glacial – Holocene benthic foraminiferal assemblages will be analyzed in piston core samples taken from MR06-04 stations 1&2.

MR04-06 Leg. 2

To reconstruct millennial-scaled changes in intermediate water oxygenation in the Bering Sea, last glacial – Holocene benthic foraminiferal assemblages will be analyzed in piston core samples taken from MR06-04 stations 23&24.

(3) Measured parameters

Foraminiferal fossil assemblages

6.10.9 Paleoceanographic and geochemical studies at the western North Pacific, Bering Sea, and Arctic Ocean: Case studies regarding application and developments of geochemical multi proxies to marine sediments

(1) Personnel
Masao Uchida (IORGC, JAMSTEC)

(2) Backgrounds and Objectives of the Study

Now we know that the high latitude regions in the Northern Hemisphere is very sensitive to global climate change. Thus it is urgent research matter for us to know detailed mechanism of the natural variations in past marine environment, as well as terrestrial environment in this region. In this study, we are planning to apply the various geochemical proxies to marine sediments collected from the western North Pacific, Bering Sea, and the Arctic Ocean in order to reconstruct the past marine environment in these high latitude regions, which provide very important information to predict the environmental changes associated with human activity. Additionally, various novel geochemical proxies are applied to marine sediments in order to enhance the precision of our interpretation regarding limited dataset of routine analysis.

The analyses used for reconstruction for past ocean environment and novel proxy developments in this study are listed as below,

1) Sea surface temperature (SST): alkenone, TEX86

2) Past ocean circulation: Stable carbon and radiocarbon isotopic analysis of foraminiferal fossil carbonate.

3) Early diagenesis and microbial alteration of organic carbon in the marine sediment: Molecular biomarkers composition and their isotopic analysis of microbial lipids.

4) Source apportioning of organic carbon to marine sediments: Compound-specific isotopic analysis of organic carbon derived from marine and terrestrial organisms.

5) Climatically-driven methane hydrate dissociation events in the last deglaciation and glacial ages: Stable carbon isotopic analysis of planktonic and benthic foraminifera.

(3) Samples

Tables 6.10.9.1, 6.10.9.2, 6.10.9.3 and 6.10.9.4 list samples collected during MR06-04 leg.1 and, 2 cruise of R/V Mirai by using multiple core sampler, pilot core sampler attached to gravity or piston core samplers, gravity core sampler, and piston core samplers respectively. Surface sediment cores will be used for reconstructing relatively recent history of combustions and terrestrial environment. Gravity and piston cores will be used for the same purpose but designated for reconstructing paleo environment.

All the multiple- and the pilot-core samples were sliced into sections with thickness of approximately 1.0 cm on board. Top 5 cm sections were stored in screw capped glass vials which were precombusted at 450°C for 12 hours, and sections below 5 cm depth were stored in plastic bags. Immediately after the sectioning, the multiple- and the pilot-core samples were frozen.

The gravity- and piston-core samples were cut into sections with 1 m depth interval immediately after sampling. Each section was vertically divided into two aliquots after 24 hours equilibration to room temperature, visual core description was performed for both aliquots, and then frozen without further subsampling/subsectioning. Only the exception is GC-33, which was sliced into subsections with thickness of approximately 2.2 cm on board and a quarter portion of each subsections was subsampled.

Table 6.10.9.1 Surface sediments collected with multiple core sampler during MR06-04 Leg.1,2 cruise

Date (mmddyy)	Core ID	Location	Lat.	Lon.	Depth(m)	HAND No.	Core length(m)*	Remarks
08.03.06	MC-01	Off Tokachi	42-30.59	144-19.64	994	HAND1	29.2	
						HAND2	29.5	
						HAND3	9.8	Catch a organisms(Brittle star?)
						HAND4	29.0	
08.04.06	MC-02	Off Tokachi	41-52.01	143-56.98	1,044	HAND1	28.6	
						HAND2	8.4	Catch a organisms(Brittle star?)
						HAND3	28.9(28.9)	
						HAND4	28.8	
08.31.06	MC-15-A	Arctic Ocean	69-59.99N	168-00.01W	48	HAND1	19.6	
						HAND2	17.8	only sections >10cm depth were sampled
						HAND5	17.6	
						HAND6	19.2	
08.31.06	MC-15-B	Arctic Ocean	70-00.01N	168.00.05W	48	HAND1	18.9	
						HAND2	19.0	
						HAND3	19.3	
						HAND4	19.6	
						HAND5	17.8	
						HAND6	18.9	
						HAND7	20.3	
						HAND8	20.4	
08.31.06	MC-14-A	Arctic Ocean	70-59.98N	165-59.85W	43	HAND1	20.7	
						HAND5	20.4	
						HAND6	20.0	
09.01.06	MC-14-B	Arctic Ocean	70-59.98N	165-59.94W	43	HAND2	20.1	
						HAND3	18.4	
						HAND4	18.4	
						HAND5	17.7	
						HAND6	18.7	
						HAND7	20.9	
						HAND8	19.4	
09.01.06	MC-13-A	Arctic Ocean	72-00.04N	165-59.97W	46	HAND1	25.8	
						HAND2	26.3	only sections >10cm depth were sampled
						HAND5	26.6	
						HAND6	26.0	
09.02.06	MC-12EX-A	Arctic Ocean	72-35.99N	166-00.04W	53	HAND1	31.5	
						HAND2	30.8	only sections >10cm depth were sampled
						HAND6	31.2	
09.02.06	MC-12EX-B	Arctic Ocean	72-36.02N	165-59.94W	53	HAND1	31.9	
						HAND2	35.1	
						HAND3	35.1	
						HAND4	34.2	
						HAND5	34.3	
						HAND6	34.1	
						HAND7	36.2	
						HAND8	34.5	
09.02.06	MC-13-B	Arctic Ocean	72-00.01N	165-60.00W	46	HAND1	23.4	
						HAND3	23.0	
						HAND4	22.7	
						HAND5	23.2	
						HAND6	23.8	
						HAND7	23.5	
						HAND8	23.6	
09.03.06	MC-12-A	Arctic Ocean	72-25.93N	166-57.85W	51	HAND1	22.2	
						HAND2	23.2	only sections >10cm depth were sampled
						HAND6	20.4	
09.05.06	MC-16-A	Arctic Ocean	68-30.03N	167-59.95W	54	HAND1	23.4	1/2 portion of each sections was subsampled
						HAND6	24.9	
09.05.06	MC-16-B	Arctic Ocean	68-29.99N	167-59.96W	55	HAND1	25.9	
						HAND2	25.3	
						HAND3	27.6	
						HAND4	25.7	
						HAND5	25.3	
						HAND6	24.3	
						HAND7	25.8	
						HAND8	24.6	
09.06.06	MC-17-A	Arctic Ocean	66-59.99N	166-59.95W	40	HAND1	26.5	
						HAND2	27.5	only sections >10cm depth were sampled
						HAND5	25.0	
						HAND6	24.3	
09.07.06	MC-19-A	Bering Sea	63-00.02N	167-29.94W	33	HAND2	20.2	
09.07.06	MC-19-B	Bering Sea	62-59.99N	167-30.01W	33	HAND1	23.4	1/2 portion of each sections was subsampled
						HAND2	24.1	
						HAND3	22.5	Small crab on the sediment
						HAND4	24.3	
						HAND5	21.8	
						HAND6	22.6	
						HAND7	24.5	
						HAND8	23.6	Small crab on the sediment

Table 6.10.9.1 (*Continued*)

Date (mmddyy)	Core ID	Location	Lat.	Lon.	Depth(m)	HAND No.	Core length(m)*	Remarks
09.08.06	MC-20-A	Bering Sea	62-00.02N	169-00.44W	37	HAND2	19.6	1/2 portion of each sections was subsampled
09.08.06	MC-20-B	Bering Sea	62-00.08N	168-59.92W	37	HAND1	17.4	
						HAND2	16.8	
						HAND3	16.6	
						HAND4	18.2	
						HAND5	17.2	
						HAND6	17.1	
						HAND7	17.4	
						HAND8	16.8	
09.10.06	MC-23-A	Bering Sea	60-09.52N	179-27.80W	1,004	HAND2	21.9	
						HAND4	22.4	
						HAND8	22.1	only sections >10cm depth were sampled
09.10.06	MC-23-B	Bering Sea	60-09.53N	179-27.86W	1,000	HAND1	22.4	
						HAND2	21.8	
						HAND3	20.7	
						HAND4	22.4	
						HAND5	22.3	
						HAND6	20.7	
						HAND7	20.9	
						HAND8	19.6	
09.11.06	MC-24-A	Bering Sea	60-15.70N	179-25.34W	851	HAND2	20.4	
						HAND4	16.9	
						HAND8	18.7	only sections >10cm depth were sampled
09.11.06	MC-24-B	Bering Sea	60-15.70N	179-25.35W	851	HAND1	21.4	
						HAND2	21.5	
						HAND3	21.5	Catch a organisms
						HAND4	21.3	
						HAND5	19.8	
						HAND6	21.4	Catch a organisms
						HAND7	20.9	
						HAND8	21.3	
09.12.06	MC-25-A	Bering Sea	60-04.49N	179-27.79W	1,158	HAND5	19.1	
						HAND8	18.3	only sections >10cm depth were sampled
09.12.06	MC-25-B	Bering Sea	60-04.50N	179-27.75W	1,158	HAND1	20.5	
						HAND2	20.4	
						HAND3	19.7	
						HAND4	20.7	
						HAND5	20.0	
						HAND6	18.9	
						HAND7	17.2	
						HAND8	18.8	
09.14.06	MC-29-A	Bering Sea	58-30.00N	167-30.04W	51	HAND8	16.8	1/2 portion of each sections was subsampled
09.14.06	MC-29-B	Bering Sea	58-29.99N	167-30.03W	51	HAND1	16.2(16.0)	
						HAND3	15.3	
						HAND4	15.9	
						HAND5	17.5	
						HAND6	18.5	
						HAND7	16.8	sectioning was failed and taken as a grab sample
						HAND8	16.4	
09.17.06	MC-33-A	Bering Sea	55-46.42N	166-13.59W	130	HAND7	28.7(30.0)	1/4 portion of each sections was subsampled

*Core length is measure on deck. Parenthetic core length is measure in laboratory(description) or dark room(sampling).

Table 6.10.9.2 Surface sediments collected with pilot core sampler attached to gravity- or piston-core samplers during MR06-04 Leg.2 cruise

Date (mmddyy)	Core ID	Location	Lat.	Lon.	Depth (m)	HAND No.	Core length(m)
09.01.06	PL-14	Arctic Ocean	71-00.01N	166-00.26W	43	HAND2	19.4
						HAND3	15.4
09.10.06	PL-23-A	Bering Sea	60-09.52N	179-27.82W	1002	HAND2	17.1
09.10.06	PL-23-B	Bering Sea	60-09.53N	179-27.82W	1000	HAND2	16.5
						HAND3	17.0
09.11.06	PL-24-A	Bering Sea	60-15.70N	179-25.34W	852	HAND3	12.3
09.11.06	PL-24-B	Bering Sea	60-15.70N	179-25.36W	853	HAND3	15.3
09.12.06	PL-25-A	Bering Sea	60-04.48N	179-27.80W	1158	HAND2	17.8
						HAND3	15.6
09.12.06	PL-25-B	Bering Sea	60-04.50N	179-27.78W	1157	HAND3	12.8

*Core length is measured on deck.

Table 6.10.9.3 Core sediments collected with gravity core sampler during MR06-04 Leg.2 cruise

Date (mmddyy)	Core ID	Location	Lat.	Lon.	Depth (m)	Core/Barrel length(m)
09.01.06	GC-14	Arctic Ocean	71-00.01N	166-00.26W	43	0.918/5
09.01.06	GC-13	Arctic Ocean	72-00.00N	166-00.01W	46	1.630/5
09.02.06	GC-12EX	Arctic Ocean	72-36.00N	165-59.97W	53	4.256/5
09.05.06	GC-16	Arctic Ocean	68-29.99N	167-59.99W	54	1.441/5
09.17.06	GC-33	Bering Sea	55-46.41N	166-13.57W	130	1.853/7

Table 6.10.9.4 Core sediments collected with piston core sampler during MR06-04 Leg.2 cruise

Date (mmddyy)	Core ID	Location	Lat.	Lon.	Depth (m)	Core/Barrel length(m)	Piston type*
08.03.06	PC-01-B	Off Tokachi	42-30.59	144-19.71	994	4.016/10	RPP-70*3&50*1
08.04.06	PC-02-B	Off Tokachi	41-52.01	143-56.95	1,043	6.593/10	Short
09.11.06	PC-23-B	Bering Sea	60-09.53N	179-27.82W	1,000	14.308/20	RPP-70*3&50*1
09.12.06	PC-24-B	Bering Sea	60-15.70N	179-25.36W	853	16.732/20	RPP-70*3&50*1
09.13.06	PC-25-B	Bering Sea	60-04.50N	179-27.78W	1,157	14.912/20	RPP-70*3&50*1

*Normal type piston is composing of stainless steel body and O-ring (size: P63). Difference between Normal type and Short type is only length (4.5cm). RPP (Rubber Plate Piston) apply rubber plates (RPP-hardness of plates*number).

6.10.10 Reconstruction of the deposition history of pyrolytic/pyrogenic residues to high latitude marine sediments: Their geochemical consequences in recent/paleo environments?

(1) Personnel

Yasuyo Koike (Tokyo University of Pharmacy and Life Sciences)
Hidetoshi Kumata (Tokyo University of Pharmacy and Life Sciences)
Masao Uchida (IORGC, JAMSTEC)

(2) Backgrounds and Objectives of the Study

Marine sediment accumulate substances from marine, continental and atmospheric environments which can provide an excellent means of evaluating and reconstructing historical changes in the past environment. Combustion of organic materials is recognized as the one most important process that influences the global environment; generating a series of greenhouse gases as well as pyrolytic/pyrogenic residues such as polycyclic aromatic hydrocarbons (PAH), and highly condensed soot carbon (black carbon: BC). Since BC absorbs solar radiation, it has direct and indirect effects on local as well as global climate. BC is biologically and chemically inert, its formation from vegetation fires and wood fuel combustion can be regarded to transfer otherwise rapidly cycling carbon from the atmosphere-biosphere cycle into a much slower cycling geological form. Elucidation of the importance of biomass-BC (or inert carbonaceous materials generated in biomass burning) to atmospheric carbon species and to carbon burial would be essential in understanding global carbon cycling.

The primary objective of this study is to reconstruct the deposition history of pyrolytic/pyrogenic residues (i.e., BC, PAH, and other classes of organic compounds that can serve as tracers for biomass burning) to the sediments from Chukchi and Bering Seas, and to investigate its relation to climatic changes/events as well as to any detectable changes in terrestrial environments of pan Chukchi and/or pan Bering areas. Through the course of this study special emphasis will be made on depicting the importance of presumably inert carbonaceous materials from biomass burning relative to the flux of carbon burial in the study area.

(3) Samples

Tables 6.10.10.1, 6.10.10.2, 6.10.10.3 and 6.10.10.4 list samples collected during MR06-04 leg.2 cruise of R/V Mirai by using multiple core sampler, pilot core sampler attached to gravity or piston core samplers, gravity core sampler, and piston core samplers respectively. Surface sediment cores will be used for reconstructing relatively recent history of combustions and terrestrial environment. Gravity and piston cores will be used for the same purpose but designated for reconstructing paleo environment.

All the multiple- and the pilot-core samples were sliced into sections with thickness of approximately 1.0 cm on board. Top 5 cm sections were stored in screw capped glass vials which were precombusted at 450°C for 12 hours, and sections below 5 cm depth were stored in plastic bags. Immediately after the sectioning, the multiple- and the pilot-core samples were frozen.

The gravity- and piston-core samples were cut into sections with 1 m depth interval immediately after sampling. Each section was vertically divided into two aliquots after 24 hours equilibration to room temperature, visual core description was performed for both aliquots, and then frozen without further subsampling/subsectioning. Only the exception is GC-33, which was sliced into subsections with thickness of approximately 2.2 cm on board and a quarter portion of each subsections was subsampled.

(4) Parameters to be determined

In order to reconstruct deposition history of combustion products to the sediments, BC, PAH, and other classes of organic compounds that can serve as tracers for biomass burning (e.g., lignin phenols, resin diterpenoides, monosaccharides, etc.) will be analyzed. Also, organic tracers from terrestrial environments will be analyzed to investigate relationship between combustion history and changes in the terrestrial environment. Isotopic analysis ($\delta^{13}C$ and $\Delta^{14}C$) will also be conducted for selected samples

that contain enough amount(s) of analyse(s) (i.e., BC and/or PAH). For the purpose of monitoring analytical errors during isolation of BC from bulk organic matter, the contents and stable isotopic composition of total organic carbon and total nitrogen (TOC and TN) will also be determined. Dry bulk density of multiple core samples will be determined in order to make depth of different sub-cores comparable each other.

(5) Instruments and Methods

BC will be analyzed according to CTO375 method by Gustafsson et al. (e.g.,). In Brief, lyophilized sediment sample is finely ground, which then heated at 375°C for 24 hours under continuous flow of air to thermally breakdown biogenic organic matter. After decalcified with 1 M HCl, the resultant refractory fraction of the sediment will be determined for contents of carbon (BC) and nitrogen (BN), $\delta^{13}C$, $\delta^{15}N$ with EA/IRMS.

Lyophilized sediment will be extracted for PAH as well as organic tracers by using dichloromethane (DCM) and/or a mixture of DCM and methanol as solvent(s). A portion of the extract will be used to determine the amount of total extractable organics. The leftover of the extract will be divided into two aliquots. One aliquot will be subjected to SiO_2 column chromatography in order to separate different classes of compounds into fractions, which then analyzed for PAH and neutral organic tracers by using GC/MS. The other aliquot will be stored for future analysis of for example, polar organic tracers from biomass burning.

Table 6.10.10.1 Surface sediments collected with multiple core sampler during MR06-04 Leg.2 cruise

Date (mmddyy)	Core ID	Location	Lat.	Lon.	Depth(m)	HAND No.	Core length(m)*	Remarks
08.31.06	MC-15-A	Arctic Ocean	69-59.99N	168-00.01W	48	HAND1	19.6	
						HAND2	17.8	only sections >10cm depth were sampled
						HAND5	17.6	
						HAND6	19.2	
08.31.06	MC-15-B	Arctic Ocean	70-00.01N	168.00.05W	48	HAND1	18.9	
						HAND2	19.0	
						HAND3	19.3	
						HAND4	19.6	
						HAND5	17.8	
						HAND6	18.9	
						HAND7	20.3	
						HAND8	20.4	
08.31.06	MC-14-A	Arctic Ocean	70-59.98N	165-59.85W	43	HAND1	20.7	
						HAND5	20.4	
						HAND6	20.0	
09.01.06	MC-14-B	Arctic Ocean	70-59.98N	165-59.94W	43	HAND2	20.1	
						HAND3	18.4	
						HAND4	18.4	
						HAND5	17.7	
						HAND6	18.7	
						HAND7	20.9	
						HAND8	19.4	
09.01.06	MC-13-A	Arctic Ocean	72-00.04N	165-59.97W	46	HAND1	25.8	
						HAND2	26.3	only sections >10cm depth were sampled
						HAND5	26.6	
						HAND6	26.0	
09.02.06	MC-12EX-A	Arctic Ocean	72-35.99N	166-00.04W	53	HAND1	31.5	
						HAND2	30.8	only sections >10cm depth were sampled
						HAND6	31.2	
09.02.06	MC-12EX-B	Arctic Ocean	72-36.02N	165-59.94W	53	HAND1	31.9	
						HAND2	35.1	
						HAND3	35.1	
						HAND4	34.2	
						HAND5	34.3	
						HAND6	34.1	
						HAND7	36.2	
						HAND8	34.5	
09.02.06	MC-13-B	Arctic Ocean	72-00.01N	165-60.00W	46	HAND1	23.4	
						HAND3	23.0	
						HAND4	22.7	
						HAND5	23.2	
						HAND6	23.8	
						HAND7	23.5	
						HAND8	23.6	
09.03.06	MC-12-A	Arctic Ocean	72-25.93N	166-57.85W	51	HAND1	22.2	
						HAND2	23.2	only sections >10cm depth were sampled
						HAND6	20.4	
09.05.06	MC-16-A	Arctic Ocean	68-30.03N	167-59.95W	54	HAND1	23.4	1/2 portion of each sections was subsampled
						HAND6	24.9	
09.05.06	MC-16-B	Arctic Ocean	68-29.99N	167-59.96W	55	HAND1	25.9	
						HAND2	25.3	
						HAND3	27.6	
						HAND4	25.7	
						HAND5	25.3	
						HAND6	24.3	
						HAND7	25.8	
						HAND8	24.6	
09.06.06	MC-17-A	Arctic Ocean	66-59.99N	166-59.95W	40	HAND1	26.5	
						HAND2	27.5	only sections >10cm depth were sampled
						HAND5	25.0	
						HAND6	24.3	
09.07.06	MC-19-A	Bering Sea	63-00.02N	167-29.94W	33	HAND2	20.2	
09.07.06	MC-19-B	Bering Sea	62-59.99N	167-30.01W	33	HAND1	23.4	1/2 portion of each sections was subsampled
						HAND2	24.1	
						HAND3	22.5	Small crab on the sediment
						HAND4	24.3	
						HAND5	21.8	
						HAND6	22.6	
						HAND7	24.5	
						HAND8	23.6	Small crab on the sediment

Table 6.10.10.1 (*Continued*)

Date (mmddyy)	Core ID	Location	Lat.	Lon.	Depth(m)	HAND No.	Core length(m)*	Remarks
09.08.06	MC-20-A	Bering Sea	62-00.02N	169-00.44W	37	HAND2	19.6	1/2 portion of each sections was subsampled
09.08.06	MC-20-B	Bering Sea	62-00.08N	168-59.92W	37	HAND1	17.4	
						HAND2	16.8	
						HAND3	16.6	
						HAND4	18.2	
						HAND5	17.2	
						HAND6	17.1	
						HAND7	17.4	
						HAND8	16.8	
09.10.06	MC-23-A	Bering Sea	60-09.52N	179-27.80W	1,004	HAND2	21.9	
						HAND4	22.4	
						HAND8	22.1	only sections >10cm depth were sampled
09.10.06	MC-23-B	Bering Sea	60-09.53N	179-27.86W	1,000	HAND1	22.4	
						HAND2	21.8	
						HAND3	20.7	
						HAND4	22.4	
						HAND5	22.3	
						HAND6	20.7	
						HAND7	20.9	
						HAND8	19.6	
09.11.06	MC-24-A	Bering Sea	60-15.70N	179-25.34W	851	HAND2	20.4	
						HAND4	16.9	
						HAND8	18.7	only sections >10cm depth were sampled
09.11.06	MC-24-B	Bering Sea	60-15.70N	179-25.35W	851	HAND1	21.4	
						HAND2	21.5	
						HAND3	21.5	Catch a organisms
						HAND4	21.3	
						HAND5	19.8	
						HAND6	21.4	Catch a organisms
						HAND7	20.9	
						HAND8	21.3	
09.12.06	MC-25-A	Bering Sea	60-04.49N	179-27.79W	1,158	HAND5	19.1	
						HAND8	18.3	only sections >10cm depth were sampled
09.12.06	MC-25-B	Bering Sea	60-04.50N	179-27.75W	1,158	HAND1	20.5	
						HAND2	20.4	
						HAND3	19.7	
						HAND4	20.7	
						HAND5	20.0	
						HAND6	18.9	
						HAND7	17.2	
						HAND8	18.8	
09.14.06	MC-29-A	Bering Sea	58-30.00N	167-30.04W	51	HAND8	16.8	1/2 portion of each sections was subsampled
09.14.06	MC-29-B	Bering Sea	58-29.99N	167-30.03W	51	HAND1	16.2(16.0)	
						HAND3	15.3	
						HAND4	15.9	
						HAND5	17.5	
						HAND6	18.5	
						HAND7	16.8	sectioning was failed and taken as a grab sample
						HAND8	16.4	
09.17.06	MC-33-A	Bering Sea	55-46.42N	166-13.59W	130	HAND7	28.7(30.0)	1/4 portion of each sections was subsampled

*Core length is measure on deck. Parenthetic core length is measure in laboratory(description) or dark room(sampling).

Table 6.10.10.2 Surface sediments collected with pilot core sampler attached to gravity- or piston-core samplers during MR06-04 Leg.2 cruise

Date (mmddyy)	Core ID	Location	Lat.	Lon.	Depth (m)	HAND No.	Core length(m)
09.01.06	PL-14	Arctic Ocean	71-00.01N	166-00.26W	43	HAND2	19.4
						HAND3	15.4
09.10.06	PL-23-A	Bering Sea	60-09.52N	179-27.82W	1002	HAND2	17.1
09.10.06	PL-23-B	Bering Sea	60-09.53N	179-27.82W	1000	HAND2	16.5
						HAND3	17.0
09.11.06	PL-24-A	Bering Sea	60-15.70N	179-25.34W	852	HAND3	12.3
09.11.06	PL-24-B	Bering Sea	60-15.70N	179-25.36W	853	HAND3	15.3
09.12.06	PL-25-A	Bering Sea	60-04.48N	179-27.80W	1158	HAND2	17.8
						HAND3	15.6
09.12.06	PL-25-B	Bering Sea	60-04.50N	179-27.78W	1157	HAND3	12.8

*Core length is measured on deck.

Table 6.10.10.3 Core sediments collected with gravity core sampler during MR06-04 Leg.2 cruise

Date (mmddyy)	Core ID	Location	Lat.	Lon.	Depth (m)	Core/Barrel length(m)
09.01.06	GC-14	Arctic Ocean	71-00.01N	166-00.26W	43	0.918/5
09.01.06	GC-13	Arctic Ocean	72-00.00N	166-00.01W	46	1.630/5
09.02.06	GC-12EX	Arctic Ocean	72-36.00N	165-59.97W	53	4.256/5
09.05.06	GC-16	Arctic Ocean	68-29.99N	167-59.99W	54	1.441/5
09.17.06	GC-33	Bering Sea	55-46.41N	166-13.57W	130	1.853/7

Table 6.10.10.4 Core sediments collected with piston core sampler during MR06-04 Leg.2 cruise

Date (mmddyy)	Core ID	Location	Lat.	Lon.	Depth (m)	Core/Barrel length(m)	Piston type*
09.11.06	PC-23-B	Bering Sea	60-09.53N	179-27.82W	1,000	14.308/20	RPP-70*3&50*1
09.12.06	PC-24-B	Bering Sea	60-15.70N	179-25.36W	853	16.732/20	RPP-70*3&50*1
09.13.06	PC-25-B	Bering Sea	60-04.50N	179-27.78W	1,157	14.912/20	RPP-70*3&50*1

*Normal type piston is composing of stainless steel body and O-ring (size: P63). Difference between Normal type and Short type is only length (4.5cm). RPP (Rubber Plate Piston) apply rubber plates (RPP-hardness of plates*number).

6.10.11 Paleo-temperature and -salinity reconstruction of the Okhotsk Sea using the planktonic foraminiferal Mg/Ca thermometry

(1) Personnel

Sagawa T. (Kochi Univ.)

(2) Objectives

I focus on the past sea surface condition change, especially on sea surface temperature (SST) and sea surface salinity (SSS), in the Okhotsk Sea on various time scale. Because SST and SSS of the Okhotsk Sea are closely related to atmospheric circulation and fresh water discharge from the Amur River, it is very important to reconstruct past sea surface condition in order to understand the climate variability of the East Asia and its relationship with the Northern Hemispheric and global climate change. Recently, alkenone based paleo SST records in the Okhotsk Sea were reported by several studies (Seki et al., 2004; Harada et al., 2006). These results indicate that SST during the last glacial maximum (LGM) was as warm as or even higher than modern condition, although diatom assemblage record indicates that the perennial sea ice cover area extended during the LGM (Shiga and Koizumi, 2000). Therefore, SST variation in the Okhotsk Sea should be examined by other geochemical paleothermometry, especially in the LGM.

I will conduct paired analysis of Mg/Ca and oxygen stable isotope of planktonic foraminifera for piston cores from the Okhotsk Sea. This method makes it possible to determine the magnitude and timing of the SST and SSS changes and their relationship in the Okhotsk Sea. Because this is the first time that the planktonic foraminiferal Mg/Ca thermometry will be applied to the Okhotsk Sea, I will also investigate the Mg/Ca-temperature relationship in this region, using the surface sediments taken by multiple corer.

6.10.12 Alkenone analysis for paleo-thermometer

(1) Personnel

Naomi Harada (IORGC, JAMSTEC)

Miyako Sato (IORGC, JAMSTEC)

Kyung Eun Lee (Korea Maritime University)

(2) Objectives

We should know about glacial and interglacial changes in environmental factors such as sea surface temperature (SST) in the Okhotsk Sea, Japan/East Sea and Bering Sea that the climate changes are thought to be close related with that in the East Asia including Japan. Since rapid climate change occurred globally during glacial and interglacial periods (e.g., Grootes and Stuiver, 1997), before human activity had a serious impact on climate, studies of those periods are important for understanding the mechanism of natural climate changes. Moreover, paleoceanographical investigations can provide data essential for the development of a climatological data set that can be used for predicting future climate.

In this cruise, we collected sediment samples to reconstruct the SST changes in the Okhotsk, Japan/East and Bering Seas by using alkenone method.

(3) Instruments and Methods

The alkenone unsaturation index, $U^{K'}_{37}$, which is derived from the relative abundance of methyl alkenones with 37 carbon atoms and two or three double bonds ($U^{K'}_{37} = (C_{37:2})/(C_{37:2} + C_{37:3})$), will be used as a proxy for a water thermometer because a linear relationship exists between $U^{K'}_{37}$ and the temperature of the water in which the alkenone producers live (Brassell et al., 1986; Prahl et al., 1988). For the alkenone analysis, a sediment sample (2–4 g dry weight) is ground into powder. The fractions containing bulk organic compounds are extracted from sediment samples with an Accelerated Solvent Extractor (ASE-200, DIONEX Japan Ltd.). The extracts are saponified in 0.5 M KOH in methanol and the neutral fraction is recovered with a pipette, dissolved in hexane, and then separated into subfractions by silica gel column chromatography using an automatic solid-preparation system (Rapid Trace SPE Workstation, Zymark, UK). An aliquot of the alkenone fraction is analyzed by capillary gas chromatography with an Agilent 6890N gas chromatograph, Agilent (USA) equipped with an fused-silica column, a cold on-column injector, and a flame ionization detector.

(4) Expected results

Sediment will be used for reconstruction of sea surface water temperature by alkenone method. From alkenone-derived SST changes, we will discuss changes of SST on millennial and centennial time scale over the past 10-100 kyr to clarify the mechanisms of abrupt climate changes and intra Northern hemispheric telleconection comparing the ice-core record from Greenland.

(5) Data archives

All the data will be published within the moratorium period and will be submitted to JAMSTEC Data

Management Office (DMO) as a publication.

6.10.13 Pore water chemical measurement

(1) Personnel

Akinari Hirota, (Division of Natural History Sciences, Faculty of Science, Hokkaido University) Leg.1-2

Akira Ijiri (Division of Natural History Sciences, Faculty of Science, Hokkaido University) Leg.2

(2) Objectives

During the Leg.1, pore water samples were taken from multiple cores (MC1 - MC7), piston cores (PC1 and PC2) and during the Leg.2, from multiple cores (MC12extra, MC12-14, MC16, MC19-26, MC30, MC31 and MC33), piston cores (PC23, PC24 and PC25) and gravity cores (GC33). Pore water samples were squeezed on board ship. The squeezing for multiple cores was carried out by pressure filtration through 0.45μm Millipore filter, using a stainless steel clamp (Manheim, 1968) at bottom water temperature (about 3°C). The pore fluid samples for piston and gravity cores were extracted on board using a stainless steel squeezer (Manheim and Sayles, 1974) in which sediment samples of about 250 cm^3 were taken for pore fluid squeezing at 50 cm intervals from the cores. Determinations of pH and alkalinity were done about PC1 and PC2 on board (Table 6.10.13.1). We will analyze concentration of major components, dissolved organic carbon and acetic acid and isotopic compositions of methane, carbon dioxide, nitrate and H_2O in pore waters.

Table 6.10.13.1 Alkalinity and pH

St.	name	depth	Alk.	pH
		[cm]	[mM]	
1	PC-1	25	4.98	8.09
		75	5.92	8.05
		125	-	-
		175	-	-
		225	-	-
		325	-	-
		350	-	-
2	PC-2	25	9.68	8.14
		75	13.74	8.14
		125	14.29	8.09
		175	15.63	8.07
		225	21.19	8.10
		275	20.95	8.05
		325	-	-
		375	21.43	8.18
		425	-	-
		475	27.12	8.20
		525	28.89	8.24
		575	-	-

(3) References

Manheim, F.T. 1968. Disposable syringe techniques for obtaining small quantities of pore water from unconsolidated sediments. Journal of Sedimentary Research, 38, 666-668.

Manheim, F.T. and Sayles, F.L. 1974. Composition and origin of interstitial waters of marine sediments, based on deep sea drill cores. In: The Sea, 5 (E.D.Golderg ed.), 527-568.

6.10.14 Late Quaternary diatom taxonomy of Okhotsk Sea, Chukchi Sea and Bering Sea sediments

(1) Personnel

Susumu Konno (Dept. of Earth & Environmental Sciences, Faculty of Science, Yamagata University) Leg.1

Richard W. Jordan (Dept. of Earth & Environmental Sciences, Faculty of Science, Yamagata University) on shore

(2) Objectives

The main aims of this project are to:

1) prepare a diatom catalogue (identification guide) for publication and laboratory use,

2) provide taxonomic support to those scientists working on palaeoenvironmental reconstruction.

(3) Methods

Sediment samples from piston, gravity and multiple cores intended for palaeoenvironmental reconstruction were subsampled for taxonomic studies. These samples will be acid-cleaned and prepared for LM and SEM observations using standard methodologies. Mountmedia-prepared slides will be observed with a Nikon Optiphot2-pol polarizing light microscope, while material mounted on aluminium EM stubs will be observed in a Hitachi S-2250N SEM. Specimens will be photographed using camera attachments.

6.10.15 Plan of land analyses of the Russian side sediments recovered during MIRAI cruise 06-04.

(1) Personnel

Gorbarenko A.S., Derkachev A., Bosin A.A., Vasilenko P.Y. (V. I.ll'ichev Pacific Ocenological Institute, Far Eastern Branch, Russian Academy of Sciences)

(2) Geochemical analyses

1) Elemental analyses of sediments using ICP-MS analyses of the sediments humidity and density (every 1cm)
2) Magnetic mineralogical analysis, magnetic granulometric, anisotropy of magnetic susceptibility (AMS), change of the geomagnetic field intensity (method resedimentation).
3) Analyses of the sediment pore water salinity.
4) Measurement of the carbonate and organic carbon, opal and chlorine content in sediments.
5) Quantities and species analyses of the diatoms, radiolarian and benthic foraminiferas in sediments.
6) Content of U, Th and its isotopes (ICP-MS, 50-100 analyses).
7) Oxygen and carbon isotope of the benthic and planktonic foraminiferas.
8) Mineralogical analyses of the heavy fraction of sediments (50-100 analyses).
9) Grain size analyses

6.10.16 Reconstruction of sea-ice variation and related climate/ocean changes in the Okhotsk, north Japan, and Bering Seas

(1) Personnel

Saiko Sugisaki (JAMSTEC IFREE4): Leg.1

Tatsuhiko Sakamoto (JAMSTEC IFREE4): Leg.1

Koichi Iijima (JAMSTEC IFREE4): Leg.1, 2

Kazumasa Oguri, Sabrou Sakai (JAMSTEC IFREE4): On shore

(2) Objectives

Our objectives are to reconstruct the glacial- interglacial scale environmental change and centennial/millennial scale abrupt climate change in the high-latitude of Northern Pacific Ocean where have a great impact to climate of eastern Asia region. Especially, we focused on how fresh water of Amur river act on sea ice formation water circulation in the Okhotsk, Northern Japan, and Bering Seas.

Our main studies are construction of correct age model of the sediment cores, especially focused on the identification of time slices (6,000 yr, 10,000 yr, last glacial stage, Heinrich event stage) and reconstruct sea ice and related oceanographic variation in the high-latitude area.

(3) Methodology

For reconstructing correct age model, we will conduct (a) accelerator mass spectrometer (AMS) ^{14}C dating of planktonic foraminifer shells (Oguri), (b) EPMA analysis of Tephras (Iijima), (c) analyses of oxygen and carbon isotopes of planktonic and benthic foraminifera (Sakai), and (d)construction of age model (Sakamoto). In addition, we will do analysis of (e) IRD counting (Sugisaki), (f) grain size analyses (Iijima), (e) optical stimulated luminescence (OSL) (Sugisaki).

Estimating the deposit age of IRD as a proxy of sea ice or iceberg process, we will try OSL analysis. The OSL technique uses the built up of a trapped electron population in natural minerals, such as quartz and feldspar, as a chronometer. The electron population of those minerals is initially set to zero by daylight exposure during transport by wind, water, or ice, and increase with time because of exposure to naturally occurring radiation from that sediments. The dating technique is usually applied into sediments that are younger than ca 150 ka. The samples are treated with hydrogen peroxide to oxidize organic material, hydrochloric acid to dissolve carbonates, and fluoboric acid to remove feldspars and micas. Heavy minerals are removed by density separation with solutions o sodium polytungstate. Coarse quartz grains of 90-125μm diameter are isolated with wet sieving and etched in 40% hydrofluoric acid.

We will analyze the sand sized IRD (>63μm) of quartz with the single grain method at Risø National laboratory. It is expected that the deposit age of IRD are agreeable with the other age data, and it will be able to cover the age span that over the applied ^{14}C age.

U-channel cased samples will be taken X-ray radiograph for IRD (>2mm diameter) counting. For grain size analyses (0.04-2000μm diameter), we will use a laser diffraction grain size analyzer, Coulter LS230 (IFREE/JAMSTEC) after removing organic matter are oxidized with hydrogen peroxide, biogenic calcium carbonate are removed with hydrochloric acid, and biogenic opal are leached with sodium

6.11 Visual core description

(1) Personnel

Sakamoto T., Iijima K., Sugisaki S. (IFREE, JAMSTEC)

Itaki T. (Pusan National Univ.)

Rella S. (Univ. of Tokyo)

Gorbarenko S., Derkachev A., Vasilenko A., and Bosin A. (POI, FEB-RAS)

(2) Introduction

On board sedimentologists were responsible for visual core descriptions (VCD) and smear slide analysis of cored sediment. Lithology of recovered material is recorded on the hand-written barrel sheets (Appendix02). All hand-written barrel sheets are scanned by flatbed scanner. In each barrel sheets, column of “Graphic Representation” is hand-written visual sketch of the cores. Color and shape of lithological features might be modified in the column in order to enhance important information of the core. The column of “Structure” indicates the presence of primary sedimentary structures, soft-sediment modification features (coring disturbance), structural features, and diagenetic features observed visually using lithological symbols (Fig.6.11.1). Intervals of lithology and any other features were noted as text in the barrel sheets.

***Sediment classification*:** Cruise MR06-04 sediment classification is based primarily on visual core descriptions and smear slide analyses. The principal lithologic name (e.g., diatom ooze, silty clay) is based on the major (>50%) sediment component. Secondary components, composing 25% to 50% of the sediment, are included as major modifiers preceding the principal name (e.g., diatom ooze, silty clay). Minor constituents, composing 10% to 25% of the sediment, are included using the term “-bearing” (e.g., diatom-bearing silty clay). The sediment modifiers are ordered so that minor modifier(s) precedes major modifier(s). Specific nomenclature for the two compositional groups, appropriate for sediments recovered during this cruise, is given below.

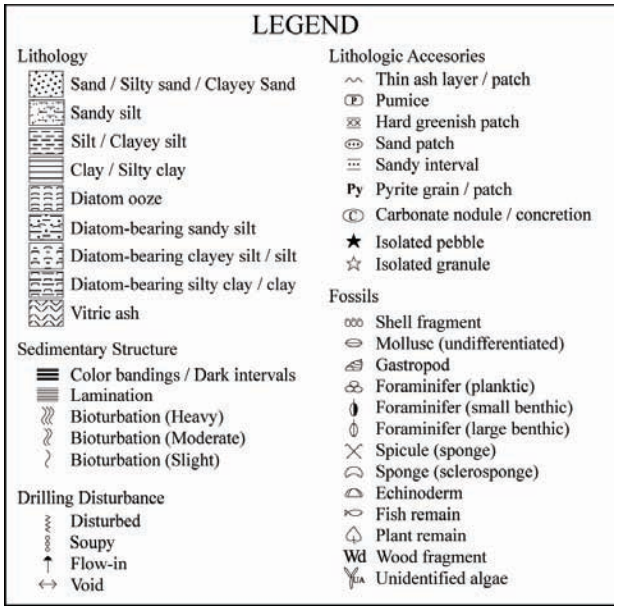

Figure 6.11.1 Legend of lithology

Siliciclastic sediments: The siliciclastic category includes sediments having >50% siliciclastic sediments. These sediments are classified on the basis of grain size, referring a ternary diagram principle names for siliciclastic sediments (from Shepard, 1954) in Mazzullo et al. (1987) (Fig.6.11.2). Siliciclastic sediment having >75% of a single component is given the name of that major component. For example, siliciclastic sediment containing 80% clay and 20% silt would be classified simply as "clay." When siliciclastic sediment consists of a two-component mixture, the major component is preceded by a modifier describing the secondary grain size. For example, siliciclastic sediment containing 70% clay and 30% silt would be classified as "silty clay."

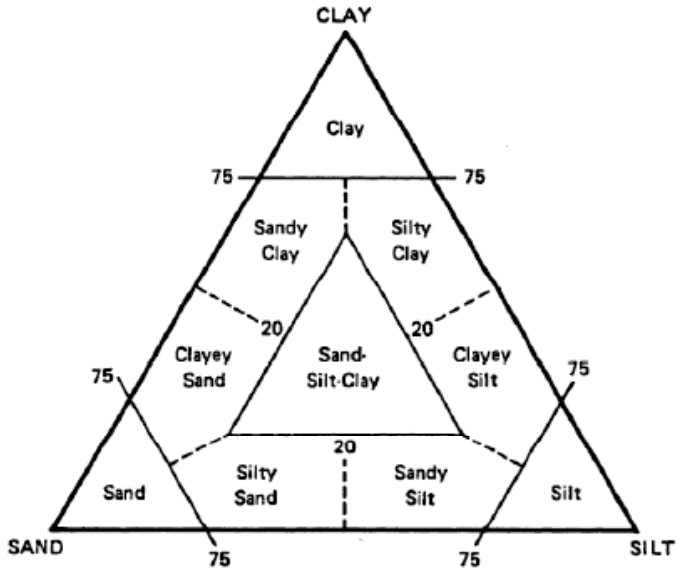

Figure 6.11.2 Ternary diagram principle names for siliciclastic sediments

Biogenic sediments: The biogenic category includes fine-grained sediments containing >50% biogenic sediments. Designation as siliceous or carbonate depends relative abundance of these two biogenic. When the biogenic component the sediment is classified as ooze. When sediments are mixed with 10% to 25% siliciclastic components, the siliciclastic component followed by the word "-bearing" is used as modifier. For example, if the sediment contains diatoms and 20% siliciclastic would be classified as "clay-bearing diatom ooze."

Bioturbation: The following scale is used to describe bioturbation as measured by the percentage of burrow features:

- Slightly bioturbated = 1%–30% bioturbation.
- Moderately bioturbated = 30%–60% bioturbation.
- Heavily bioturbated = 60%–90% bioturbation.

Total mixing of sediment by bioturbating organisms produces homogeneous sediment with an appearance similar to nonbioturbated sediments that result from the deposition of material of homogeneous color and grain size. Therefore, a bioturbation scale cannot be applied to homogeneous sediment with confidence.

Color: The color of the sediment cores noted in the "Color" column in the barrel sheet are recorded as hue and chroma attributes of color determined using Munsell Soil Color Charts (1971).

Samples: In the "Sample column" of the barrel sheets, intervals of smear slide samples were record as ID of SS with its intervals in the section.

Coring disturbance: Deformation and disturbances of sediment that clearly resulted from the coring process are illustrated in the barrel sheets. The degree of coring disturbance is described using the categories listed below (blank regions indicate the absence of coring disturbance):

- Slightly disturbed = bedding contacts that are slightly bent.
- Moderately disturbed = bedding contacts that are extremely bowed.
- Very disturbed = bedding that is completely disturbed
- Soupy or flow-in = intervals that are water-saturated (soupy or have otherwise lost all aspects of original bedding resulting from flow-in.

Depth adjustments: Length and intervals of each section of the recovered cores were often shifted during core processing on shipboard, especially splitting whole-round core into two half-split cores (see "6.8.3.1 Multi-Sensor Core Logging"). This artificial depth shift resulted in discrepancy of measurement intervals of MSCL for whole rounded core with the intervals of VCD and color reflectance measurement. In order to avoiding inconsistency of the intervals and length of the core, a "depth sheet" including information of core length measured several times on board during core processing (see "6.8.3.1 Multi-Sensor Core Logging"). For the split cores, MWJ marine technicians put pinpricks in the intervals of 1cm at the side of sediment material beside core liner just after split core on deck. The any intervals of color reflectance measurement and VCD followed the intervals of pinpricks if the section has expanded or shrunk during core processing on board.

(2) Summarized lithology with physical properties

All shipboard VCD information of the hand-written barrel sheets was summarized as major and minor sediment lithology with major features into "lithology" column as Figs. 6.11.3 to 6.11.40 using graphic patterns listed in Fig. 6.11.1. Because of the limited scale of the core summaries, the graphic lithology column and lithologic symbols usually shows only the major layers, intervals exceeding 20 cm in thickness, or other notable characteristics. Descriptions and locations of thin, interbedded, or minor lithology or thin color banding that could not be depicted in the Lithology column should be referred in original hand-written barrel sheets in the Appendix02.

Results of physical properties measurements including magnetic susceptibility, gamma-ray attenuation density, and color reflectance plotted together with summarized lithology column. Measurement errors resulting from voids, fractures, disturbed intervals, and edge materials in the top and bottom of the section were omitted in this profiles with evaluation based on the VCD.

Figures 6.11.9, 6.11.14, 6.11.17, 6.11.21, and 6.11.26 include correlation and initial age model on shipboard among cores at same station of 4, 5, 6m, and 7, respectively.